STUDIES OF THE ELECTRIC DISCHARGE AND ITS APPLICATION FOR THE EXCITATION OF HIGH POWER GAS LASERS

by

Ayham A. Yahya B.Sc., M.Sc.

A DOCTORAL THESIS

Submitted in partial fulfilment of the requirements for the award of Ph.D. of the Loughborough University of Technology, 1990.

Supervisor: Dr. J. E. Harry

Department of Electronic and Electrical Engineering

To my parents

ABSTRACT

The electric discharge has been studied in static and fast flow gases at gas pressures between 50 mb and 1 b over a range of current of between 10 mA and 1.5 A representative of its application to the excitation of high power gas lasers.

The investigations have shown that the glow to arc transition is a cathode phenomenon which may oscillate between a glow and arc discharge at the transition current. The oscillation appears to be inherent where neither the glow nor the arc is stable at the transition current. The glow to arc transition has no effect on the positive column characteristics.

The contraction of the positive column and the decrease in its voltage gradient as the current is increased appeared to be related to the thermal conductivity of the gas which indicates that the formation of streamers in the discharge column in a fast gas flow is a local constriction due to thermal instabilities.

The multiple electric discharge has been investigated and analysed and compared with an equivalent single electric discharge. The investigation showed that the coalesced part of the column has the same characteristics of a single discharge column with the same current and the discharge column coalesces so as to operate at the minimum voltage which supports the Steenbeck minimum principle. A mathematical model was established for the coalescence of the multiple discharge based on Steenbeck's minimum principle which has been demonstrated experimentally by applying an external magnetic field to the discharge column.

The behaviour of the positive column in a fast gas flow was investigated and mathematical models were established for the contraction of the positive column by the shear stress force due to the flow profile of the gas flow in the laminar and turbulent flow regimes using gas injection nozzles to demonstrate the effect of the flow

profile on the contraction of the discharge column and a diffusing injection nozzle has been proposed as the optimum design.

An injection nozzle-electrode was designed and tested by replacing the original cylindrical injection nozzle-electrode in a 5 kW CO_2 laser at a gas pressure of 50 mb. The new nozzle-electrode has resulted in a 50% reduction in the gas mass flow rate.

ACKNOWLEDGEMENTS

It is my pleasure to acknowledge the kind advice, encouragement and patience of my supervisor and friend, Dr. J. E. Harry, throughout this work.

I am grateful to the Iraqi Government for the grant that made this work possible. I would also like to thank the technicians who have helped me in constructing the equipment.

Finally, my sincere thanks go to my family for their understanding and encouragement.

CONTENTS

LIST OF FIGURES

CHAPTER 4

CHAPTER 5

CHAPTER 6

LIST OF TABLES

LIST OF SYMBOLS

		unit
a	Distance between two conductors.	mm
A	Area.	m^2
c_p	Specific heat of the gas.	J kg^{-1} $°C^{-1}$
d	Diameter.	mm
e	Electron charge.	C
E	Voltage gradient.	V mm^{-1}
E_1	Voltage gradient of the coalesced column.	V mm^{-1}
E_2	Voltage gradient of the non coalesced column	V mm^{-1}
E_a	Energy.	J
F	Force.	N
F_L	Compression force due to laminar flow.	N
F_M	Compression force due to magnetic field.	N
F_b	Axial force along the discharge column.	N
F_T	Compression force due to turbulent flow.	N
H	Magnetic flux.	A m^{-1}
I	Current.	A
I_s	Stabilising impedance current.	A
k	Thermal conductivity	mW $mm^{-1}K^{-1}$
L	Electrode separation.	mm
n	Number.	-

N	Neutral particle density.	m^{-3}
N_A	Avogadro's number.	-
p	Pressure.	b
P_E	Electric discharge power input.	W
P_H	Waste heat power.	W
P_L	Laser power output.	W
P_{Lc}	Power of convective cooled laser.	W
P_{Ld}	Power of diffusion cooled laser.	W
r	Radius.	mm
R	Gas constant.	$J\ mol^{-1}K^{-1}$
R_d	Reynolds number.	-
t	Time.	s
T	Temperature.	°C
U	Gas velocity.	$m\ s^{-1}$
u_d	Electron drift velocity.	$m\ s^{-1}$
U_m	Weighted mean velocity.	$m\ s^{-1}$
U_r	Gas velocity at the axis of the tube.	$m\ s^{-1}$
U_s	Gas velocity.	$m\ s^{-1}$
u_t	Thermal molecular speed.	$m\ s^{-1}$
v	Volume.	m^3
V	Voltage.	V
V_a	Anode fall voltage.	V
V_c	Cathode fall voltage.	V
V_d	Discharge voltage.	V
V_p	Voltage drop along the positive column.	V
V_s	Voltage drop across the stabilising impedance.	V
x	Length.	mm

y	Distance.	mm
η	Efficiency.	-
θ	Angle.	degree
λ	Mean free path.	m
λ_e	Electron mean free path.	m
μ	Dynamic viscosity.	kg $m^{-1}s^{-1}$
μ_o	Permeability of air.	H m^{-1}
ρ	Gas density.	kg m^{-3}
τ	Shear stress.	N m^{-2}
τ_L	Shear stress due to laminar flow.	N m^{-2}
τ_T	Shear stress due to turbulent flow.	N m^{-2}

CHAPTER 1

INTRODUCTION

Since the discovery of the electric discharge, its luminous and colourful emissions have fascinated observers for more than a century. Efforts in investigating it have been rewarded by many interesting discoveries which often appear now to be far removed from the original field. The discharge itself appeared to be a complex phenomenon and the way in which it functions remained a mystery. Today different sciences, such as plasma physics, atomic physics, communication and others, owed their very existence either directly or indirectly to the electric discharge. In the meantime, the demonstration of a laser by Maiman (1960), and a gas laser by Javan et al (1961), has opened a new era of the applications of electric discharge for their excitation. Since then a compact laser which is capable of delivering several kilowatts or even megawatts has been a target for many scientists for many different applications.

Electric discharges using a.c., d.c. or radio frequency (rf) current at low gas pressure (30-150 mb) are used to produce CW output lasers such as CO and CO_2 lasers, while pulsed discharges at high gas pressure (200 mb up to several atmospheres) are used to produce pulsed output lasers such as CO, CO_2 and excimer lasers. Many of the lasers commercially available today use electric discharge technology developed in the 1970's. The CO_2 laser is used in industry for material processing such as cutting, welding, drilling and surface treatment. The majority of high power CO_2 lasers installed in industry are d.c. discharge excited lasers making the potential for significant improvements in methods of d.c. discharge excitation techniques very attractive. New interest has developed in the CO laser for its better results in material processing and the capability of transmission through optical fibre, as well as the excimer lasers where its short wavelength (170-350 nm) is suitable for photo-chemical processing. Major national and international programmes have been undertaken to develop new lasers technology involving CO, CO_2 and excimer lasers

to meet the demands for higher laser outputs (10-50 kW) of the industrial users; programmes such as the European EUREKA and BRITE programmes, and the Japanese Ministry of International Trade and Industry (MITI).

1.1 THE PRESENT WORK

The initial interest was directed first towards the rare gas monohalide excimer lasers. Excimer lasers have either an unbound or weakly bound lower lasing level. As a result, the life time of this level is generally short enough to prevent blocking the molecule transition to the ground state. This removes a major obstacle to the operation of CW excimer laser, however, excimer lasers have always been operated in the pulsed mode (30-400 ns). This is because the gas pressure in the discharge cavity must be higher than 400 mb (Wang 1976) which leads to a rapid local constriction within the discharge column due to thermal instabilities which quench the laser action (Hogan et al 1980), and the depletion of the halogen donor molecule which also causes column constriction within the discharge column and premature termination of the laser output (Hogan et al 1981, Osborne et al 1986). If a uniform discharge column could be maintained by limiting the current flow to the discharge, a longer pulse duration or even CW laser output may be obtained. This led to the construction of a XeCl laser with an output pulse duration of 1.5 μs (Taylor and Leopold 1985).

It was assumed in the early stage of this work that a CW excimer laser might be possible if a uniform d.c. discharge column could be maintained at atmospheric pressure without constriction, where the electron energy in the positive column, determined by the E/N ratio (Nighan 1970), would be suitable for carrying out the selective molecular transition. A promising way to overcome the constriction of the discharge column is to combine the electric discharge with various gas flow configurations

to cool the discharge column and to increase the column voltage gradient. This technique has already been used successfully in CO_2 lasers at low pressure (50-150 mb) to maintain a uniform discharge column and cool the discharge convectively. The combination of the fast gas flow with the electric discharge has resulted in high power CO_2 lasers (> 10 kW) which were out of reach with the still gas (sealed tube) lasers and output power per unit length of up to about 8 kW/m (Evans 1987), compared with 64 W/m in the sealed tube lasers (Demaria 1973).

The present work is involved in investigating the characteristics of the electric discharge and particularly the positive column in still and flowing gases and the interaction of the gas flow with the discharge column. The results have been dedicated to the excitation of CO_2 lasers since the excimer laser gas mixture is expensive and extremely poisonous, but, the results should be applicable to the excitation of excimer lasers since their operational conditions determined by the E/N ratio (Greene and Brau 1978), are similar to the pulsed CO_2 laser (Nighan 1970). It was believed that a uniform discharge column maintained at pressure higher than that of the conventional CO_2 lasers (> 200 mb) would be useful for the excitation of CW excimer lasers as well as CW CO_2 and CO lasers and could lead to a more compact laser head and reduction in the size of the bulky recirculating system. The results could also have a potential application in chemical synthesis where the appropriate electron energy needed for selective chemical transition can be provided in a convectively cooled uniform positive column and the conventional thermal processes could destroy the reactants or the final products (Suhr 1973, Traus et al 1989).

1.2 THE THESIS STRUCTURE

The structure of the thesis is shown in Fig. 1.1. Chapters 2,4 and 5 are concerned mainly with the fundamentals of electric discharges, while chapters 3,6 and 7 are involved in the applications of electric discharge in gas lasers.

A review of the electric discharge is given in Chapter 2 which includes the theory and physical characteristics of each region of the glow and arc discharge. The stabilising requirements of the electric discharge are discussed. The multiple discharge, the electric discharge in a fast gas flow and the use of electric discharge for the excitation of gas laser are described.

Chapter 3 presents a review of the d.c. electric discharge techniques used for the excitation of CW CO_2 and CO lasers. This includes the electrode arrangements, the discharge cavity and the gas flow configurations. The electrode arrangement for the transversely excited atmospheric pressure (TEA) lasers is also reviewed.

Chapter 4 describes the initial experimental work carried out to investigate the characteristics of the electric discharge in a still gas. The investigation is carried out in different gases over a wide range of pressure.

Chapter 5 describes the investigations carried out on the characteristics of the positive column which include the emission spectra of the positive column at the glow to arc transition, the column voltage gradient in relation to Steenbeck's minimum principle, and the multiple discharge positive column.

Chapter 6 describes the investigation carried out on the interaction of the fast gas flow with the discharge column at atmospheric pressure using different gas

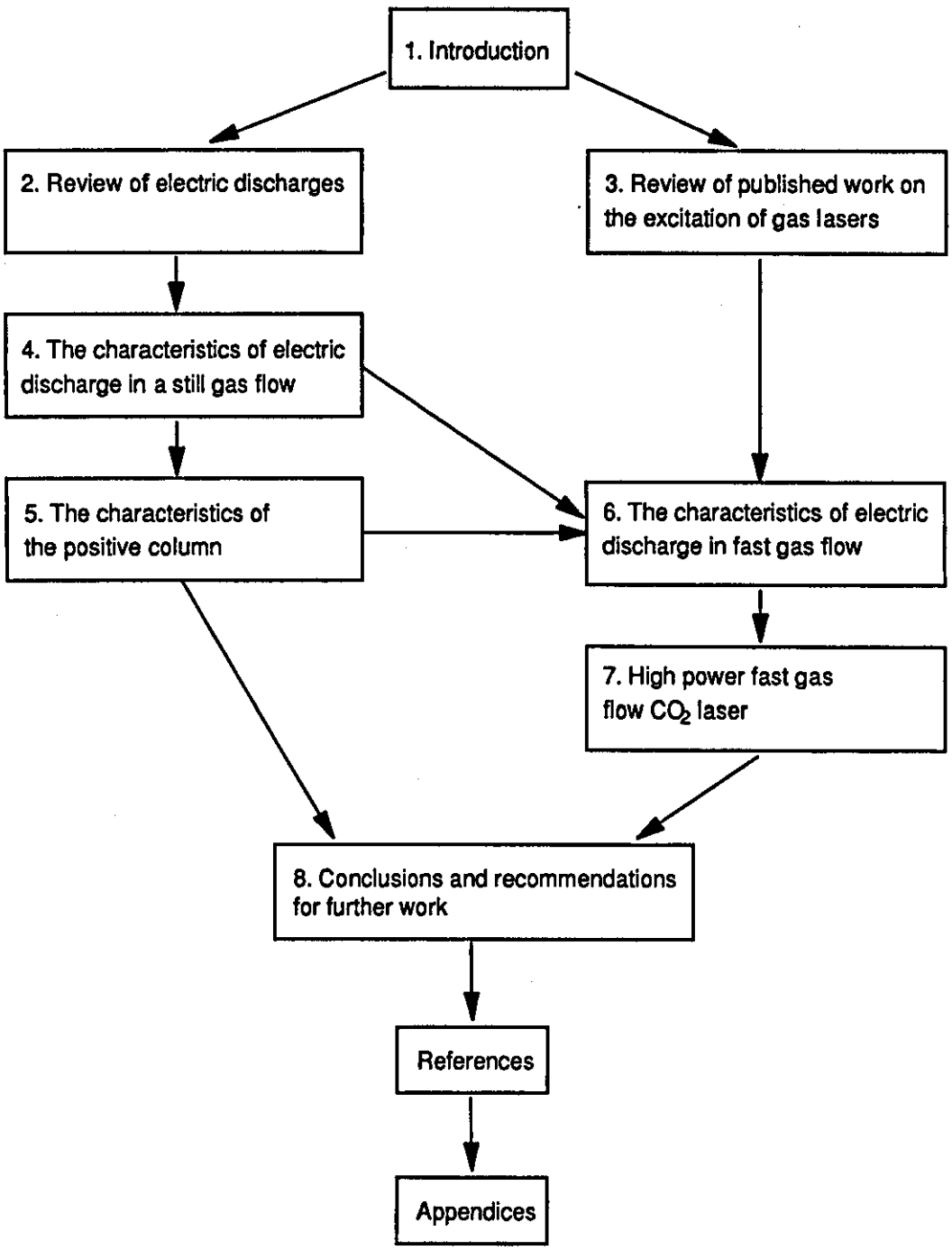

Fig. 1.1 The structure of the thesis.

injection methods by considering the force applied by the flow on the column, and theoretical analysis is given for the laminar and turbulent flow regimes.

Chapter 7 describes the investigation carried out to examine results obtained from this study on a fast axial gas flow 5 kW CO_2 laser at low pressure (50 mb) using different electrode configurations and showing improvements with new injection nozzles.

The conclusions of this study and the recommendations for further work are presented in Chapter 8.

The technical specifications for the scanning monochromator used to investigate the emission spectrum of the positive column are given in Appendix 1. A review on Steenbeck's minimum principle is presented in Appendix 2. The technical specifications of the 5 kW CO_2 laser used in the investigations of Chapter 7 are given in Appendix 3.

CHAPTER 2

REVIEW OF ELECTRIC DISCHARGES

2.1 INTRODUCTION

Gases are, in general, very good insulators, however, they can be made to pass an electric current under certain circumstances. The electric gas discharge is a phenomenon which is observed when an electric current passes through a gaseous medium.

There are many types of discharge but all are characterised by the presence of free charges and an electric field. Accelerated by the electric field, the electrons collide with the free gas molecules giving rise to elastic collisions, excitation, ionisation and sometimes the formation of negative ions. Radiation in the form of emitted photons is produced and gives rise to the luminosity of the electric discharge. The positive ions produced from these collisions are accelerated in the opposite direction towards the cathode. Secondary electrons may be released from the cathode surface by the positive ion bombardment which further contribute to the ionisation process.

The different types of electric discharge can be grouped in two main categories;
(i) non self-sustained discharges, which are characterised by the need for an external ionising source and once this source ceases to act, the electric current through the gas disappears;
(ii) self-sustained discharges, where sufficient electrons are released within the discharge to maintain the electric current and therefore can survive after the removal of the external ionising source which gave rise to them.

2.2 THE ELECTRIC DISCHARGE CHARACTERISTICS

Electric discharges can be established in different gases over a very wide range of gas pressure and carry currents ranging from microamps to more than 10^6 A. The discharge current can be steady, alternating at low or high frequency or transient of very short duration.

The voltage current characteristics of a steady current electric discharge may be determined using a circuit such as that shown in Fig. 2.1. The general nature of the voltage current characteristics of a steady current electric discharge is shown in Fig. 2.2. The discharge characteristics can be generally classified into three main groups according to the visual appearance and the ionisation mechanism as follows;

(i) the Townsend or dark discharge;
(ii) the glow discharge, and;
(iii) the arc discharge.

The characteristics of an electric discharge or the range of the different discharge regions in terms of current depend upon the nature of the gas, the electrode material, the nature of the applied voltage and the constants of the external circuit.

The Townsend discharge is a non self-sustained discharge and characterised by a very low current ($I < 10^{-6}$ A). The discharge is invisible because the density of the excited species which emit visible light is correspondingly low. Since it is a non self-sustained discharge, it requires an external ionising agent such as heat or radiation (X-rays or ultraviolet rays), to produce electrons either directly in the gas or from the cathode.

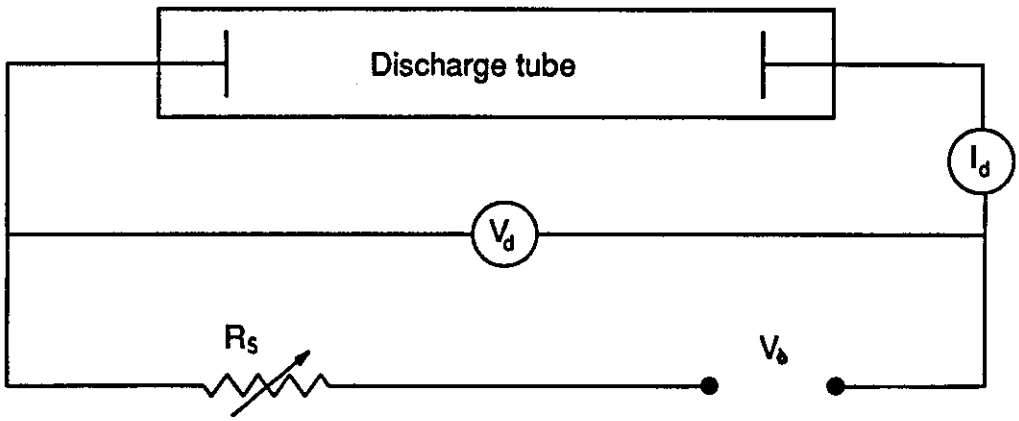

Fig. 2.1 Circuit used to investigate the voltage current characteristics of an electric discharge.

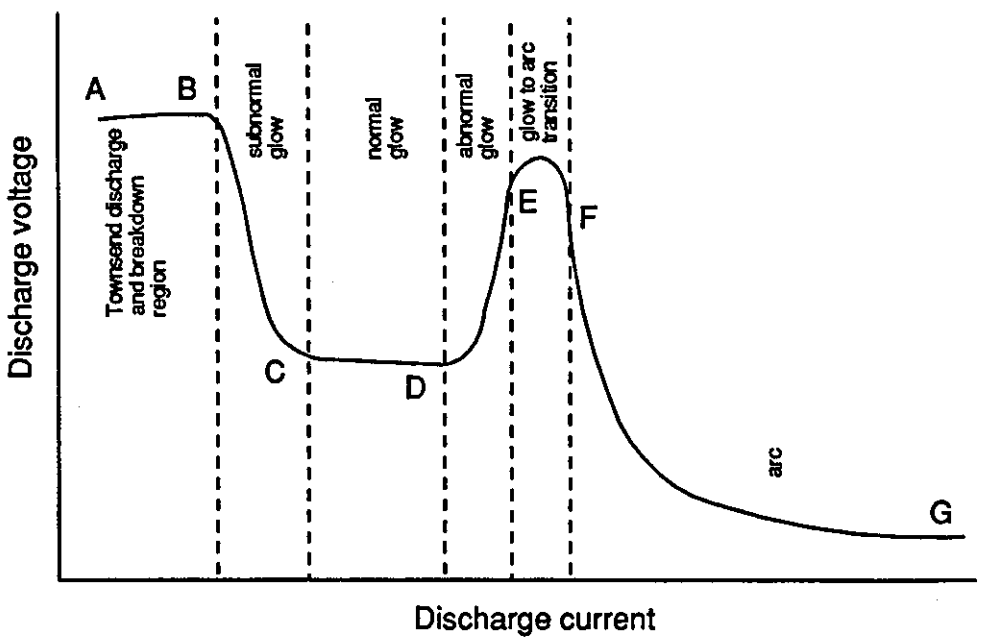

Fig. 2.2 The generalised voltage current characteristic of an electric discharge.

If the current in the Townsend discharge is increased by increasing the supply voltage V_o or decreasing the stabilising resistance R_s, the current will increase abruptly by several orders at some point. This is the breakdown point which depends on the gas pressure, the type of gas, the separation and shape of the electrodes. Once breakdown has occurred, the discharge will take the form of a glow or an arc depending on the circuit and gas conditions. The discharges are both luminous and self-sustained, and the emitted spectrum depends on the type of the gas and the degree of ionisation.

The glow and arc discharges are of special interest since they are self-sustained and they are widely used especially for gas lasers excitation in the CW and pulsed modes (Harry 1974).

2.3 THE GLOW DISCHARGE

The glow discharge derives its name from the luminous region near the cathode. If a glow discharge is established between two cold plane metal electrodes in a cylindrical vessel of few tens of mm radius filled with a gas at pressure of 0.1-1 mb and a current of the order of 1 mA, the visible light emitted from the discharge is distributed over the length of the tube as shown in Fig. 2.3(a). The Aston dark space and the cathode glow are not always clearly visible especially at high pressure (> 100 mb). As the pressure decreases, the negative glow and the Faraday dark space expand at the expense of the positive column which may disappear completely. When the gas pressure increases above, about 0.1 mb, it is seen that the negative zones contract towards the cathode. Above 100 mb only the Faraday dark space is clearly visible.

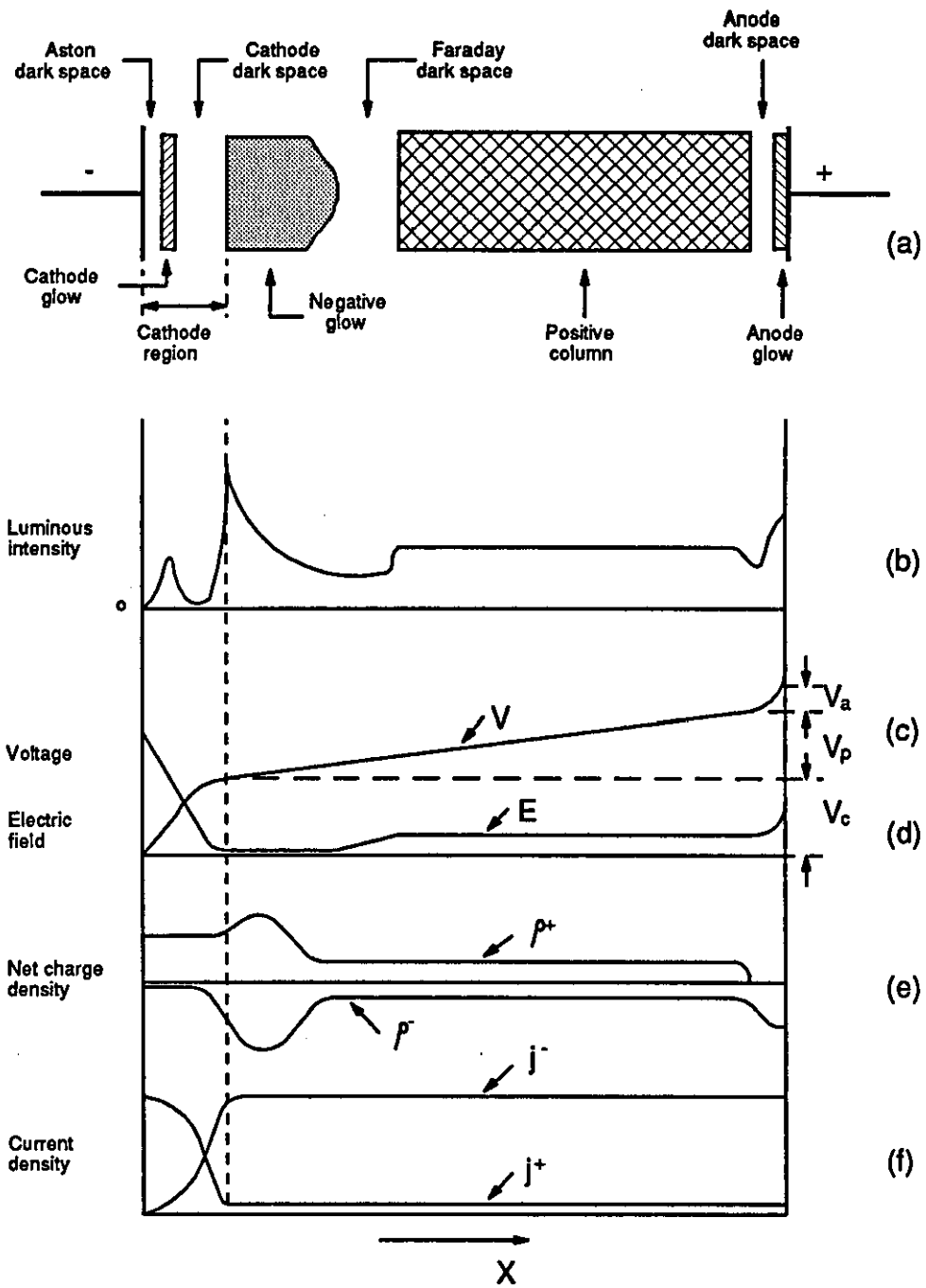

Fig. 2.3 Normal glow discharge. The shaded areas are luminous. (von Engel 1957)

The positive column always fills the remainder of the gap, but it contracts radially at higher pressures. If the distance between the electrodes decreases, the positive column diminishes in the same ratio without the size of the other zones varying. If the cathode is moved transversely, all zones up to the Faraday dark zone are displaced with it. These observations indicate that the regions at and near the cathode are essential to sustaining the glow discharge and that the positive column merely acts as a conducting path for the current.

The distribution of the voltage along the glow discharge is shown in Fig. 2.3(c). The voltage does not vary linearly as a function of the distance from the electrodes due to the effect of the space charge (Fig. 2.3e). The discharge voltage is mainly made up of;

V_c = cathode fall voltage
V_p = voltage drop along the positive column
V_a = anode fall voltage

The cathode fall voltage (the voltage across the cathode region which extends from the cathode to the anode side of the cathode dark space) is high (100-450 V), which indicates the high electric field across this region as shown in Fig. 2.3(d). The positive column voltage varies linearly along its length and, therefore, the electric field along its length is constant. The anode fall voltage (the voltage across the anode glow and anode dark space regions) is determined by the type of the gas and it is approximately equal to the first ionisation potential of the gas (Papoular 1965). The discharge current is mainly electronic rather than ionic because of the greater mobility of the electrons. The net charge density and the current density distribution along the discharge are shown in Fig. 2.3(e) and (f) respectively.

The conduction process in the glow discharge and the related distribution of the emitted light, voltage, net charge density and current density have been described extensively (Cobine 1958, von Engel 1965), but, little attempt has been made to explain them.

The glow discharge is normally obtained at low pressure, but it is known that it can be maintained in a similar form at high pressure up to and above 1 atm. The discharge in this pressure range is usually called a high pressure glow discharge. It can be obtained in air (Gambling and Edels 1954), and other gases (Fan 1939).

2.3.1 The Glow Discharge Cathode Region

The glow discharge cathode region is the region stretching from the surface of the cathode to the start of the negative glow with a corresponding cathode fall voltage V_c. If the discharge is operating in the region CD of Fig. 2.2, the negative glow covers only part of the cathode surface and the cathode fall, dark space and current density at the cathode remain constant and independent of the discharge current; this is the normal cathode fall regime. When the negative glow covers the cathode, an increase in the discharge current produces an increase in the cathode fall voltage (region DE in Fig. 2.2) and the current density increases but the thickness of the dark space decreases; this is the region of the abnormal cathode fall.

The magnitude of the cathode fall voltage depends mainly on the type of the gas and the cathode material (Table 2.1), and varies slightly with pressure and the electrode spacing.

cathode:	He	Ne	A	H_2	N_2	air	Hg	*gas/voltage*
Cu	177	220	130	214	203	375	450	CO:484, CO_2:460
Zn	143	..	119	184	216	280	..	O_2:354, CO:480
Hg	143	..	..	337	226	..	340	..
Al	140	120	100	170	180	230	245	Cl_2:280, O_2:310
C	..	..	..	280	..	424	475	CO:525
Mo	109	107	103	..	..	..	..	..
W	..	125	..	..	..	..	305	..
Fe	150	150	165	250	215	270	300	O_2:290, Xe:306, K:80, Cs:340
Ni	160	140	130	271	200	226	275	..
Pt	165	152	130	276	216	277	..	O_2:364, Cl_2:275
K	60	68	64	94	170	180	..	K:80

Table 2.1 Normal cathode fall voltage in volts (von Engel 1965).

In general, the cathode fall voltage is low for alkali cathodes in rare gases and high for ordinary metals in Hg, O_2, and CO_2. A given cathode shows a larger fall voltage in molecular gases than in rare ones.

As the laser excitation process takes place in the positive column, the power in the cathode fall region is wasted and does not contribute to the excitation power of the gas lasers and as a result the axial lasers are normally more efficient than the transverse ones.

2.3.2 The Glow Discharge Positive Column

The positive column is bounded at one end by the Faraday dark space and at the other by the anode. It is so called because it connects the negative zones to the anode. It is the most luminous part of the discharge after the negative glow. The positive column is not really necessary for maintaining a glow discharge, although it can be the largest part of the discharge. The axial voltage gradient is constant and hence the number of positive and negative charges per unit volume or per unit length of column does not vary. The temperature of the positive ions is slightly higher than the gas temperature and the electron temperature can be many times higher. The axial voltage gradient decreases with increasing current at a fixed pressure, and tends to increase with pressure for a fixed current. The current in the positive column is primarily carried by electrons because of the small mobility and drift velocity of ions.

The positive column region is important as it has many applications especially for gas lasers as it is the medium where the laser excitation process takes place.

2.3.3 The Glow Discharge Anode Region

In general, the electric field at the anode attracts electrons from the positive column and repels the positive ions. Consequently, a negative space charge is set up in front of it. The field rises, and an anode fall develops. Because of the increased probability of excitation, the luminosity increases slightly giving rise to the positive glow.

The voltage across the space charge is called the anode fall potential V_a, which occurs over a relatively short distance typically of the order of one mean free path of an electron (Brown 1966). Electrons flowing across

the negative space discharge region must generate the same rate of positive ions to flow into the positive column as flow out of the other end into the Faraday dark space. If this condition is not met, insufficient positive ions are produced at the anode end of the column and the negative space charge region grows so that the anode fall rises, and more ionisation occurs until enough positive ions are generated to rectify the situation.

2.4 THE ARC DISCHARGE

If the discharge current is increased beyond the abnormal glow region (DE in Fig. 2.2) by increasing the input voltage or decreasing the stabilising resistance in Fig. 2.1, the discharge changes into an arc passing through the unstable glow to arc transition region EF. A convenient definition of an arc is given by comparing its cathode region with that of a glow discharge. The cathode of the glow has a fall of potential of about 100 to 400 V and a low current density. Except at high pressure and currents, the positive column often fills the containing vessel. Thermal effects do not contribute to the working of the cathode of a glow discharge, and the light emitted from the region near the cathode has the spectrum of the gas. The arc cathode, however, has a fall of potential of the order of 10V, and a very high current density (10^2 to 10^4 A/mm^2). Thermal effects are essential to its working, and the light emitted has the spectrum of the vapour of the cathode material. The positive column is constricted near the two electrodes.

Fig. 2.4 gives the spatial distribution of the gas temperature, the potential, and the current density in a long arc. Different distribution of potential and current density can be seen in the arc than that in glow especially near the cathode which implies that the mechanism of electron emission from the cathode is

different in the arc than that in glow. The distance between the electrodes may vary from a few microns to several metres.

Arcs may be operated at low pressure (10^{-2} mm Hg) or high pressure (several atmospheres). The difference between high and low pressure arcs is the temperature of the positive column. The temperature in the high pressure column is usually of the order of 5000 to 6000 K, and the ions, electrons and gas atoms are in thermal equilibrium (Fig. 2.5). The gas temperature of low pressure arcs is not more than a few hundred degrees Celsius. The high pressure arc can have a high power density input but a non-uniform radial distribution of the temperature. Only a narrow filament along the axis of the arc column is heated by the current and the thermal energy is transferred to the rest of the gas by convection and conduction. Electric arcs do not normally enable a uniform volume of ionised gas to be obtained.

2.5 THE GLOW TO ARC TRANSITION

When the current in a glow discharge between cold metal electrodes in a gas at a pressure of 0.1 - 1 atm is gradually increased, the voltage across the discharge is seen first to rise (region DE in Fig. 2.2). However, when the current exceeds a critical value, the voltage suddenly drops to about 1/10 or less of its former value and an arc forms. Since there is usually a constant resistance in series with the discharge, the sudden drop in voltage is accompanied by a sudden increase in current. The luminous area at the cathode surface contracts to a small area, the cathode spot. At the same time the gas in the discharge column increases to a very high temperature. This change in behaviour is the glow to arc transition which can be represented by the region EF on the generalised voltage current characteristic of an electric discharge in Fig. 2.2.

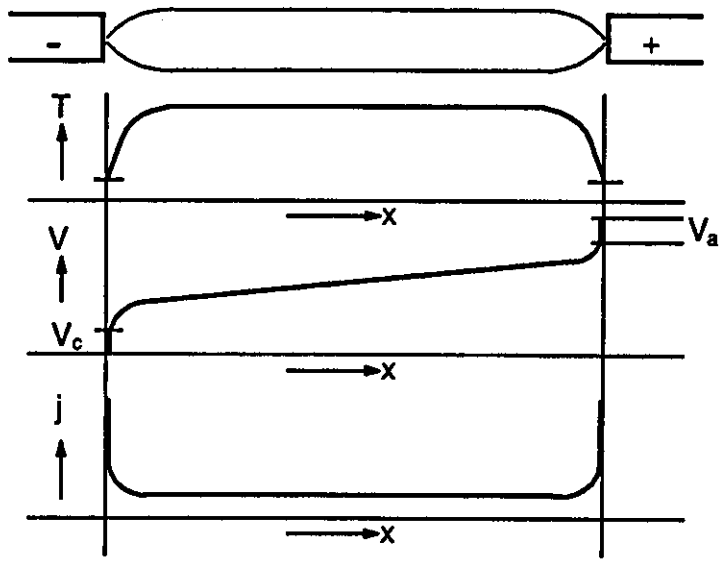

Fig. 2.4 Gas temperature T, potential V, and current density J as a function of position x along the axis of a long arc (von Engel 1965).

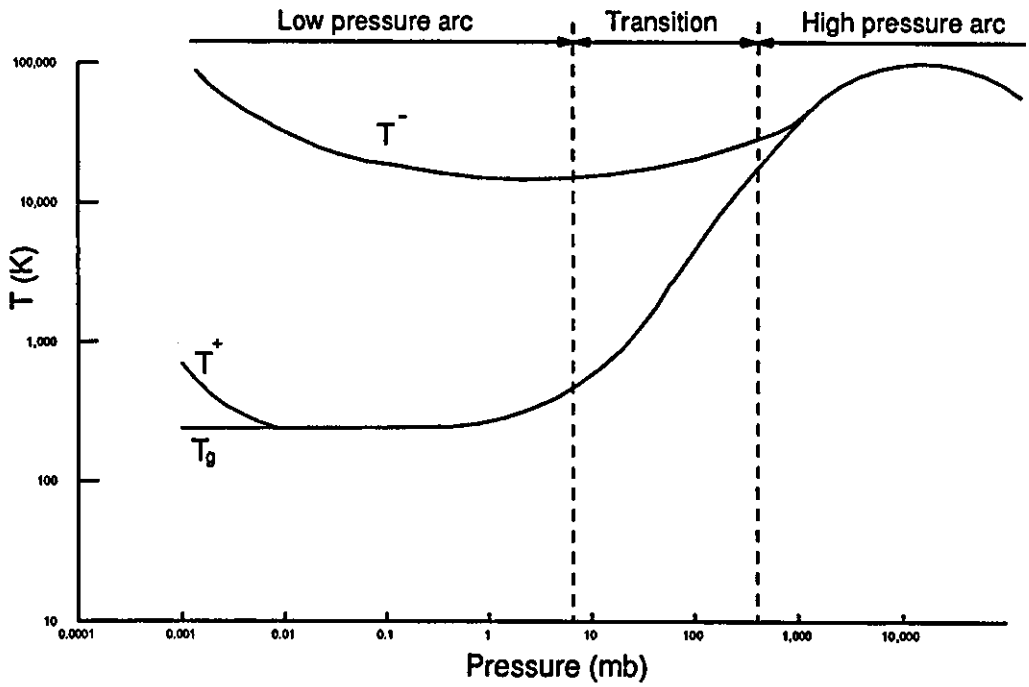

Fig. 2.5 The temperature of the electron, positive ion and gas in the positive column (Hoyaux 1968).

The discharge current at which the glow to arc transition occurs puts an upper limit on the electrical power input to a glow discharge. The arc discharge is unsuitable for exciting the CO_2 laser because of the requirement for the average gas temperature to remain below 270 °C to avoid populating the lower laser levels and destroying the population inversion (Demaria 1973). The electron temperature in the arc discharge also can be much less than 1 eV which is not enough to obtain an efficient energy transfer from the electric discharge to the laser transitions for lasers such as CO_2, CO and N_2 lasers (Nighan 1970).

Mixed forms of glow and arc discharges can be observed. In Hg vapour, small mobile arc spots can be formed on a liquid Hg cathode to which either a diffused glow-like positive column or a constricted arc-like column is attached. Also known are cathodes with glows covering the whole Hg surface with either a diffused or narrow constricted column joined to it. Which of the four different forms develops depends on the discharge current, gas pressure and dimension of the containing vessel (von Engel 1983).

The glow to arc transition associated with the cathode may be divided into thermionic and non-thermionic mechanisms. Cathodes made of refractory materials (such as tungsten or carbon) can reach temperatures high enough for thermionic emission to occur. The increase in current produced by the thermionic emission increases the number of the positive ions hitting the cathode surface which heats the cathode enabling a lower voltage to maintain a given discharge current. Under these conditions the glow to arc transition occurs (Cobine 1958). A detailed review of the thermionic mechanism for the glow to arc transition is given by Meek and Craggs (1953).

The non-thermionic mechanism of glow to arc transition is not directly dependent upon raising the cathode to high temperature to liberate the large number of electrons required. The work of Westberg (1959), Hancox (1960), and Maskrey and Dugdale (1966) suggest that the main mechanism for the glow to arc transition occurring with non-thermionic cathodes (such as copper) is dependent upon the presence of insulating particles on the cathode surface which become charged by positive ion bombardment to a potential high enough to cause breakdown, producing a burst of vapour. Once the vapour is produced, the increased conductivity of the region causes a local increase in current density which further increase the amount of vapour produced and the high current density arc root is established. An extensive review of the non-thermionic glow to arc transition is given by Lutz (1974).

2.6 FAST GAS FLOW ELECTRIC DISCHARGE

The voltage gradient of the positive column which is of the order of 0.1 V/mm under still gas flow conditions with a typical CO_2 laser gas at 40 mb can be increased to approximately 20 V/mm in a flowing gas with all other parameters held constant. This wide variation in the value of electric field strength makes the choice of operating conditions for an electric discharge used to selectively excite laser transitions particularly important if efficient laser excitation is to be achieved. The ratios E/p and E/N are used to identify the optimum conditions for efficient pumping of the laser mediums such as CO_2, CO, N_2 and excimer (Nighan 1970, Greene and Brau 1978). The fast gas flow also cools the discharge convectively which increases the laser output power obtainable per unit length of discharge by several orders of magnitude (Demaria 1973). The gas flow can be axial (McLeary and Gibbs 1973), or transverse (Sato et al 1985) to the

discharge, and the flow velocity can be subsonic (Harry and Evans 1988), or supersonic (Shirahata and Fujisawa 1973).

In the fast gas flow electric discharge, the glow to arc transition may occur in the positive column (also referred to sometimes as column constriction, streamer formation and glow collapse). The discharge becomes unstable and collapses into arc-like filaments or streamers and is accompanied by a substantial drop in the electron energy (below 1 eV) which results in the collapse of the population inversion in the laser and hence the laser output (Wasserstrom et al 1978).

The cause of the streamers appears to be that a non-uniformity in the gas flow or discharge current density leading to uneven heating of the gas (Eckbreth and Owen 1972), which may appear to be similar to a high pressure arc column. Theoretical treatment to predict the growth time of instability for a range of electrical input power densities has been developed by Nighan and Wiegand (1974). Decreasing the gas residence time (< 1 ms) in the discharge cavity so that collapse of the unstable glow does not have time to occur, and controlled introduction of gas with turbulent mixing produced a uniform discharge at a higher power density than before under otherwise similar conditions (Wiegand and Nighan 1975).

2.7 DISCHARGE STABILISATION

The electric discharge, generally, has a negative dynamic resistance, therefore, the discharge is usually stabilised by a resistance (for a d.c. supply) or an impedance (for an a.c. supply) in series with the discharge and the power supply. The minimum condition for

maintaining a stable electric discharge is defined by the Kaufmann criterion (Kaufmann 1900), which may be expressed mathematically as;

$$\frac{dV}{dI} + \frac{dV_s}{dI_s} \geq 0 \qquad 2.1$$

where $\frac{dV}{dI}$ is the dynamic resistance of the discharge and $\frac{dV_s}{dI_s}$ is the stabilising impedance.

The stabilising resistance is represented by the load line on the generalised voltage current characteristic of the discharge in Fig. 2.6. When the supply voltage is V_{i1}, the load line cuts the discharge characteristic at the points A, B, C and D. From equation 2.1, the points A and C are unstable while the points B and D are stable. The stable operating point depends on the method of starting the discharge. If it is started by short circuiting the electrodes, an arc discharge will be obtained at point D. If the discharge is started by decreasing the stabilising resistance R slowly, the glow discharge will be maintained at B. Increasing the supply voltage to V_{i2} while keeping the stabilising resistance R fixed, the operating points are obtained at F or H.

Varying the value of the stabilising resistance R results in changing the load line slope. Low current glow or arc discharge operating points such as A or C, respectively, can be obtained by increasing the stabilising resistance and the supply voltage. The complete discharge voltage current characteristic, therefore, may be investigated by varying the supply voltage and the stabilising resistance.

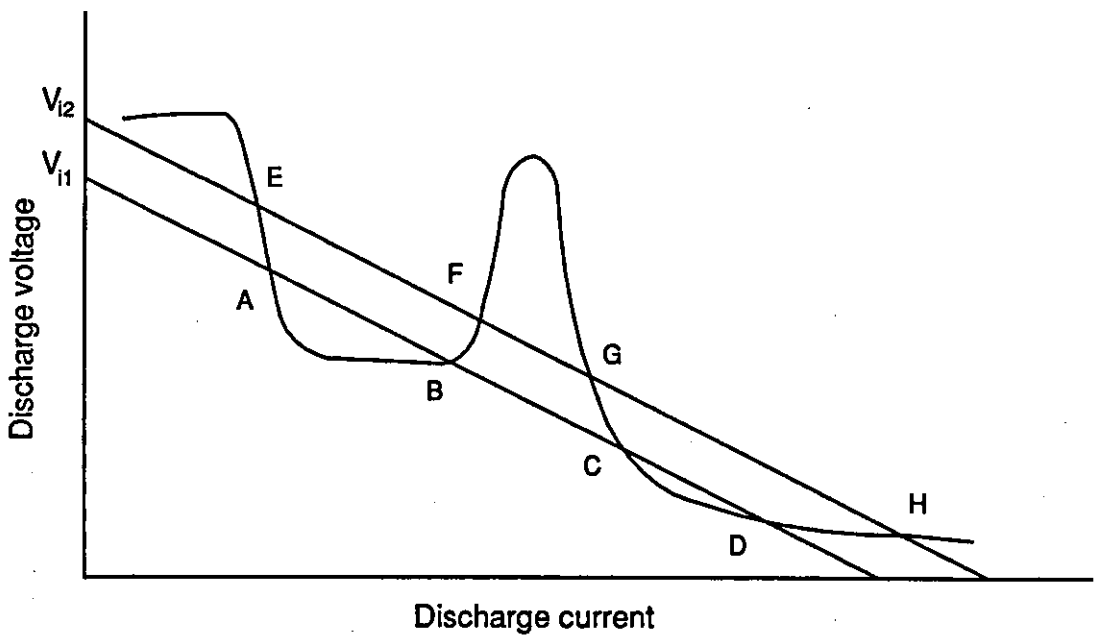

Fig. 2.6 The generalised voltage-current characteristic curve and the load line.

2.8 MULTIPLE DISCHARGES

Multiple discharges may be defined as a number of individual discharges which are operated in close proximity to each other so that they interact electromagetically. The discharges may be separate or coalesced and the direction of currents can be parallel so that they attract each other or anti-parallel so that they repel, or a combination of parallel and anti-parallel (Harry and Knight 1986).

Multiple discharges can be obtained using separate power supplies or transformers with separate secondary windings with individual stabilising resistances for each discharge (Fig. 2.7). More than one discharge cannot be normally operated from a common power supply due to the common stability resistance and the negative dynamic resistance of the discharge where one discharge will exist and the other will extinguish. More than one separate discharge can, however, be maintained (Fig. 2.8), if separate resistances are used to stabilise each discharge (Harry and Knight 1981).

Quasi-multiple discharges incorporating either multiple cathodes coupled to a single anode or multiple anodes coupled to a single cathode have been reported for transverse CO_2 lasers (Hill 1971, Eckbreth and Davies 1972, Lancashire et al 1977).

Multiple arc discharges have been used to obtain a large volume of ionised gas for applications including metal melting and reduction of ores (Harry and Knight 1983, Harry 1983). Multiple glow discharges have been used for the excitation of fast flow CO_2 lasers (Saleh 1981, Harry and Saleh 1982, Evans 1987).

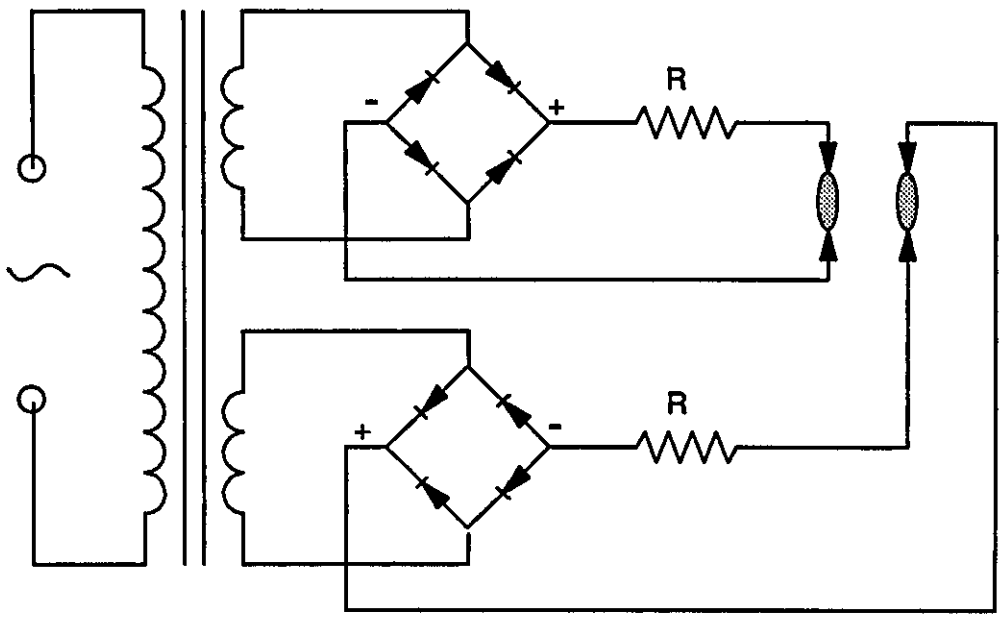

Fig. 2.7 Multiple discharge using two separate secondary windings with individual stabilising resisters.

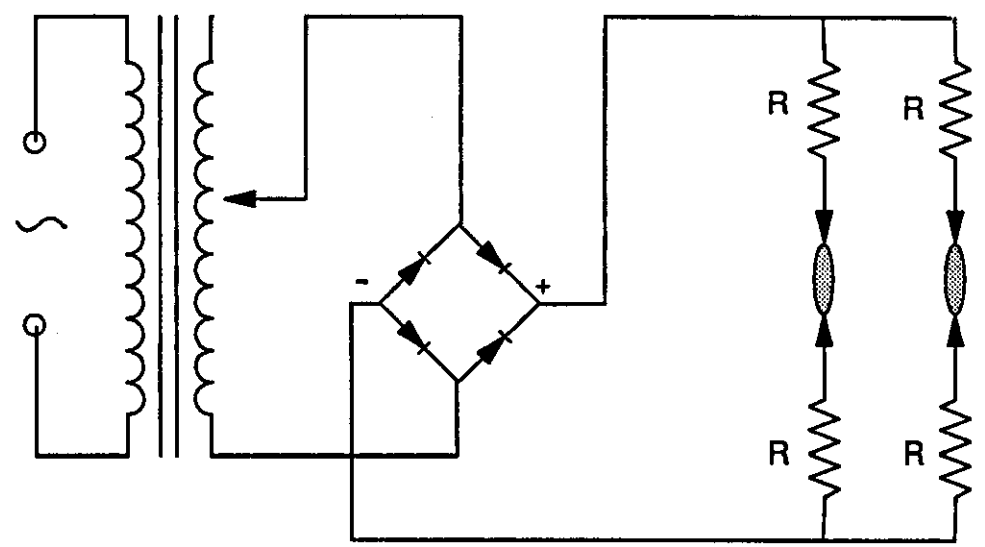

Fig. 2.8 Multiple discharge using single power supply with separate stabilising resistors.

2.9 THE ELECTRIC DISCHARGE FOR THE EXCITATION OF GAS LASERS

Gas lasers are the most versatile class of lasers; within this classification fall the shortest wavelength laser (116 nm), the longest wavelength laser (10.6 μm), the highest efficiency laser(> 30%), and the most powerful CW laser(> 400 kW). Gas lasers can be excited by a wide variety of techniques that include the use of optical systems, electrical discharges, electron beams, chemical-flow combinations and thermo-gasdynamic expansion. The mechanisms for creating population inversion in gas lasers include electron excitation or ionisation, molecular dissociation, chemical reactions, the formation of excited-state complexes, Penning ionisation, and resonant energy transfer. Some representative examples of gas lasers are listed in Table 2.2 showing their pumping techniques and the excitation process.

The different laser excitation processes are determined by the electron energy in the discharge column to achieve ionisation or excitation of the atoms or molecules in the laser gases. For efficient excitation of the molecular gas mixture, the excitation cross section requiresan average electron energy determined by the ratio E/N (electric field per neutral particle density), of the discharge column (Nighan 1970, Greene and Brau 1978).

lasers	lasers type	mode	method of excitation	pumping process
He-Ne	neutral atom	CW	elec. disc.	excitation
Ar, Kr, Xe	ion gas	CW, pulse	=	ionisation
Sn, Zn, Pb	metal vapour	CW	=	=
CO_2, CO	molecular	CW, pulse	elec. disc. or thermo-gasdynamic expansion.	excitation
N_2	=	pulse	elec. disc.	=
excimer	=	=	elec. disc. or e-beam	excited-state complexes
HF, HCl	=	CW, pulse	chem.-flow combination	chemical reaction
HgBr	=	pulse	elec. disc. or photo-dissociation	molecular dissociation

Table 2.2 Some known gas lasers (Svelto 1982, Measures 1984).

Analytical studies (Nighan and Bennet 1969, Nighan 1969, 1970) have provided the percentage of the fractional power transferred from the electrons to N_2, CO, and CO_2 molecules as a function of E/N and average electron energy. Fig. 2.9 presents the energy level diagram of lower vibrational levels of CO_2 and N_2 molecules. Fig. 2.10 presents the fractional power transferred from the electrons to N_2 and CO_2 molecules in a gas mixture of CO_2:N_2:He = 0.1:0.1:0.8 by mass. For an E/N value of approximately 10^{-14} V.mm^2, 65% of the electron energy goes directly into the CO_2 (001) upper level and effectively

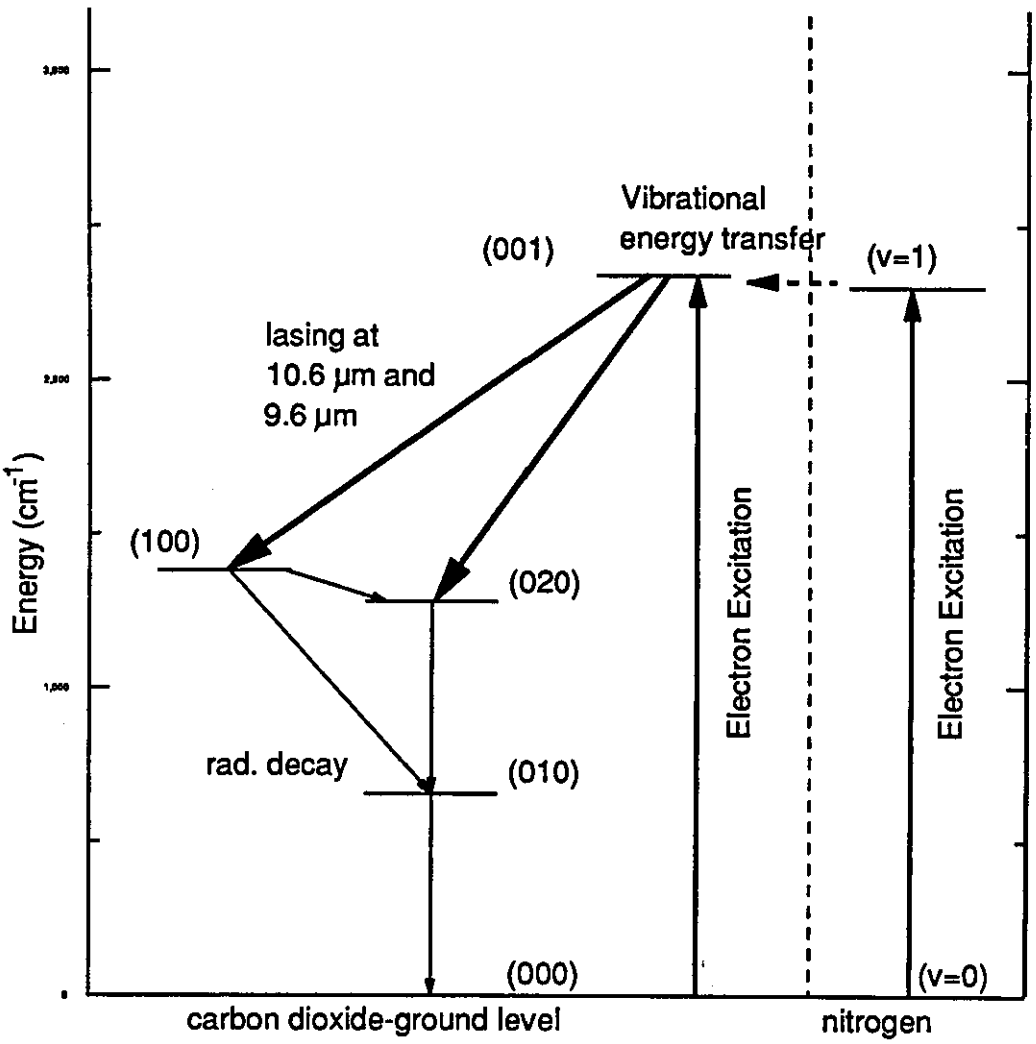

Fig. 2.9 Simplified energy level diagram for CO_2 and N_2 molecules.

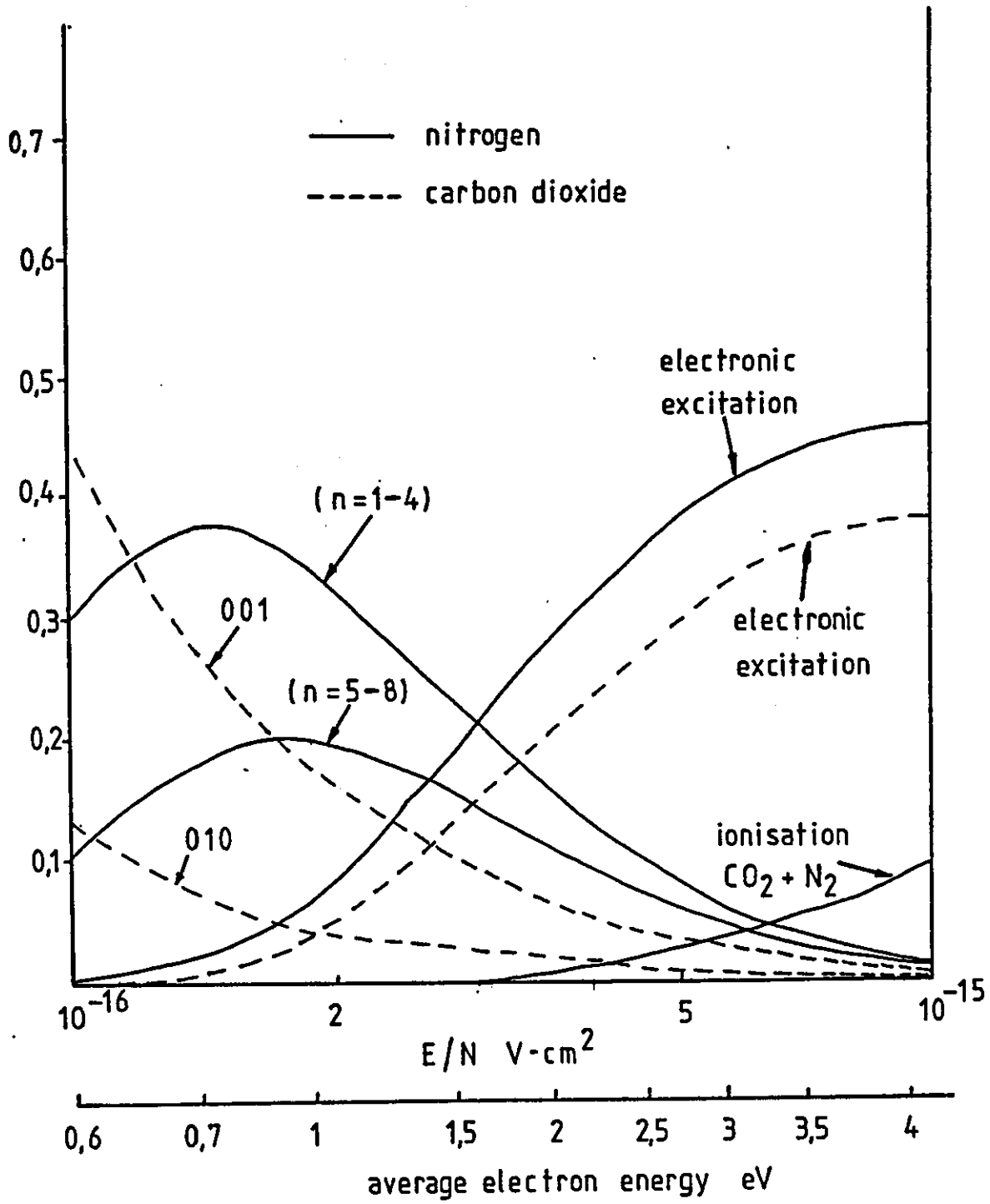

Fig. 2.10 Fractional electron power transfer to CO_2 and N_2 in a (10% CO_2: 10% N_2: 80% He) gas mixture (Nighan and Bennet 1969).

all the energy goes into vibrational excitation of either CO_2 or N_2. For an E/N value of about 10^{-13} V.mm^2, more than 80% of the electron energy goes into electronic excitation of CO_2 and N_2. Although the electronic excitation is considered as electron energy loss process, it is a necessary part of sustaining ionisation in the electric discharge.

The employment of the high mass flow rate of the laser gases through the optical cavity to cool the laser medium convectively and to control the ratio E/N by controlling the electric field of the discharge column has led to a substantial increase in the output power capability of CO_2 electric discharge lasers (Demaria 1973). Apart from the requirement to cool the laser gas below 200 K, CO lasers operate with a configuration similar to that of CO_2 devices (Sato et al 1982).

2.10 SUMMARY

The two types of the self-sustained electric discharge, the glow and arc discharges, as well as the characteristics and properties of the different regions have been described. The conditions for stable operation of glow and arc discharges have been defined. The properties of the electric discharge in a fast gas flow as well as the multiple discharge have been explained. The use of electric discharge for the excitation of gas lasers has been presented.

CHAPTER 3

REVIEW OF PUBLISHED WORK ON THE EXCITATION OF GAS LASERS

3.1 INTRODUCTION

The production of a uniform non contracted electric discharge of chosen E/N over a wide range of pressure is of great interest for its use in high power CW CO and CO_2 gas lasers and chemical synthesis. An effective method of producing a uniform discharge is to operate the electric discharge in a flowing gas. The use of gas flow with the electric discharge can help in controlling the ratio E/N, and therefore, the electron energy for selected transition necessary for the laser action to take place (Nighan 1970), or efficient chemical reactions to take place (Boenig 1988), and to dispose of the waste heat, which could destroy the laser action (Cheo 1967, Hill 1970), or some of the products of chemical synthesis (Suhr 1973), by convecting it out of the discharge.

To maintain the electron temperature to around 1 eV, it is necessary to maintain a stable glow discharge. However, when the gas pressure or the discharge current are increased, the glow discharge becomes unstable and collapses into arc-like filaments or streamers (Wiegand and Nighan 1975). This instability of the glow discharge is accomplished by a substantial drop in the electron energy well below the required 1 eV, which results in the annihilation of the lasing or chemical processes.

The report of CW laser action in a CO_2 gas electric discharge was made by Patel (1964 a,b). These early reports gave detailed characteristics of both the CW and pulsed power spectra of the CO_2 laser. The possibility of a laser that uses the vibrational-rotational transitions of the ground electronic state of CO was initially proposed by Legay and Legay-Sommaire (1964). Pulsed laser action on these transitions was subsequently observed by Patel and Kerl (1964) in the same year at about the same time that laser action in CO_2 first was reported.

An important advance for the CO_2 laser was the use of a mixture of nitrogen and CO_2 as the active medium. The use of N_2 for obtaining higher power output and efficiency from a CO_2 laser was discovered almost simultaneously by Legay and Legay-Sommaire (1964) and Patel (1964c). The increase in average power by the addition of N_2 is caused by the N_2 - CO_2 vibrational energy transfer (Fig. 2.9). Similar results were obtained by adding N_2 to the CO laser gas (Patel 1965).

Another important advance for the CO_2 laser was the discovery that increased power output and efficiency could be obtained if He was added to the gas mixture (Moeller and Rigden 1965, Patel et al 1965). The best operation was found to be a mixture of CO_2, He, and N_2. Adding He to the CO laser gas mixture enabled a CO laser with an output power and efficiency comparable to that of CO_2 to be obtained (Osgood and Eppers 1968, Osgood et al 1970, Eppers et al 1970). This was accomplished by direct excitation of CO: N_2: He or CO: air :He mixtures and a liquid nitrogen cooled tube after the suggestion made by Patel (1966) that the gain in the CO laser could be considerably enhanced by operating at low temperature.

It is believed that the role of He is to cool the gas by aiding in the depopulation of a lower vibrational energy level, which serves as a blockage for the transfer of molecules down to the ground state, without significantly interfering with the upper laser level. In addition, He also plays an equal important role in maintaining the energy distribution of electrons within the discharge in the proper range for more efficient excitation of the molecules.

3.2 TYPES OF HIGH POWER CW CO AND CO_2 LASERS

The CW gas lasers can be divided into two main groups with respect to the configuration of the electric discharge: the longitudinal or axial electric discharge lasers and the transverse electric discharge lasers. In the longitudinal or axial discharge lasers the optical axis is along the discharge, while in the transverse discharge lasers the optical axis is transverse to the discharge. The longitudinal or axial lasers can be divided into three groups with respect to the gas flow: the sealed-off tube gas lasers, slow gas flow and the fast gas flow lasers.

In the sealed tube axial discharge laser the waste heat generated in the electric discharge is removed by diffusion to the discharge tube wall which can be cooled by a flowing fluid jacket. The slow gas flow laser is similar to the sealed tube laser but the gas flows axially with low flow rate (typically 60 - 70 l/s, Patel et al 1965), to remove the gas dissociation products generated within the discharge. In the fast gas flow laser the waste heat is removed mainly by convecting it out of the discharge region with the fast gas flowing with subsonic velocity (Harry and Evans 1988), or supersonic velocity (Wasserstrom et al 1978). A schematic diagram of each of the three types of axial electric discharge lasers is shown in Fig. 3.1.

The transverse discharge lasers can be divided into two groups with respect to the gas flow: the transverse-flow and discharge lasers, and the transverse-flow cross-discharge lasers. In the transverse-flow and discharge laser, the gas flow is axial with the discharge while the optical axis is perpendicular to them. In the transverse-flow cross-discharge laser the gas flow is perpendicular to the discharge and both are perpendicular to the optical axis. A schematic diagram for each of the two types is given in Fig. 3.2.

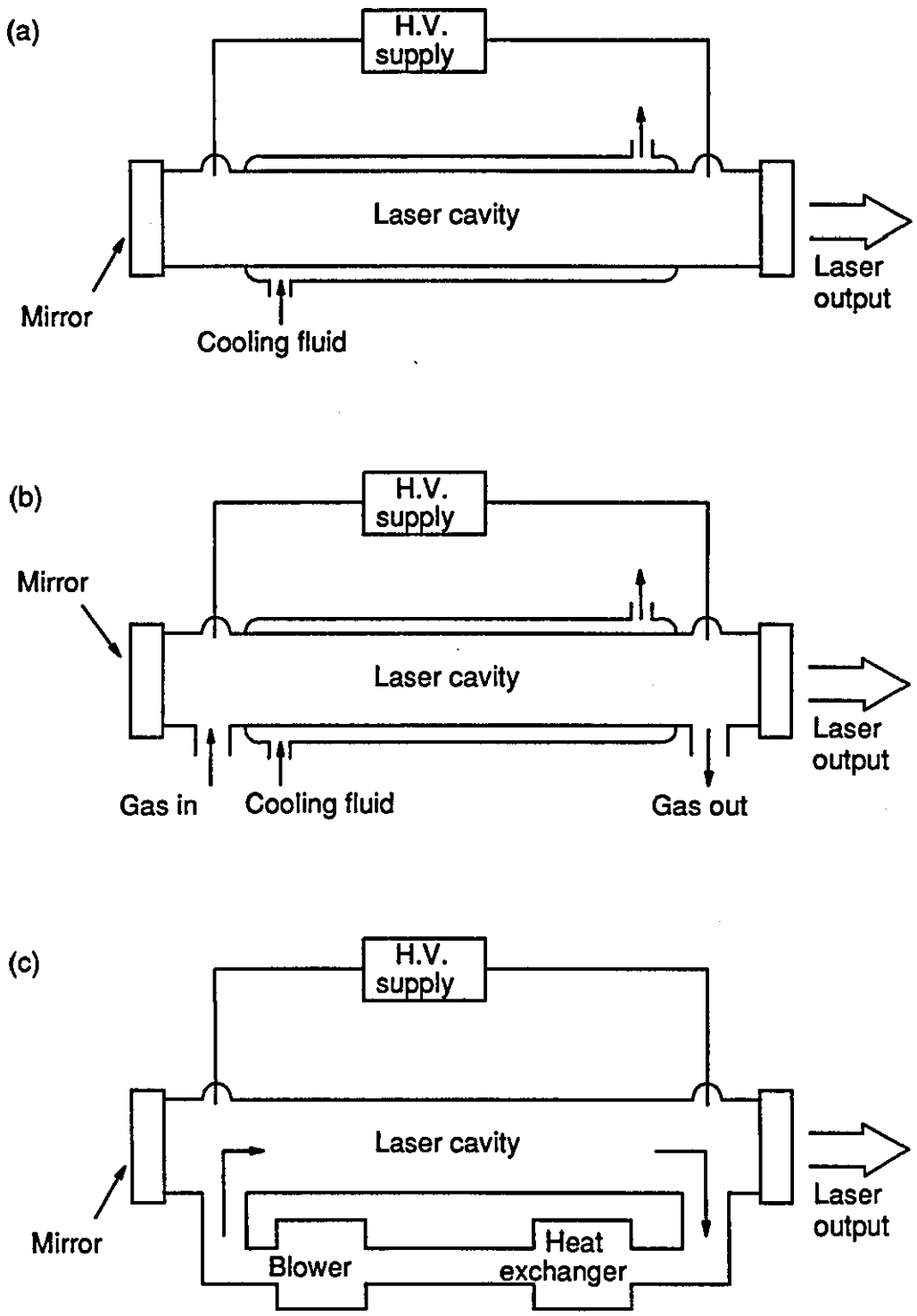

Fig. 3.1 The three different types of axial discharge laser.

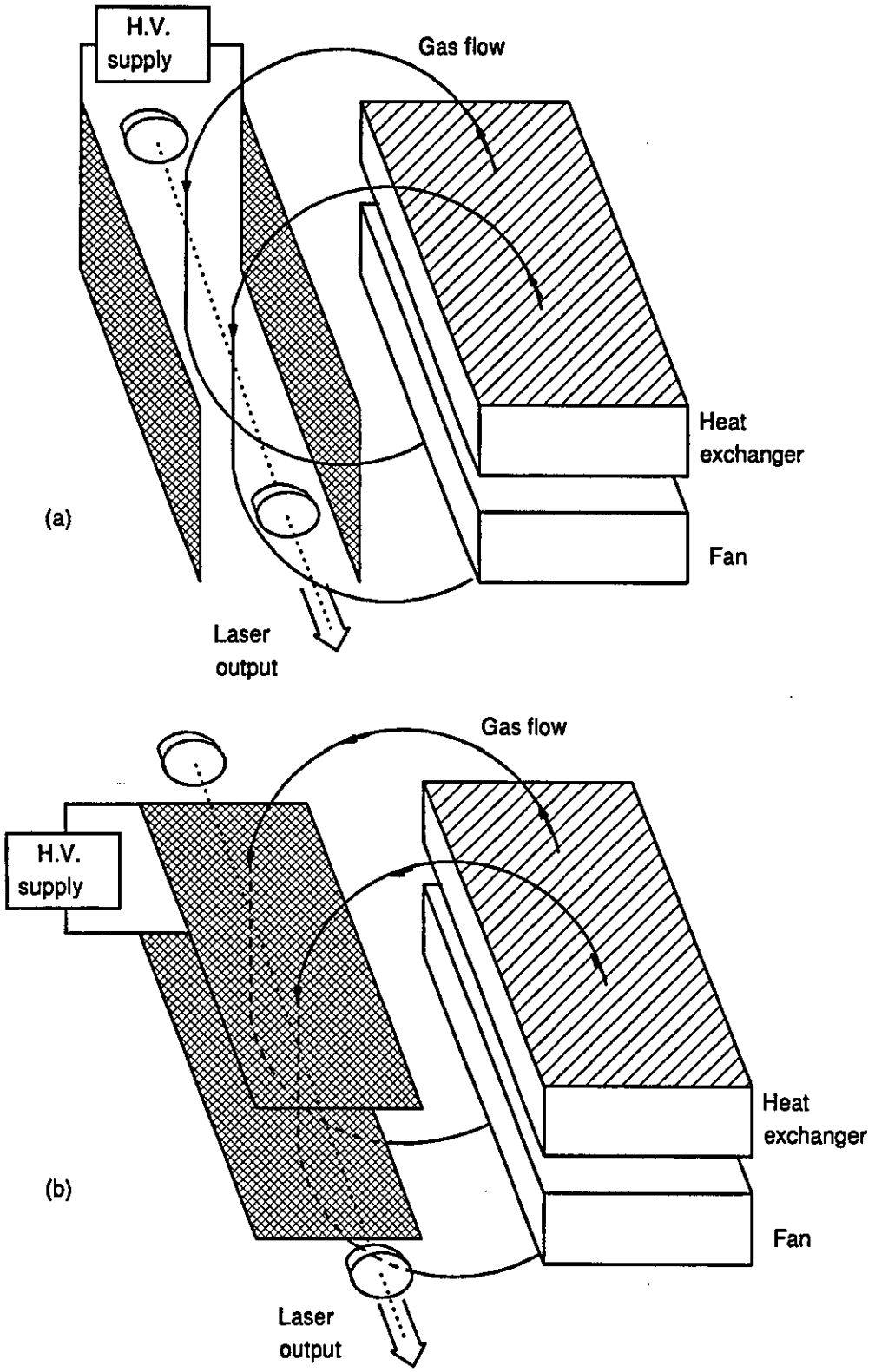

Fig. 3.2 The two different types of the transverse discharge laser.

The design of the CO laser is similar to that of the CO_2 laser except for the operating temperature which should be below 200 K (Sato et al 1982).

3.3 THE SLOW AXIAL GAS FLOW LASER

The slow flow laser, like the sealed tube laser, relies upon diffusion of the waste heat generated in the electric discharge to the water or oil cooled discharge tube. The temperature of the gas must remain below about 500 K in the CO_2 laser and below 200 K in the CO laser, to maintain a high conversion efficiency. The rate of heat transfer from the gas to the discharge tube wall limits the maximum laser power obtainable from this configuration.

In the sealed tube CO_2 laser, dissociation products are formed during the discharge as follows;

$$2CO_2 \longrightarrow 2CO + O_2$$

Catalytic regeneration of the carbon dioxide from the dissociation products is increased by adding H_2O vapour to the CO_2, He and N_2 gas mixture (Witteman 1967), which promotes the recombination reaction,

$$H_2O \longrightarrow OH + H$$
$$CO^* + OH \longrightarrow CO_2^* + H$$

Alternatively, a low ionisation potential gas, such as xenon, can be used, which reduces the number of CO_2, O_2 and CO ions in the discharge (Clark and Wada 1968).

In the slow flow axial laser, the gas is passed through the discharge cavity to remove the dissociation products before a large concentration builds up and reduces the gain of the active medium (Smith 1968, Tunnen et al 1974). An increase in the tube diameter increases the tendency

of the gas to overheat at the centre of the tube because of the longer diffusion path to the cooled surface of the discharge tube, thus no increase in laser power per unit length of discharge is achieved. An increase in the gas pressure increases the density and heat capacity of the medium which would result in an improvement in the heat transfer mechanism, but, increasing the pressure will result in decreasing the uniformity and the diameter of the glow discharge due to the increased discharge power density and the waste heat generated within the discharge which will reduce the gain of the laser cavity.

The laser power from a slow flow CO_2 laser device is limited to 100 W/m (Demaria 1973). Discharge tubes can be placed optically in series so that the total length of the discharge is increased and higher laser output can be obtained. A laser using two sections was reported by Roberts et al (1967), with a total discharge length of 8.2 m and laser output power of 820 W corresponding to 100 W/m length of discharge at an electrical to optical efficiency of 22%.

3.4 THE CONVECTIVE COOLING OF ELECTRIC DISCHARGE

Waste heat can be removed by convection rather than by diffusion by using fast gas flow through the discharge tube. If the gas is moved at a speed U in a flowing gas system, the ratio of laser power achieved with a diffusion-cooled (P_{Ld}), and with a convective-cooled (P_{Lc}) laser is simply proportional to the ratio of the characteristic cooling times (Demaria 1973);

$$\frac{P_{Ld}}{P_{Lc}} \propto \frac{\lambda u_t}{dU} \qquad 3.1$$

where P_{Ld} = power of diffusion cooled laser
P_{Lc} = power of convective cooled laser

λ = mean free path of the laser molecules in the gas mixture

u_t = thermal molecular speed

d = discharge diameter

U = gas velocity

Since 3.1 is much smaller than unity, for even relatively slow gas flow velocities, the advantages of convective cooling over diffusion cooling are readily apparent.

If the gas flows through a cross sectional area A of a rectangular laser cavity of thickness x (Fig. 3.3), and, assuming that an electric discharge power P_E is loaded to this volume and the laser extraction efficiency is η, then the laser output power P_L is given by;

$$P_L = \eta P_E \qquad 3.2$$

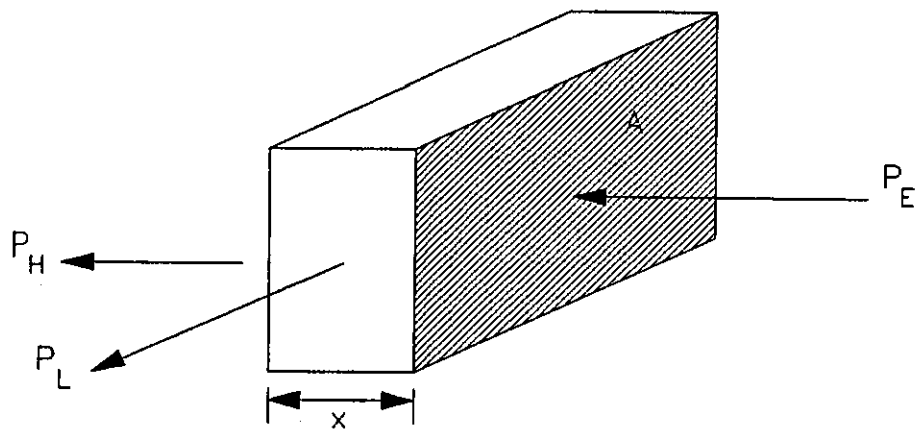

Fig. 3.3 Schematic of a volume of gas of length x and area A.

and the waste heat power P_H is;

$$P_H = (1-\eta)P_E = \left(\frac{1-\eta}{\eta}\right)P_L \qquad 3.3$$

where,

$$P_H = \rho c_p U \frac{\Delta T}{\Delta x} v \qquad 3.4$$

where ρ = gas density
c_p = specific heat of the gas
U = the velocity of the flow
v = the volume

substituting equation. 3.4 in equation. 3.3, we obtain;

$$P_L = \rho c_p U \Delta T A \left(\frac{\eta}{1-\eta} \right) \qquad 3.5$$

Equation. 3.5 shows that the output power density per unit volume can be increased without any increase in the gas pressure and temperature but by increasing the gas mass flow rate. The overall output power per unit length can be scaled with the mass flow rate in gas transport convection lasers enabling multi-kilowatt laser performance from relatively compact lasers (Deutsch et al 1969, Tiffany et al 1969, Targ and Tiffany 1969).

3.5 THE GAS FLOW TURBULENCE

Experimental studies (Eckbreth and Davies 1972, Wiegand and Nighan 1975) have shown that increasing the discharge input power by increasing the mass flow rate cannot continue indefinitely since it is limited by the formation of arc-like filaments or streamers within the discharge and the subsequent collapse of the discharge voltage. However, by controlling the gas flow field, the velocity profile and flow turbulence within the discharge, the uniform glow discharge column can maintained up to higher currents without constriction which limits the discharge input power (Eckbreth and Owen 1972).

A theoretical analysis (Nighan and Wiegand 1974) of the stability of high power CO_2 laser discharges showed that the growth time of arc instabilities in the glow discharge was of the order of 1 ms over a wide range of pressure (27-270 mb). From this analysis, it was concluded that an important role of the gas flow is not only to remove heat from the discharge but also to remove the plasma instabilities from the discharge region in a time less than that required for the collapse of the glow discharge to occur. A series of tests were conducted by Wiegand and Nighan (1975) to determine the dependence of the power density at which the collapse of the glow occurred on the gas residence time in the discharge.

The stability and uniformity of the discharge is found to be further enhanced if additional turbulence is introduced near the upstream electrode (Hill 1971, Wiegand and Nighan 1975). The oblique shock waves created in the supersonic gas flow passing through a Laval nozzle which is placed between the anode and the cathode were found to be effective in the generation of a large homogeneous discharge volume and delaying the glow collapse (Hill 1971, Shirahata and Fujisawa 1973, Wasserstrom et al 1978).

3.6 THE FAST AXIAL GAS FLOW LASER

Deutsch et al (1969) described a CO_2 laser using a fast axial gas flow discharge in a short discharge tube of 100 mm long with an inside diameter of 13.5 mm. A schematic diagram of the system is given in Fig. 3.4. The system was capable of producing an output power per unit length of 1.4 kW/m at a gas pressure of 90 mb. A laser power of 140 W was obtained at an efficiency of up to 11.7% and a discharge current of 150 mA.

A 20 W compact fast axial gas flow CO_2 laser was reported by Tyte (1970) with a discharge length of 100 mm and tube diameter of 7 mm (Fig. 3.5). The optimum gas pressure in the laser tube was 120 mb giving a laser output power per unit length of 200 W/m at a discharge current of 40 mA.

A CO_2 laser using a fast axial gas flow discharge was developed by the Welding Institute, later manufactured by Control Laser UK (Fig. 3.6). The laser was capable of delivering an output power of 2 kW using four discharge tubes 750 mm long and 34 mm inside diameter. The maximum discharge current per tube was 150 mA limited by the onset of streamers and the maximum tube output per unit length was 667 W/m. The stabilisation of the discharge is achieved by rapidly expanding the recirculating gas through a nozzle which creates an axially symmetric turbulence flow field in the discharge region (Fig. 3.7a). Only one tungsten anode rod is used per discharge tube resulting in poor utilisation of the laser cavity in the anode region. The anode configuration was subsequently developed by Control Laser UK where better utilisation of the gas flow was obtained in diffusing the discharge in the anode region (Fig. 3.7b), which resulted in increasing the output power up to 3.5 kW.

A high power compact fast axial gas flow CO_2 laser has been developed at Loughborough University using multiple discharge and gas injection at the upstream anodes (Evans 1987). An output laser power of up to 5 kW was obtained from an active cavity of 630 mm long and 93 mm wide at a relatively high efficiency of about 23 percent. The gas injection at the anodes with a mass flow rate of up to 0.031 kg/s combined with the multiple discharge has enabled a diffused discharge at a discharge current of up to 1.8 to be obtained.

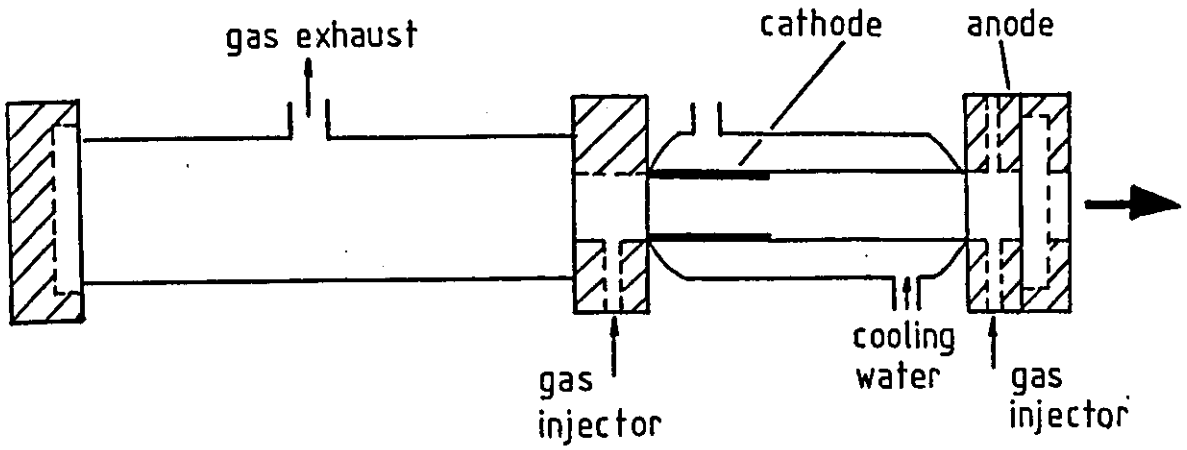

Fig. 3.4 Fast axial flow laser (Deutsch 1969).

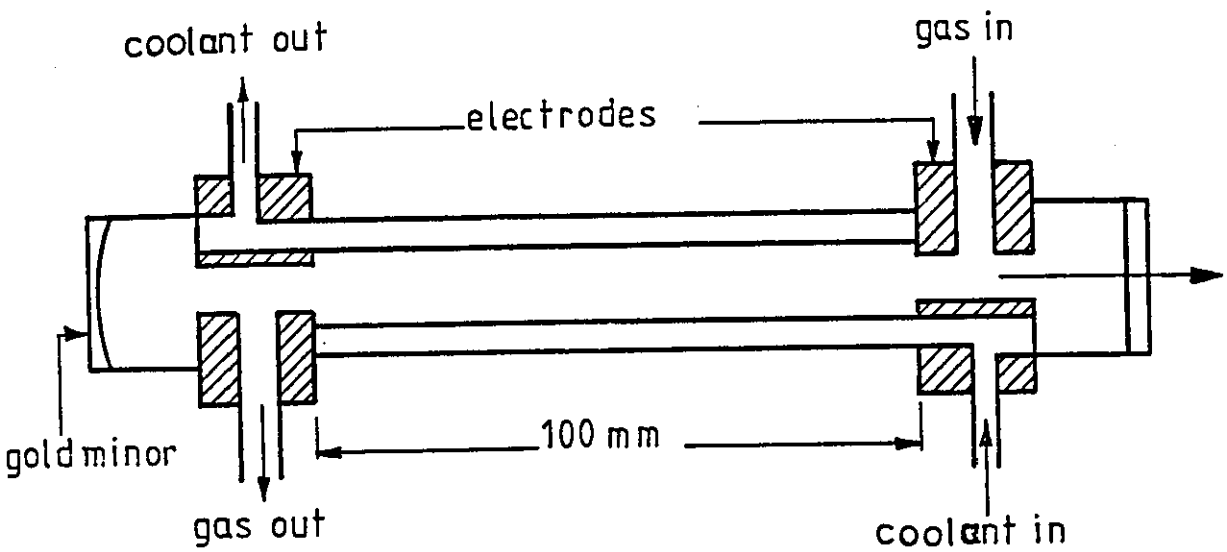

Fig. 3.5 Compact small bore fast axial flow laser (Tyte 1970).

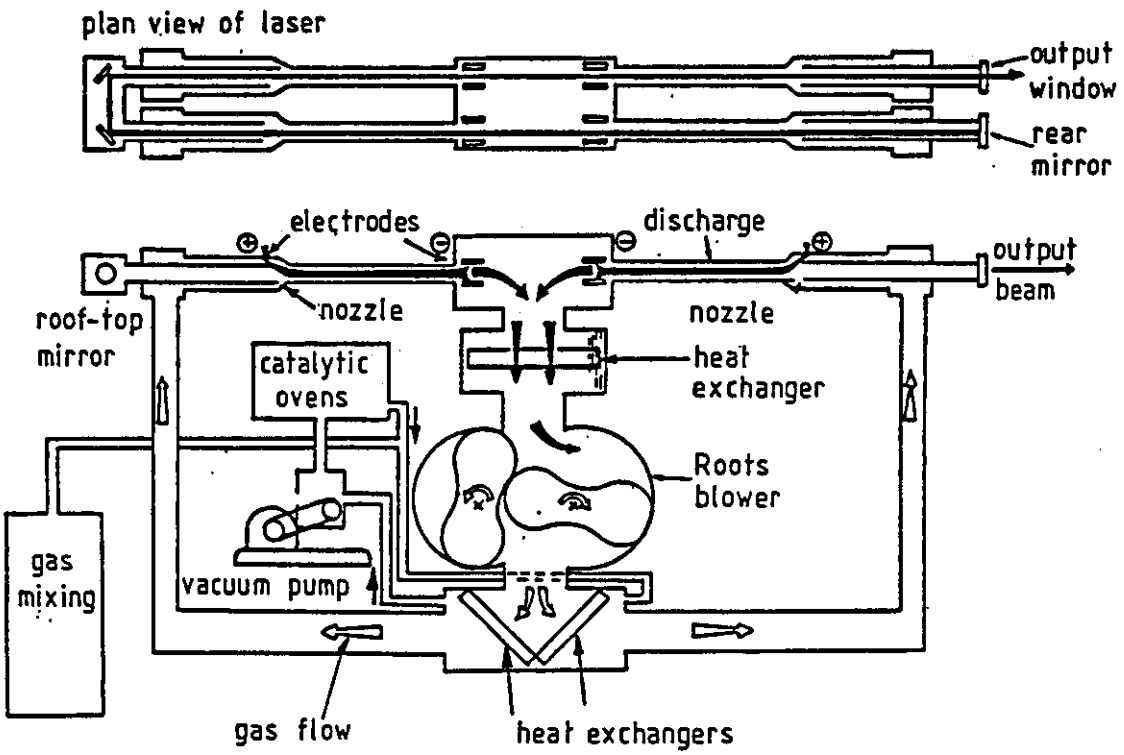

Fig. 3.6 The Control 2 kW fast axial flow laser.

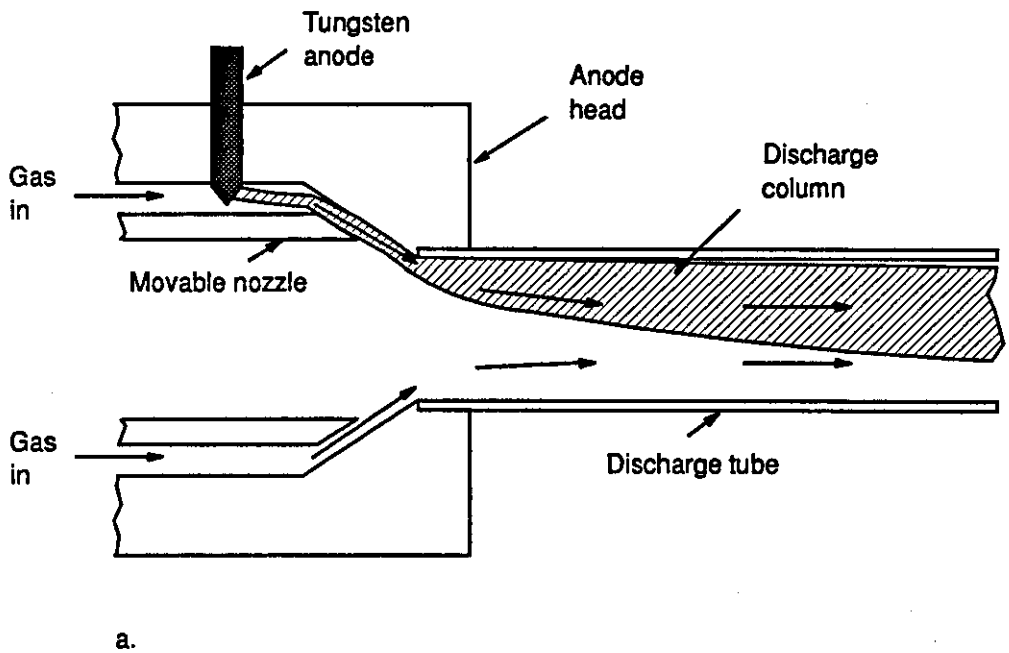

a.

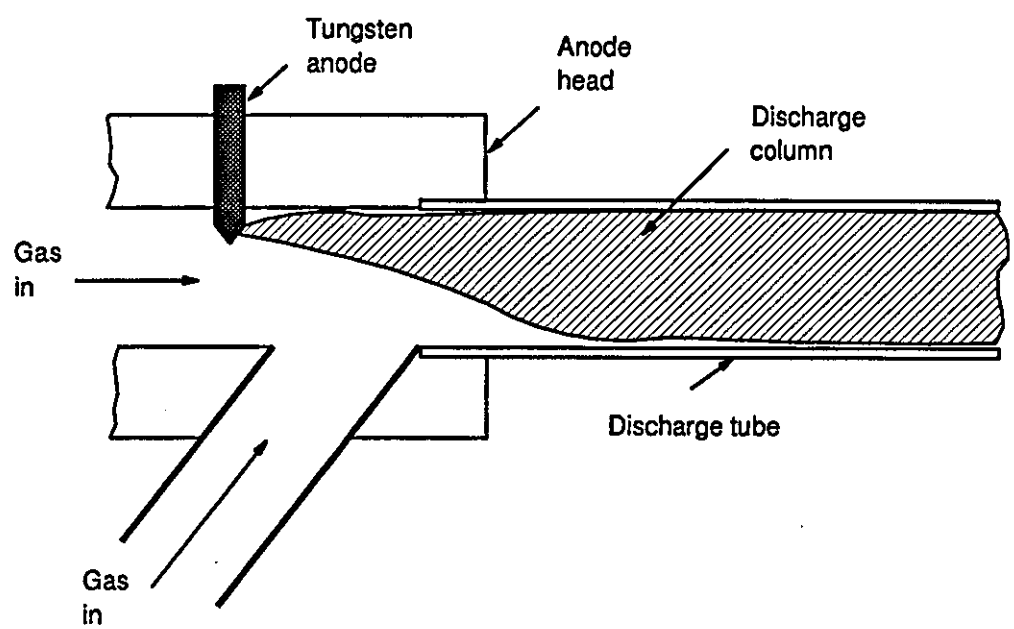

b.

Fig. 3.7 The flow conditioning nozzle used in the Control laser.

a. The original nozzle.

b. The developed nozzle.

3.7 ATMOSPHERIC PRESSURE FAST AXIAL GAS FLOW ELECTRIC DISCHARGE

The production of a uniform non contracted electric discharge at higher pressures than those used at present (>150 mb) is of great interest since it could result in several advantages, such as higher power density and the use of smaller gas transport pumps. Nevertheless, little work has been reported on atmospheric pressure d.c. discharges because of their tendency to contract into a narrow arc-like channel as the discharge input power is increased.

Chebotaev (1973) reported a non contracted axial discharge excited in subsonic and supersonic gas flows at pressures of 1-2 b in a discharge tube of 40 mm diameter and 200 mm long (Fig. 3.8). The discharge was in helium with various different additives such as CO_2, N_2 and air, at a discharge current of several tens of milliamps.

The first CW CO_2 laser at atmospheric pressure was reported by McLeary and Gibbs (1973) using a fast axial gas flow discharge. Two discharge tubes of 200 mm long each and inside diameter of 19 mm were used in series. Common anode was used in the middle and two cathodes at the two ends. The gas was radially fed at sonic velocity near the upstream common anode (Fig. 3.9). The flow conditioning near the upstream anode enabled a uniform discharge to be sustained in the two discharge tubes. An output laser power in excess of 500 W was obtained using three pairs of discharge tubes at an efficiency of 4.5 percent.

3.8 THE TRANSVERSE DISCHARGE LASER

The transverse discharge lasers are divided into two groups; the transverse- flow and discharge lasers, and the transverse-flow cross-discharge lasers. The electric

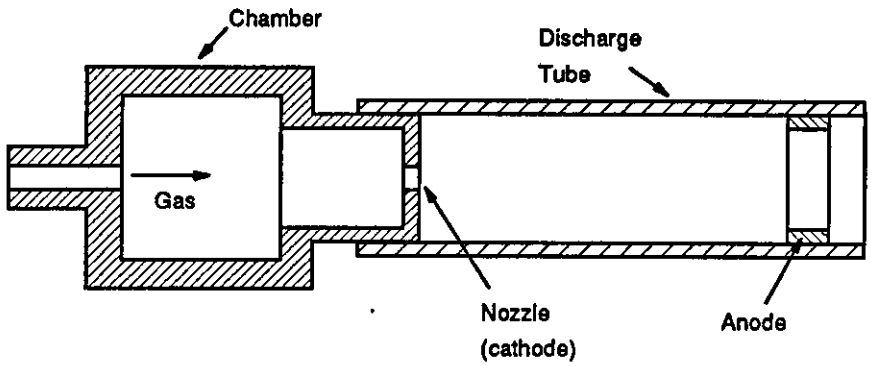

Fig. 3.8 Atmospheric pressure discharge tube (Chebotaev 1973).

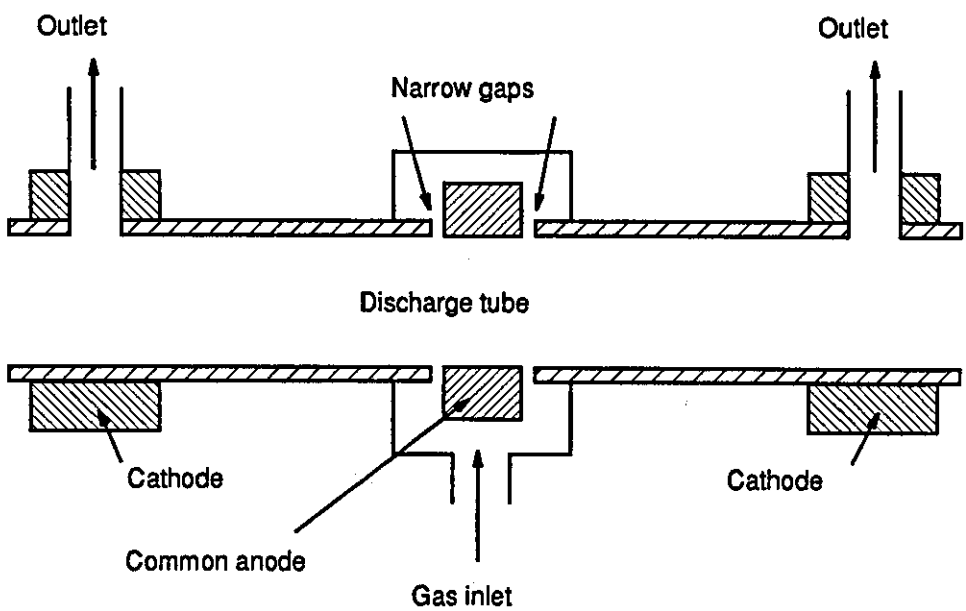

Fig. 3.9 A CW atmospheric pressure fast axial flow laser (McLeary and Gibbs 1973).

discharge in the transverse discharge laser is perpendicular to the optical axis. Its discharge voltage (~3 kV) is low compared with the discharge voltage of the axial discharge laser (~15 kV) due to the small electrode separation (typically 30-50 mm), and the total current (up to 20 A) is higher than the axial discharge current. The low discharge voltage reduces the maximum electrical to optical efficiency because the fall voltage (which does not contribute to laser action) represents a higher proportion of the total discharge voltage.

3.8.1 The Transverse-Flow and Discharge Laser

In the transverse-flow and discharge laser configuration, the gas flow and discharge current are collinear and perpendicular to the optical axis. The interaction between the gas flow and the discharge column, therefore should be the same as in the axial flow discharge except that the gas has shorter dwell time in the discharge column.

Hill (1971) reported the application of fast transverse flow using aerodynamic flow conditioning techniques to produce a large volume uniform glow discharge over a wide range of gas pressure (40-200 mb and up to 1 b). The CO_2 laser amplifier (Fig. 3.10) incorporated a number of individually stabilised multi-pin anodes positioned immediately downstream of an array of rods used to shed vortices around each of the anodes. The vortices caused rapid diffusion of the plasma, thus minimising the thermal gradients. A nozzle array placed downstream of the anodes further enhanced mixing by driving the flow supersonic, then shocking it back to subsonic. The nozzles are non-conducting so that the individual discharges are electrically isolated during mixing. The individual anodes were electrically stabilised by 20 k ohm resistors and operated up to a maximum current of 133 mA per anode. The cathode (located

1 m downstream), was a common wire array aligned with the flow. A maximum electrical power of 100 kW was coupled into the discharge cavity which had a volume of 43 1.

Another transverse flow convection CO_2 laser amplifier using flow conditioning techniques was reported by Eckbreth and Davies (1972). The laser is shown schematically in Fig. 3.11. A number of flow conditioning methods were applied including a range of vortex generators and rectangular apertures placed near the upstream tungsten cathode pins. Each cathode pin was separately stabilised through resistors to spread the discharge across the 600mm x 25 mm channel. Turbulence in the discharge region created by the vortex generators was found to improve the stability of the discharge and enabled the power in the discharge to be raised from 11 kW to 16 kW.

Eckbreth and Owen (1972) employed four adjustable baffles upstream of a multi-pin cathode (which were aligned with the flow and separately stabilised), to modify the turbulence level and velocity profile in the discharge zone (Fig. 3.12). The anode was two common bars positioned downstream. The time averaged turbulence level and the velocity profile were determined by hot-wire anemometry. The experiments indicated that it is important to establish a uniform velocity profile in the discharge region in order to prevent the premature onset of discharge instabilities. It was believed that the turbulence level is also important in delaying the onset of discharge instabilities.

Kasamatsu et al (1986) reported a transversely excited CW CO_2 laser giving an output power of up to 10 kW at an efficiency of 19 percent. The system incorporated multiple bar cathodes and anodes made of three copper tubes combined with gas flow at 65 m/s. The study included comparison with a conventional multi-pin cathode and modification from previously reported system (Kasamatsu et al 1982,

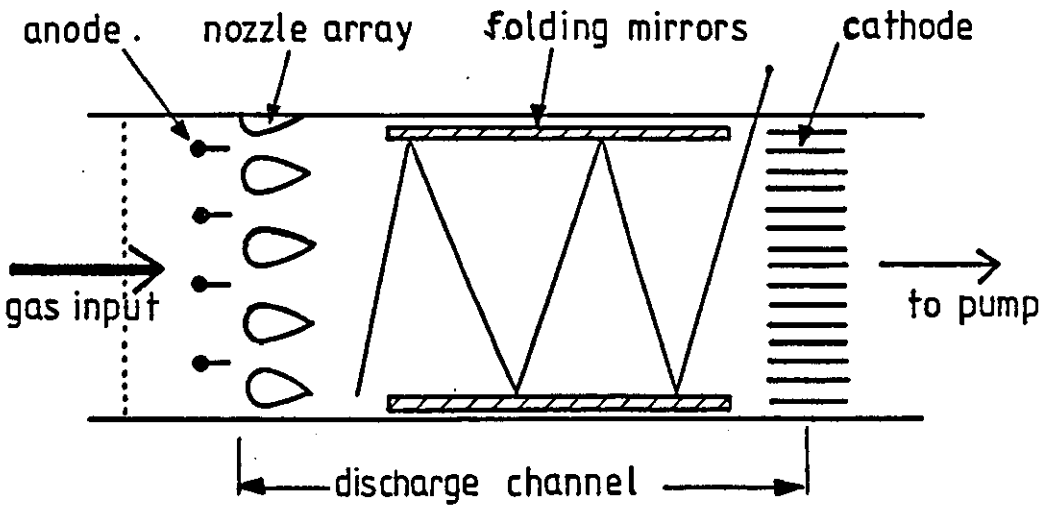

Fig. 3.10 Fast transverse-flow and discharge laser (Hill 1971).

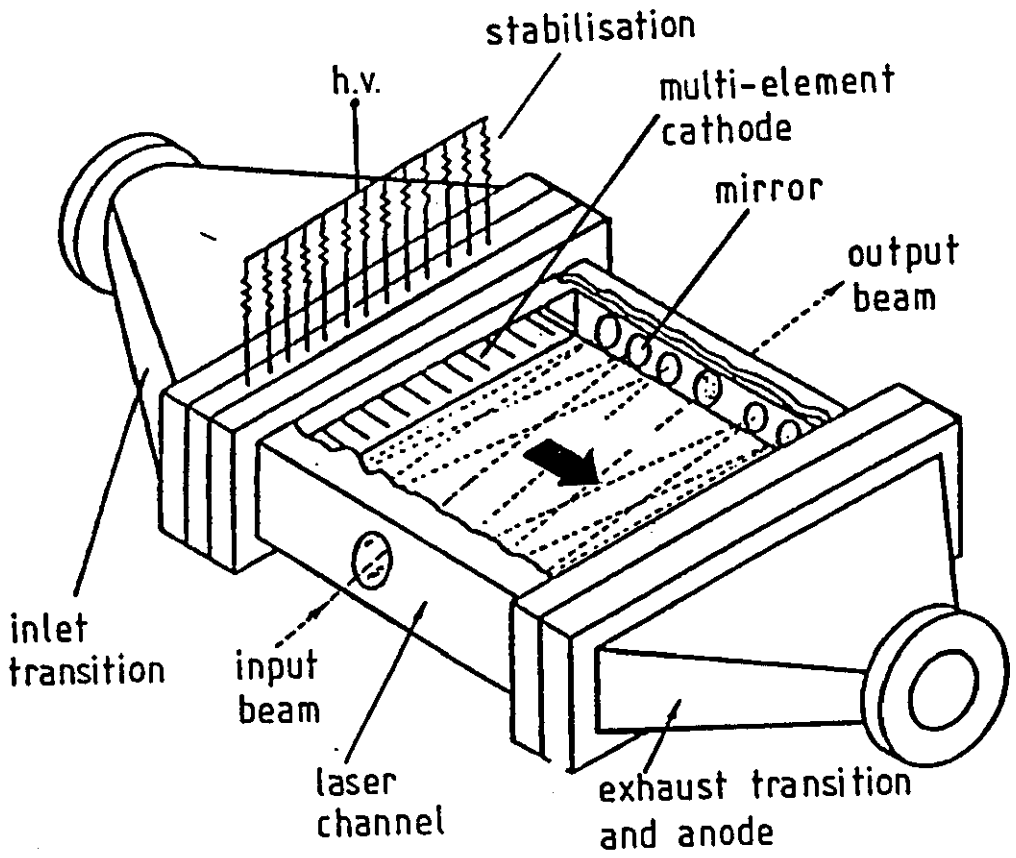

Fig. 3.11 Fast transverse-flow and discharge laser amplifier (Eckbreth and Davies 1972).

Kasamatsu and Shiratori 1986). More uniform discharge at high current (10 A) was obtained with the new cathode configuration than at low current (3 A).

3.8.2 The Transverse-Flow Cross-Discharge Laser

In the transverse-flow cross-discharge laser configuration, the gas flow is perpendicular to the electric discharge and both are perpendicular to the optical axis. The gas flow in this configuration provides effective convective cooling at relatively slow flow velocities (typically 30-50 m/s). However, the discharge column has a tendency to deflect downstream which could be a disadvantage for the continuous operation of the laser.

The first CW CO_2 laser using a transverse-flow cross-discharge configuration was reported by Tiffany et al (1969) which is shown schematically in Fig. 3.13. The laser was able to give 1.1 kW output power from 1 m active length at a tube efficiency of 8% and overall efficiency of 6% including losses in the recirculating blower.

Lancashire et al (1977) has described the NASA high power closed cycle CO_2 laser which was designed to generate up to 70 kW of CW output laser power. The transverse flow laser incorporated multi-pin cathodes to a plane anode system for a self-sustained d.c. discharge as well as an electron beam to preionise the discharge (Fig. 3.14). The laser was operated in the pressure range of 150-240 mb with transverse gas velocities of up to 150 m/s.

The Ferranti CL5 kW CO_2 laser developed by the Culham Laboratory had two pairs of distributed electrodes forming two cavities 50 mm x 50 mm x 1000 mm placed optically in series (Fig. 3.15). Each set of electrodes incorporates multiple anodes to a single bar cathode which operates at a d.c. discharge current of 14 A and a discharge voltage

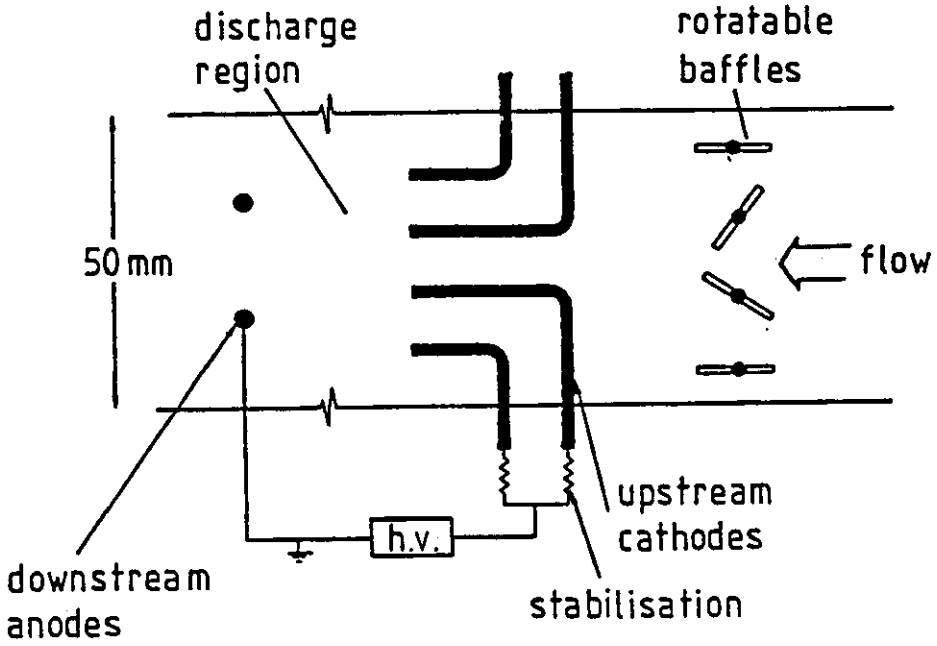

Fig. 3.12 Schematic of baffle-electrode geometry for a transverse flow and discharge laser (Eckbreth and Owen 1972).

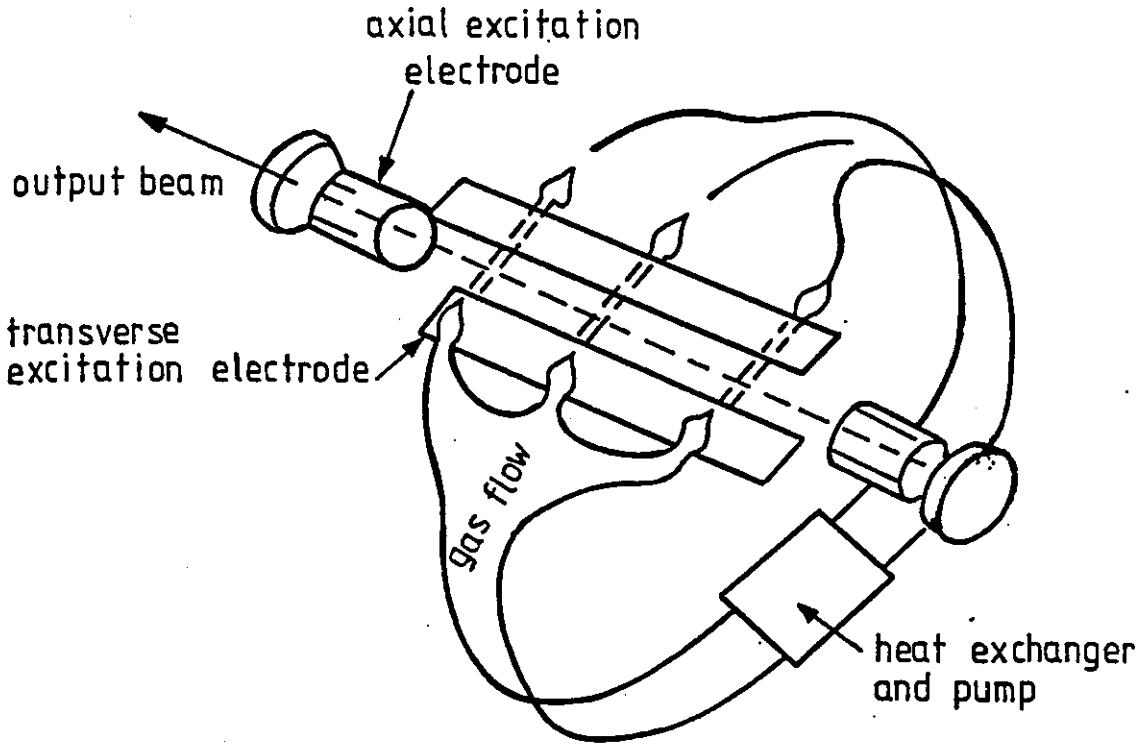

Fig. 3.13 The transverse-flow cross-discharge laser (Tiffany et al 1969).

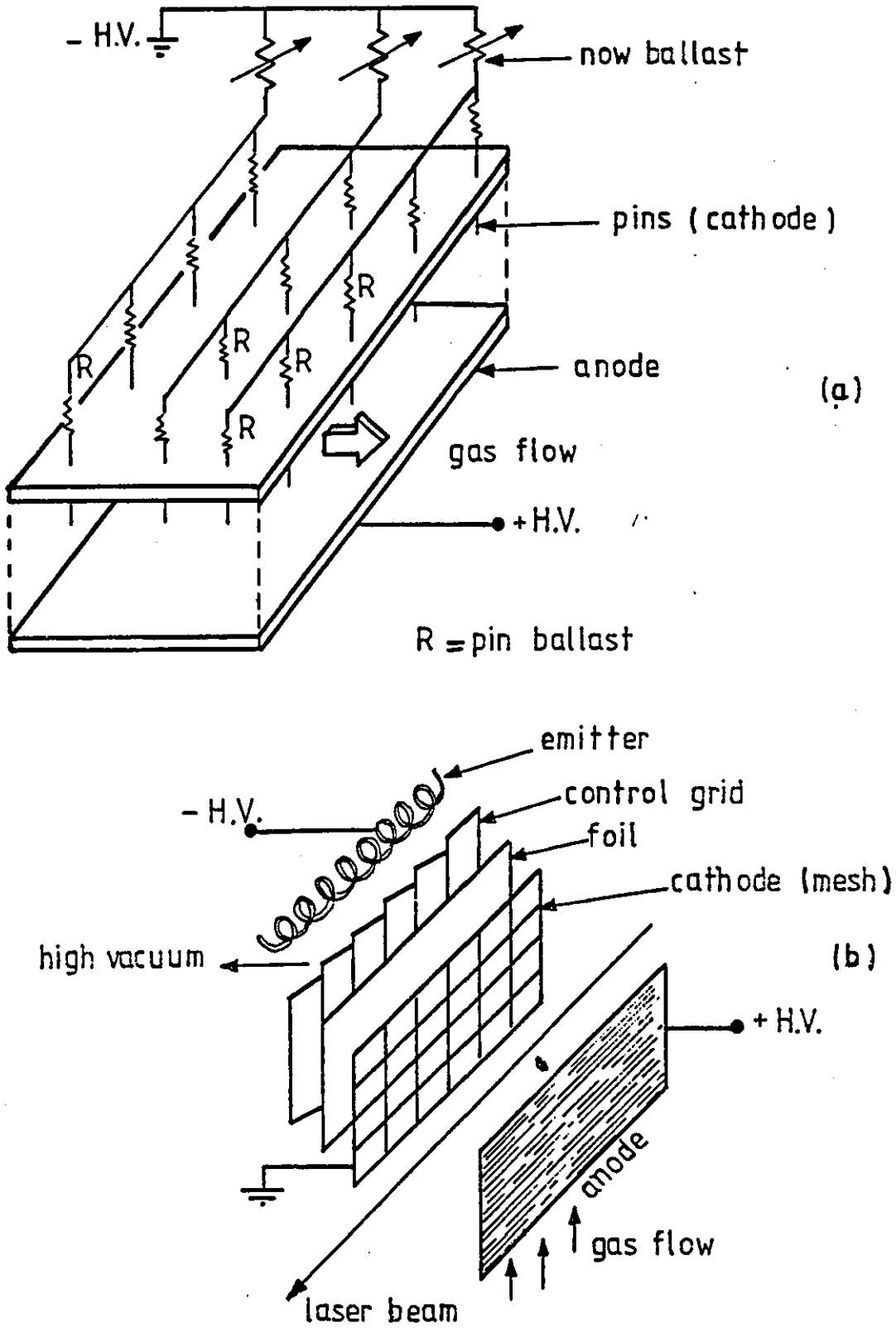

Fig. 3.14 The NASA high power CO_2 laser (Lancashire et al 1977)
(a) pin to plane self-sustained configuration
(b) electron beam sustained configuration

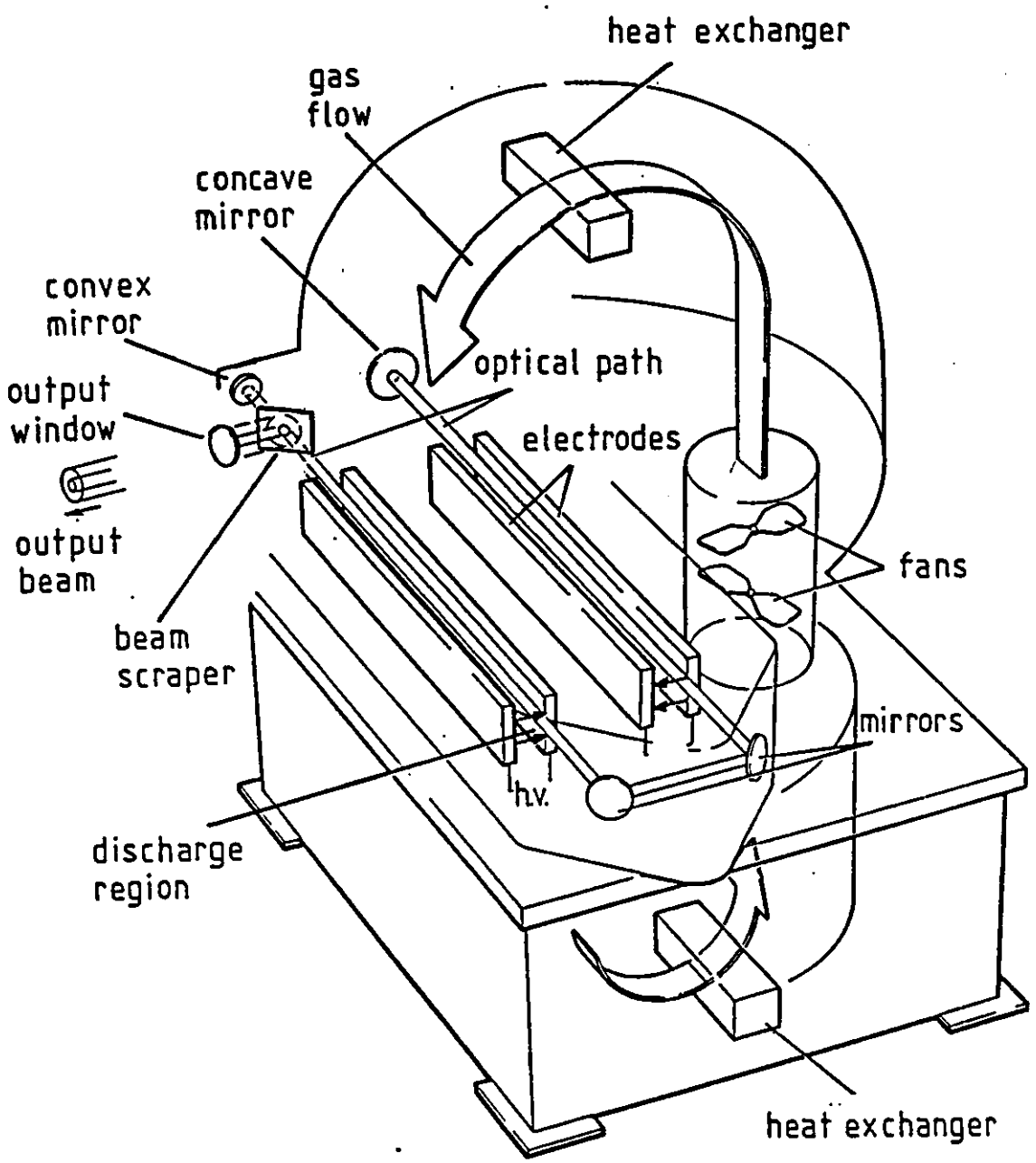

Fig. 3.15 The Ferranti CL5 transverse-flow cross-discharge laser

of 2 kV giving an electrical to optical efficiency of 9%. The recirculated laser gas passes through the discharge with a gas flow velocity of 50 m/s at gas pressure of 66 mb.

The transverse-flow cross-discharge configuration has been used for the excitation of CO laser because of the good discharge convective cooling provided by the transverse gas flow. Sato et al (1985) reported a transverse-flow cross-discharge CO laser at an output power of up to 770 W corresponding to 1.82 kW/m which is shown schematically in Fig. 3.16. The laser is excited by a transverse self-sustained d.c. glow discharge which occurs between the hollow-type cathode array and planar anode at an optical conversion efficiency of 16.3%. The laser gas which is pre-cooled by liquid nitrogen passes through the discharge at flow velocity of 15 m/s.

Saito et al (1987) reported a 3.1 kW CO laser using transverse-flow cross-discharge configuration with multiple hollow-type cathodes to a planar anode (Fig. 3.17). The laser power was obtained with a discharge cavity length along the optical axis of 1240 mm corresponding to laser power per unit length of 2.5 kW/m at an optical conversion efficiency of 14.1%. The gas flow velocity was 40 m/s in the discharge region at a temperature range of 120 K-room temperature. The gas pressure was 130 mb in the discharge region.

3.9 THE TRANSVERSELY EXCITED ATMOSPHERIC PRESSURE (TEA) LASERS

The atmospheric pressure electric discharge in a fast gas flow has been used for the excitation of CW CO_2 lasers, but the glow discharge instabilities occur at a relatively low current (< 40 mA), (Hill 1971, McLeary and Gibbs 1973), therefore, atmospheric pressure electric discharges are normally used for pulse excitation of gas

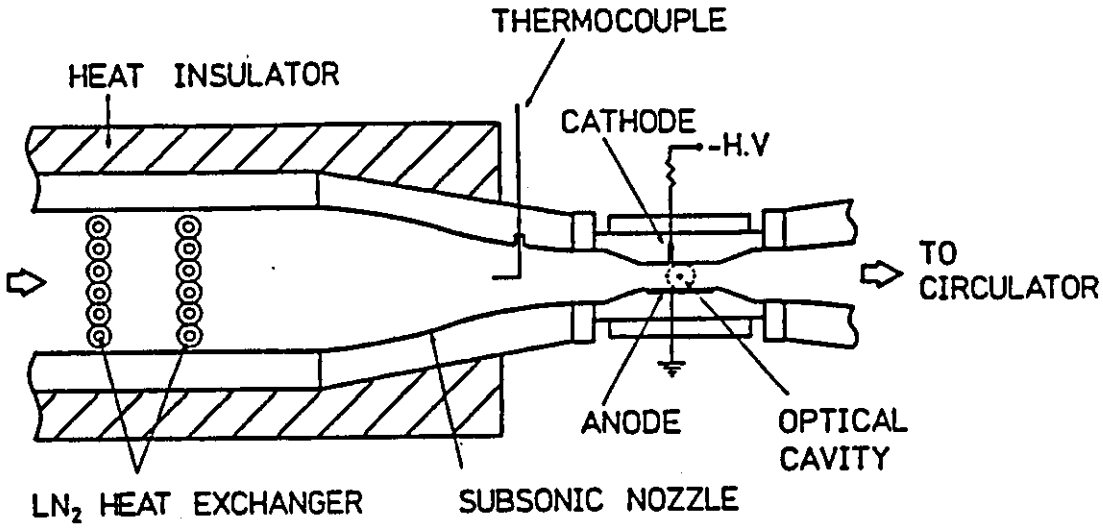

Fig. 3.16 Schematic of the transverse-flow cross-discharge CO laser (Sato et al 1985).

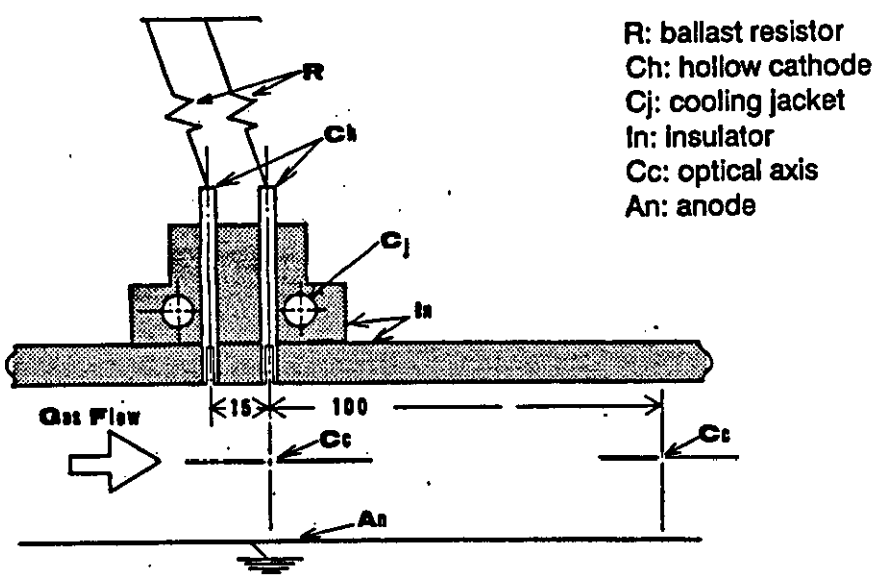

Fig. 3.17 Schematic of the transverse-flow cross-discharge CO laser (Saito et al 1987).

lasers such as CO_2, CO and excimer lasers. Pulsed outputs with large output energies per unit volume of the discharge (10-50 J/l) can be obtained, (Svelto 1982). The pulse duration is again limited by the glow to arc transition which is characterised by the formation of arc like filaments associated with an abrupt reduction in the discharge voltage. To counteract this, the pulse duration is made sufficiently short (a fraction of a microsecond) so that the discharge instabilities have no time to develop.

The first demonstration of the pulsed CO_2 laser was at low pressure (~ 80 mb) using a longitudinal discharge excited by a high voltage pulse transformer (Hill 1968). The use of pulsed longitudinal discharges at atmospheric pressure is not practical due to the very high voltage (~ 3 kV/mm), required to break down the gap, and operation at atmospheric pressure has been confined to short discharges transverse to the optical axis.

The first report of a transversely excited atmospheric pressure CO_2 laser was by Beaulieu (1970). The electrode configuration, shown in Fig. 3.18, utilises a separately stabilised multi-pin cathode and single bar anode transverse to the laser axis. The laser was able to produce pulses with energies of up to 150 mJ and a peak power of up to 0.5 MW.

The resistively stabilised electrodes result in reduced overall efficiency due to the I^2R losses, while premature arc filaments occur in a discharge between two continuous single electrodes. Laflamme (1970) used a double discharge configuration (Fig. 3.19), where a small source of energy is supplied to the auxiliary discharge to preionise the main discharge gap so that well distributed free electrons can initiate a homogeneous discharge between the two continuous single anode and cathode.

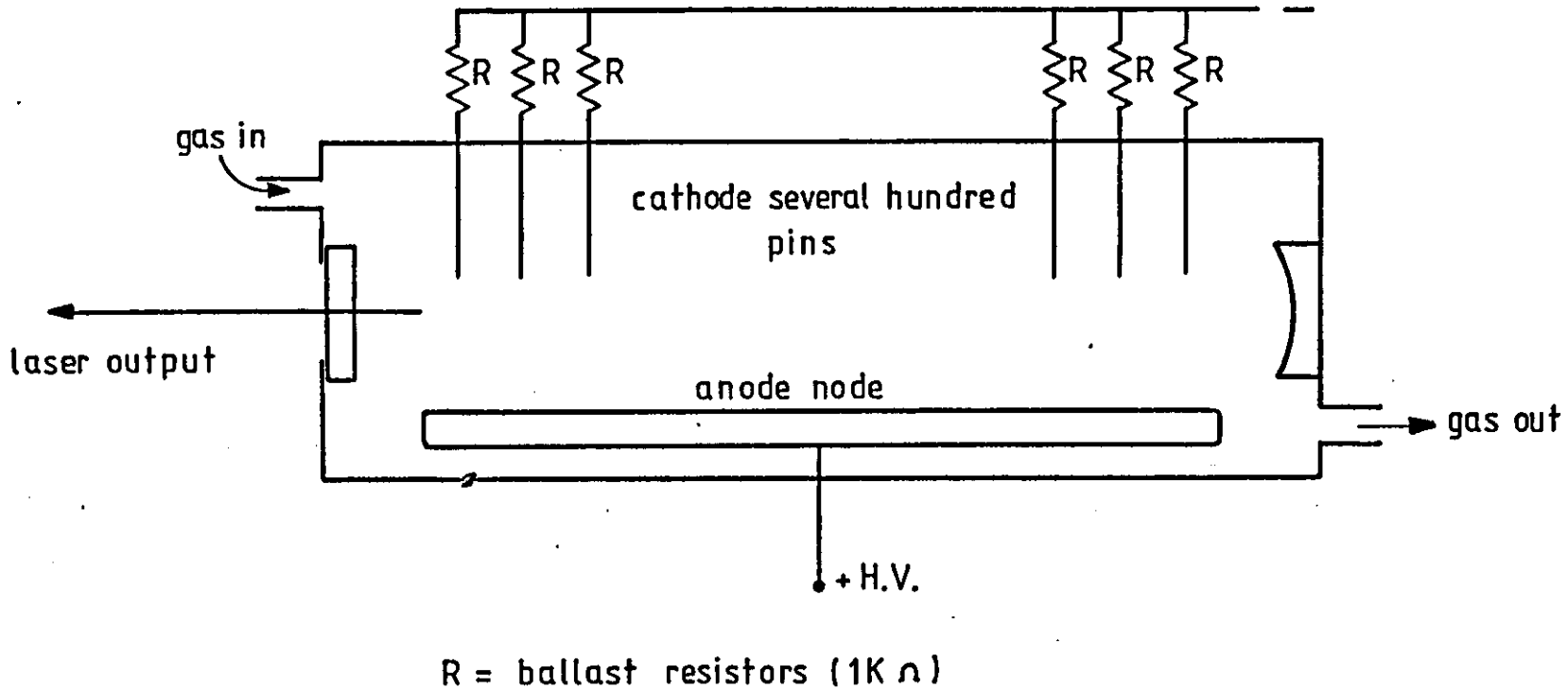

Fig. 3.18 The TEA CO_2 laser configuration (after Beaulieu 1970).

Various techniques have been used subsequently later to preionise the gap incorporating corona discharges, arc discharges and photo-ionisation. The highest output power density of a TEA CO_2 laser was reported by Marchetti et al (1982) using circularly profiled electrodes and ultraviolet preionisation generated from a single spark gap (Fig. 3.20), and the system delivered output pulses with peak power in excess of 1.6 MW with a peak output power density of 500 MW/l at a pressure of 1 b. The output laser pulse was 70 ns full wave half maximum (FWHM) wide.

Laser action in TEA CO lasers has been reported using various techniques similar to those used in TEA CO_2 lasers. An extensive review of the different techniques used for the excitation of CO laser was given by Mann (1976).

The excimer laser, which is inherently a high pressure laser (> 400 mb), can be excited by using similar techniques to those used in TEA CO_2 lasers. Extensive reviews on the excimer lasers and their excitation techniques have been given by Brau (1979), and Hutchinson (1980).

3.10 SUMMARY

The CW gas lasers can be divided into two main groups with respect to the configuration of the electric discharge; the longitudinal (axial) electric discharge lasers and the transverse electric discharge lasers.

The longitudinal or axial discharge lasers can be divided into three groups with respect to the gas flow; the sealed tube gas lasers, the slow axial gas flow discharge lasers and the fast axial gas flow discharge lasers, while, the transverse discharge lasers can be divided into two groups with respect to the gas flow; the transverse-flow and discharge lasers and the

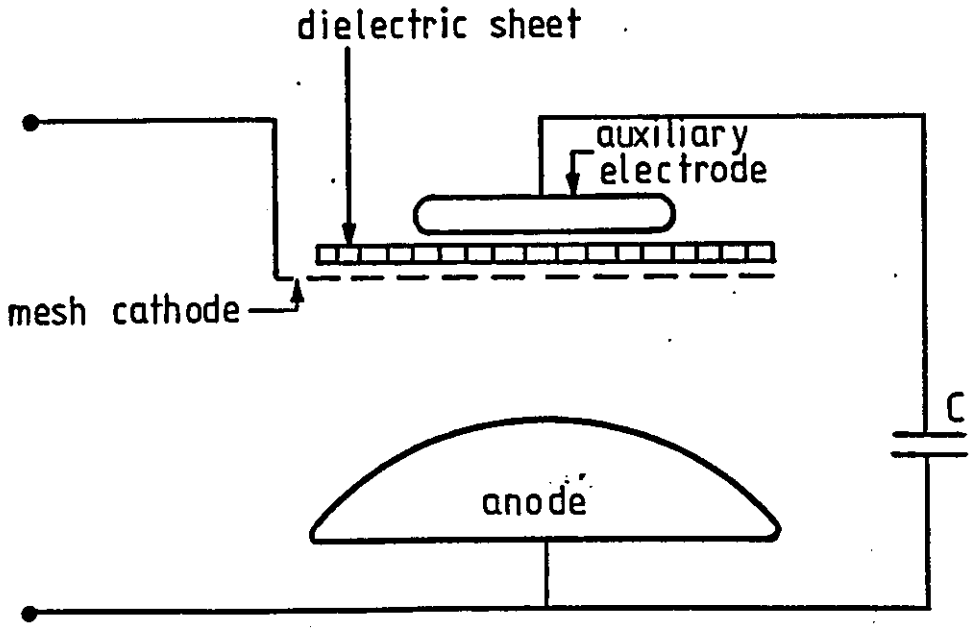

Fig. 3.19 The TEA laser electrode configuration with preionisation (Laflamme 1970).

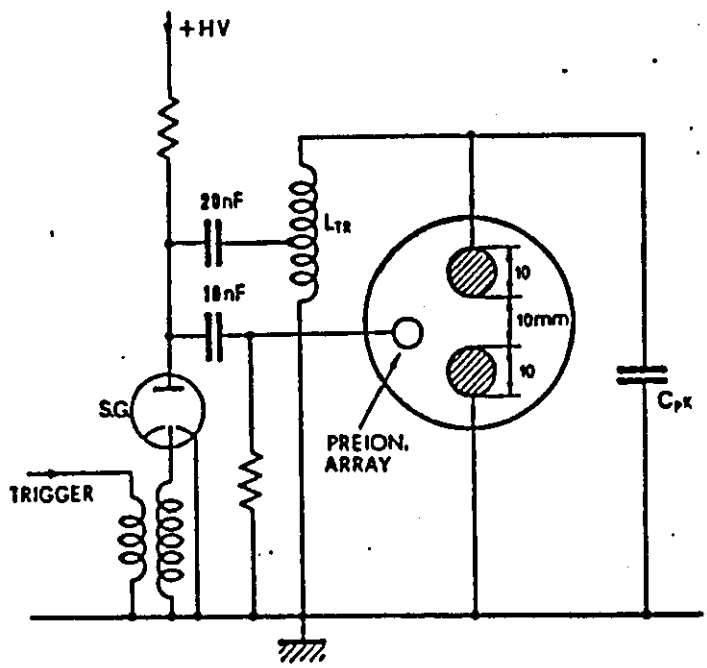

Fig. 3.20 Schematic of the TEA CO_2 laser (Marchetti et al 1982).

transverse-flow cross-discharge lasers. The different types of the CW gas lasers have been described and published work relative to each type has been reviewed.

The transversely excited atmospheric pressure (TEA) laser configuration has been described and related published work has been reviewed.

Tables 3.1 and 3.2 summarise the electrode configuration of the fast axial gas flow and the transverse gas flow lasers as well as their performance characteristics reviewed in this chapter.

Laser	Power output (W)	Input power density (mW/mm^2)	Discharge current (A)	Cathode type	Anode type	Reference
CO_2	140	15.7	0.15	single	single	Deutsch et al (1969)
CO_2	20	31	0.04	single	single	Tyte (1970)
CO_2	2000	-	-	single	single	Control laser 2kW
CO_2	5000	5	1.5	multiple	multiple	Evans (1987)
-	-	-	40-70	sigle	single	Chebotaev (1973)
CO_2	500	35	-	single	single	McLeary and Gibbs (1973)

Table 3.1 Fast axial gas flow lasers

Laser	Power output (W)	Input power density (mW/mm^2)	Discharge current (A)	Cathode type	Anode type	Reference
CO_2	19000	12	-	single	multiple	Hill (1971)
CO_2	2050	38	-	multiple	-	Eckbreth and Davies (1972)
-	-	-	1.2	multiple	single	Eckbreth and Owen (1972)
CO_2	10000	-	10	multiple	single	Kasamatsu et al (1986)
CO_2	1100	-	-	-	-	Tiffany et al (1969)
CO_2	5900	16	-	multiple	single	Lancashire et al (1977)
CO_2	5000	12	28	single	multiple	Ferranti (CL5)
CO	770	-	3.5	multiple	single	Sato et al (1985)
CO	3100	-	8	multiple	single	Saito et al (1987)

Table 3.2 Transverse gas flow lasers

CHAPTER 4

THE CHARACTERISTICS OF AN ELECTRIC DISCHARGE IN A STILL GAS FLOW

4.1 INTRODUCTION

The experimental data available on the static characteristic of low pressure (30-100 mb), and high pressure (1 b) glow discharges (Fan 1939, Gambling and Edels 1954, von Engel 1965) shows that both forms of glow discharge have a high cathode fall voltage (150-400 V) and low cathode current density (0.1-100mA/mm^2) compared with those which normally exist in arcs (10-20 V and 10^4 A/mm^2 respectively). The atmospheric pressure glow discharge has received less attention because of its contracted positive column compared with the low pressure glow discharge and it is essentially a low current discharge, although currents of up to 12 A have been obtained in H_2 (Fan 1939).

Low pressure glow discharges are used for the excitation of CW gas lasers such as CO and CO_2 lasers. Low current axial glow discharges (20-60 mA) have been used in sealed tube CO_2 lasers (Carbone 1967, Witteman 1967). High current glow discharges (up to 2 A) in a fast axial gas flow have been used in high power CO_2 laser (Harry and Evans 1988), and even higher current glow discharges (up to 12 A) have been used in a transversely excited CW CO_2 laser (Kasamatsu et al 1986). The discharge current is normally limited by the formation of streamers within the discharge which is also referred to in the literature as a glow to arc transition (Nighan and Wiegand 1974, Eckbreth and Owen 1972, Wasserstrom et al 1978).

The glow to arc transition normally occurs at lower currents (40 mA, Hill 1971) in fast flow atmospheric pressure glow discharges, therefore the atmospheric pressure discharge is normally used in the form of a pulse which is characterised by a high energy density (1-5 J/l), but the pulse duration is also limited by the on set of glow discharge instability.

It is proposed here that if the nature of the glow to arc transition in still and fast gas flows is understood and can be suppressed or shifted up to higher current, it may be possible to operate high power CW gas lasers at atmospheric pressure.

This chapter investigates the static characteristic of the electric discharge at low pressure in different gases as well as at atmospheric pressure to attempt to understand the glow to arc transition and its influence on the positive column behaviour in still gas.

4.2 THE POWER SUPPLY AND MEASUREMENT EQUIPMENT

The power supply (Fig. 4.1), was designed to supply a variable D.C. voltage of up to 12 kV at a total current of up to 1.5 A. The high voltage 3 phase transformer, the high voltage bridge rectifier and the load resistors were contained in a metal cabinet. The discharge electrodes were contained in a metal enclosure with perspex panels to provide electrical safety. The electrical circuit used for the electric discharge tests is shown in Fig. 4.2. The discharge current was measured using an analog multimeter, and, the discharge voltage was measured using a high voltage probe with high input impedance (1000 M ohm), connected to a digital multimeter. Fig. 4.3 shows a general view of the test equipment.

4.3 LOW PRESSURE ELECTRIC DISCHARGE

A series of tests were carried out to investigate the behaviour of the electric discharge over a wide range of gas pressure. The electrode arrangement used in these tests is shown schematically in Fig. 4.4. Copper electrodes were used in a Pyrex tube of 93 mm ID. The anode end was a semi-sphere of 20 mm diameter. The cathode was a circular sheet of copper of 90 mm diameter. The

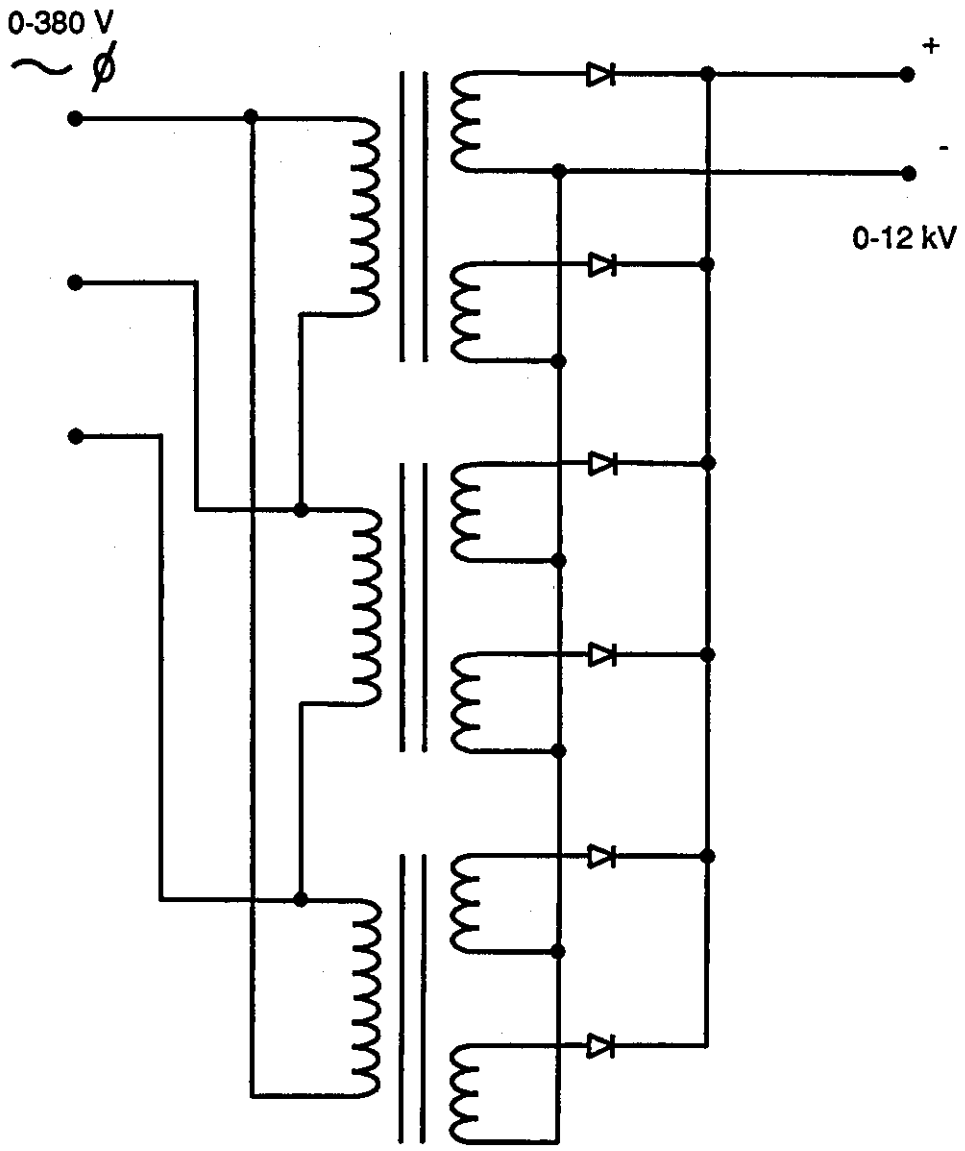

Fig. 4.1 High voltage d.c. power supply

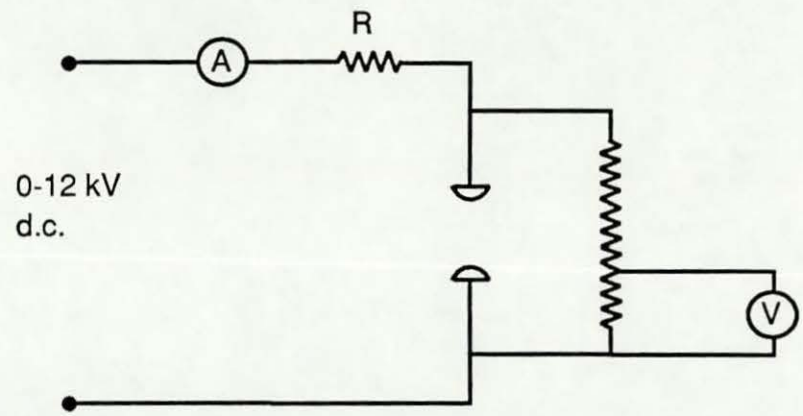

Fig. 4.2 The electric discharge and measurement circuit

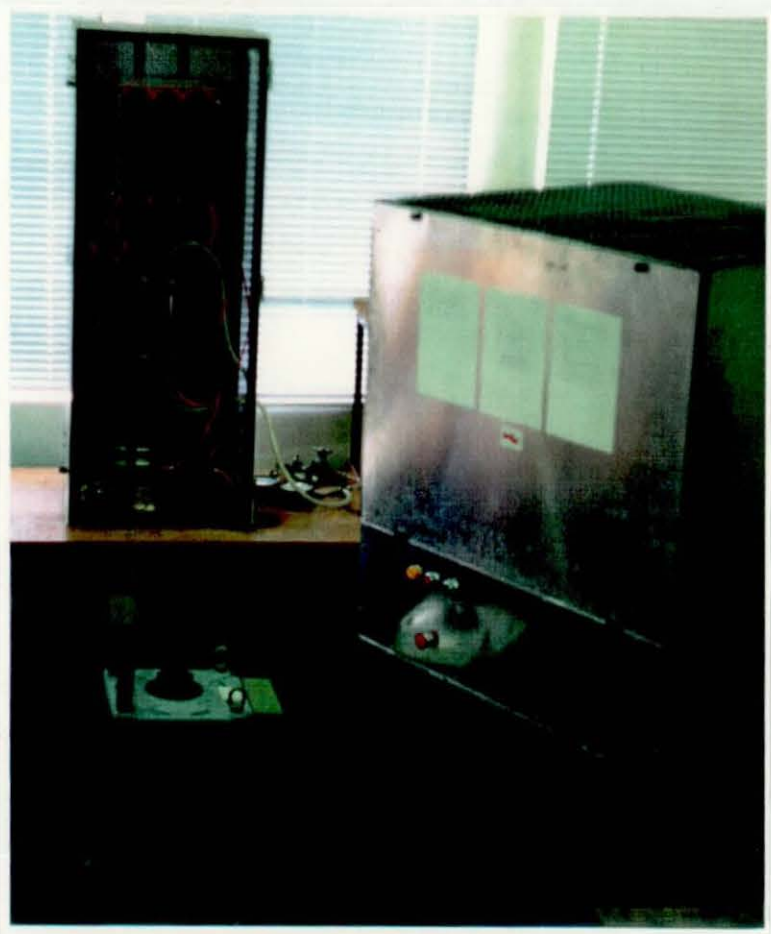

Fig. 4.3 General view of the tests equipment

discharge was initiated by evacuating the discharge cavity to a low pressure (< 50 mb) so that the open circuit voltage (0-12 kV) was able to break down the gap at the critical value.

Fig. 4.5 shows a schematic diagram of the gas supply system. A single stage rotary vacuum pump was used to evacuate the discharge cavity; the gas was supplied from a gas cylinder. The discharge cavity was pumped down and flushed with gas many times to ensure high gas purity.

4.3.1 Electric Discharge in Air

The voltage-current characteristics of the electric discharge in air for different values of pressure for 50 mm electrode separation are shown in Fig. 4.6. At 50 mb, the negative glow covered the whole cathode surface area at around 1.2 A and an abnormal glow developed. At 100mb, the negative glow as well as the positive column appeared contracted compared with the 50 mb discharge, however, a normal glow discharge was obtained up to 1.5 A, but, the negative glow did not cover the whole cathode area, and an abnormal glow was beyond the current capability of the power supply. At 200 mb, the discharge was more contracted, however, a normal glow was obtained up to 1.0 A, and, a glow to arc transition took place as the current was increase further without showing abnormal glow. At atmospheric pressure, the discharge appeared more contracted than before and a normal glow was obtained only up to 0.8 A and the glow to arc transition occurred as the current was increased further without showing abnormal glow.

The variation of the glow discharge voltage with pressure at different values of current in air is shown in Fig. 4.7. The relation is not linear and the voltage tends to level-off at high pressure (>500 mb at 0.2 A and >200 mb at 0.8 A). This indicates the increasing

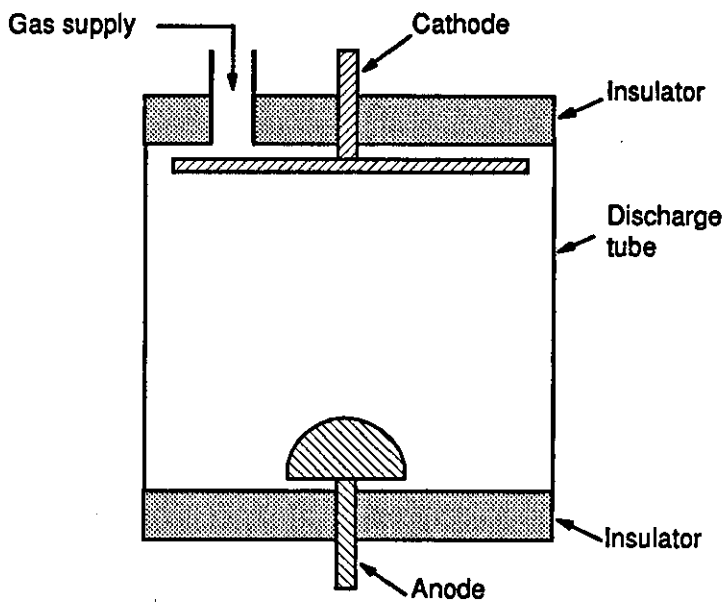

Fig. 4.4 Electrode arrangement for the low pressure electric discharge

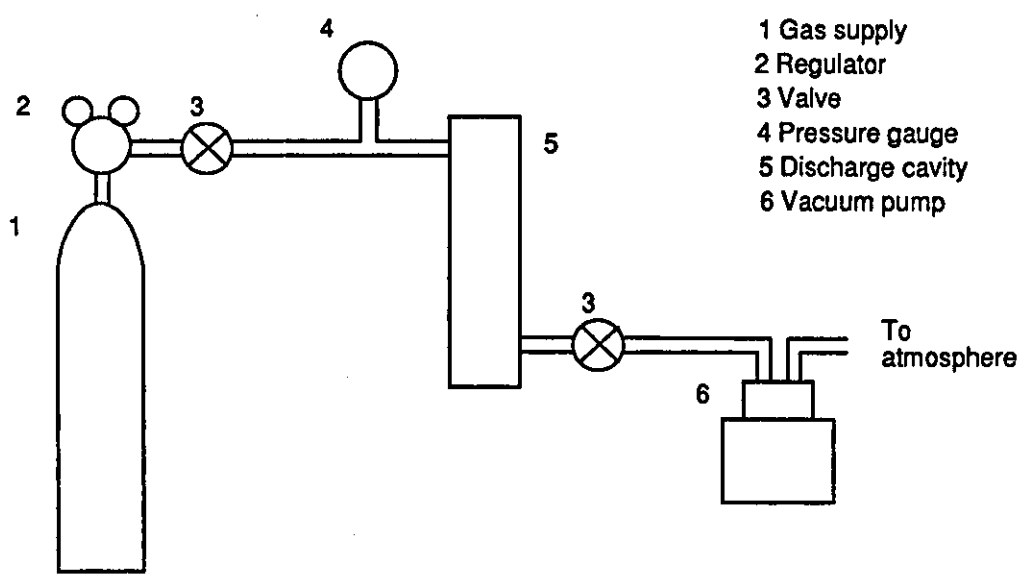

Fig. 4.5 The gas supply system

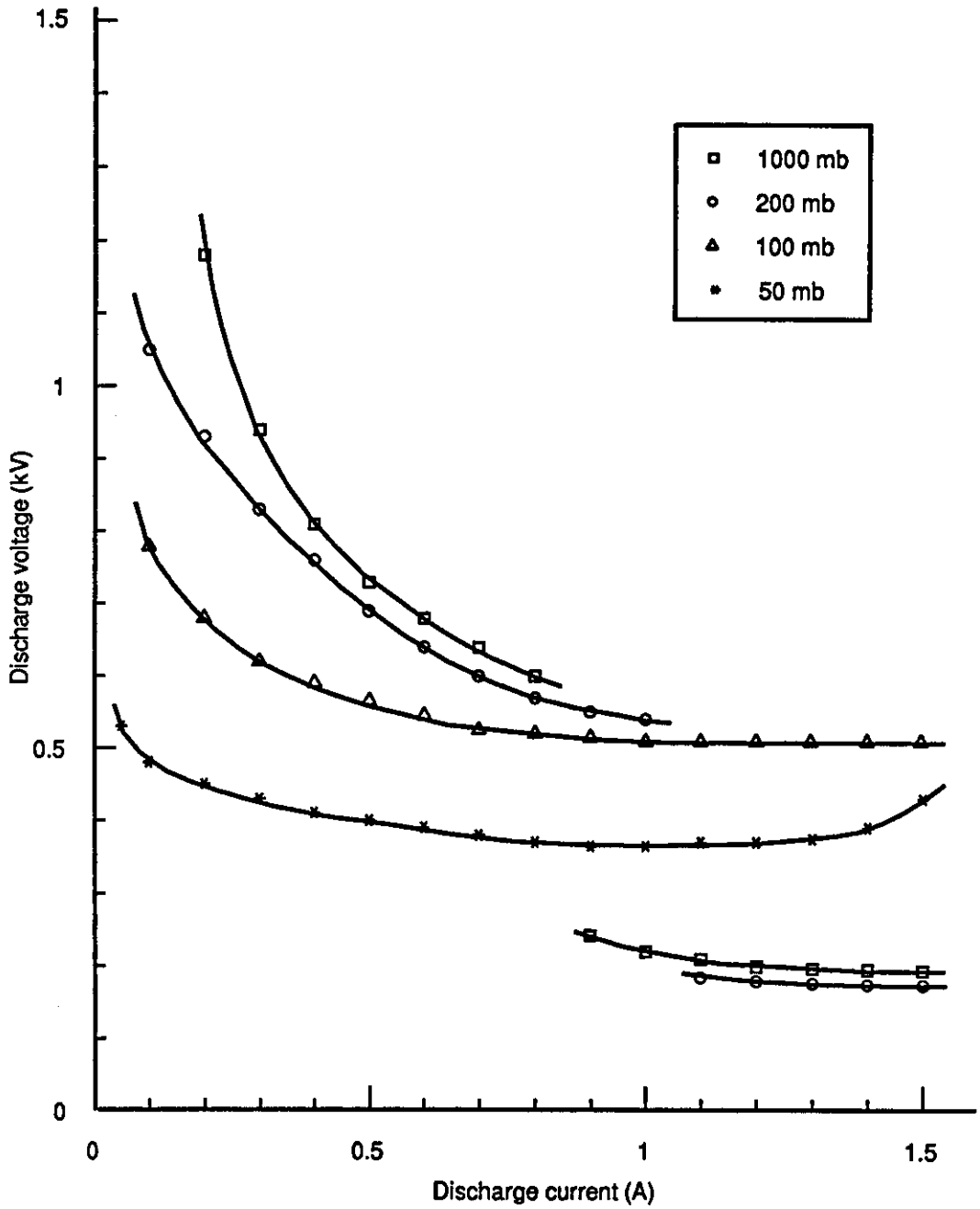

Fig. 4.6 The voltage-current characteristic in air at different values of gas pressure

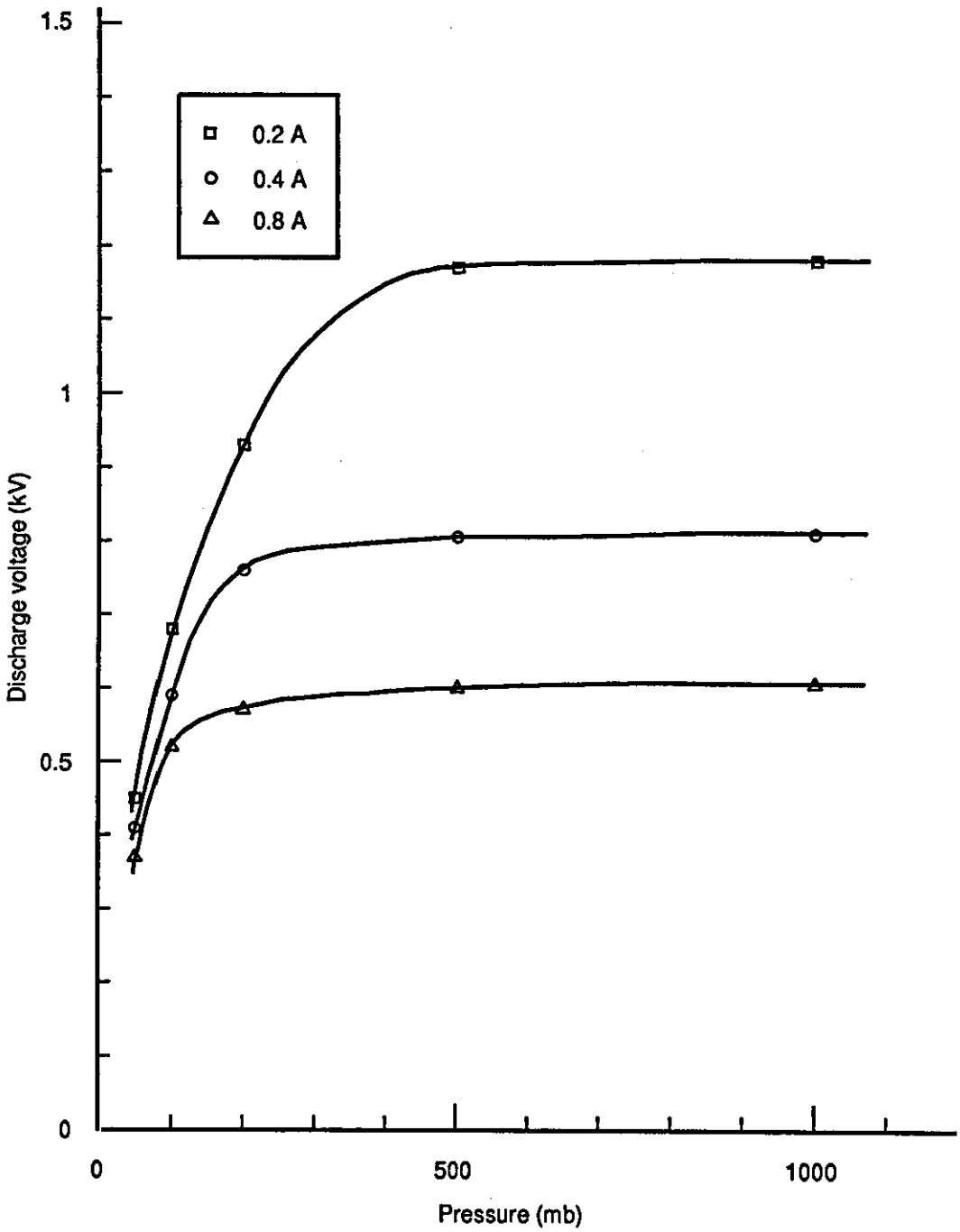

Fig. 4.7 Variation of discharge voltage with gas pressure in air for a 50 mm long discharge

thermal ionisation process due to the contraction of the positive column as the discharge current and/or the pressure are increased.

4.3.2 Electric Discharge in CO_2 Laser Gas Mixture

The static characteristic of the electric discharge in a standard gas mixture of CO_2 laser (82% He: 13.5% Ne: 4.5% CO_2 by volume) was studied to investigate the behaviour of the electric discharge used in gas lasers. The voltage-current characteristics in a standard CO_2 laser gas mixture at different values of pressure are shown in Fig. 4.8. At low pressure (100 mb), the negative glow covered the cathode surface at 1.1A and an abnormal glow started to develop. As the pressure was increased the discharge appeared to contract but less rapidly than in air. At 200 mb and up to 500 mb, a normal glow was obtained up to 1.5 A without any sign of an abnormal glow. At atmospheric pressure, a normal glow was obtained up to 1.2 A and a glow to arc transition took place as the current was increased further.

The variation of the glow discharge voltage with pressure at different values of current in the CO_2 laser gas mixture is shown in Fig. 4.9. The relation is almost linear unlike the results in air. This relation indicates that the variation of E/p (the electric field per unit pressure) of the positive column is nearly linear with pressure and, therefore, electrons are still playing the major role in the ionisation process (field ionisation) at high pressure. This indicates that excitation of a high power high pressure CO_2 laser may be possible with effective and homogeneous cooling to the positive column.

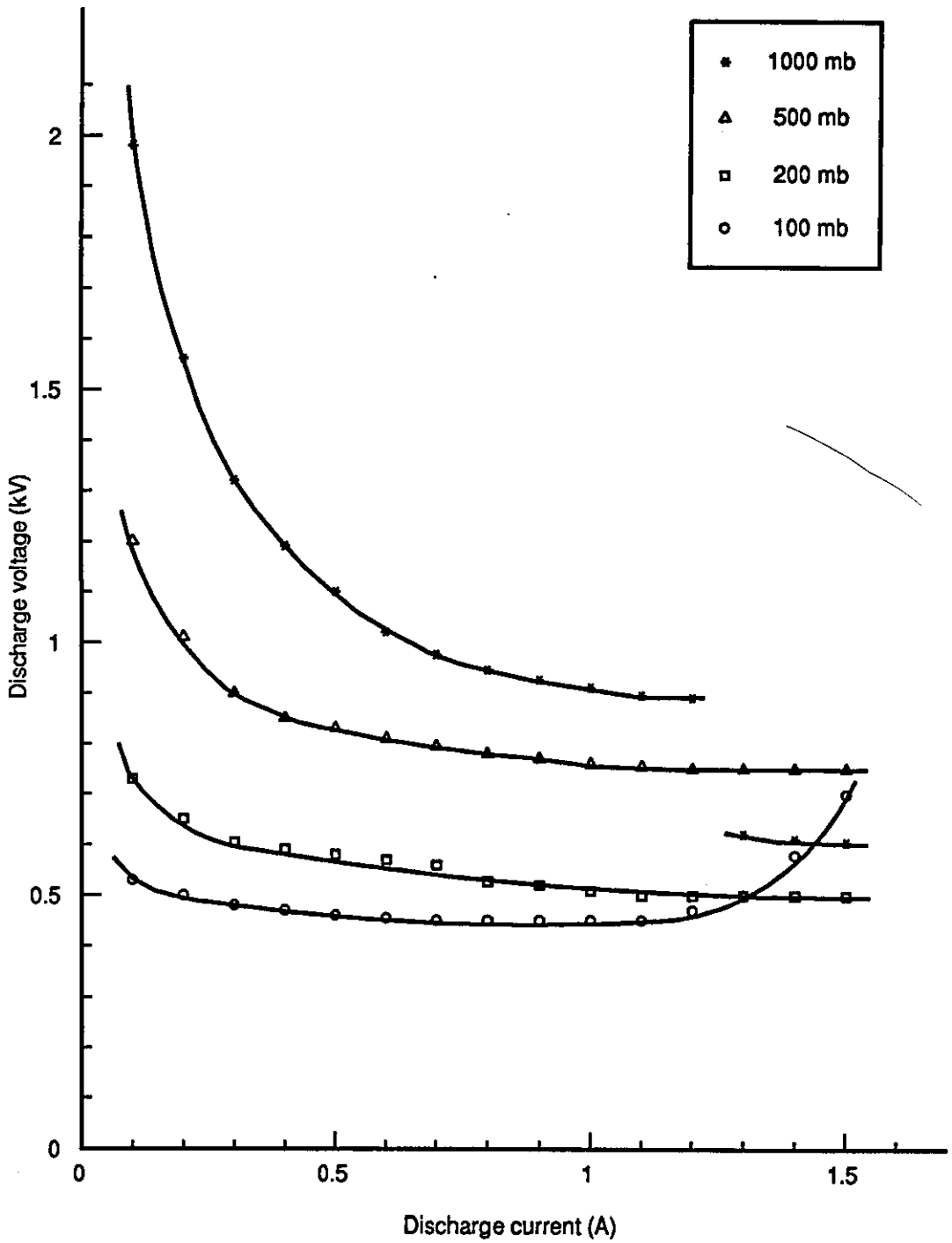

Fig. 4.8 The voltage-current characteristics in CO_2 laser gas mixture at different values of gas pressure

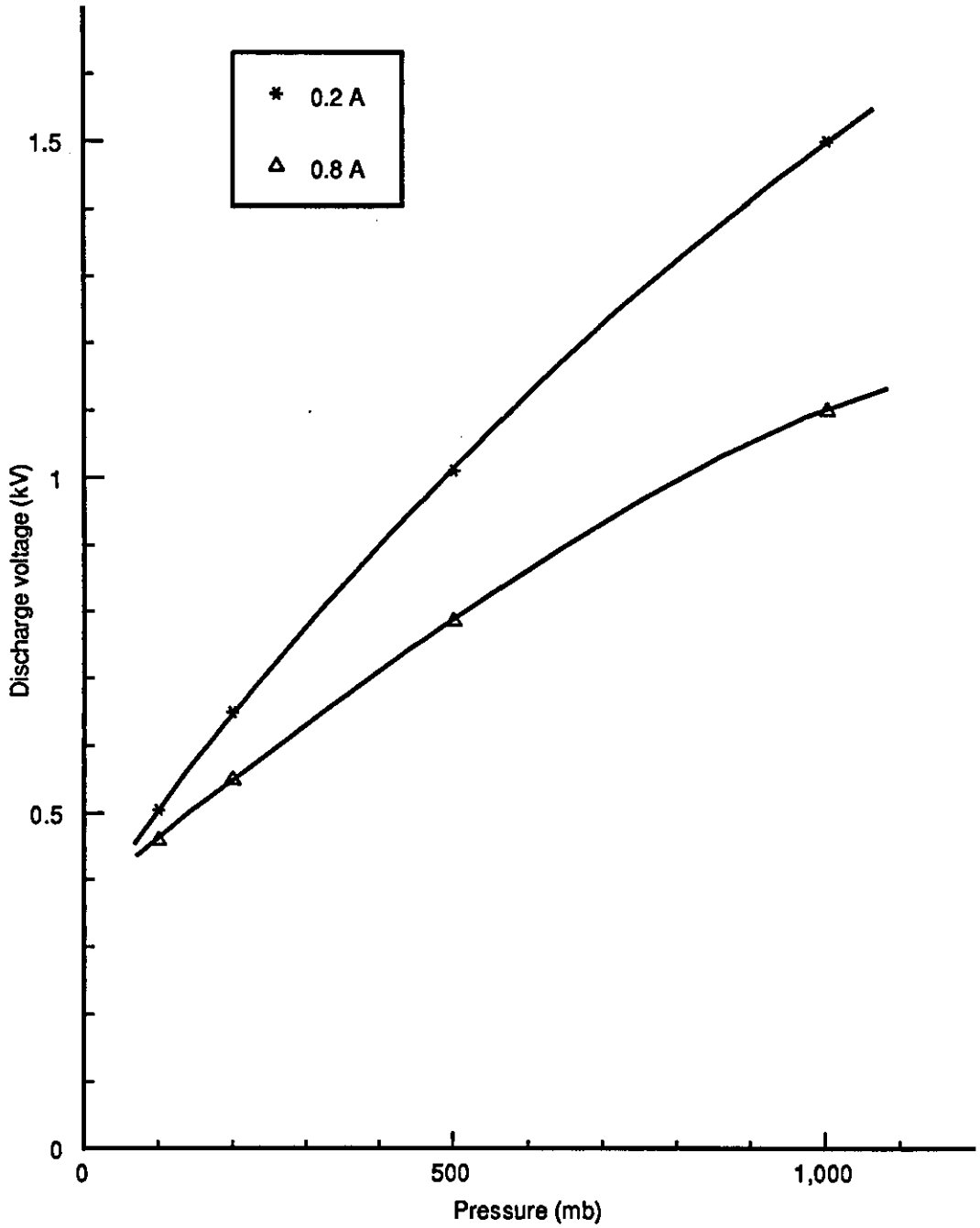

Fig. 4.9 Variation of discharge voltage with pressure in CO_2 laser gas mixture at different values of current

4.4 THE ATMOSPHERIC PRESSURE ELECTRIC DISCHARGE

A series of tests were carried out to study the electric discharge characteristic at atmospheric pressure in different gases. Copper electrodes were used in a Pyrex glass tube of 22 mm ID. No special care was taken of the electrode surface finish. The cathode was water cooled and its diameter was 20 mm. The electrode arrangement is shown schematically in Fig. 4.10. The discharge was initiated by touching the two electrodes and then separating them apart.

4.4.1 Electric Discharge in Air

The voltage-current characteristics for different values of electrode separation in air at atmospheric pressure are shown in Fig. 4.11. The broken curve is derived from the 10mm long discharge characteristic curve. At low current, the discharge voltage is high. As the discharge current is increased, the discharge voltage falls sharply at first then tends to become constant before the glow to arc transition takes place at 0.5 A. The discharge voltage variation with current is solely due to the variation of the positive column voltage gradient since the sum of the electrodes drop and the voltage across the Faraday dark space and negative glow is constant (von Engel 1965).

Repeating the tests many times, the glow to arc transition appeared to take place mostly at 0.5 A, although in some tests the glow discharge was extended up to 0.8 A. The glow to arc transition occurred without showing an abnormal glow and some times temporary transitions identified visually and by a temporary drop in voltage occurred at lower currents before a stable arc was established. The cathode negative glow current density, measured by a travelling telescope, was about 120 mA/mm^2 close to the 125 mA/mm^2 reported by Fan (1939). The negative glow current density was constant and independent

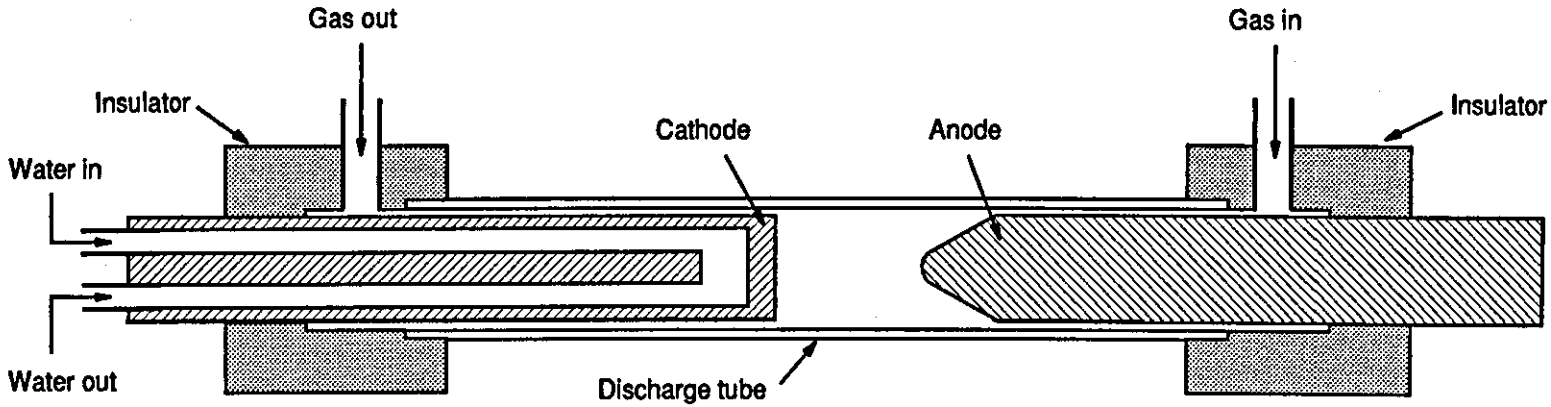

Fig. 4.10 Electrode arrangement for the atmospheric pressure electric discharge

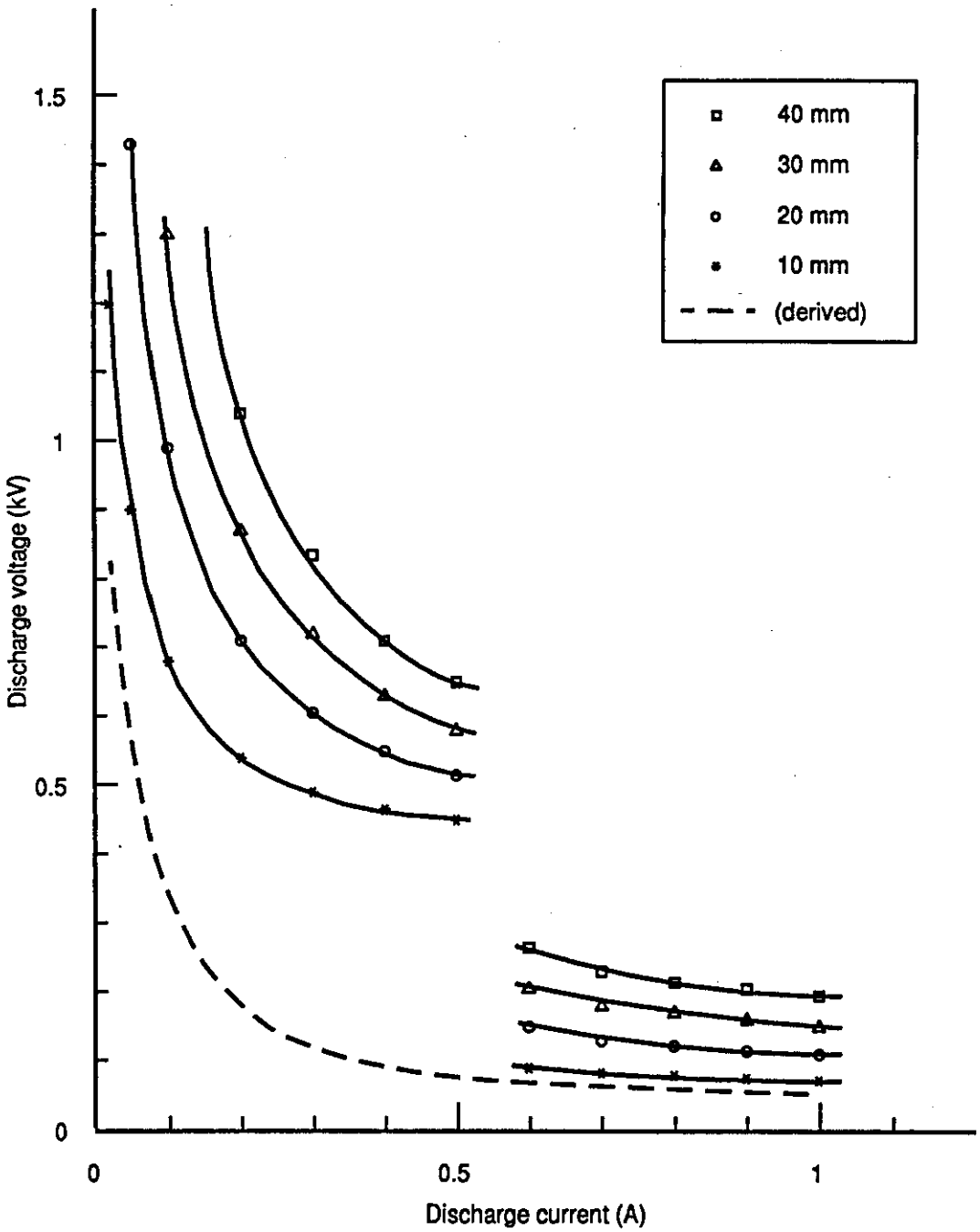

Fig. 4.11 The voltage-current characteristics in air at atmospheric pressure

of current as the negative glow covered only part of the cathode surface and, therefore, no abnormal glow developed.

The variation of the discharge voltage with the electrode separation at different values of current for glow and arc discharges is shown in Fig. 4.12. The relation is approximately linear since the voltage gradient along the positive column is approximately constant at a constant current. Extending these straight lines to intersect the voltage axis, they give a zero-length voltage of 375 V. This value is independent of current and it represents the sum of the cathode and anode fall voltages. This value is some times identified as the cathode fall voltage since the anode fall voltage is only of the order of 10-15 V.

Fig. 4.12 shows that the voltage gradient along the arc column is not markedly different from that along the glow column before the transition. To show the effect of the glow to arc transition on the positive column characteristic, the zero-length voltage is subtracted from the voltage-current characteristic curve of the glow discharge for the 10 mm long discharge as an example. This gives the voltage-current characteristic for the positive column for this gap which is represented by the broken line in Fig. 4.11. The figure shows that the curve continues smoothly in the transition region where the voltage along the positive column after the transition is just below the arc voltage. This difference in the voltage (~15 V) represents the cathode fall voltage of the arc discharge.

4.4.2 Electric Discharge in CO_2 Laser Gas Mixture

The voltage-current characteristics of the electric discharge in a standard CO_2 laser gas mixture at atmospheric pressure for different values of electrode

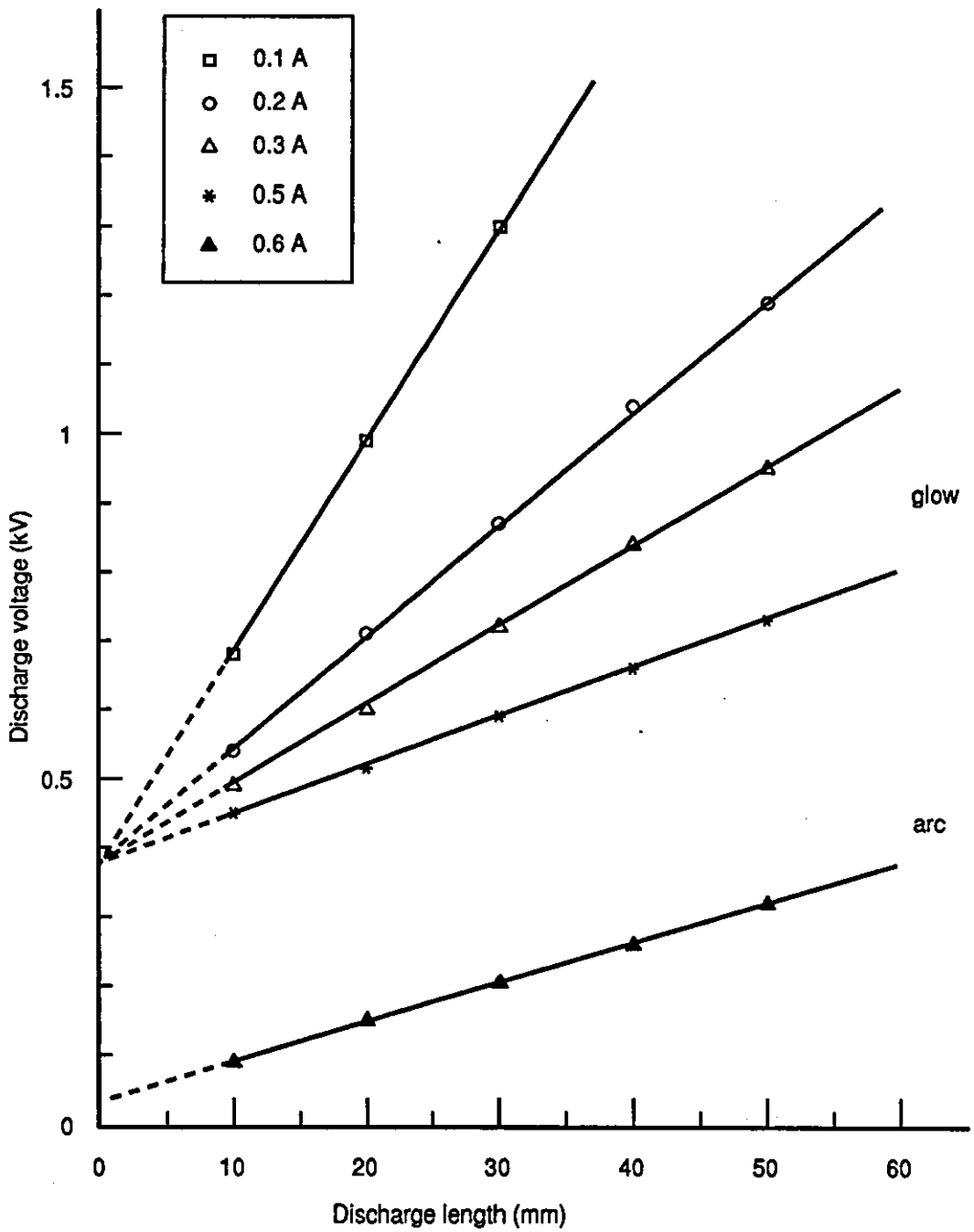

Fig. 4.12 Variation of discharge voltage with electrode separation in air at atmospheric pressure

separation are shown in Fig. 4.13. The broken line curve is derived from the 10 mm long discharge characteristic curve. Stable glow discharges could be extended up to 1.2 A before the transition occurred. Apart from the difference in the discharge current at which the glow to arc transition took place, the static characteristics are similar to the discharge characteristics in air. The glow to arc transition also occurred before the abnormal glow.

The negative glow in the CO_2 laser gas mixture covered a larger area than the negative glow in air, therefore, the current density was smaller (about 17 mA/mm^2). Although, the negative glow in the CO_2 laser gas mixture did not cover the whole cathode surface area before the glow to arc transition took place, Fig. 4.14 shows a gradual then steep increase in the negative glow current density with increase in the discharge current.

The spread of the negative glow in the CO_2 laser gas mixture over a larger area than in air makes it more suitable to demonstrate the abnormal glow discharge at atmospheric pressure, and a copper cathode 3 mm diameter was used to provide a smaller cathode surface area (7 mm^2). The voltage-current characteristic is shown in Fig. 4.15. As the discharge current was increased to 120 mA the negative glow covered the cathode surface area. When the current was increased further, the discharge entered the abnormal glow region which is shown by the increase in the discharge voltage before the glow to arc transition took place at 150 mA.

The variation of discharge voltage with electrode separation at different values of current is shown in Fig. 4.16. The straight lines which represent the voltage gradient along the positive column intersect the voltage axis giving a zero-length voltage of 385 V. This value is used to derive the static characteristic of the positive column for the 10 mm long discharge. The broken line in

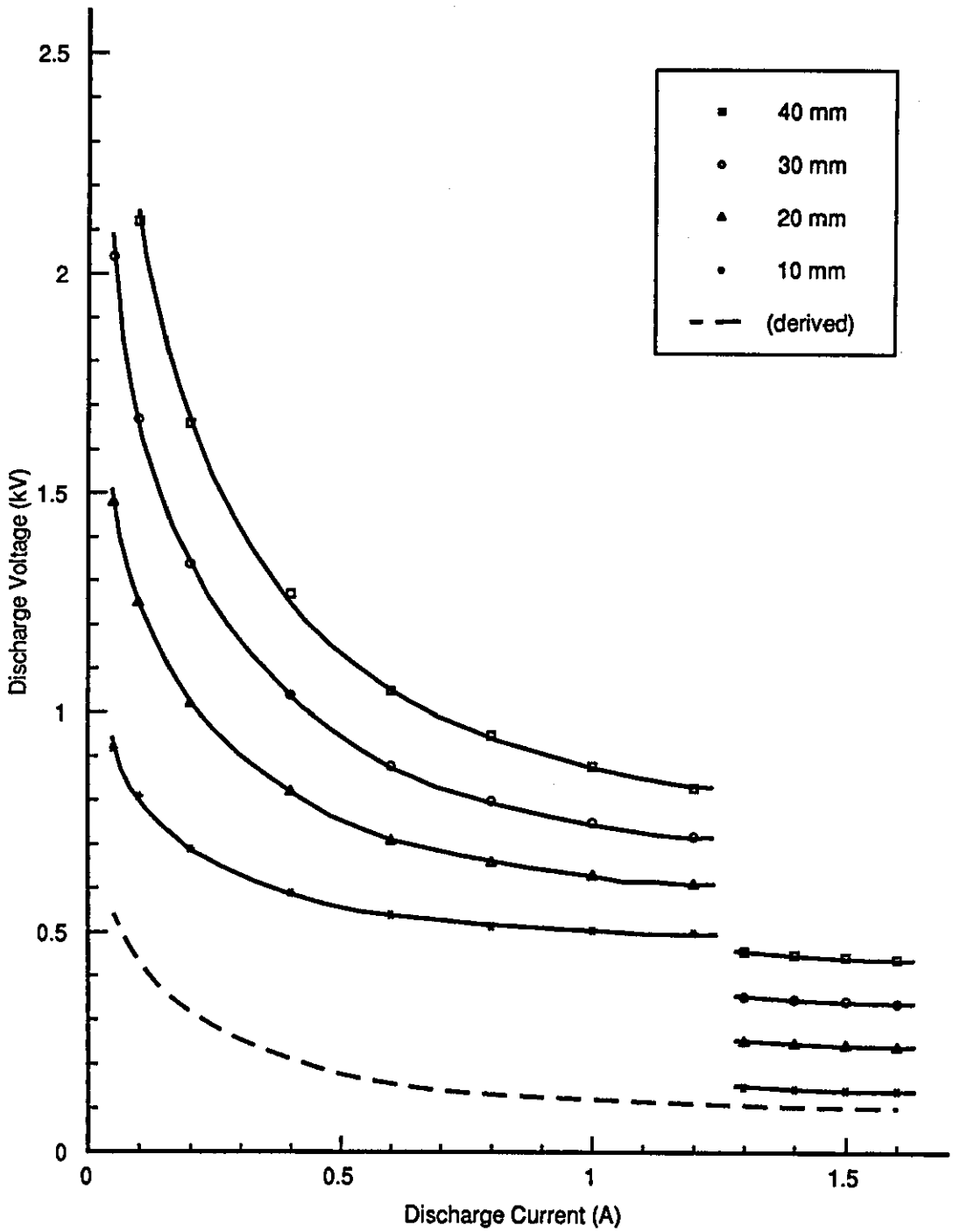

Fig. 4.13 The voltage-current characteristics in CO_2 laser gas mixture at atmospheric pressure

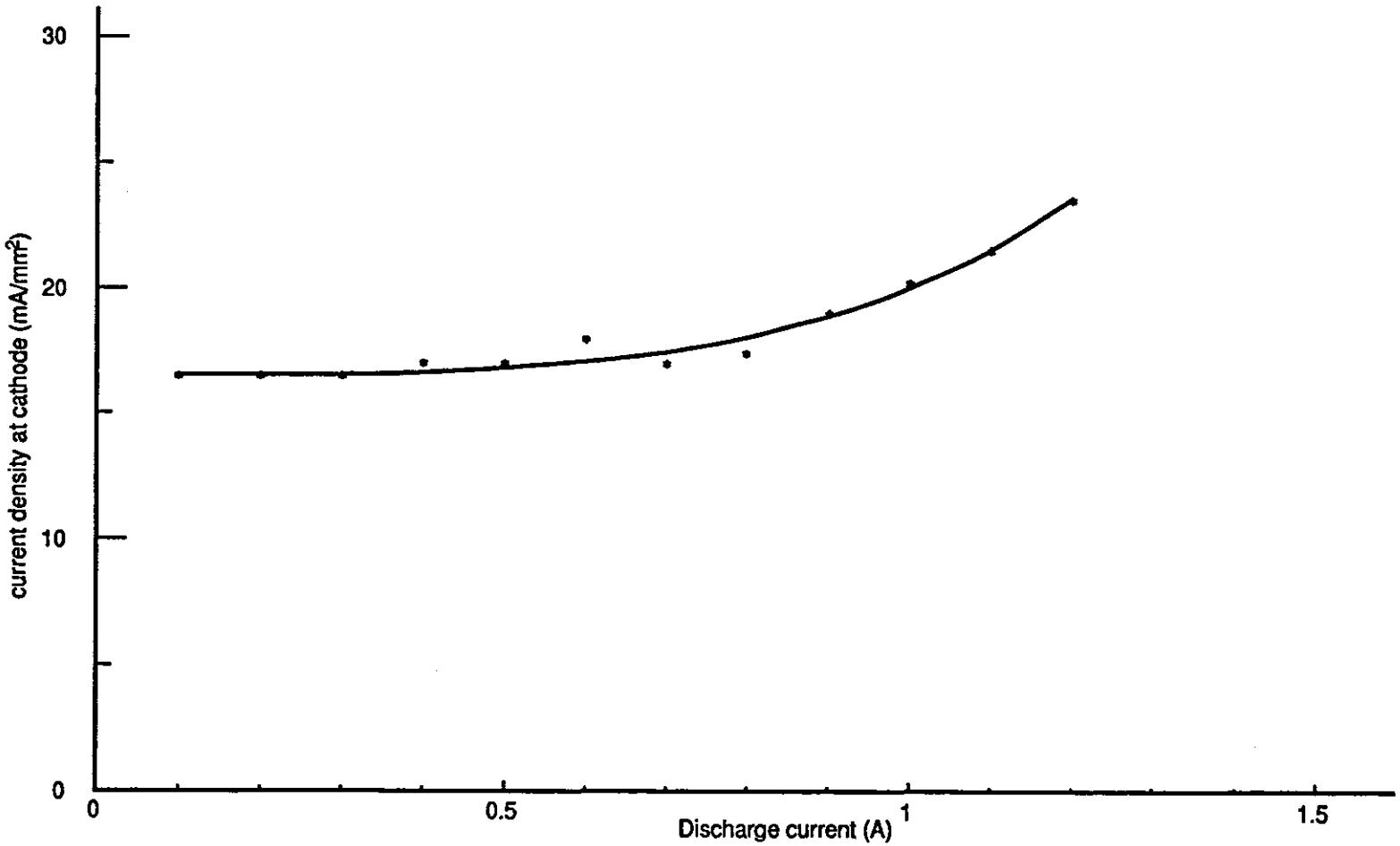

Fig. 4.14 Variation of current density at the cathode with discharge current in CO_2 laser gas mixture at atmospheric pressure

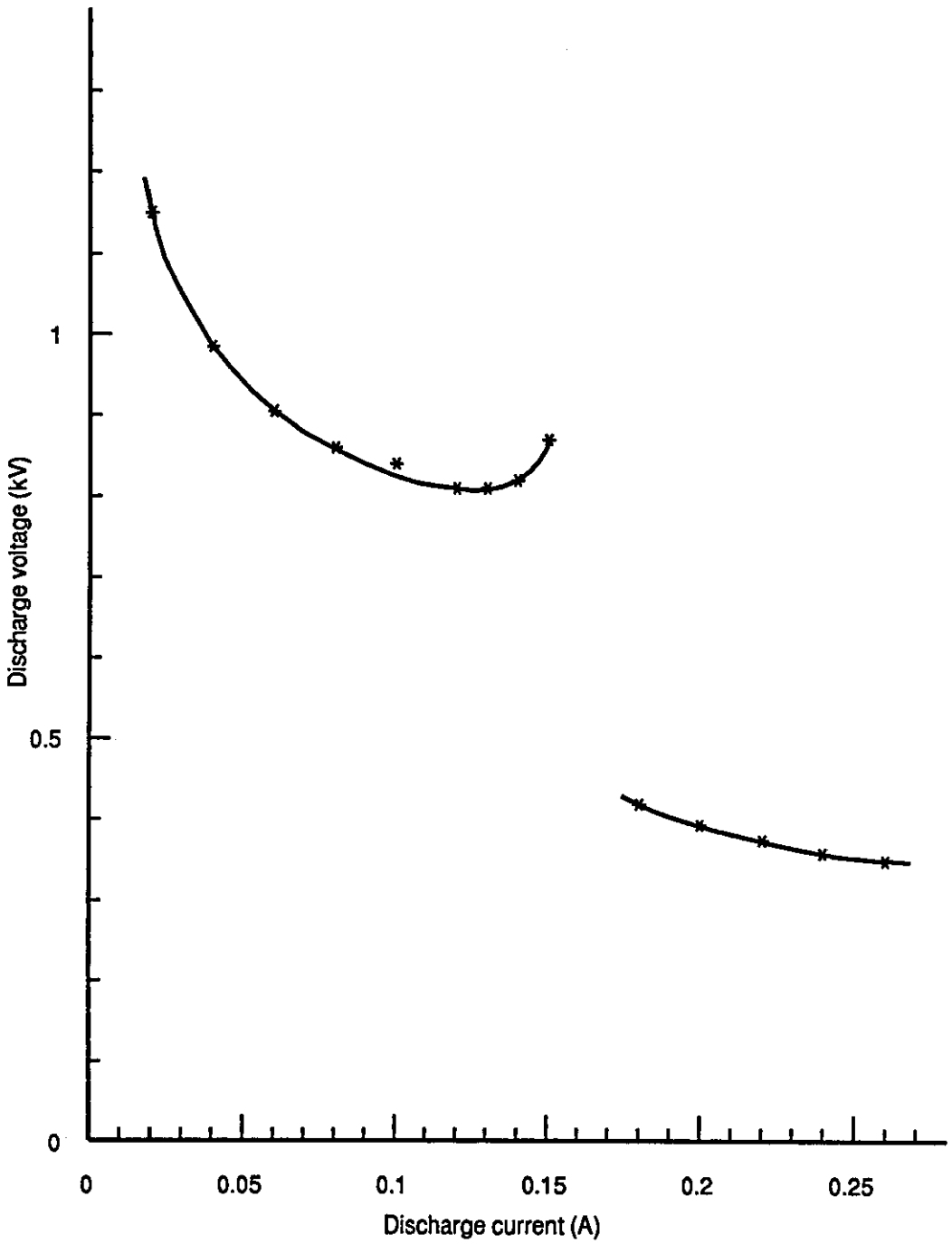

Fig. 4.15 The V-I characteristic in CO_2 laser gas mixture at atmospheric pressure with 3 mm cathode diameter

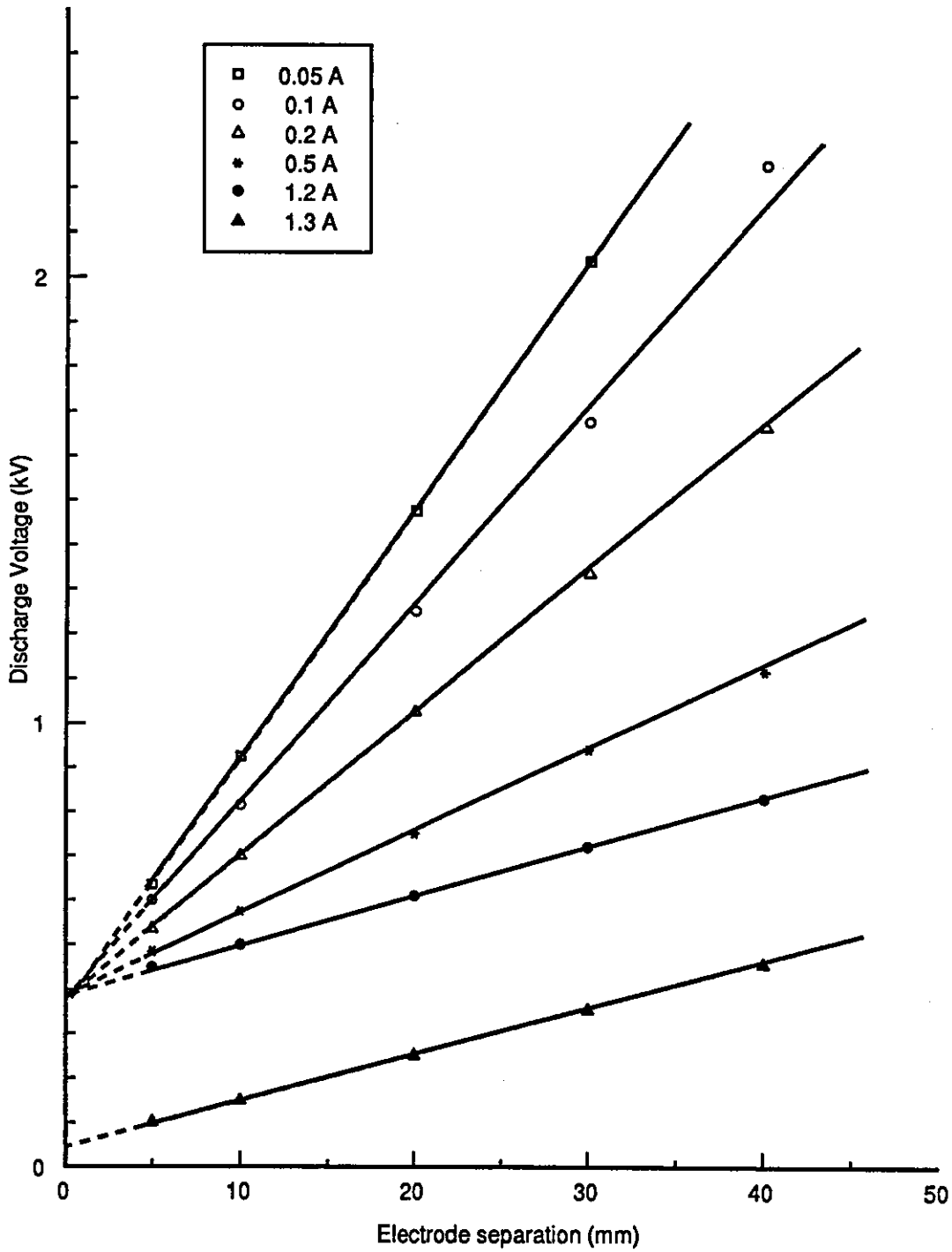

Fig. 4.16 Variation of discharge voltage with electrode separation in CO_2 laser gas mixture at atmospheric pressure

Fig. 4.13 which represents this characteristic shows clearly that the glow to arc transition is only a cathode region phenomenon without any influence on the positive column.

4.4.3 Electric Discharge in He and Ar

The static characteristic of an electric discharge in helium (which is a base for most of the gas laser mixtures), and argon (which is widely used in arc welding), at atmospheric pressure has been studied for comparison with the results obtained for air and the CO_2 laser gas mixture. The variation of the discharge voltage with current in He (purity 99.995%) and Ar (purity 99.998%) at atmospheric pressure is shown in Fig. 4.17 and Fig. 4.18 for different values of electrode separation. The glow to arc transition occurred at about 1.0 A in both cases.

Figs. 4.19 and 4.20 show the variation of discharge voltage with electrode separation at different values of current in He and Ar respectively. The two figures give the zero-length voltages of 210 V (He), and 140 V (Ar) for copper electrodes. These values are used to derive the positive column static characteristic for the 10 mm long discharge shown in Figs. 4.17 and 4.18. The positive column characteristic curves (the broken lines) show no discrete transitions. It is interesting to note that the V-I characteristic for argon (Fig. 4.18) shows that the discharge voltage levels out well before the glow to arc transition takes place in the cathode region.

4.5 THE POSITIVE COLUMN CHARACTERISTIC

The voltage-current characteristics derived for the positive column for the 10 mm long discharge in air, He, Ar and CO_2 laser gas mixture are shown in Fig. 4.21. The

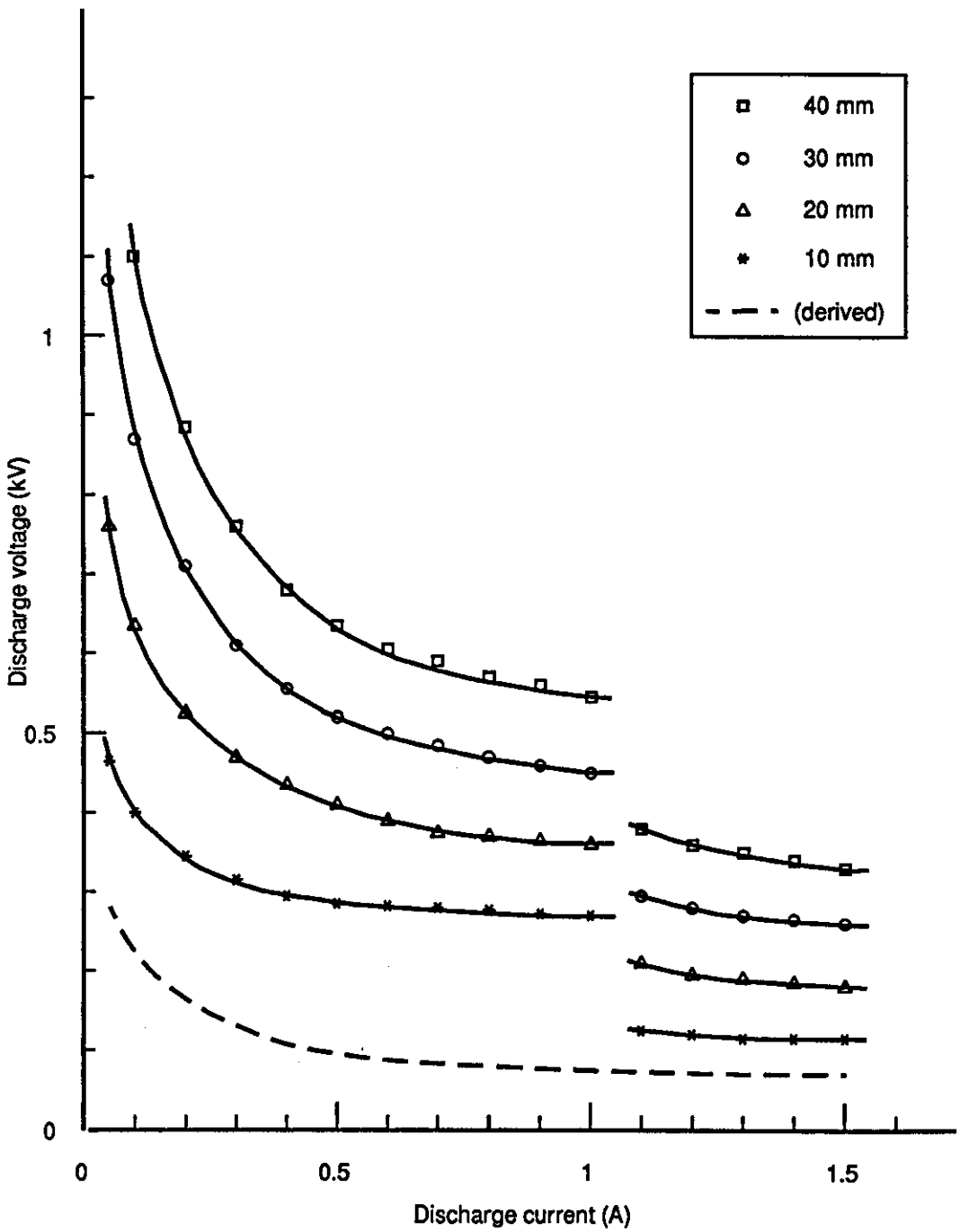

Fig. 4.17 The voltage-current characteristics in He at atmospheric pressure

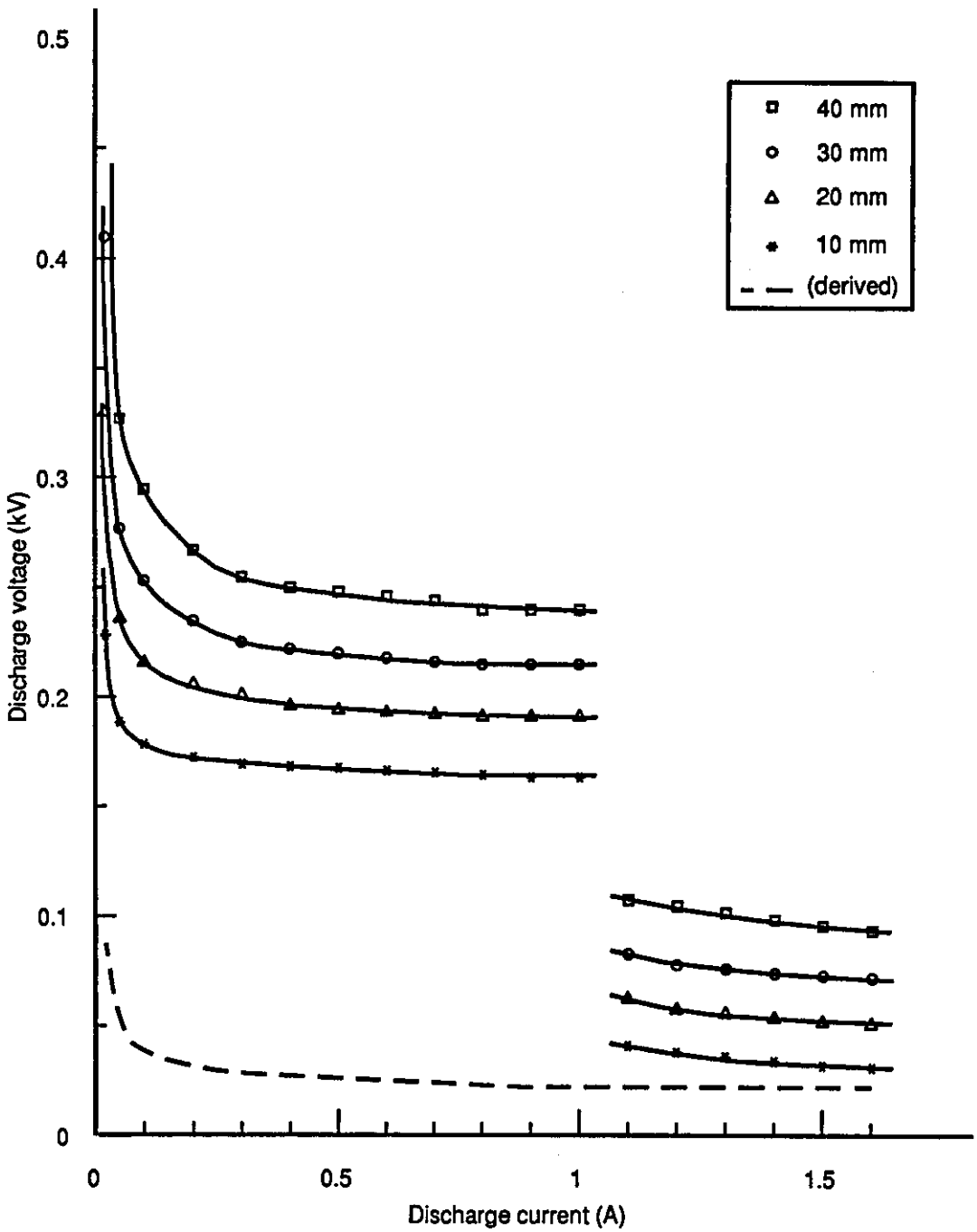

Fig. 4.18 The voltage-current characteristics in Ar at atmospheric pressure

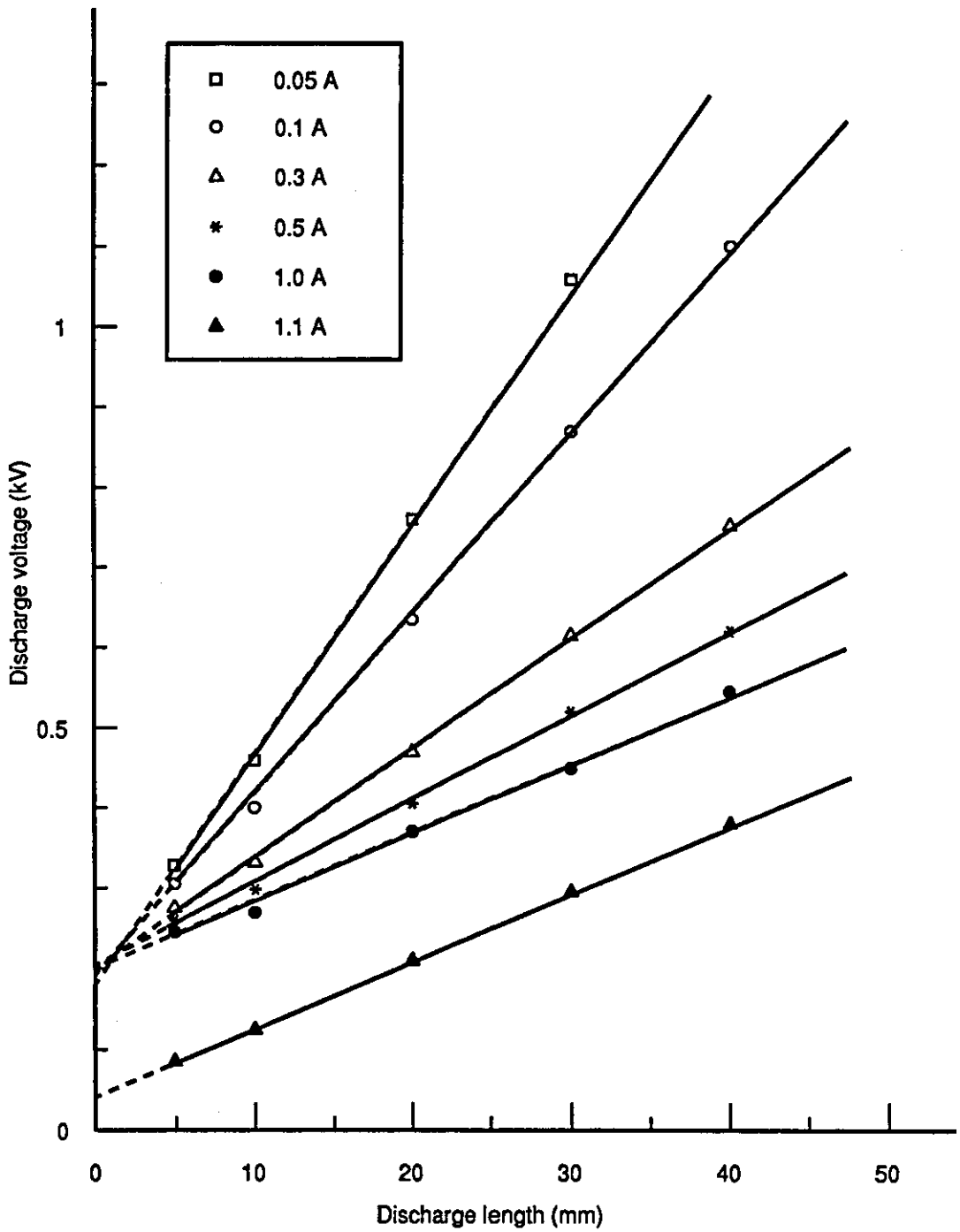

Fig. 4.19 Variation of discharge voltage with electrode separation in He at atmospheric pressure

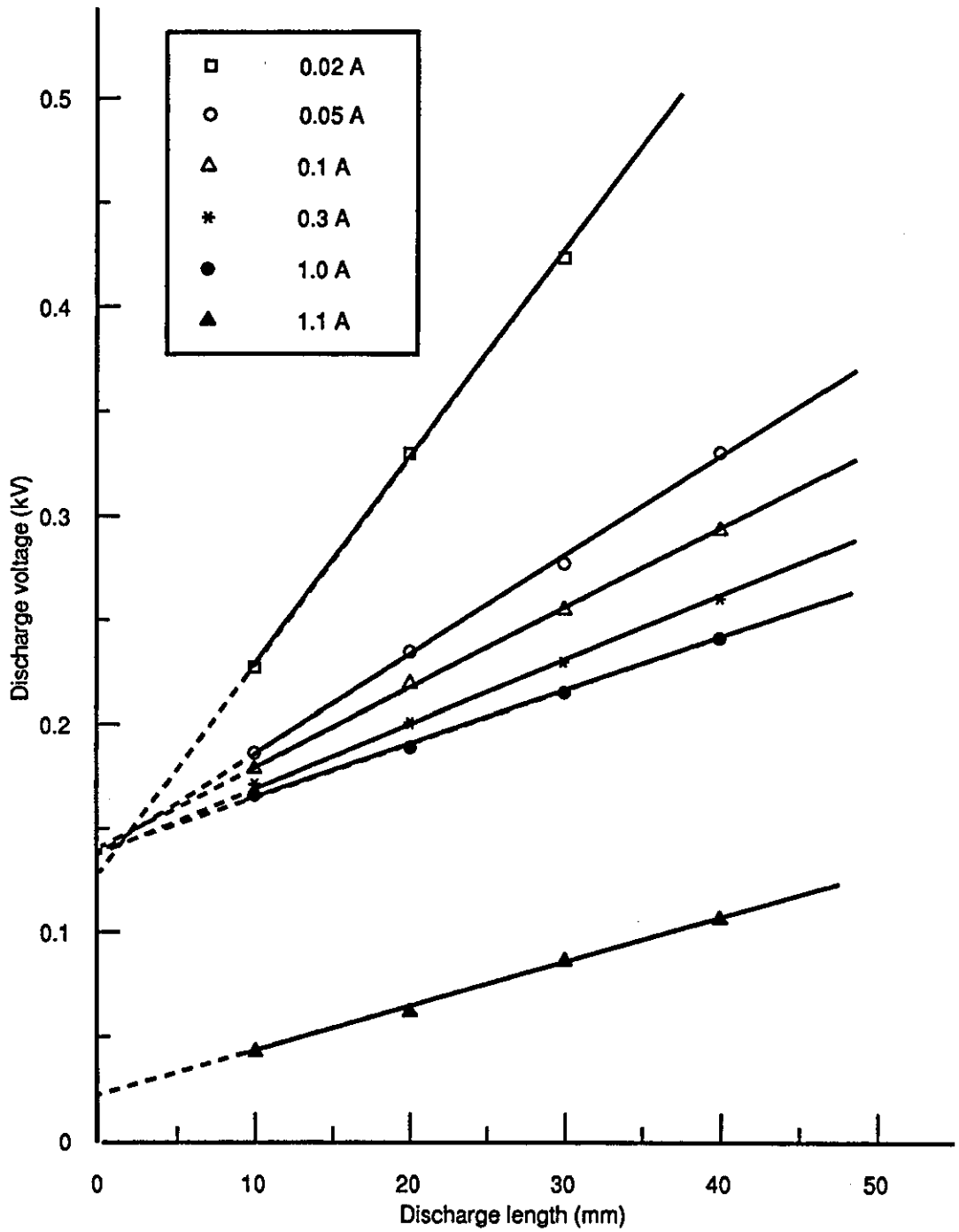

Fig. 4.20 Variation of discharge voltage with electrode separation in Ar at atmospheric pressure

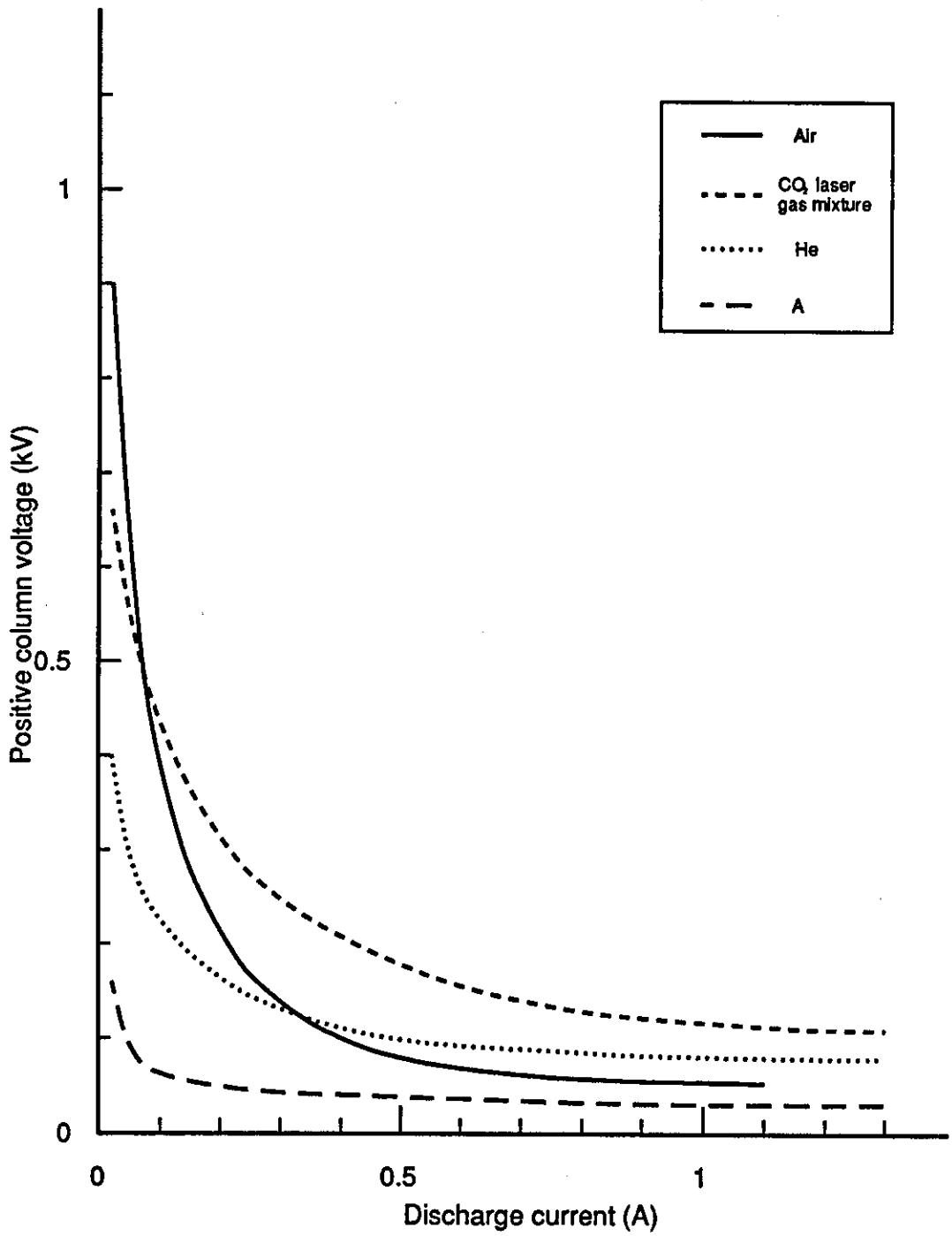

Fig. 4.21 The voltage-current characteristics derived for the positive column for different gases at atmospheric pressure

different characteristic curves show that the voltage along the positive column decreases rapidly and then tends to become constant as the discharge current is increased. The positive column voltage is independent of the glow to arc transition in the cathode region. Fig. 4.11 (air) shows the glow to arc transition occurring before the positive column voltage gradient has become constant while Fig. 4.18 shows the glow to arc transition occurring in Ar well after the voltage has become constant.

The discharge characteristic curves derived for the positive column show that there are two different regions of the self-sustained discharge positive column. The first is the low current region where the voltage decreases sharply as the current is increased which is the subnormal glow region, and second, where the voltage is almost constant with current which is the normal glow (when the cathode is in the glow regime) and arc (when the cathode is in the arc regime).

It is concluded that glow and arc are two meaningless terms when used to describe the positive column and the real change in the positive column characteristic is between the subnormal and the normal glow.

The positive column behaviour in the subnormal and normal glow is thought to be due to the two different ionisation processes, the field and thermal ionisation processes. At low current, the positive column is relatively cold and the ionisation is mostly by electrons (field ionisation). The ionisation process needs a high electric field to accelerate the electrons to a high enough velocity to ionise the gas molecules by electron-molecule collision. As the current is increased, the gas temperature increases and the molecules gain enough energy to ionise each other by molecule-molecule collision (thermal ionisation). The voltage falls down steeply with increase in current, as the electrical resistance of the ionised column is reduced. The voltage

stays constant as the current is increased further and slower electrons are able to sustain the discharge and carry the current in the discharge column. The discharge column voltage is always the minimum according to Steenbeck's minimum principle which is investigated in Chapter 5.

Cooling the positive column limits the molecule-molecule ionisation process. This increases the force which causes the voltage gradient to increase and maintain the flow of current in the discharge by giving more energy to the electrons and enhance the electron-molecule ionisation process. As the cooling of the positive column causes the increase of the electron energy, molecular transition selection may be possible by controlling the cooling of the discharge.

The rate of decrease in the discharge voltage in the subnormal glow varies from one gas to another and it is suggested that it is related to the thermal conductivity of the gas. Table 4.1 shows the thermal conductivity of gases used in the tests at 1 b, at different temperatures. The thermal conductivity at low temperature (300-5000 K) should be considered, as the relatively cold gas surrounding the ionised column may play a significant role in convecting the heat out of the discharge column. Argon, which has a low thermal conductivity, has a very steep subnormal characteristic. This may be because the gas temperature in the positive column becomes hotter with increase in current in argon due to the low thermal conductivity of the relatively cold gas around the column compared with the other gases, and the shift from the subnormal to the normal glow in argon occurs over a narrow range of current. Fig. 4.22 shows two photographs of the discharge in Ar at 0.02 A and 0.05 A. The difference in the diameter and the light intensity of the positive column is obvious over this narrow range of current. The same difference has been observed over wider ranges of currents in other gases (Fig. 4.21).

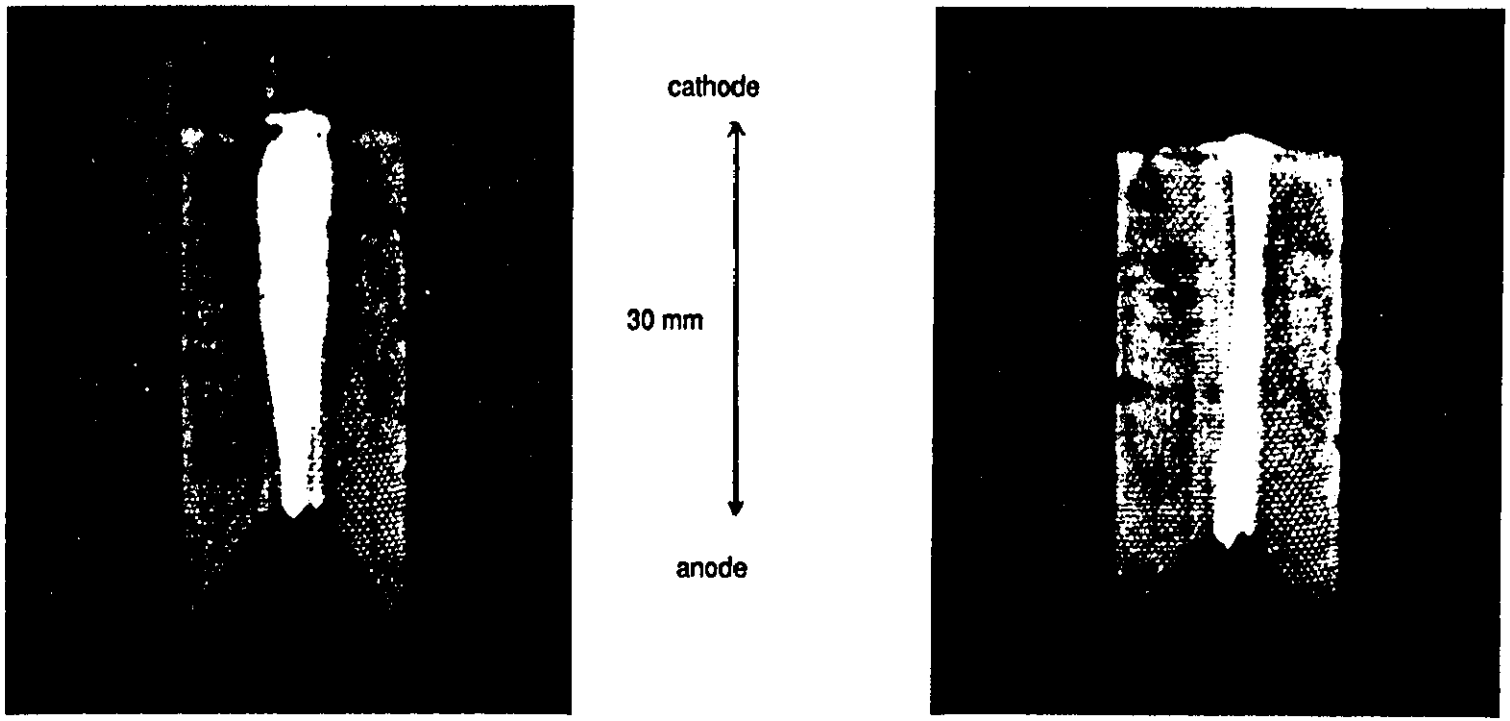

Fig. 4.22 Electric discharge in Ar at atmospheric pressure at currents of (a) 0.02 A, and (b) 0.1 A

T °K gas:	300	600	1000	2000	3500
He	0.1499	0.247	0.363	0.62	0.958
N_2	0.02598	0.0441	0.0631	0.1146	0.1915
Ar	0.01772	0.0301	0.0427	0.0692	0.106

Table 4.1 The thermal conductivity, k, mW $mm^{-1}K^{-1}$ of He, N_2 and Ar at different temperatures, (the values are extracted from Touloukian et al 1970).

The variations of positive column voltage, diameter and current density with discharge current in the CO_2 laser gas mixture are shown in Fig. 4.23. The positive column diameter was measured with a travelling telescope. The diameter of the luminous column was considered as an approximation. In the subnormal glow region the positive column appeared diffused. Initially, as the current was increased, the diameter d expanded to A then contracted to B, but, the current density J increased and continued to increase up to D, and the voltage decreased. As the current was increased further, the positive column started to expand again slowly to C, but, the current density started to decrease to E, while the voltage tended to stay constant. The first positive column expansion is thought to be due to the low degree of ionisation of the discharge column at low current, and the second expansion is due to the low gas density in the column due to its high temperature as the current was increased further.

4.6 THE OSCILLATION PHENOMENON AT THE GLOW TO ARC TRANSITION

The tests have shown that as the discharge current is increased, prior to the glow to arc transition, the electric discharge behaves in either of two ways in the cathode fall region;

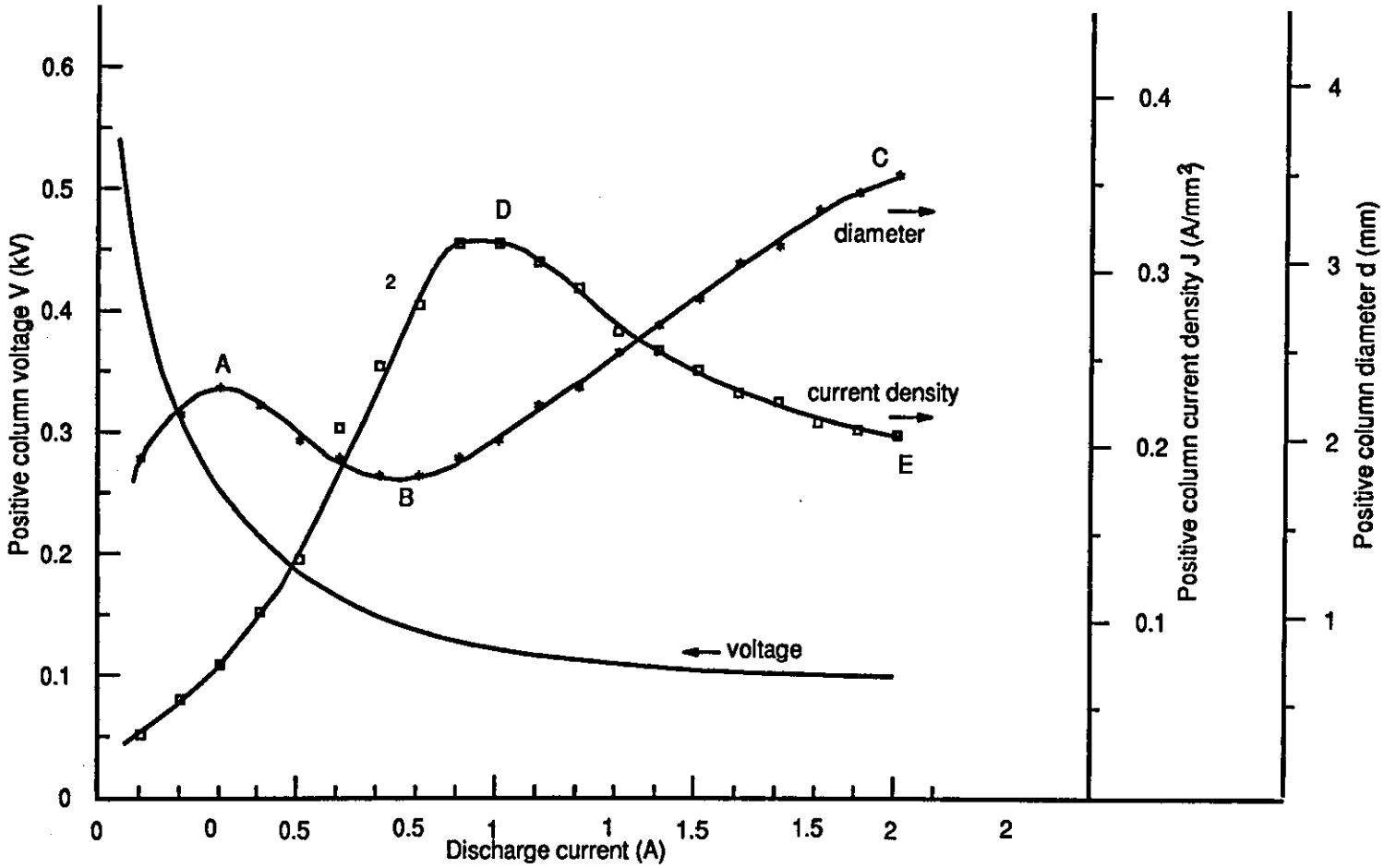

Fig. 4.23 Variations of the positive column voltage, diameter, and current density with current in CO_2 laser gas mixture at atmospheric pressure

(i) If the cathode surface area is relatively small, then, increasing the current beyond the value at which the glow covers the whole cathode surface area results in more concentrated space charge in front of the cathode. Therefore, the cathode fall increases and the discharge enters the abnormal glow region (Fig. 4.15).
(ii) If the cathode surface area is relatively large (compared with the negative glow area), then, at high current, the positive column contracts before the negative glow covers the whole cathode surface. The positive column contraction slows down the negative glow expansion and at high current the negative glow current density increases (Fig. 4.14), which also results in more concentrated space charge in front of the cathode.

In both cases the power density increases in the cathode fall region as the current is increased. At a critical current, the discharge suddenly changes to the arc, with a sudden increase in the current density at the cathode and a sudden reduction in the cathode fall voltage.

The discharge voltage prior to and after the transition was measured using a high voltage probe connected to an oscilloscope. A 10 k ohm resistive load was connected in series with the discharge. The discharge voltage appeared to be oscillating between the glow and the arc discharge voltages implying that the discharge in the glow to arc transition region was not stable either in the glow mode or in the arc mode. Fig. 4.24a shows the discharge voltage waveform prior to the transition which shows the voltage oscillation with a glow discharge voltage predominating. Fig. 4.24b shows the discharge voltage waveform just after the transition which shows the voltage oscillation with an arc predominating. The oscillation appears to be not regular and more than 5 transitions per second can be seen. Over the oscillating

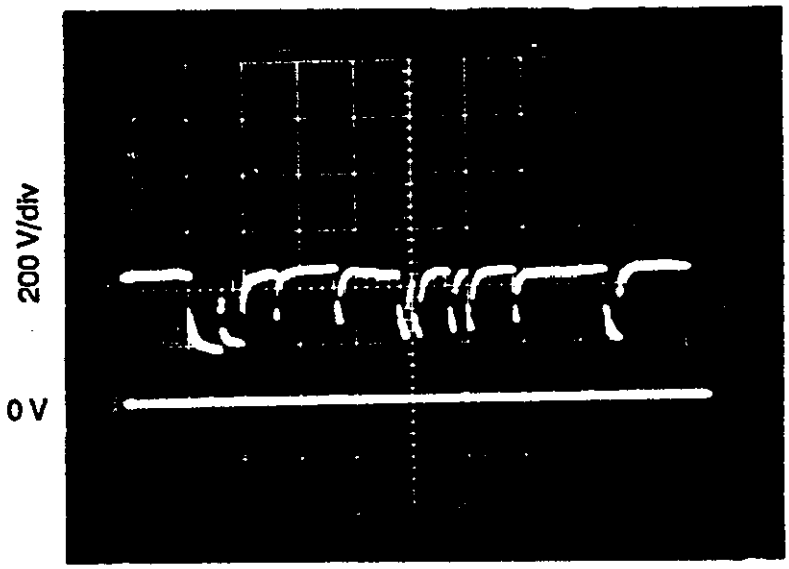

(a)

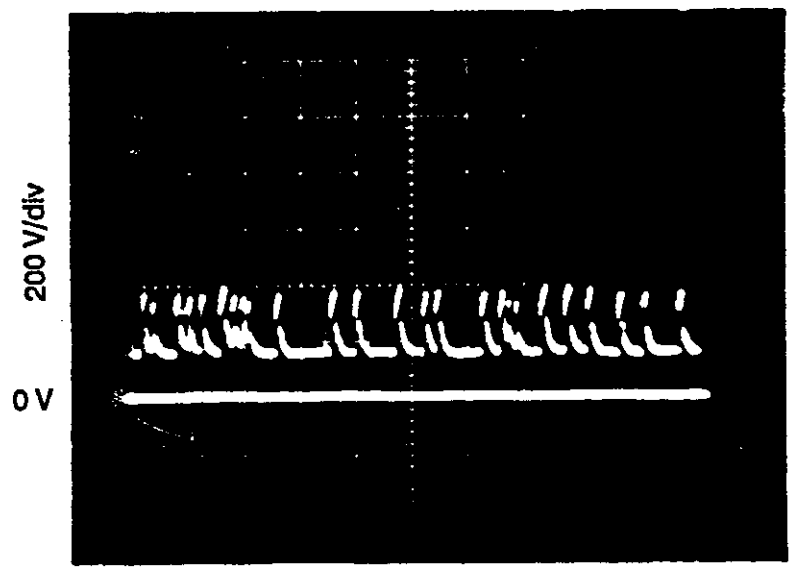

(b)

Fig. 4.24 Voltage waveform at the glow to arc trasition in air for 10 mm long discharge at current of 0.4 A,
(a) before transition
(b) after transition

region, the discharge prior to the transition appeared visually as a stable glow and after the transition as a stable arc.

The phenomenon of oscillation between glow and arc discharges at the glow to arc transition can be explained by considering the different emission processes. In the glow discharge, the cathode fall voltage is high due to the space charge in front of the cathode which extends a substantial distance away from the cathode (depending on the pressure). Prior to the transition, as the current is increased, the current density at the cathode increases, and, the power dissipated as heat in the cathode fall region is concentrated in a small region which heats up the cathode. At a critical current the discharge suddenly changes to an arc accompanied by a sudden reduction in the cathode fall voltage due to the change in distribution of the space charge in front of the cathode as the space charge decreases and moves closer to the cathode surface due to the different electron emission process at the cathode (Cobine 1958). At this point, just after the transition, the power dissipated as heat in the cathode fall region is considerably reduced due to the reduction of the cathode fall voltage, and it may not be possible to maintain the electron emission process in the arc mode at the cathode. As the discharge starts to terminate, the discharge voltage starts to increase, where the open circuit voltage is higher than the discharge voltage, and at a critical voltage the electron emission process in the glow mode at the cathode fall is restored. If the current is increased further, the discharge stays longer in the arc regime as the power dissipated as heat at the arc cathode fall region is increased until the current has become high enough to maintain the electron emission process of the arc at the cathode.

4.7 SUMMARY OF RESULTS

(i) This investigation has shown that a high power glow discharge in a still gas is possible even at high pressure and the glow discharge is solely a cathode fall region phenomenon and has no influence on the positive column characteristic.

(ii) The glow to arc transition at the cathode can oscillate between a glow and arc discharge, neither of which is stable with time at the transition current.

(iii) As the current is increased, the rate of contraction of the positive column accompanied by the reduction of its voltage gradient is higher in a gas of low thermal conductivity which implies that the domination of the thermal ionisation process over the field ionisation process causes the positive column contraction and the reduction in its voltage gradient.

(iv) The high power glow discharge in a still gas is not necessarily suitable for gas lasers excitation where the positive column is contracted and electron temperature is not sufficient for molecular transitions due to the domination of the thermal ionisation process over the field ionisation process.

(v) Expectation of a high power high pressure CO_2 laser is possible with effective and homogeneous cooling of the positive column which can also be used to control the energy of the electron for the selected transition and is more efficient if the discharge has the cathode root in the arc mode.

CHAPTER 5

THE CHARACTERISTICS OF THE POSITIVE COLUMN

5.1 INTRODUCTION

The static discharge characteristics were investigated over a wide range of pressure in different gases in the previous chapter. It was shown that the positive column characteristic is independent of the glow to arc transition (Fig. 4.21), and there is a gradual change from predominantly field ionisation to thermal ionisation with increasing current.

Gas laser excitation processes usually occur in the positive column of the discharge, where over a limited range of gas pressure and discharge current, the electrons have the appropriate energy for the required excitation transitions. Increasing the discharge current and the gas pressure is an important objective to increase the laser output power and the power density, but, they are limited by the contraction of the positive column where the gas temperature increases, which quenches the laser excitation process, and the electron temperature decreases due to the reduction in the discharge voltage.

A fast flow gas injected into the discharge has been used in α CO_2 laser, to convectively cool the discharge and to increase the electron temperature by diffusing the discharge column and increasing its voltage gradient (Evans 1987). The electrical input power to the fast gas flow discharge is however limited by the formation of streamers within the positive column which is accompanied by an abrupt reduction in the discharge voltage.

This chapter investigates the different features of the positive column under conditions relative to the electric discharge techniques used for laser excitation. The investigation includes a theoretical model for the electric discharge behaviour in multiple discharges.

5.2 THE EMISSION SPECTRUM AT THE GLOW TO ARC TRANSITION

The interactions of ions and electrons with each other and with the neutral particles affect the radiation spectrum of the plasma in several ways. The structure of the emission spectrum of the positive column is therefore a reflection of the particle densities and their energy distribution. As the discharge current is increased the thermal ionisation process dominates the field ionisation process in the positive column, this is also reflected in the radiation spectrum.

A series of tests therefore have been carried out to examine the emission spectra of the positive column at different values of discharge current in order to show the effect of the glow to arc transition on the spectrum of the positive column. The tests were carried out in helium and argon chosen for their relatively simple spectrum.

5.2.1 The Scanning Monochromator For Measuring The Radiation Spectrum

The radiation spectrum emitted from the positive column was measured using a scanning monochromator (Appendix 1) which enabled the complete spectrum over the range 200 nm to 930 nm to be displayed on an oscilloscope.

Light from the source was directed into the monochromator via a flexible fibre-optic light-guide (2.5mm active diameter) and dispersed into a spectrum by a diffraction grating mounted in an Ebert optical configuration (Fig. 5.1). Light from the output slit of the monochromator was directed into a photomultiplier, and the output was amplified and displayed on an oscilloscope. A complete spectrum was produced by the

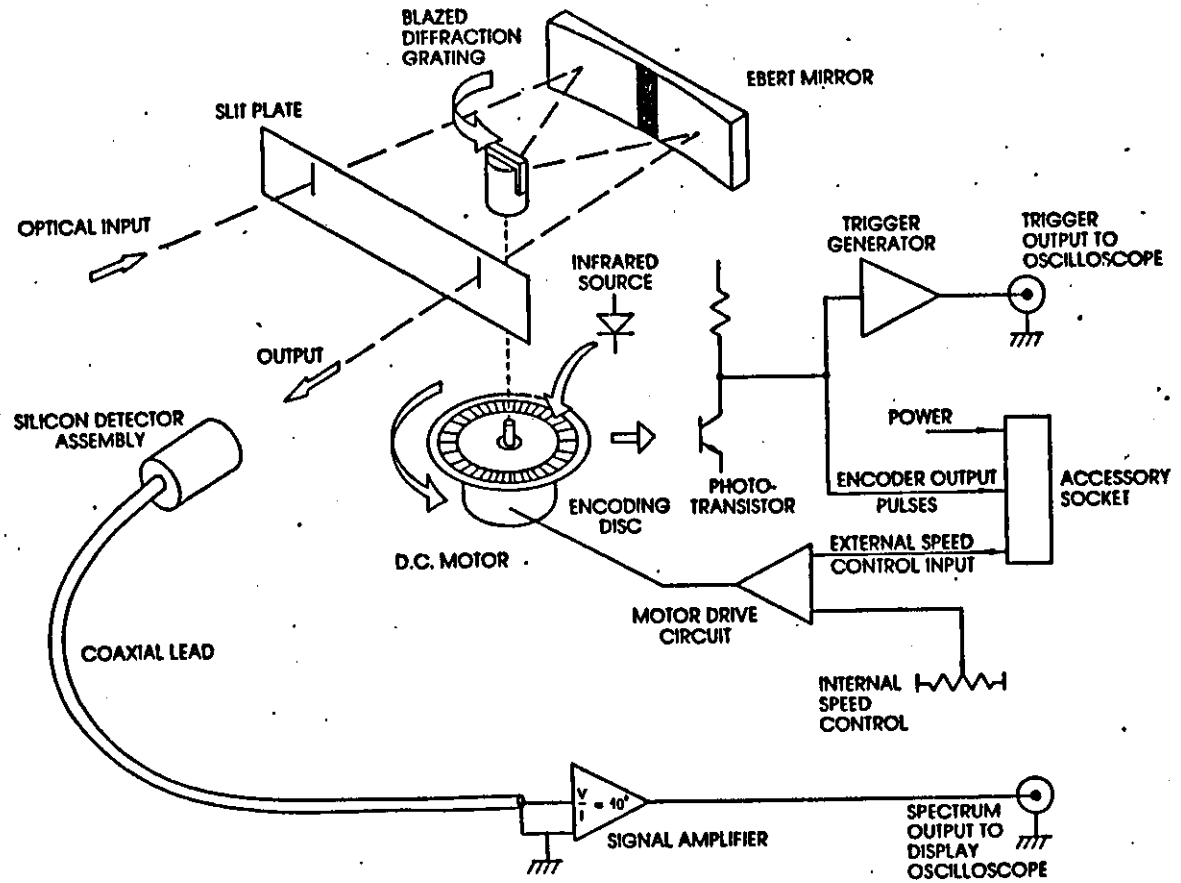

Fig. 5.1 Schematic of optical system for measuring the emission spectrum of the positive column (after Angus 1980)

rotation of the diffraction grating at a scanning rate of approximately 10 Hz. The Wavelength scale was generated by a shaft encoder attached to the rotating diffraction grating and was also displayed on the oscilloscope. The wavelength can be measured to an accuracy of ±0.5 nm between 400 nm and 700 nm, and to ±1 nm for the remainder of the spectrum between 200 nm and 930 nm, by using a moveable cursor pulse generated as part of the wavelength scale. The relative intensity of spectral lines was measured using the wavelength marker pulse in conjunction with a sample and hold circuit.

The optical bandwidth of the monochromator was set at 10 nm using input and output slits so that the resolution was just adequate for the intensity of the radiation to be measured.

The electric discharge electrode assembly discussed in the previous chapter (Fig. 4.10) was used as the source. The input to the fibre-optic light guide was positioned at less than 10 mm from the positive column; the discharge was 40mm long so that the radiation from the fall regions could be neglected.

5.2.2 The Positive Column Emission Spectrum

The emission spectra of the electric discharge positive column in He at atmospheric pressure at three different values of current are shown in Fig. 5.2. The emission spectrum at 0.2 A where the discharge was in the subnormal glow region (Fig 4.17), is shown in Fig. 5.2a. The emission spectra of the positive column at 0.9 A and 1.0 A where the discharge was a glow at 0.9 A just before the transition and an arc at 1.0 A after the transition are shown in Figs. 5.2b and c respectively. The difference in the emission spectra just before and after the glow to arc transition appears to be insignificant apart from the emission intensity.

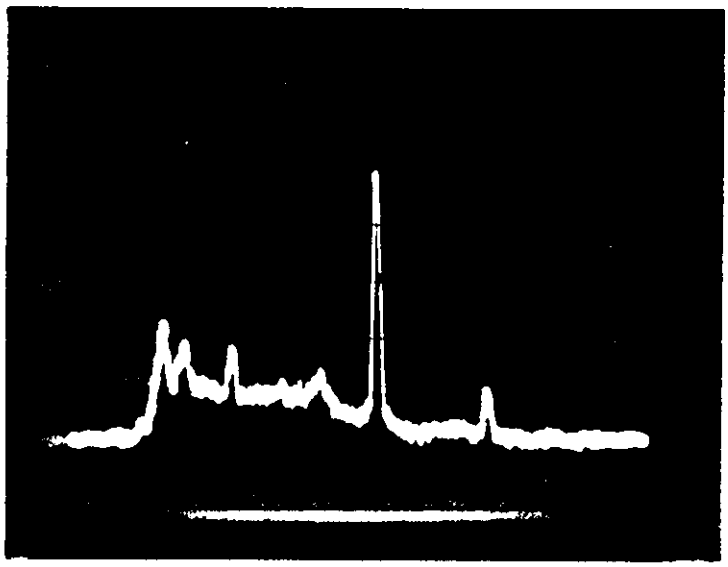

(a)

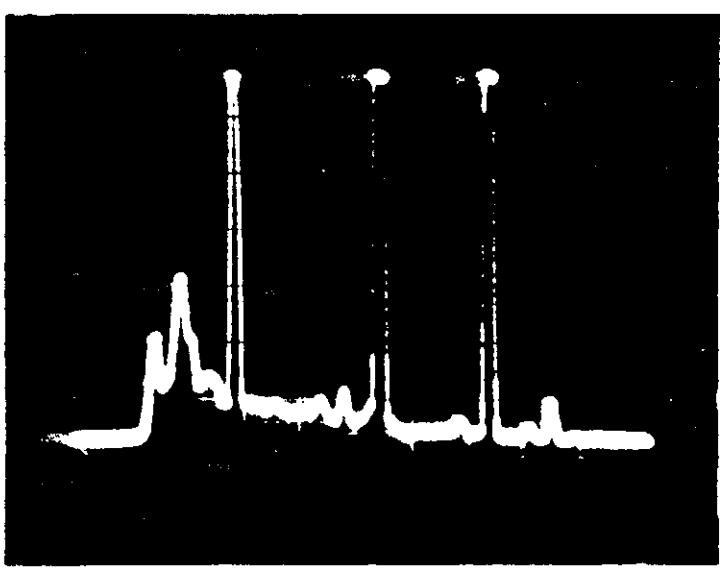

(b)

Fig. 5.2 The emission spectrum of the positive column in He at (a) 0.2 A, (b) 0.9 A and (c) 1.0 A

(c)

Fig. 5.2 (Continued)

The emission spectra of the electric discharge positive column in Ar at atmospheric pressure at three different values of current are shown in Fig. 5.3. The emission spectra before and after the glow to arc transition at 0.9 A and 1.0 A (Fig. 4.18), are shown in Figs. 5.3b and c respectively. The difference between the two again appears insignificant while the difference between them and the spectrum of the subnormal glow at 0.1 A (Fig. 5.3a) is obvious.

The investigations of the emission spectrum of the positive column indicate that the behaviour of the positive column is unaffected by the glow to arc transition which takes place in the cathode region. The difference appears to happen only between the subnormal and the normal glow where the electric field along the positive column changes with current and the ionisation process appears to change accordingly.

5.3 THE POSITIVE COLUMN BEHAVIOUR UNDER EXTERNAL FORCE

A high velocity gas flow recirculated through the laser cavity is normally used to increase the laser output power by cooling the discharge convectively. The fast flow gas affects the laser output in two ways;
(i) cooling and diffusing the discharge column so that the discharge current can be increased enabling the input power to be increased.
(ii) cooling and diffusing the discharge column causes its voltage gradient to increase, therefore the E/N ratio can be varied in order to obtain the optimum value for the electron energy needed for selected transitions.

To study the fast flow electric discharge characteristic, the voltage-current characteristic has been taken as a measure for the discharge properties and its suitability for the laser excitation in the same way as in a still gas (Saleh 1981, Evans 1987).

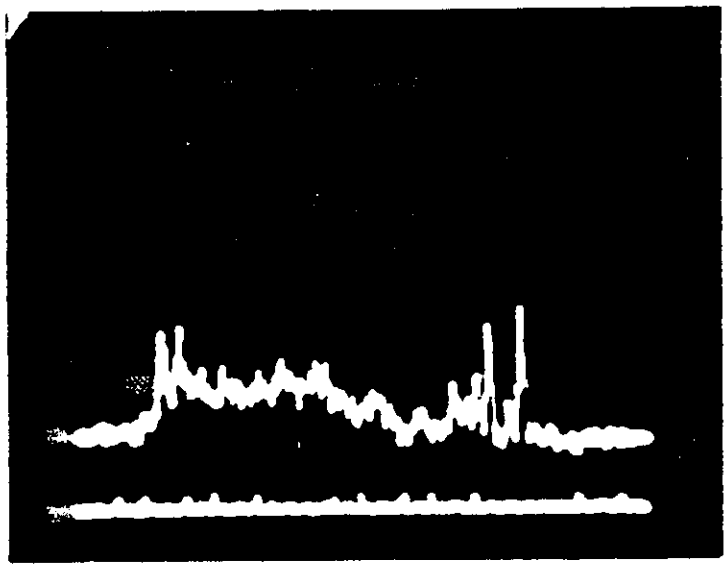

(a)

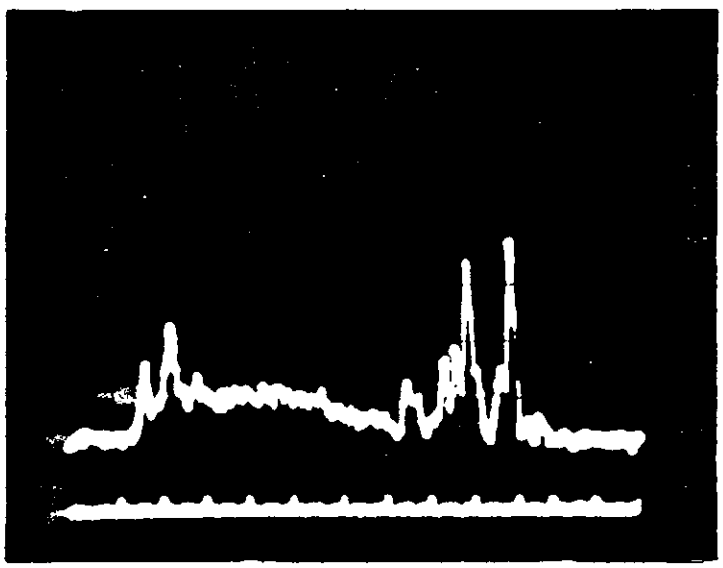

(b)

Fig. 5.3 The emission spectrum of the positive column in Ar at (a) 0.1 A, (b) 0.9 A and (c) 1.0 A

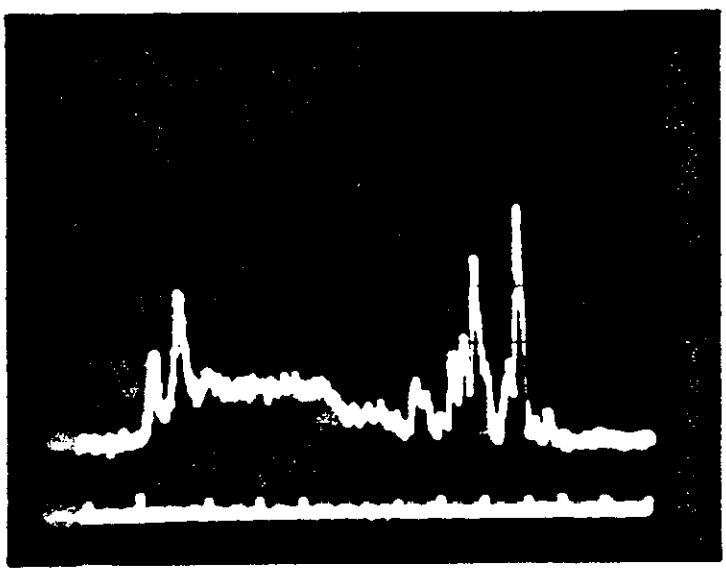

(c)

Fig. 5.3 (Continued)

5.3.1 The Positive Column Voltage Gradient

The radial distribution of the electron and gas temperatures in the positive column at different pressures are shown in Fig. 5.4. At low pressure (< 10 mb), the gas temperature is low and constant across the diameter, while the electron temperature is high and almost constant across the diameter. At high pressure (> 500 mb), the column contracts and the gas and electron temperatures become high along the column axis forming a bell shape distribution and the two temperatures are almost equal. These changes in the gas and electron temperature distributions occur gradually and continuously with increase in pressure.

It was shown in Chapter 4 that if the discharge current is increased at low pressure, the discharge column also contracts, therefore similar changes in the gas and electron temperature distributions occur.

In the fast gas flow electric discharge, low temperature gas is injected into the discharge column. The thermal ionisation process which is caused by molecule-molecule collisions due to the high gas temperature is therefore suppressed. This increases the force which causes the column voltage gradient to increase, which increases the electron temperature and the field ionisation processes start to dominate.

Diffusing a high current discharge has a similar effect to operating the discharge with still gas in the subnormal glow region where the discharge current density is low and the voltage gradient is high (Fig. 4.23).

The general voltage-current characteristic of the positive column in a still gas is shown in Fig. 5.5. At any current, the positive column will have a cross section so that the voltage gradient is a minimum (Fig. 5.6). This is known as Steenbeck's minimum principle (Appendix

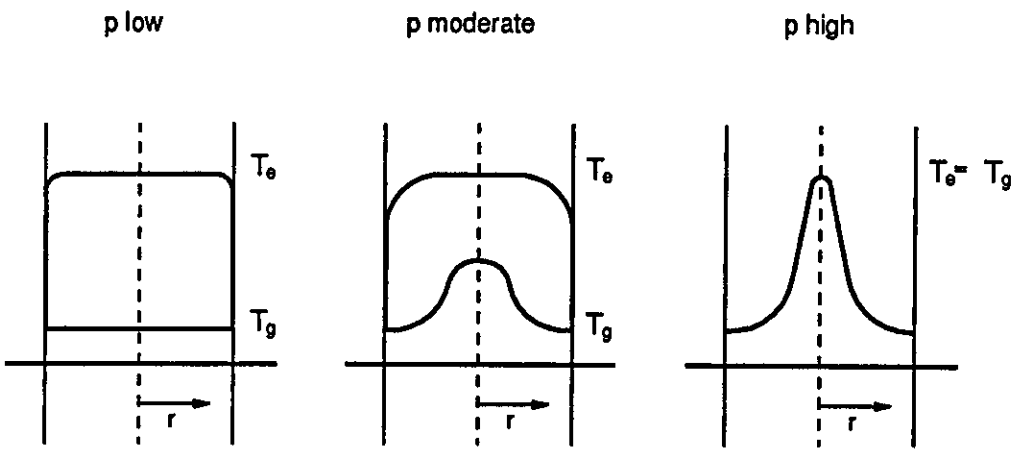

Fig. 5.4 Radial distribution of electron and gas temperatures T_e and T_g at various pressures

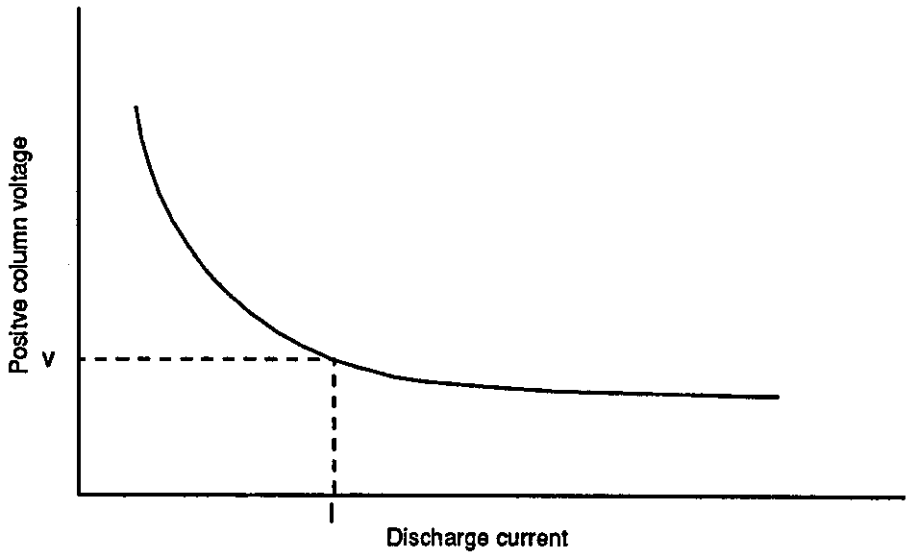

Fig. 5.5 The general V-I characteristic of the positive column

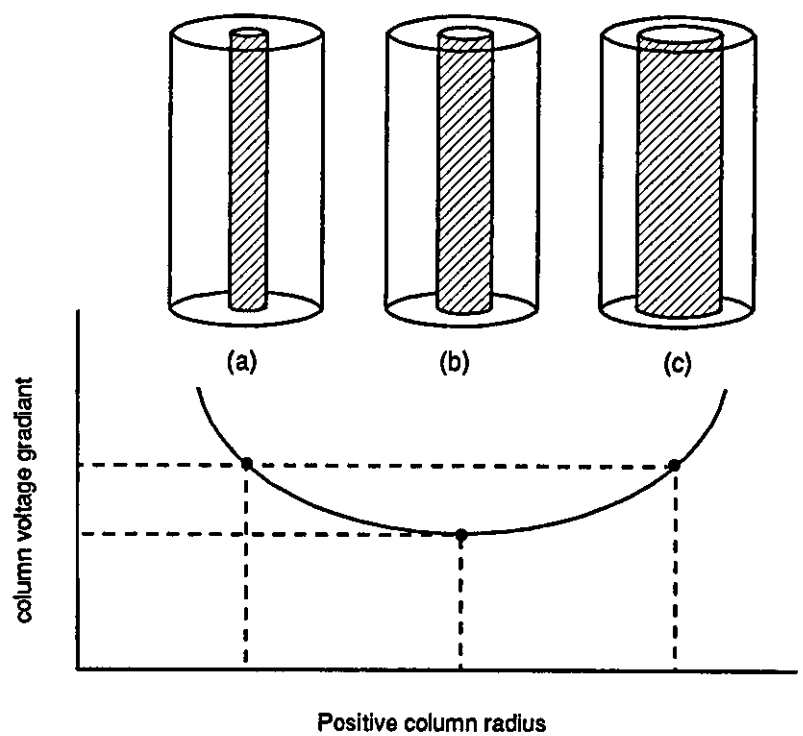

Fig. 5.6 Variation of the positive column voltage gradient with the radius

2), and can be expressed as

$$dE/dT = 0 \quad \text{or} \quad dE/dr = 0$$

which implies that for a given current and boundary conditions the positive column has a radius or temperature such that the electric field strength of the positive column is a minimum. This implies that an increase in the column voltage gradient may be caused by diffusing the discharge or by causing it to contract. Fast gas flow can diffuse or contract the discharge column causing the column voltage gradient to increase (Chapter 6).

5.3.2 Investigations Of Steenbeck's Minimum Principle

It was shown in Chapter 4 that if the discharge current is increased, the positive column contracts, the current density increases and the column voltage gradient decreases, whereas forcing the column to contract without increasing the current also increases the current density but according to the minimum principle the column voltage gradient increases.

Considering the discharge voltage as a measure for studying the discharge characteristic in fast gas flow can be misleading according to the minimum principle. It was proposed in this study to examine the minimum principle with respect to the increase of the column voltage gradient by forcing the column to contract. An electromagnetic field was applied to force the discharge column to contract. The electromagnetic field has no physical contact with the discharge column unlike the gas flow as the cooling effect can also be responsible for increasing the voltage gradient.

A conductor carrying d.c. current was used to provide an electromagnetic field which provides a constricting force to the discharge column of a multiple discharge around the conductor. The multiple discharge used four pairs of 6 mm diameter copper electrodes around an axial conductor and confined in a cylindrical Pyrex tube of 94

mm ID (Fig. 5.7). The magnetic field was provided by an axial conductor which was a water cooled copper tube inserted inside a narrow Pyrex tube (5 mm ID) to insulate it from the discharge and was designed to carry a dc current of up to 1000 A. A single power supply was used for the multiple discharge with separate stabilisation of each electrode as shown in Fig. 5.8. The axial conductor current was supplied from a separate power supply (Fig. 5.9), which was limited to 700 A.

The discharge was operated in He at 50 mb - 100 mb. At 50 mb the discharge surrounded the axial conductor uniformly (Fig. 5.10). At 100 mb the discharge was coalesced forming a long single positive column in the middle branching at the ends to the four pairs of electrodes (Fig. 5.11). The current passing through the axial conductor was parallel to the discharge current so that the electromagnetic force would attract the discharge radially towards the axial conductor and compress it as shown in Fig. 5.12.

5.3.2.1 The contracted discharge characteristic

The voltage-current characteristics of the coalesced multiple discharge in He at a pressure of 100 mb at three different values of current in the axial conductor are shown in Fig. 5.13. The discharge voltage increases as the axial current is increased, although the discharge length remains constant. At high axial current the discharge was more compressed and partially surrounding the axial conductor sheath as shown in Fig. 5.12b. The variation of the discharge voltage with the axial current at a constant value of discharge current (0.4 A) is shown in Fig. 5.14. The relation is approximately linear and shows the considerable effect of the axial current and the resultant compression force on the discharge voltage which starts to increase at around 300 A.

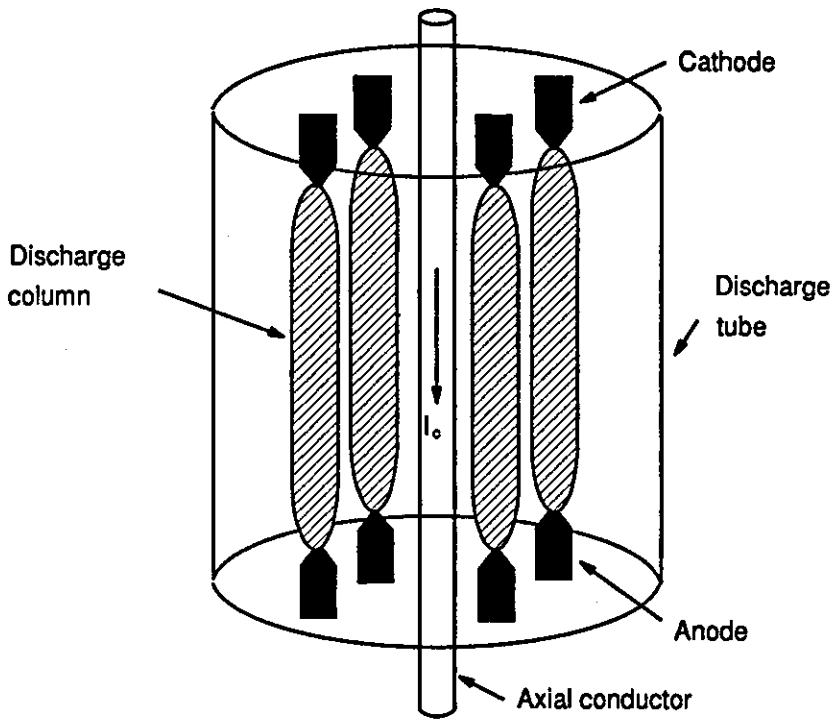

Fig. 5.7 The electrode arrangement of the multiple discharge

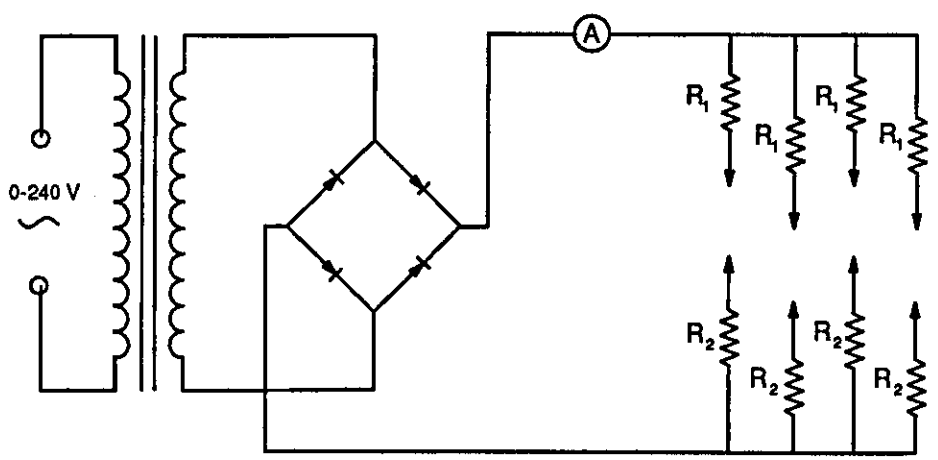

Fig. 5.8 The multiple electric discharge circuit

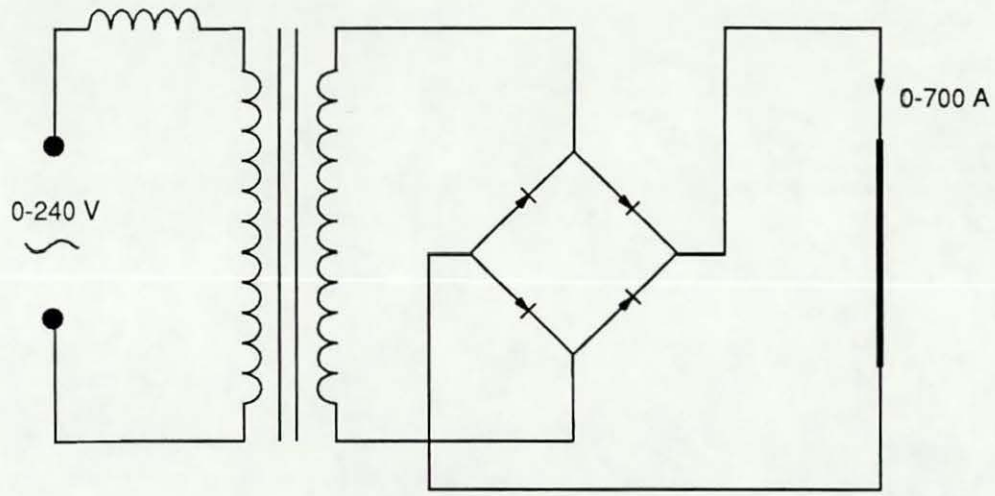

Fig. 5.9 The axial conductor current supply circuit

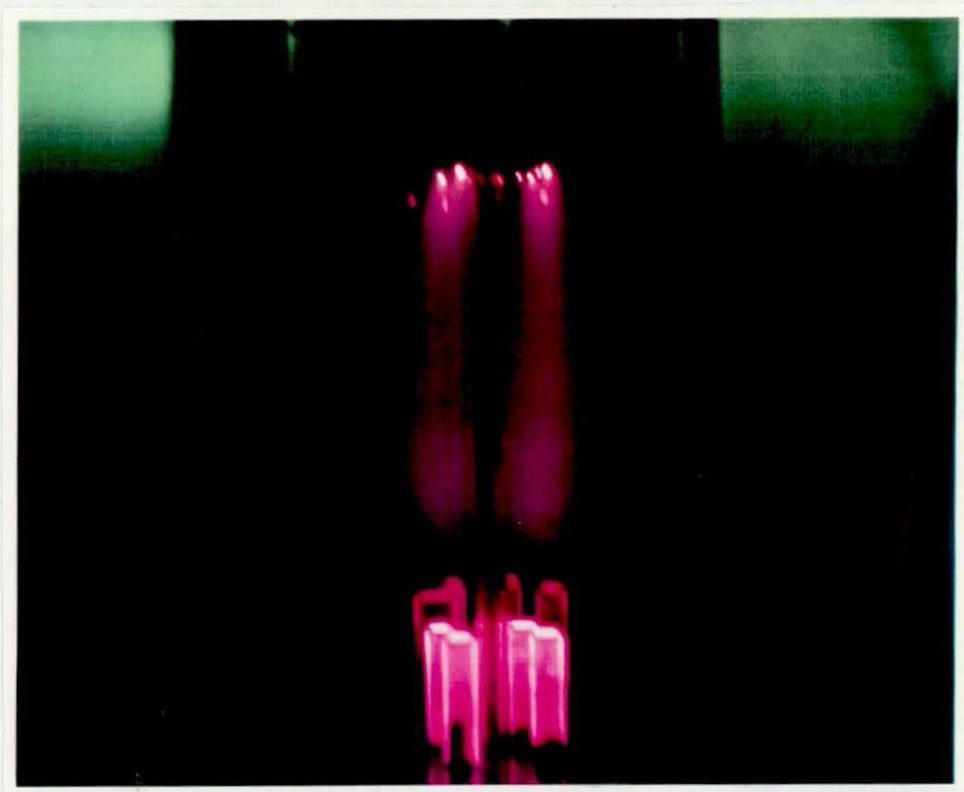

Fig. 5.10 Multiple electric discharge in He at 50 mb (second image is due to reflections).

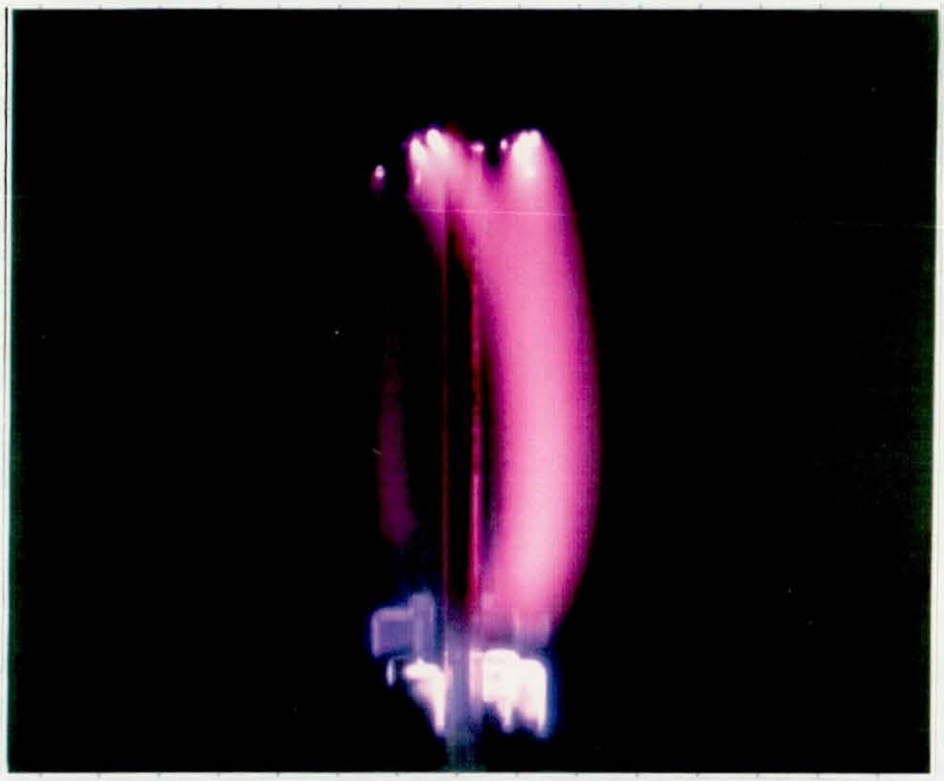

Fig. 5.11 The coalesced multiple discharge at 100 mb in He (second image is due to reflections).

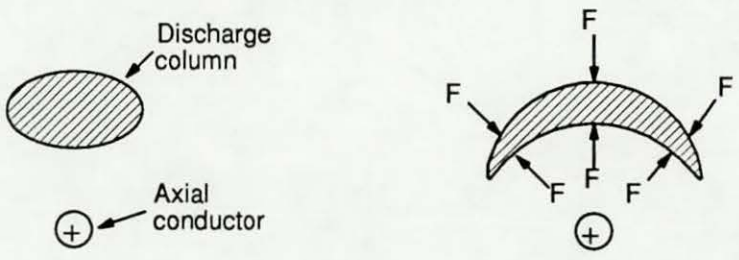

Fig. 5.12 Cross section of the coalesced discharge column
a. no current is passing through the axial conductor
b. current is passing through the axial conductor

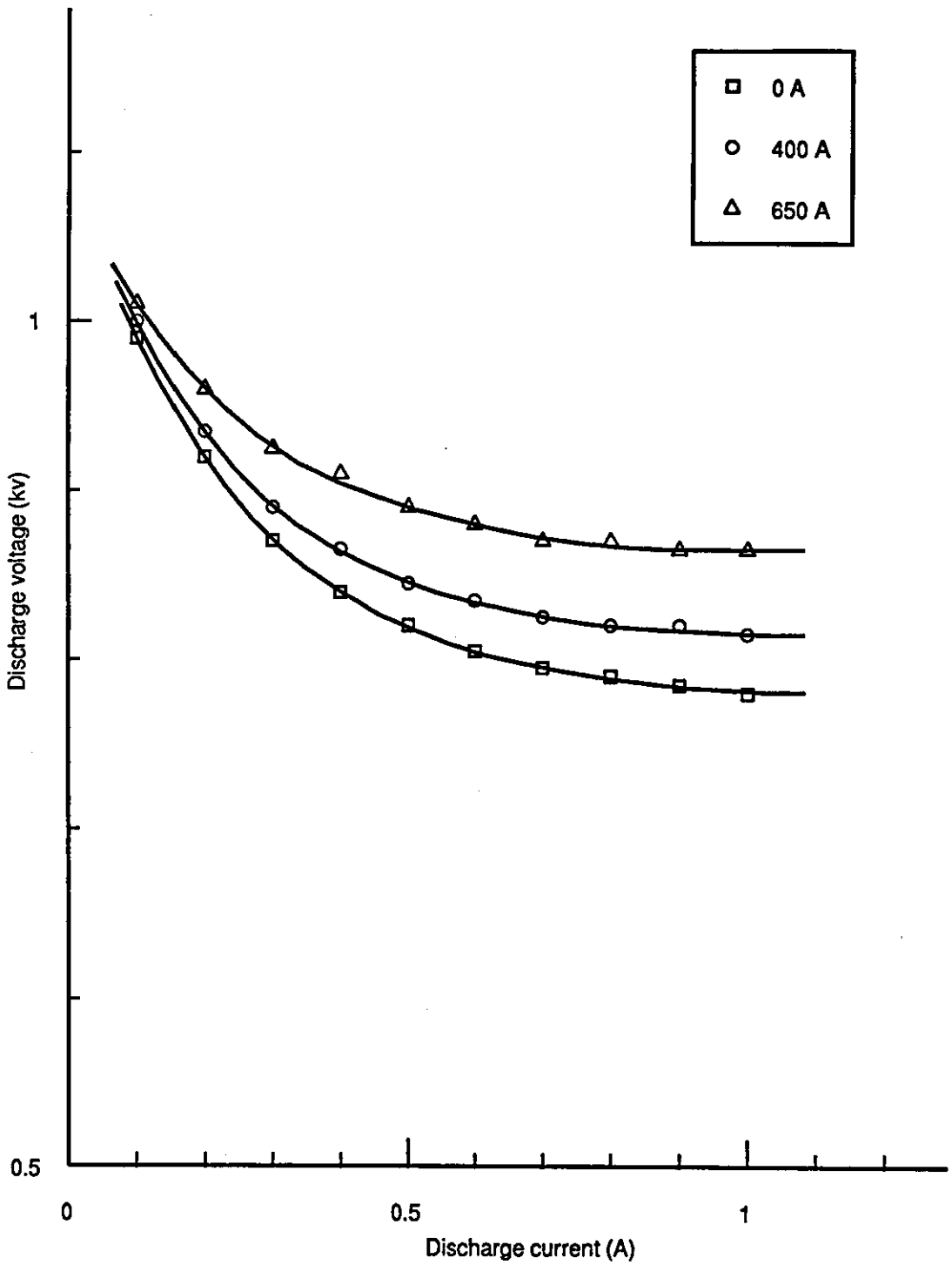

Fig. 5.13 The voltage-current characteristics of a coalesced multiple discharge at different values of axial current

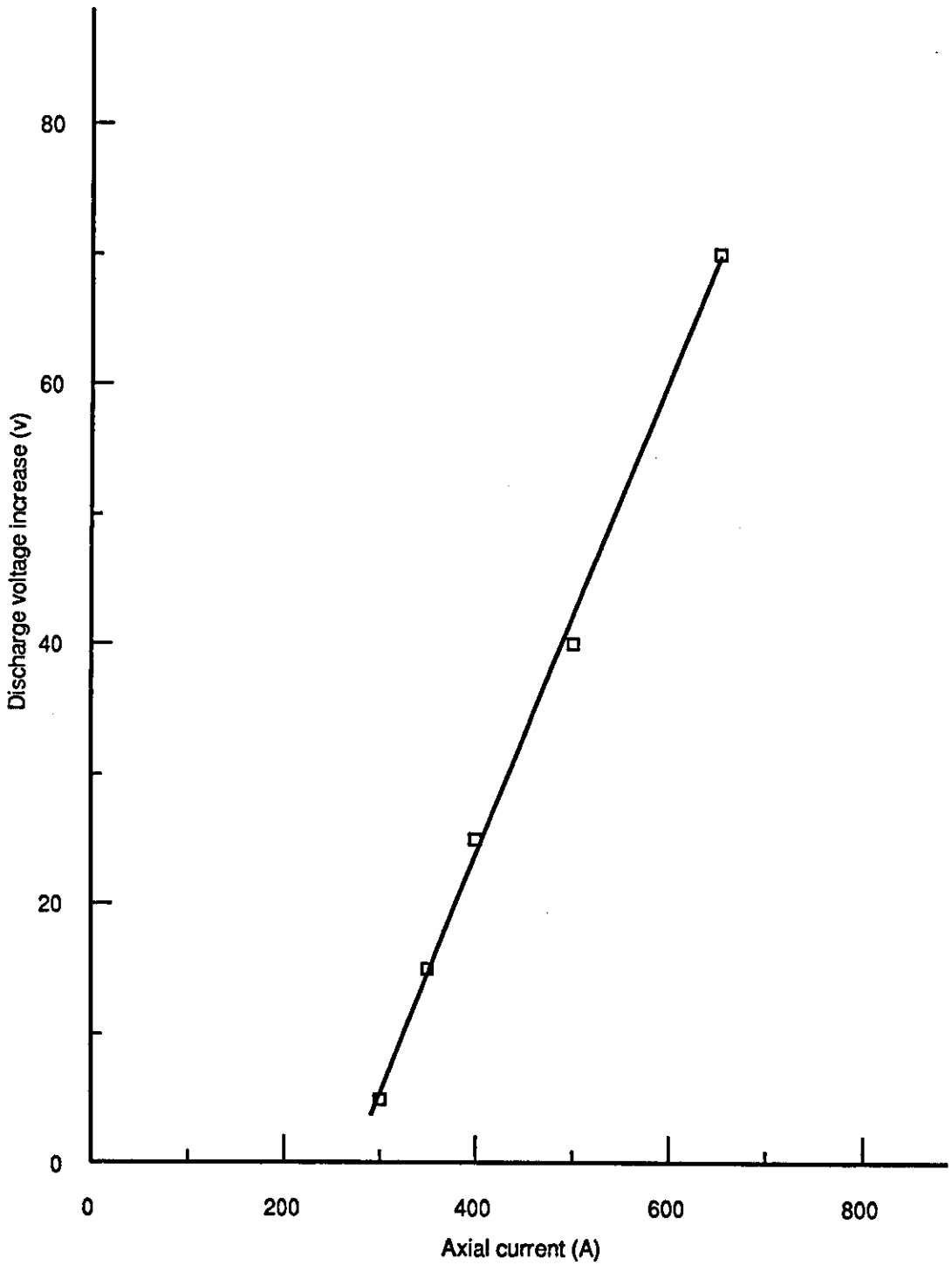

Fig. 5.14 The increase of the discharge voltage due to the axial current

At 50 mb at which the discharge uniformly surrounded the axial conductor, the axial current had no effect on the discharge shape or the discharge voltage even at its highest values. The uniformly distributed multiple discharge forms a cylindrical conductor and according to Ampere's law there is no electromagnetic field inside the cylinder;

$$\oint H.dl = I \qquad 5.1$$

The electromagnetic field due to the axial current, therefore, has no interaction with the discharge electromagnetic field and there is no attraction force between them.

5.3.2.2 Discussion of results

This investigation has shown clearly that contracting the discharge increases the column voltage gradient in a similar way to diffusing the discharge. This is consistent with Steenbeck's minimum principle.

A fast gas flow which could diffuse the discharge can also contract the discharge depending on the way the gas is injected into the discharge. In some applications of electric discharges, including gas lasers, the ratio E/N is an important factor as a measure for the electron energy needed for a specific molecular transition (Nighan 1970), but according to this investigation, the use of the similarity principle and its application to the reduced electric field E/p or E/N is justifiable only when the discharge is in the same mode however it has been applied by many to discharges in varying gas flows for which it is no longer valid. Under these conditions it can give completely erroneous results for example a constricted discharge may have the same voltage gradient as a diffused discharge although the ionisation process

in the constricted column is predominantly thermal ionisation while in the diffused discharge it is field ionisation.

5.4 MULTIPLE ELECTRIC DISCHARGE

Multiple arc discharges have been used to produce large volumes of ionised gas (Knight 1984), and a multiple glow discharge has been used in a large bore fast axial flow CO_2 laser (Harry and Evans 1988).

A series of tests were carried out to investigate the characteristics of the parallel and antiparallel multiple electric discharges in comparison with the single electric discharge characteristics, to examine the relation between the coalescence of the multiple discharge columns and Steenbeck's minimum principle.

5.4.1 Parallel Multiple Electric Discharge

A series of tests were carried out on a parallel discharge using the discharge arrangement shown in Fig. 5.7. A single power supply with individual stabilisation of each electrode was used. The voltage-current characteristics of a single, double coalesced and double non-coalesced discharges in He at pressure 500 mb are shown in Fig. 5.15, where the electrode separation was 105 mm and the separation distance between the two pairs of electrodes for the coalesced discharge was 15 mm.

The non-coalesced double discharge has the same discharge voltage as a single discharge with half the double discharge current. For example, at a current of 0.2 A the single discharge voltage is 1.28 kV which is the same voltage for the non-coalesced double discharge with current of 0.4 A. This can be explained because the non-coalesced multiple discharge behaves just like a

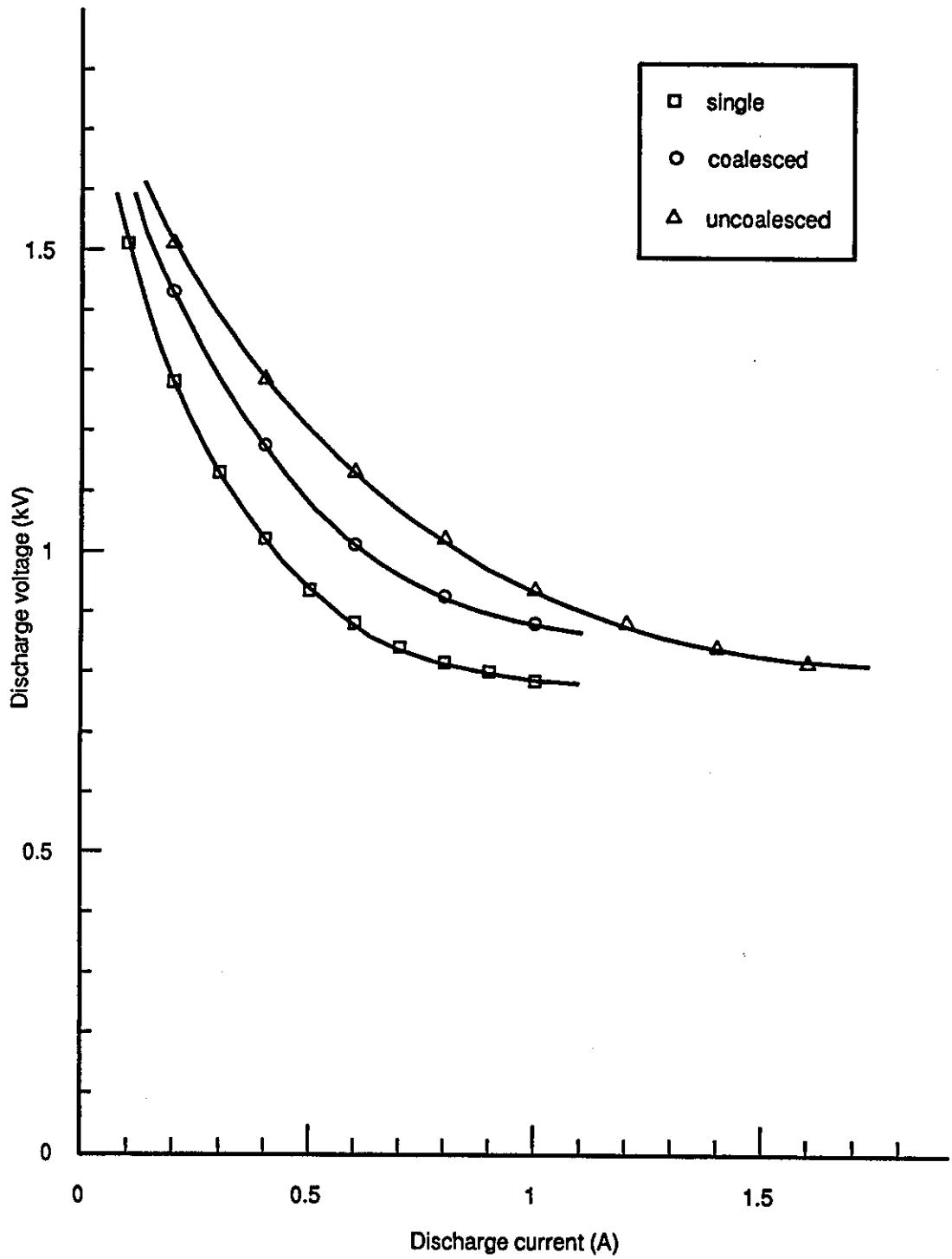

Fig. 5.15 The voltage-current characteristics of single and double discharge in He

number of individual single discharges with no thermal or electromagnetic interaction between them. The non-coalesced double discharge voltage is more than the single discharge voltage at the same current according to the voltage-current characteristic of the single discharge, however, the coalesced discharge voltage is more than the single discharge voltage at the same current but less than the non-coalesced discharge voltage.

The variation of the discharge voltage with the electrode separation for 0.4 A single discharge and 0.4 A coalesced and non-coalesced double discharge is shown in Fig. 5.16. The relation is approximately linear. The 0.4 A single discharge curve and the 0.4 A non-coalesced double discharge curve (which also represents a 0.2 A single discharge) intersect the voltage axis giving a zero-length voltage of 180 V, which is approximately equal to the cathode fall voltage. The 0.4 A coalesced double discharge curve is approximately parallel to the 0.4 non-coalesced double discharge curve. This can be explained if only the coalesced part of the discharge changes its length by extending the electrode separation, i.e. the coalesced part of the 0.4 A double discharge has the same voltage gradient as the 0.4 A single discharge positive column. The voltage difference between the single and the coalesced discharges is due to the non-coalesced parts branching at the two ends. By reducing the electrode separation and keeping the separation distance between the two pairs of electrodes at 15 mm, the coalesced discharge separates into two single discharges at the electrode separation of 55 mm.

From Fig. 5.16, it is clear that the discharge remains non-coalesced below 55 mm where the discharge voltage is less than the coalesced discharge voltage at that spacing, and coalesced above 55 mm where the discharge voltage is less than the non-coalesced discharge voltage. This

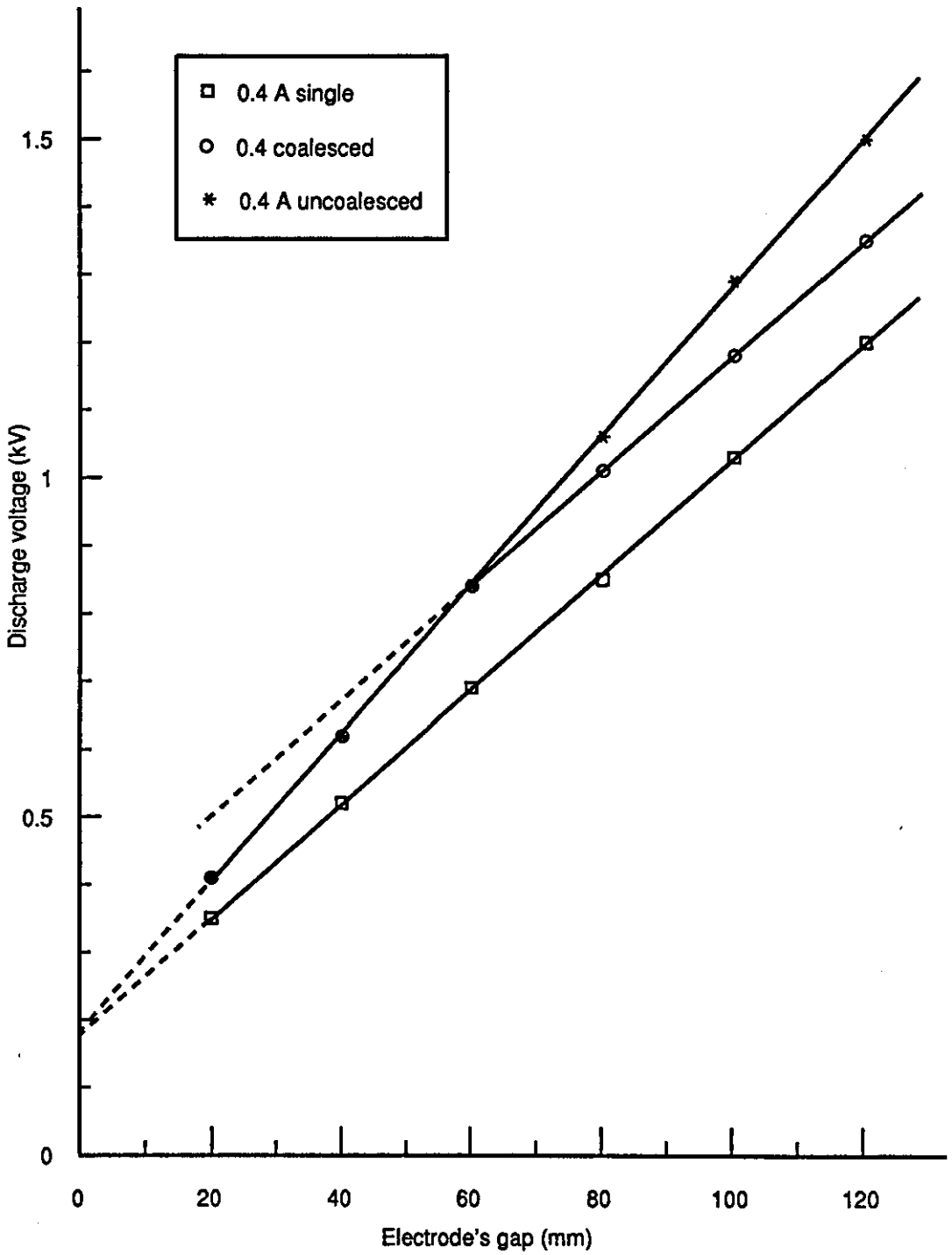

Fig. 5.16 Variation of the single and double discharge voltage with the electrode separation at a discharge current of 0.4 A

phenomenon where the discharge is coalesced or non-coalesced whichever has the less voltage represents another illustration of Steenbeck's minimum principle.

5.4.2 The Double Discharge Coalescence Model

A simple model for the coalesced double discharge can be presented by considering the Steenbeck's minimum principle. For an electric discharge with electrode separation L and separation distance $2y$ between the two pairs of electrodes (Fig. 5.17), the discharge voltage could be written as follows;

$$V_d = V_a + V_c + E_1(L - 2y\tan\theta) + \frac{2y}{\cos\theta}E_2 \qquad 5.2$$

where V_a and V_c are the anode and cathode fall voltages respectively, E_1 and E_2 are the voltage gradient of the coalesced and non-coalesced parts of the positive column respectively and θ is the coalescence angle. According to Steenbeck's minimum principle V_d should be minimum, therefore,

$$\frac{dV_d}{d\theta} = -2yE_1\frac{1}{\cos^2\theta} + 2yE_2\frac{\tan\theta}{\cos\theta} = 0 \qquad 5.3$$

$$E_1\frac{1}{\cos\theta} = E_2\tan\theta \qquad 5.4$$

$$\frac{E_1}{E_2} = \tan\theta\cos\theta = \sin\theta \qquad 5.5$$

$$\theta = \sin^{-1}\frac{E_1}{E_2} \qquad 5.6$$

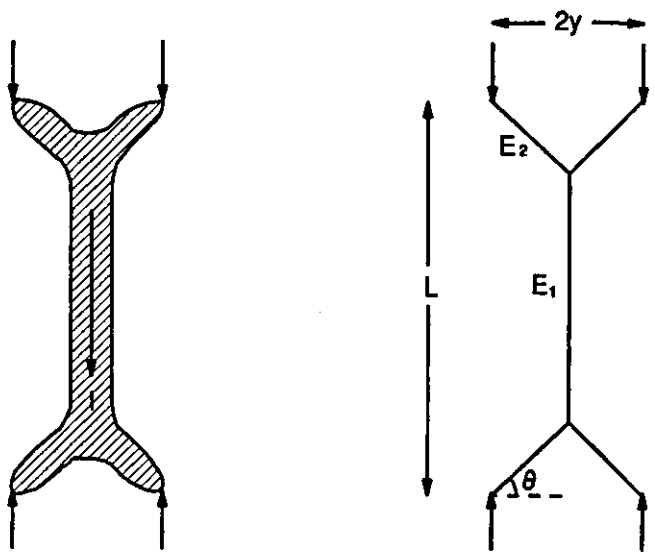

Fig. 5.17 Coalesced double discharge

The value of the coalescence angle θ is around 50° for the discharge current range available which is consistent with visual observation. This model which is based on Steenbeck's minimum principle is consistent with the actual behaviour of the coalesced discharge without considering the electromagnetic attraction force.

5.4.3 The Effect of the Electromagnetic Force on the Electric Discharge

The force between two parallel conductors is given by;

$$F = \frac{\mu_o I_1 I_2}{2\pi a} \qquad 5.7$$

In order to investigate to what extent the electric discharge is affected by the electromagnetic force, a 100 mm long discharge in He at 500 mb was subjected to an electromagnetic force from a conductor carrying a current parallel to the discharge (Fig. 5.18). The separation between the conductor and the discharge column was 60 mm. A discharge of 0.4 A showed no sign of attraction towards the conductor which carried a current of up to 50 A (Fig. 5.19), which is equivalent to a multiple discharge with the two columns 15 mm apart (the separation used in the coalesced discharge investigation), and each carrying current of 12.5 A. Increasing the conductor current to 100 A for the same separation of 60 mm (which is equivalent to 25 A, 15 mm apart) had a considerable effect on the 0.4 A discharge column bending towards the conductor (Fig. 5.20).

It is concluded that the electromagnetic force has only a very minor role in coalescing a discharge over the current range used.

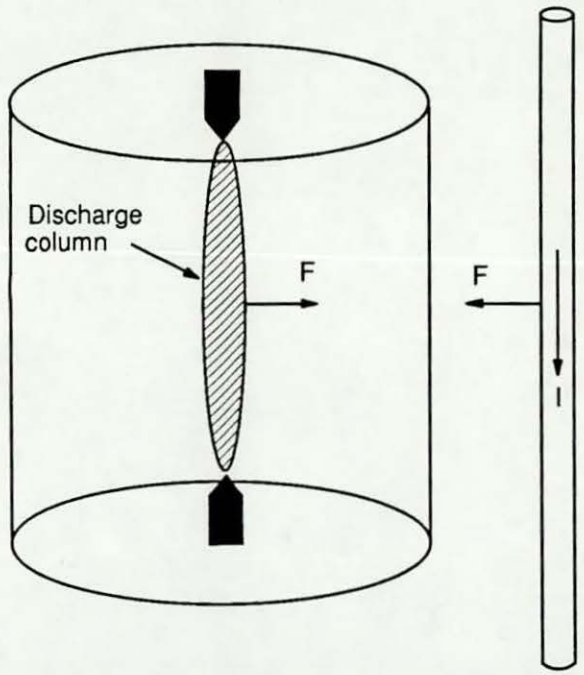

Fig. 5.18 The conductor and the electrode arrangement

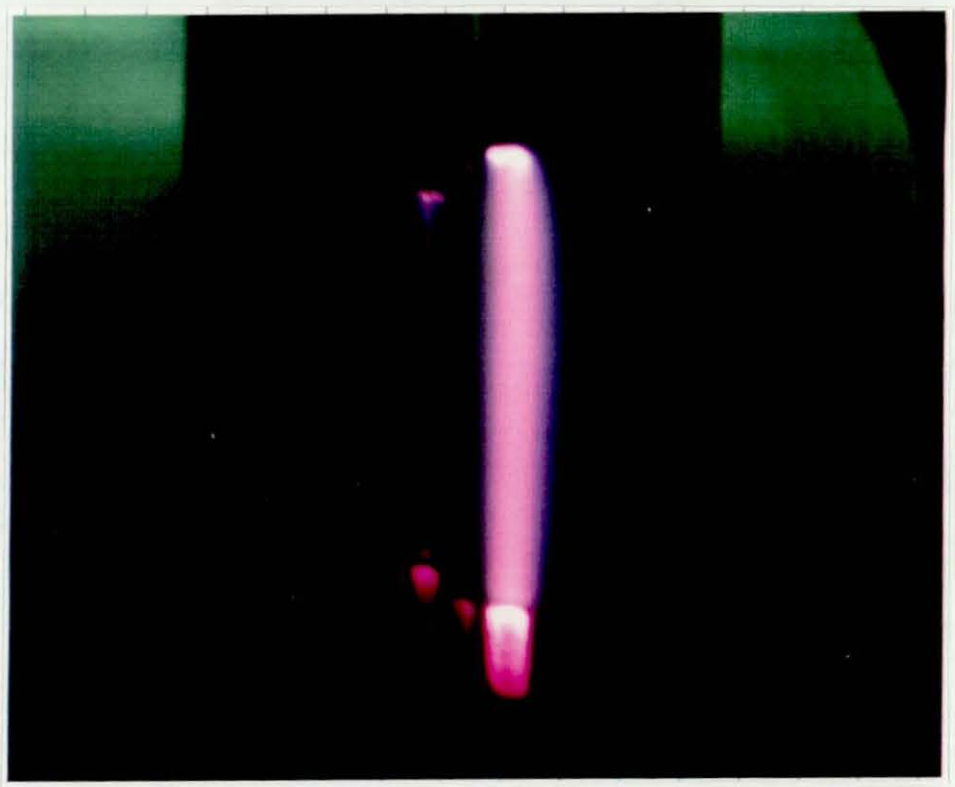

Fig. 5.19 Electric discharge in He at 500 mb parallel to a conductor carrying a current of 50 A (second image is due to reflections).

5.4.4 Minimum Voltage and the Balance of Forces

It is proposed here that the minimum principle could be understood in a different way based on the balance of forces.

If a discharge is subject to an electromagnetic force F, then the discharge will bow in the direction of the force (Fig. 5.21), and its length and, therefore, its voltage will increase. Assuming that the discharge current is due to electrons only, then the discharge current I is given by;

$$I = \frac{ne}{t} = \frac{neu_d}{x} \qquad 5.8$$

where ne is the number of electrons passing in a time t, u_d is the electron drift velocity and x is the increase in the discharge length. The energy added to the discharge E_a by extending it is then;

$$E_a = neV = \frac{IVx}{u_d} \qquad 5.9$$

where V is the voltage across x. This energy is equal to a potential energy which is a result of a force F_p which tries to pull the discharge against the force F, therefore,

$$E_a = F_p x = \frac{IVx}{u_d} \qquad 5.10$$

then,

$$F = \frac{E_a}{x} = \frac{IV}{u_d} \qquad 5.11$$

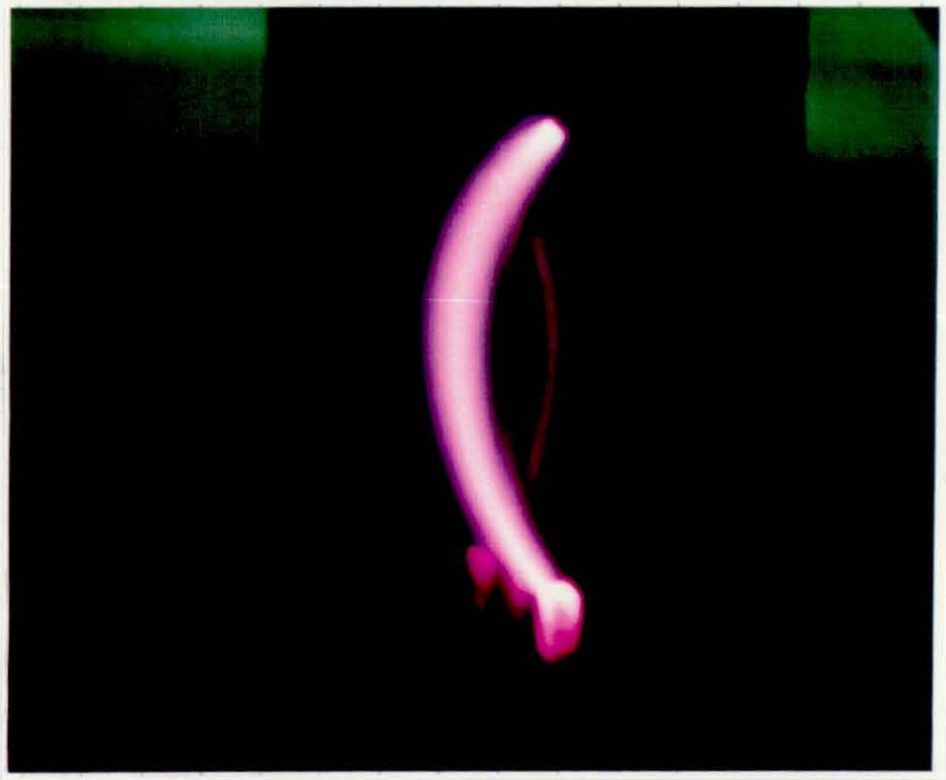

Fig. 5.20 Electric discharge in He at 500 mb parallel to a conductor carrying a current of 100 A (second image is due to reflections).

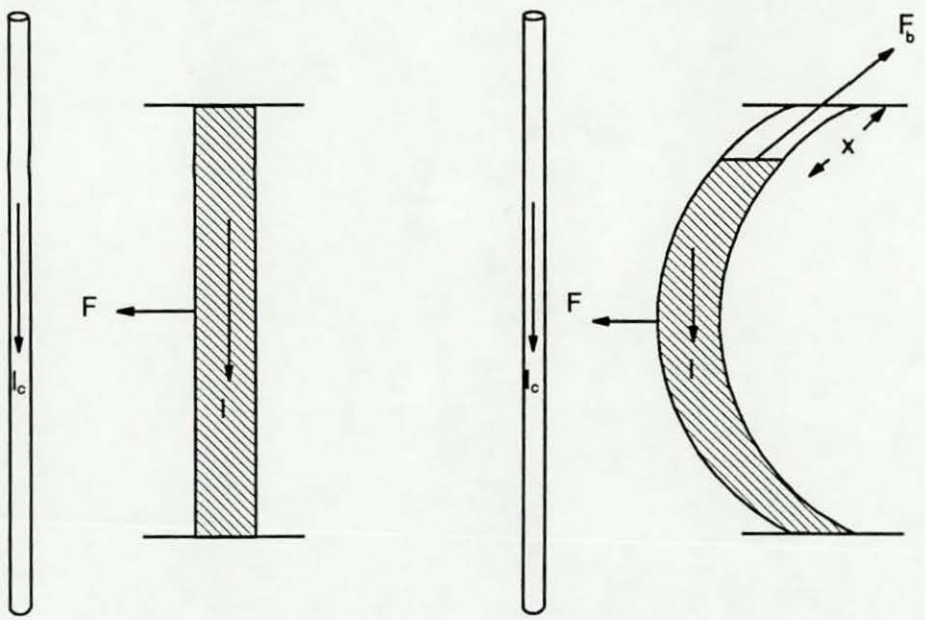

Fig. 5.21 The forces acting on the discharge

In the absence of the force F, the force F_p will pull the discharge back so that it becomes shorter with less voltage across it. This is consistent with Steenbeck's minimum principle.

Although this model is based on an electric discharge subjected to an external force, a model should be possible on the balance of forces which decides the relation between the minimum voltage and the discharge diameter.

5.4.5 Antiparallel Multiple Discharge

A series of tests were carried out to examine the behaviour of the antiparallel double discharge. The electrode arrangement is shown in Fig. 5.7. The electrode separation was 100 mm and the distance between the two pairs of electrodes was 15 mm. The current was supplied to the two discharges by two separate power supplies as shown in Fig. 5.22. The discharge was operated in He at 500 mb. The discharge was started with a single discharge with a 0.2 A discharge current recorded by the ammeters A_1 and A_2 (Fig. 5.23a). When the second power supply was switched on, two discharges carrying 0.1 A recorded by the ammeters A_3 and A_4, were started between the two adjacent electrodes and the first discharge intensity was reduced (Fig. 5.23b). By increasing the second power supply current to 0.2A, the first discharge was extinguished and the intensity of the second two discharges was increased (Fig. 5.23c).

It was shown in the parallel multiple discharge tests that with the electrode configuration and current range used, the electromagnetic force interaction between the two columns is insignificant. This should also be case where the discharges are antiparallel. The extinction of the main discharge column and the formation of the two columns between the adjacent electrode is therefore due to a different reason. It is not possible for a single

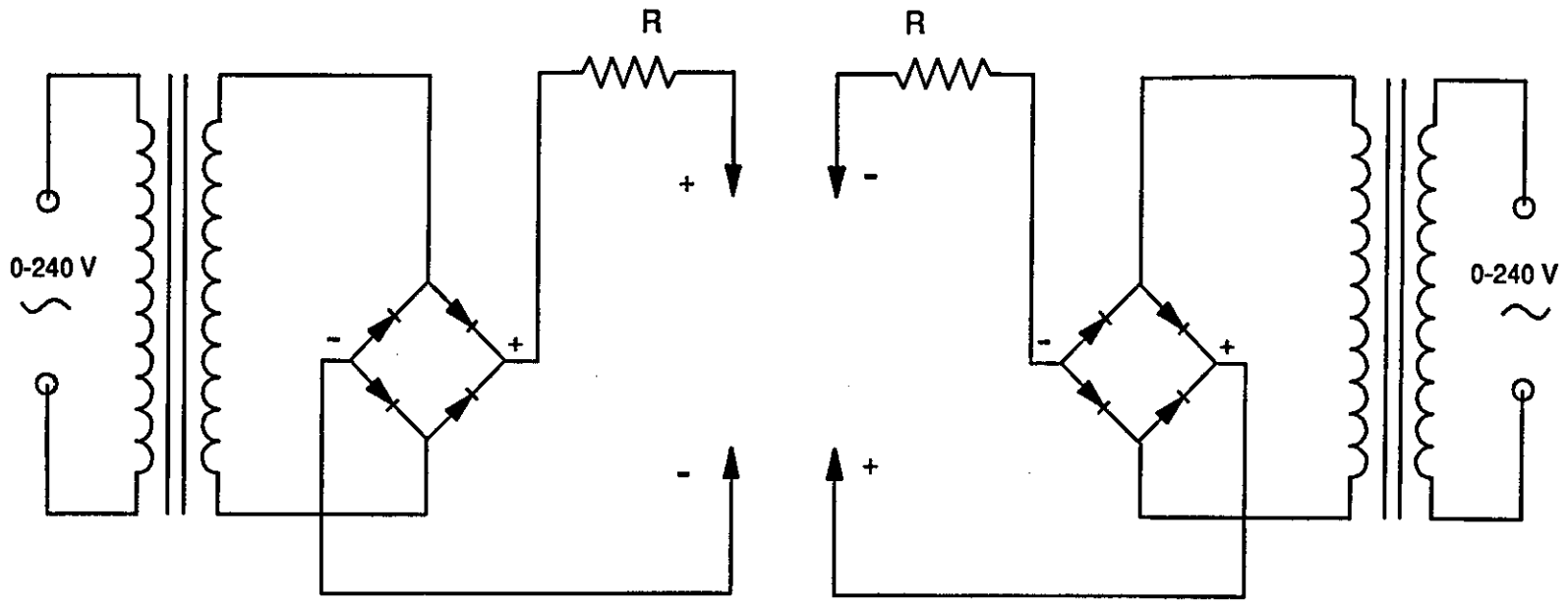

Fig. 5.22 Antiparallel multiple discharge circuit

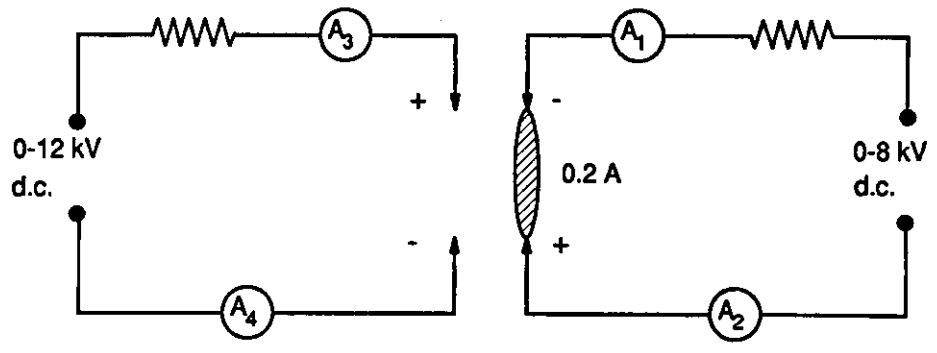

a.

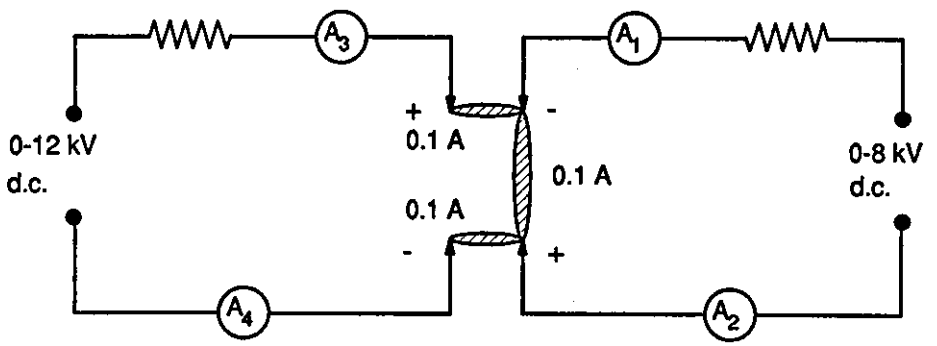

b.

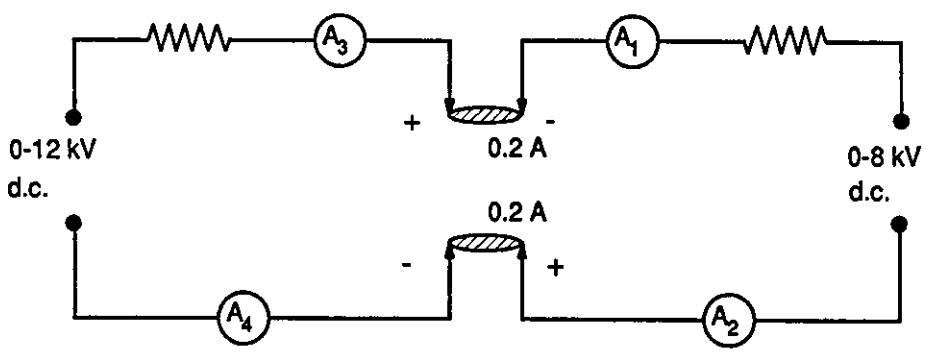

c.

Fig. 5.23 Antiparallel multiple discharge

column to carry two opposite currents, and, if therefore the coalescence is not possible, non-coalesced discharge columns must exist which will take the shortest distance between the adjacent electrodes rather than the original electrode gap with a lower discharge voltage than the voltage of the alternative longer discharge.

The existence of the two non-coalesced columns between the adjacent electrodes rather than along the 100 mm electrode separation is another example of the Steenbeck's minimum principle

5.5 SUMMARY OF RESULTS

(i) The emission spectrum of the positive column has shown no change around the glow to arc transition indicating that the glow to arc transition has no effect on the positive column characteristic.

(ii) A considerable change in the spectrum emission of the positive column was seen between the subnormal and the normal glow which is due to different molecular excitation states and ionisation mechanisms.

(iii) Steenbeck's minimum principle has been illustrated experimentally. Contracting as well as diffusing the positive column causes its voltage gradient to increase.

(iv) Since the voltage gradient increases with constriction (leading to thermal ionisation), or diffusion (leading to field ionisation), the E/N ratio is not necessarily a useful measure of the suitability of an electric discharge for laser excitation.

(v) A multiple discharge coalesces to operate at the minimum voltage and if this is not achieved it will remain non-coalesced.

(vi) The electromagnetic interaction between the parallel multiple discharges has a minor role in the coalescence at currents below ~25 A.

(vii) A simple mathematical model for the coalesced double discharge has been established based on the minimum voltage principle.

(viii) The minimum voltage has been related to a balance of forces acting on the glow discharge considering an external force affecting the discharge.

(ix) The advantage of the multiple discharge is the distribution of the discharge current between more than one electrode but it has no apparent advantage in the positive column since a coalesced column has the same characteristics as a single discharge column carrying the same current.

CHAPTER 6

THE CHARACTERISTICS OF AN ELECTRIC DISCHARGE IN A FAST GAS FLOW

6.1 INTRODUCTION

The voltage-current characteristic of the positive column in static gas flow and the effect of forces on the column due to external fields have been investigated and analysed in the previous chapter.

The use of convection cooling in high power molecular laser discharges is well known and the laser output power of CO_2 and CO lasers, may be scaled with the mass flow rate as an alternative to increasing the discharge length (Cool and Shirley 1969, Hill 1970). The gas injection to the discharge is crucial for the formation of a diffused high power density discharge and the power density is still limited by the constriction of the positive column (Hill 1971, Harry and Evans 1988).

Aerodynamic and gas injection techniques have been used to increase the threshold of the electrical power density at which the positive column constricts to form streamers in the fast gas flow electric discharge; it has been suggested that turbulent flow is necessary for the discharge column diffusion (Eckbreth and Owen 1972, Shirahata and Fujisawa 1973, Harry and Evans 1987).

This chapter investigates the interaction of the fast gas flow with the positive column at atmospheric pressure. The forces applied by the fast gas flow on the positive column are considered and analysed for the laminar and turbulent flow regimes.

6.2 THE GAS FLOW SYSTEM

A fast gas flow at atmospheric pressure was obtained in the discharge cavity using the system shown in Fig. 6.1. An oil-free diaphragm compressor was used to compress the gas at up to 8 b into a 120 l reservoir. The gas was then released through the discharge cavity and discharged

to the atmosphere. The gas flow was measured with a gas volume flow meter and the pressure was measured at the entrance to the discharge cavity. The gas velocity in the discharge cavity could be calculated knowing the gas volume flow rate and the discharge cavity cross section.

The gas used in the tests was air since the discharge characteristic of the positive column in air was shown to be similar to that of the CO_2 laser gas mixture and the study was concerned with the behaviour of the discharge column in the fast flow gas and not the molecular transition used for excitation.

6.3 THE FAST AXIAL GAS FLOW ELECTRIC DISCHARGE

A series of tests were carried out on a fast flow gas electric discharge in air at atmospheric pressure for different electrode arrangements. To show the effect of an axial gas flow on single glow discharge, initially, a normal glow discharge was obtained with no gas flow at 0.1 A between two electrodes 20 mm apart positioned axially in a Pyrex tube 10 mm ID (Fig. 6.2a). By introducing the gas flow over a range of gas velocities (10-300 m/s) in the discharge cavity, the discharge column became contracted, and was straight and parallel to the gas flow and continued on downstream until it touched the side of the downstream electrode (Fig. 6.2b). As the gas flow velocity was increased, the discharge column touched the side of the electrode further downstream.

The variation of the discharge voltage with the gas velocity is shown in Fig. 6.3. The discharge voltage showed a steep rise as the gas flow was introduced. This is believed to be due to the column contraction where it was shown before (Chapter 5) that as the discharge column is forced to contract its voltage gradient rises which is consistent with Steenbeck's minimum principle. The discharge voltage increased more slowly as the gas

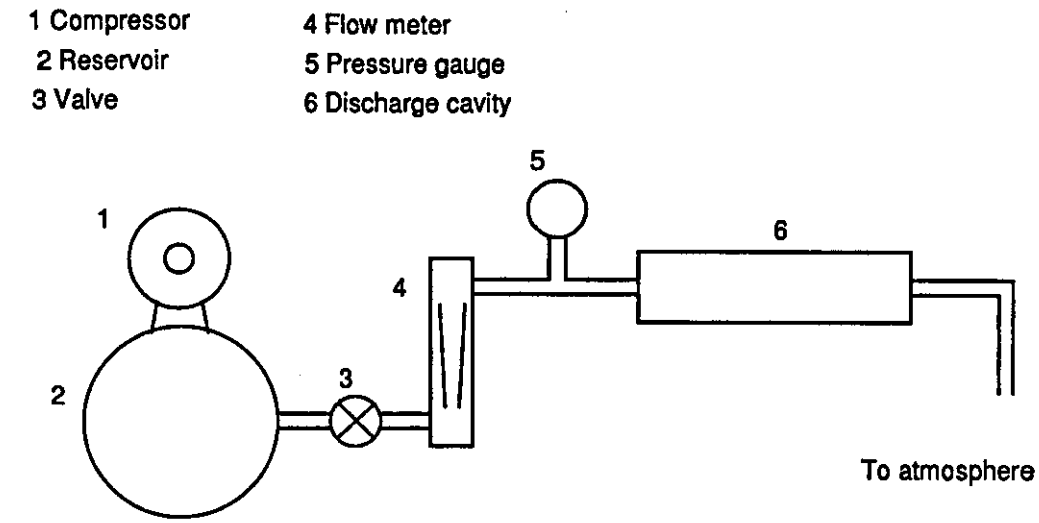

Fig. 6.1 The gas flow system.

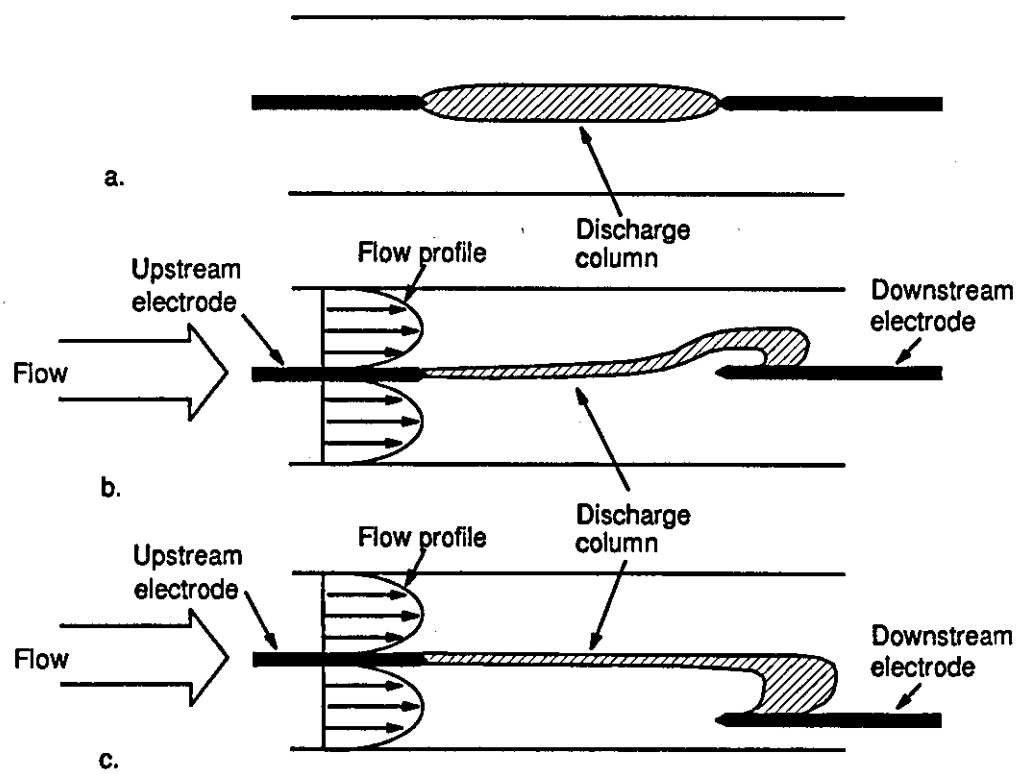

Fig. 6.2 Single discharge in still and fast flow gas.

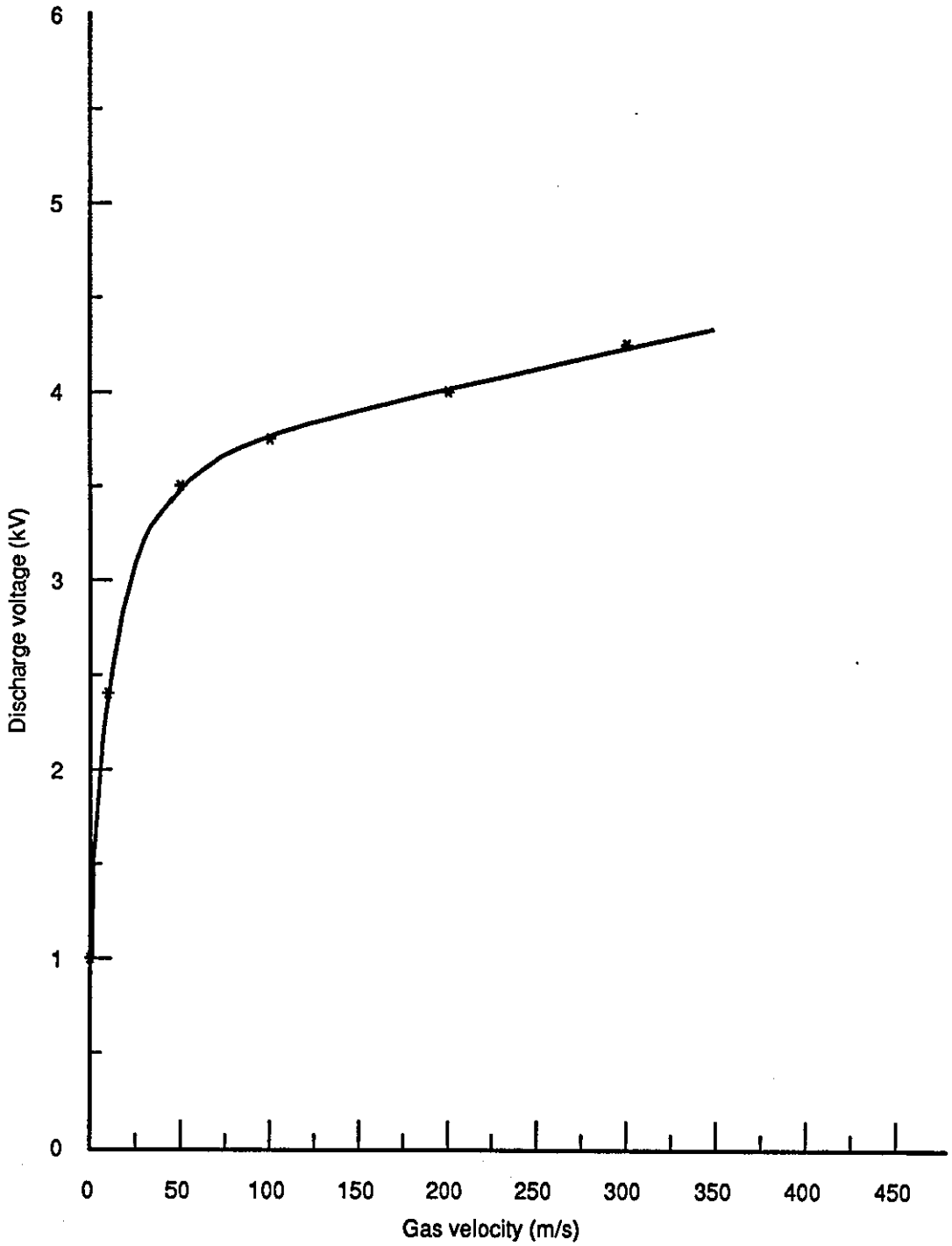

Fig. 6.3 Variation of the discharge voltage with gas velocity at a discharge current of 0.1 A.

velocity increased due to the increased contraction of the discharge column and increase in the length of the discharge as it was carried further downstream by the gas flow before it touched the downstream electrode. The discharge column diameter was not constant along its length as it was becoming wider downstream, and it was not possible to separate the effects of constriction and increase in length on the voltage. It is interesting to mention that at high gas velocities (~200 m/s) the gas flow could not carry the contact point downstream any further.

The downstream electrode was moved across the diameter of the tube to show the effect of the location of the downstream electrode on the discharge column behaviour. This did not change the discharge column behaviour or its location along the tube except near the downstream electrode where it contacted the electrode transversely (Fig. 6.2c).

The above tests were repeated reversing the polarities of the electrodes to show the effect of the different polarities on the discharge column behaviour. The tests showed the same results and behaviour with the opposite polarities.

Multiple discharges have been used to obtain a high power large bore glow discharge for the excitation of a high power CO_2 laser using slow axial gas flow (Saleh 1981), and fast axial gas flow (Harry and Evans 1988). To show the effect of the upstream as well as the downstream multiple electrodes on the discharge column behaviour, two separately stabilised electrodes were placed downstream instead of the single electrode. The static glow discharge was a single coalesced column, branched downstream to the electrodes (Fig. 6.4a). By introducing the gas flow, the discharge column was also contracted and parallel to the gas flow except near the downstream

electrodes (Fig. 6.4b). Reversing the polarities of the upstream and the downstream electrodes showed no difference in the discharge behaviour.

The two multiple electrodes then were placed upstream and the single electrode downstream (Fig. 6.5a). By introducing the gas flow the static gas column which is a single column branching at the two multiple electrodes became two columns starting from the upstream electrodes parallel to each other and to the gas flow and conducting to the single electrode downstream (Fig. 6.5b). Reversing the polarities also showed no difference in the discharge behaviour.

Two observations were made on the effects of the gas flow on the discharge column;
(i) the discharge column tends to follow the gas flow streamlines where the downstream electrode location did not affect the location of the discharge column (Fig. 6.2c). This is also shown by the branched column to the two upstream electrodes forming two columns starting from the upstream electrodes parallel to the gas flow streamlines (Fig. 6.5).
(ii) the gas flow forces the discharge column to contract just like pushing two cotton threads diverging from a single point to each other (Fig. 6.2). This contraction force appears to be due to the shear stress force between the gas flow streamlines layers.

6.4 THE FAST GAS FLOW SHEAR STRESS OVER THE UPSTREAM ELECTRODE

When a fluid flows in a tube with a uniform velocity U, a boundary layer gradually builds up until it reaches the centre of the tube. The velocity profile is then said to be fully developed, and may be assumed not to vary further down the tube. There are two main types of flow, laminar and turbulent flow. In the laminar flow fluid

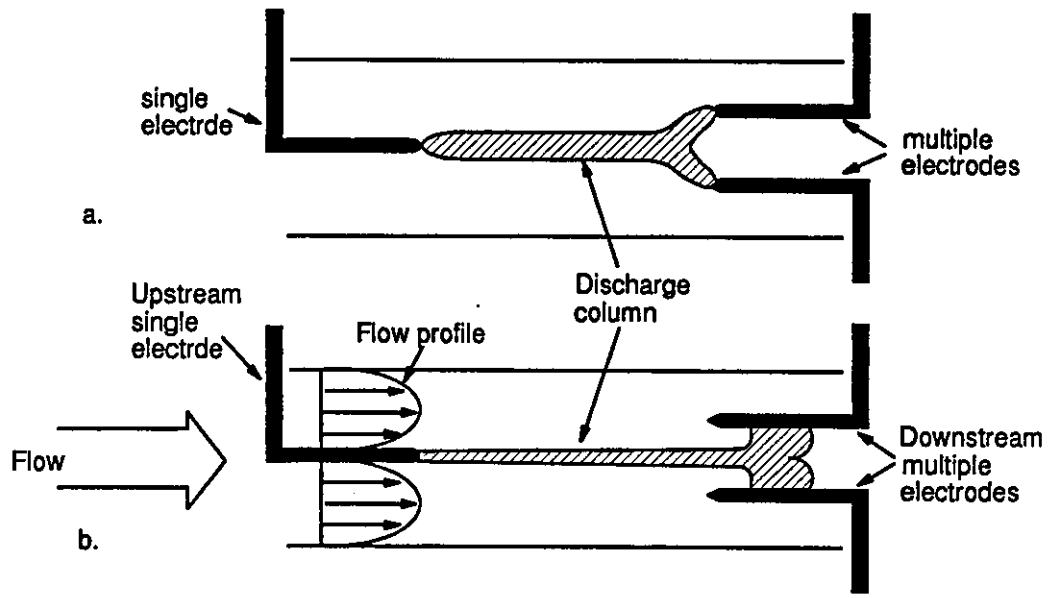

Fig. 6.4 Multiple downstream electrodes discharge in still and fast flow gas.

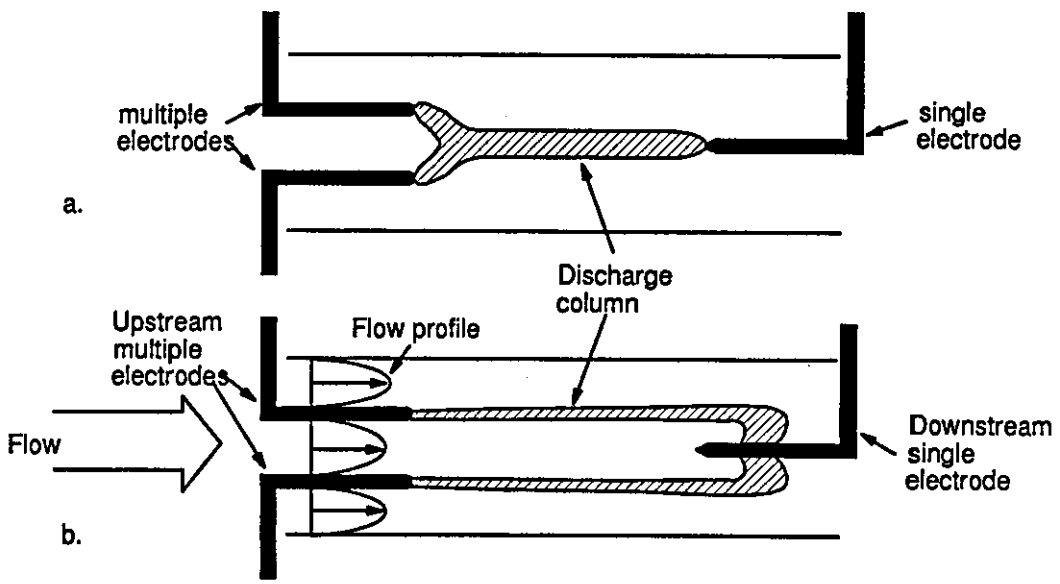

Fig. 6.5 Multiple upstream electrodes discharge in still and fast flow gas.

elements move in continuous paths, or streamlines, without mixing with the fluid in adjacent paths. In the turbulent flow, eddy motion of individual elements fluctuate in the direction of the flow and perpendicular to it. The conditions for laminar or the turbulent flow are determined by the Reynolds number which is defined by,

$$R_d = \frac{\rho U_m d}{\mu} \qquad 6.1$$

where d is the tube diameter, U_m is the weighted mean velocity, ρ is the fluid density and μ is the dynamic viscosity. The two types of flow profile are shown in Fig. 6.6.

6.4.1 The Laminar Flow Shear Stress

When a gas flows in a tube, it is always assumed that the fluid velocity adjacent to the surface is zero, i.e. there is no slip between the fluid and the surface, then, the gas velocity varies from zero on the wall surface to its maximum in the centre of the tube. Accordingly, a shear stress τ will exist and at any point in the gas and it is proportional to the velocity gradient (dU/dy) at that point, Fig. 6.7. The constant of proportionality is the dynamic viscosity μ of the gas, so that,

$$\tau = \mu(dU/dy) \qquad 6.2$$

Assuming that the gas properties are independent of temperature, then, for a fully developed laminar flow, the velocity profile of a gas flowing through a cylindrical tube is parabolic and is given by (Douglas et al 1985);

$$\frac{U}{U_r} = 2\left(\frac{y}{r}\right) - \left(\frac{y}{r}\right)^2 \qquad 6.3$$

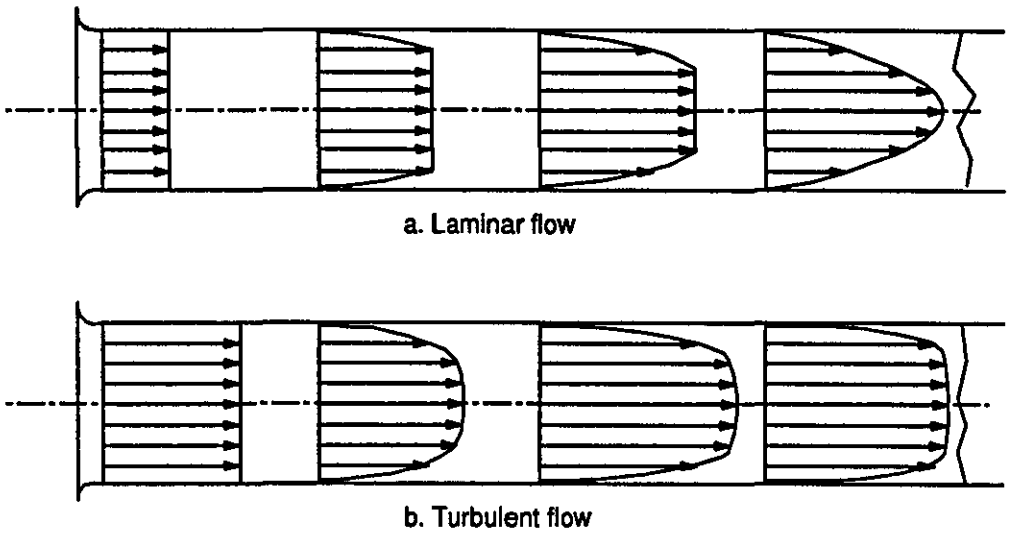

Fig. 6.6 Establishment of a fully developed velocity profile in a tube (after Douglas et al 1985).

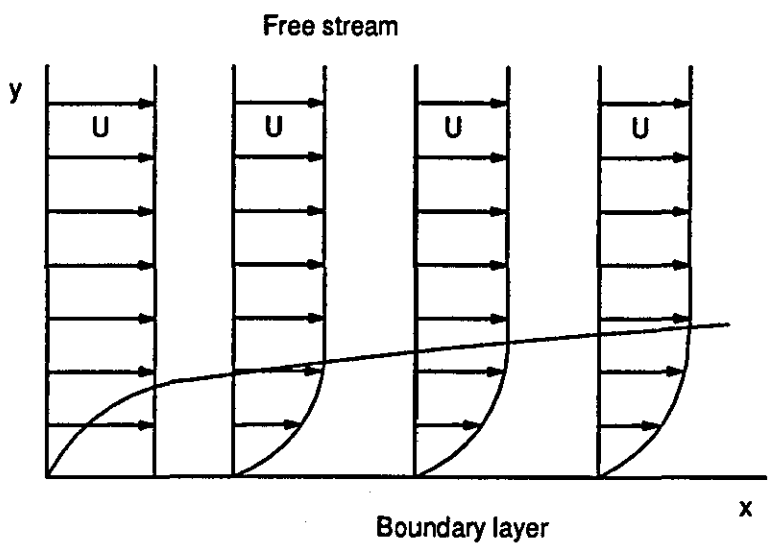

Fig. 6.7 The shear stress in the fluid

where r is the radius of the tube, U_r is the gas velocity at the axis of the tube and U is the gas velocity at a distance y from the tube wall. From equations 6.2 and 6.3, we get,

$$\tau = \frac{2\mu U_r}{r}\left(1-\frac{y}{r}\right) \qquad 6.4$$

The shear stress between two layers is, then,

$$\tau_1 - \tau_2 = \frac{2\mu U_r}{r^2}(y_2 - y_1) \qquad 6.5$$

To show the effect of the shear stress due to the flow profile of the laminar flow on the discharge column it is assumed that the upstream electrode is annular and of the same internal diameter of the tube and butted to it so as to form a continuous surface, (Fig. 6.8). If a discharge exists between the upstream electrode and a downstream electrode, the discharge column which starts from the end of the upstream electrode fall region diverges in that region to form the fully developed discharge column somewhere downstream as shown in Fig. 6.8. When the gas flows through the tube in the laminar flow regime, the shear stress given by equation 6.5 applies a force on the diverging discharge column and forces the column to contract.

6.4.2 The Turbulent Flow Shear Stress

For a fully developed turbulent flow, Prandtl has shown that, as an implication of experimental relation, the velocity profile follows a 7th power law (Douglas et al 1985), so that,

$$\frac{U}{U_r} = \left(\frac{y}{r}\right)^{\frac{1}{7}} \qquad 6.6$$

Applying equation 6.2 to equation 6.6, we get,

$$\tau = \frac{\mu U_r}{7r}\left(\frac{r}{y}\right)^{\frac{6}{7}} \qquad 6.7$$

The shear stress between two layers is, then,

$$\tau_1 - \tau_2 = \frac{\mu U_r}{7r}\left\{\left(\frac{r}{y_1}\right)^{\frac{6}{7}} - \left(\frac{r}{y_2}\right)^{\frac{6}{7}}\right\} \qquad 6.8$$

Equations 6.5 and 6.8 show that the shear stress between the gas flow layers for both laminar and turbulent flow is independent of the pressure but it depends on the flow velocity and the dynamic viscosity of the gas.

Comparing equation 6.5 with equation 6.8 and the laminar and turbulent flow profiles in Fig. 6.6 it shows that the shear stress is much higher in the turbulent gas flow near the tube wall than in the laminar gas flow for the same tube diameter. This is because of the steep turbulent flow profile near the tube wall. On the other hand the shear stress is less in the centre of the tube in the turbulent flow than in the laminar flow for the same tube diameter and this is because of the relatively plane flow profile in the central region of the tube in the turbulent flow.

In a typical upstream electrode configuration such as a pin electrode (Fig. 6.2) or an annular electrode (Fig. 6.8), the steep flow profile adjacent to the electrode is inevitable and the shear stress due to that forces the discharge column to contract. For the same tube diameter, the flow profile of the turbulent flow adjacent to the electrode is much steeper than that of the laminar flow, and therefore, the contraction force is higher.

6.4.3 The Comparison of the Different Contraction Forces

The discharge positive column in a static gas flow contracts as the current increases due to its self-electromagnetic field. The contraction force is given by,

$$F = \frac{\mu . I^2}{2\pi r} \qquad 6.9$$

where I is the discharge current and r is the column radius. To compare this force in a fast gas flow axial discharge with the contraction force from the shear stress due to the gas flow on the column in the centre of the tube, the following data has been obtained from a 5 kW CO_2 laser (Evans 1987),

discharge current = 2 A
discharge tube ID = 93 mm
gas velocity U_r = 300 m/s

For comparison, a hypothetical cylinder within the discharge along the axis of the tube of 20 mm diameter was considered. The equivalent discharge current in the cylinder is 0.093 A assuming uniform current density. Putting the values of the radius and the current in equation 6.9, the contraction force acting on the cylinder due to its self electromagnetic field will be

$$F_M = \frac{4\pi \times 10^{-7} \times (0.093)^2}{2\pi \times 0.01} = 1.73 \times 10^{-7} \ N \qquad 6.10$$

If the gas flow is in the laminar flow regime, then, the shear stress over the hypothetical discharge column could be calculated using equation 6.5 by putting $\mu_{He}(T = 250C^{\circ}) = 2.85 \times 10^{-5} kg/m.s$, $y_1 = 0.0365m$, $y_2 = r = 0.0465m$, and so that,

$$\tau_L = 0.079 \ N/m^2 \qquad 6.11$$

Considering the area A over which this stress is developed as a cylindrical area with radius equal to 5 mm which is half the radius of the hypothetical cylinder and 1 m long, then, the contraction force acting on the cylinder due to the laminar flow shear stress will be

$$F_L = \tau A \qquad 6.12$$

so that,

$$F_L = 0.079 \times 0.031 = 2.5 \times 10^{-3} \ N \qquad 6.13$$

If the gas flow is in the turbulent flow regime, then equation 6.8 gives,

$$\tau_T = 6.06 \times 10^{-3} \ N/m^2 \qquad 6.14$$

and, the contraction force due to the turbulent flow shear stress will be

$$F_T = 1.9 \times 10^{-4} \ N \qquad 6.15$$

Comparing the magnitude of the three different forces acting on the discharge along the axis of the tube, the model calculations indicate that the discharge self electromagnetic force is less than the shear stress contraction force due to the turbulent flow which is lower than the shear stress contraction force due to the laminar flow.

6.5 THE CYLINDRICAL INJECTION NOZZLE

Four cylindrical injection nozzles have been used as anodes in a multiple discharge at 60 mb to produce a high power CO_2 laser of up to 5 kW (Evans 1987). A cylindrical

injection nozzle was designed to examine the behaviour of the discharge column at atmospheric pressure where the column diameter is less than at low pressure so it can be traced along the gas flow.

The gas flow and the electrode configuration are shown in Fig. 6.9. As the gas flow was introduced the steep flow profile adjacent to the wall of the nozzle forced the column to contract along side the wall of the nozzle, and as the gas diffused out of the nozzle to the tube, the steep flow profile forced the discharge column away out of the fast flow region to the stagnation region. This behaviour of the positive column implies that the gas flow has not been exploited efficiently in diffusing the discharge column and cooling it convectively.

6.6 THE DIFFUSION OF THE DISCHARGE COLUMN IN THE FAST AXIAL GAS FLOW

It was concluded before that the discharge column always follows the gas flow streamlines; this was shown by the two columns which were parallel to each other and to the flow streamlines due to the two upstream electrodes (Fig. 6.5b). If many electrodes separately stabilised were located upstream instead of the two, there will be many columns parallel to each other and to the streamlines. This means that if a single electrode was used upstream and the discharge column was diffused upstream over a wide area, then, the column will stay diffused along the gas flow where it will behave as if it was many individual columns parallel to each other and to the gas flow.

For effective cooling of the discharge column, it is necessary for the gas flow streamlines to pass through the cross section of the discharge column. But, as it was shown before, the steep flow profile adjacent to the upstream electrode surface whether it is an annular electrode (Fig. 6.8) or pin electrode (Fig. 6.2) is an

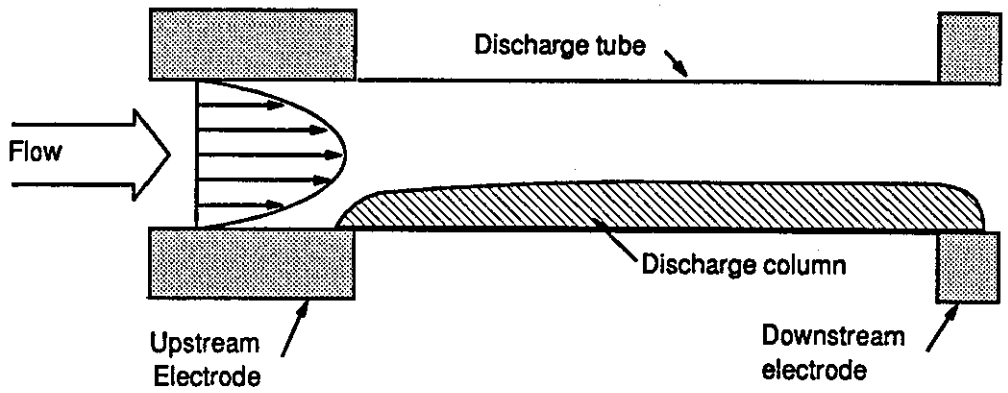

Fig. 6.8 Electric discharge in fast gas flow with annular electrode

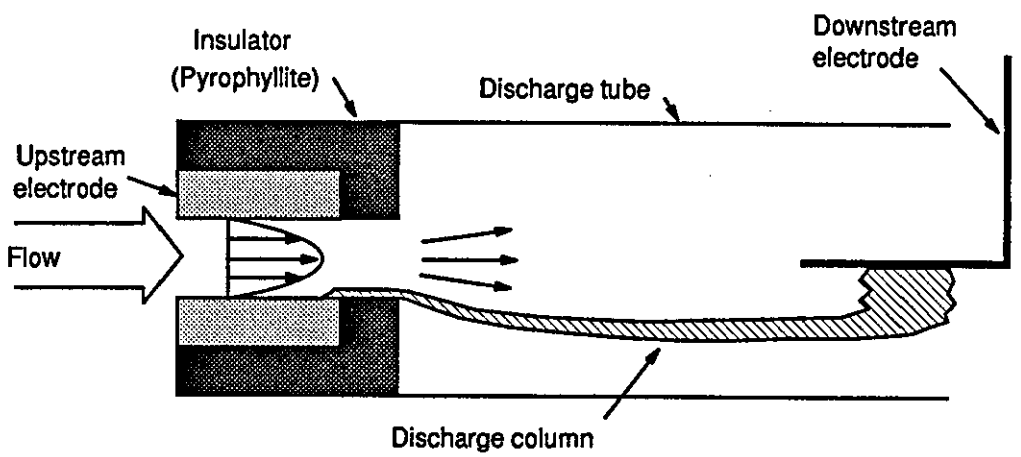

Fig. 6.9 The discharge column out of the flow stream in the stagnation region behind the insulator

inherent effect which always forces the discharge column to contract out of the fast flow region due to the high shear stress in this region.

The discharge column was modelled by treating it as a flexible object compressed by the gas flow which applies a shear stress on its surface. However, the discharge column is an ionised gas region surrounded by an un-ionised gas which is contracted by the injection of cold un-ionised molecules. If a flexible body is compressed by an external force, it applies an opposite expansion force where the final shape is decided by the balance between the two forces. This opposite force applied by the discharge column against the contraction force has not been considered yet.

The contraction of the discharge column causes the voltage gradient to increase as shown in the previous chapter. The steep flow profile adjacent to the upstream electrode forces the discharge column to contract and pushes the column out of the fast gas flow region to the slow flow region. This means that the discharge column is not effectively cooled by convection and although its voltage gradient is high due to the contraction, the thermal ionisation process dominates the field ionisation process. The increase in voltage gradient which results from the constriction force will increase the force which diffuses the contracted discharge column by ionising a wider column within the fast flow region. Cooling the column effectively by convection also increases the force which causes its voltage gradient to increase where more field ionisation is needed to compensate for the loss in the thermal ionisation process. The final column cross section is decided by the balance between the flow contraction force and the expansion forces which governs the voltage gradient. The balance between the different forces will happen at a lower voltage in between the two high voltages which is the minimum voltage according to Steenbeck's minimum principle.

It is concluded that although a steeper flow profile applies more contraction force on the discharge column, the high voltage gradient due to the contraction causes the column to diffuse more over the high gas flow region. This means that steeper flow profile is better for effective column cooling by convection.

It was shown before that the turbulent flow profile is much steeper adjacent to the walls than the laminar flow profile for the same tube diameter and the same gas flow rate. This means that the turbulent flow is more effective in cooling the discharge column convectively.

6.7 THE RECTANGULAR INJECTION NOZZLE

A gas flowing in a narrow tube has a steeper flow profile adjacent to the walls than that in a large diameter tube for the same gas flow rate and gas flow regime. To demonstrate the effect of the gas flow profile on the contraction of the discharge column, a rectangular nozzle was suggested in which the difference between the two different contraction forces on the discharge column can be shown due to the two different flow profiles across its length and height. The difference between the column contraction across the length and across the height therefore is only due to the flow profile while the gas flow rate and the gas flow regime is the same.

The upstream electrode was placed behind the nozzle so that the discharge column carried by the gas flow passes through the rectangular nozzle (Fig. 6.10). The flow profile across the rectangular height (3 mm), should be steeper adjacent to the nozzle walls (Fig. 6.11a) and to the pin electrode surface (Fig. 6.11b) than the flow profile across the rectangular length (6 mm). Introducing the fast gas flow to the discharge, the discharge column appeared more contracted across the rectangular height

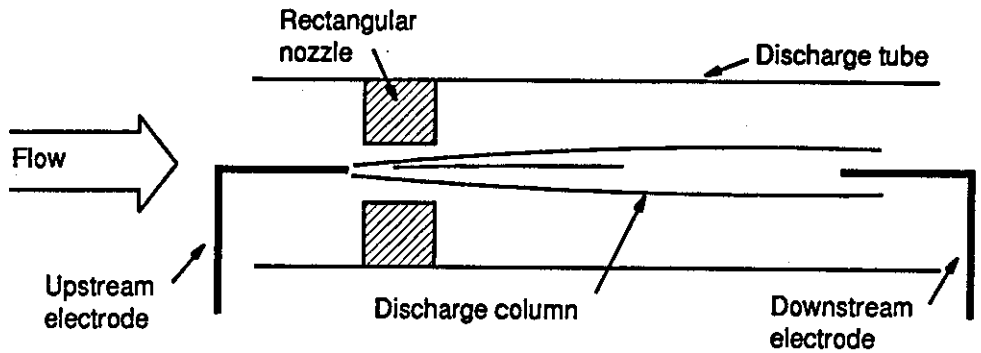

Fig. 6.10 Fast flow axial discharge using a rectangular nozzle

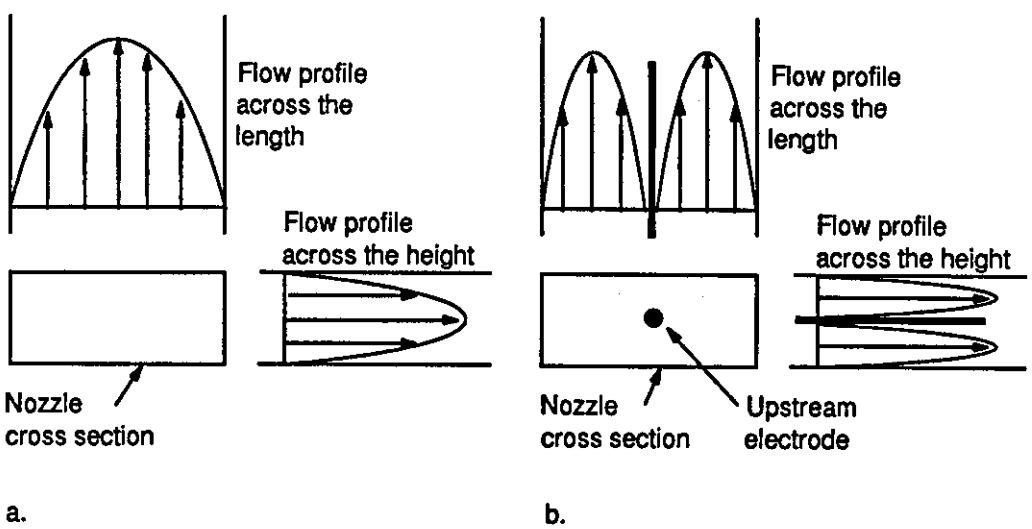

Fig. 6.11 The gas flow profile in a rectangular nozzle

than across the rectangular length. This is due to the higher shear stress across the height than the shear stress across the length.

The discharge column being more contracted across the nozzle height does not mean that the column is diffused and convectively cooled across the nozzle length. This is because the slow flow region across the length is wider.

6.8 THE TRANSVERSE GAS FLOW ELECTRIC DISCHARGE

The behaviour of the discharge column in the downstream electrode region was mentioned before (Fig. 6.2b), where the column contacted the side of the downstream electrode and as the gas velocity increased, the contact point was carried further downstream up to a limit. The shape of the discharge column around the downstream electrode implies that the column followed the streamlines along which the flow pattern was expected as shown in Fig 6.12. The discharge column then touched the downstream electrode by crossing the streamlines.

Studying the behaviour of the electric discharge in a transverse gas flow is useful to understand the downstream electrode region. A 5 mm long discharge was held in a transverse gas flow (Fig. 6.13). At discharge current of 0.3 A and gas flow of 15 m/s, the discharge voltage waveform is shown in Fig. 6.14. The flowing gas appeared to carry the discharge column away in its direction of flow causing a rise voltage. When the discharge is long enough, the discharge voltage becomes high enough to break down the gap again which could be seen as straight sparks across the minimum electrode gap.

At higher gas flow (25 m/s) at the same discharge current, the rate of the rise in voltage and voltage repetition frequency increased (Fig. 6.15). This shows

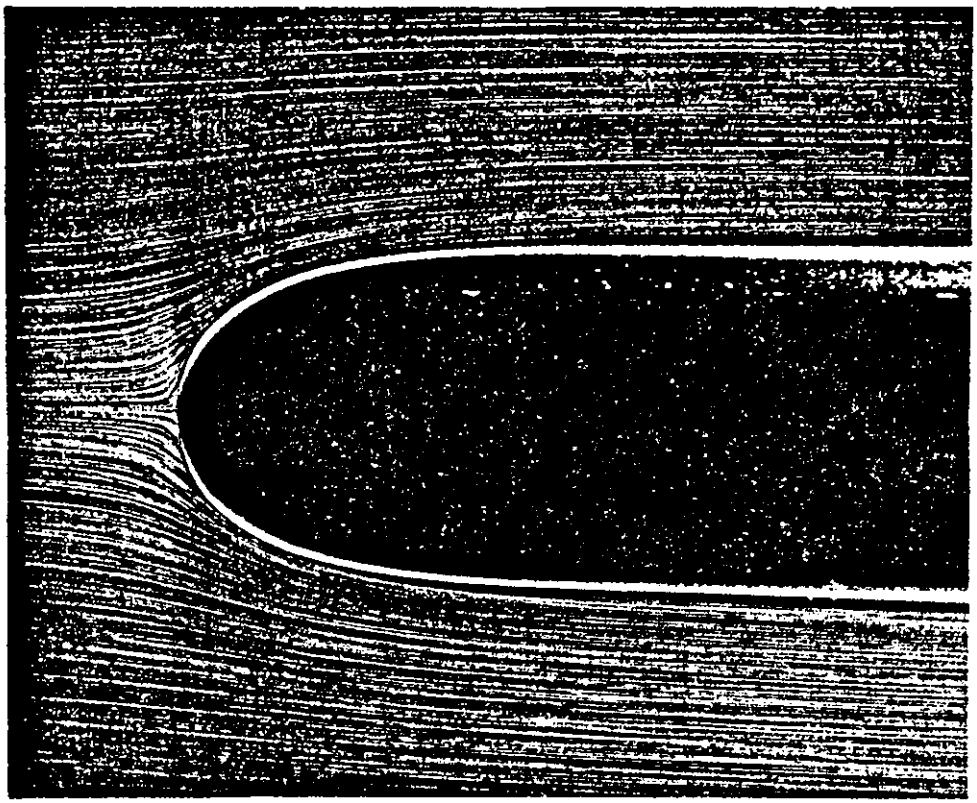

Fig. 6.12 The pattern of the gas flow past a round end rod (the gas flow is from left to right). (After Van Dyke 1982)

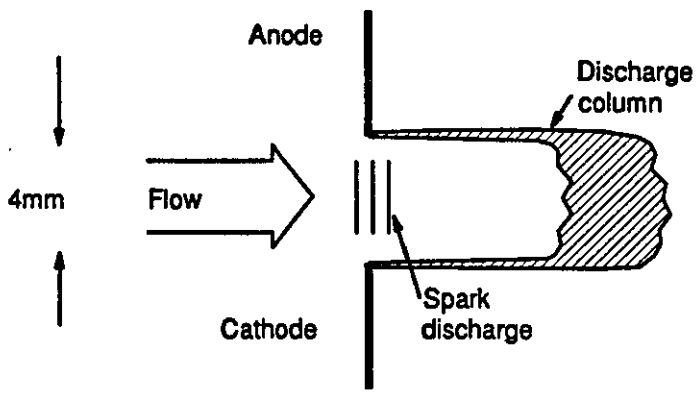

Fig. 6.13 The fast gas flow transverse discharge at atmospheric pressure

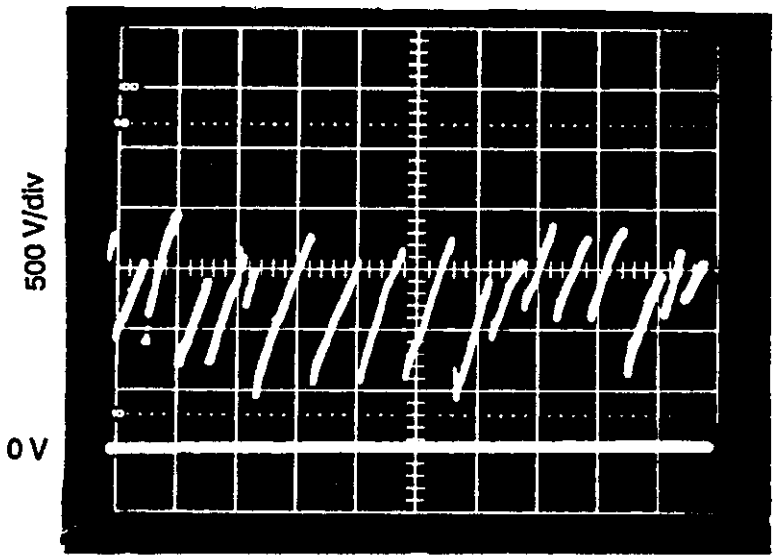

Fig. 6.14 The voltage waveform of the transverse discharge at gas flow of 15 m/s.

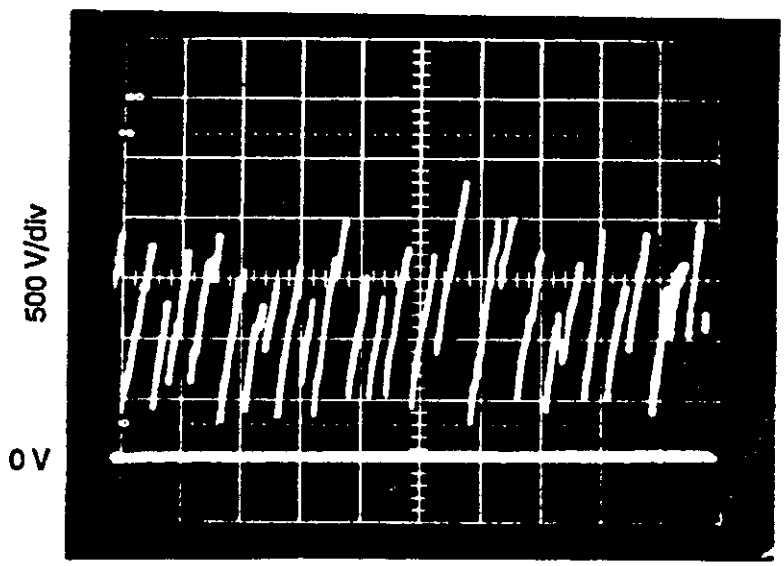

Fig. 6.15 The voltage waveform of the transverse discharge at gas flow of 25 m/s.

that each cycle the discharge voltage for the longest column possible carried away by the flow was just enough to break down the gap again. These tests show also that the electric discharge is unstable in the transverse gas flow and the discharge column is always forced to be parallel to the flow confined by the flow streamlines.

6.9 THE DISCHARGE COLUMN IN THE STAGNATION REGION

A test was carried out to show the behaviour of the electric discharge in the stagnation region formed in front of the upstream electrode. A rod 3mm diameter with flat end was used as the upstream electrode, inserted axially in a Pyrex tube 20 mm ID. Another rod was inserted downstream 20 mm apart (Fig. 6.16a). The flow pattern around the upstream electrode was expected to be as shown in Fig. 6.17. Over a wide range of velocity (10-300 m/s), the discharge column was contracted and parallel to the flow streamlines starting from the upstream fall region which appeared as a narrow point located on the edge of end of the upstream electrode (Fig. 6.16b).

It was concluded that as the steep flow profile pushes the discharge column towards the stagnation region, the transverse component of the eddies in the stagnation region forces the discharge column out of this region. The result is a contracted discharge between the steep flow profile region and the eddies region.

6.10 THE DIFFUSING INJECTION NOZZLE

Vortex generators are frequently used behind the upstream electrode to create vortices in front of it on the assumption that the vortices are able to mix the discharge with the gas flow and diffuse it (Hill 1971, Wiegand and Nighan 1975, Evans 1987). Although the vortices are able to diffuse the discharge and increase the threshold at which the streamers form under some

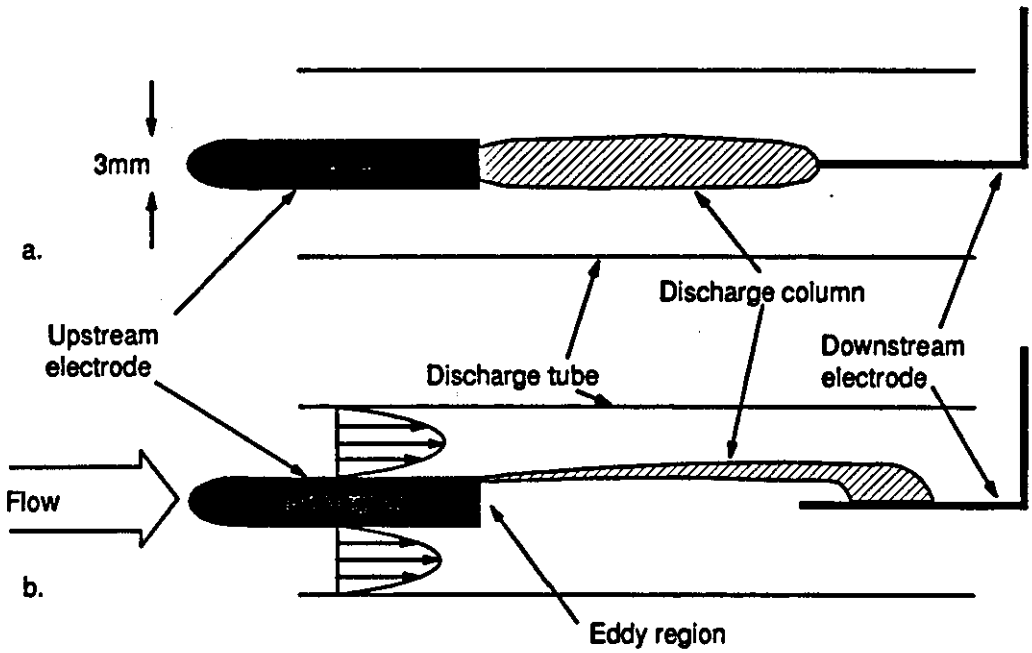

Fig. 6.16 The discharge column behaviour in the stagnation region

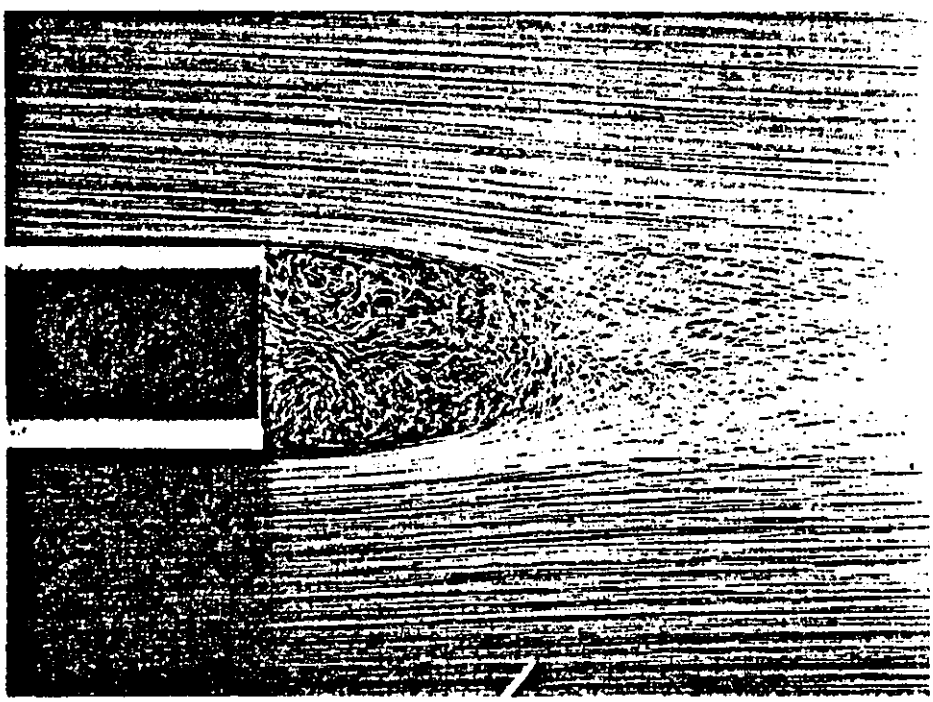

Fig. 6.17 The gas flow pattern around a flat cut rod (the gas flow is from left to right). (After Van Dyke 1982)

conditions at low pressure, the present results indicate that the diffusion is not due to the discharge mixing but that the vortices disturb the stagnation region and force the discharge column to the flow streams, but the discharge column diffusion in this case is still limited because of the steep flow profile adjacent to the upstream electrode.

A convergent-divergent diffuser located in front of the upstream electrode was designed (Fig. 6.18a) to minimize the stagnation region in front of the upstream electrode and to have a plane flow profile in the discharge column. The gas flow streamlines here are forced to converge in front of the electrode, squeezing the stagnation region and passing the throat with an almost plane flow profile. As the gas flow streamlines diverge in the diffuser , it is expected that the discharge column will be diffused by following the streamlines.

A copper electrode 1mm diameter was placed behind a diffuser made of pyrophyllite with a 3 mm diameter throat and diverging angle of 12°. The nozzle diffused the gas into a Pyrex tube (5 mm ID). The downstream electrode was placed along the axis of the tube so that the electrode gap was 20 mm. At a gas velocity of up to 300 m/s in the throat, the discharge column of up to 0.1 A appeared contracted in the throat and then diffused in the divergent part of the diffuser following the diverging flow streamlines (Fig. 6.18b). When the discharge current was increased above about 0.1A, the discharge column started to contract. This is because the flow profile is never completely plane in front of the upstream electrode and when the discharge current is increased the current density will increase more in the low gas velocity region forming a hot constricted column.

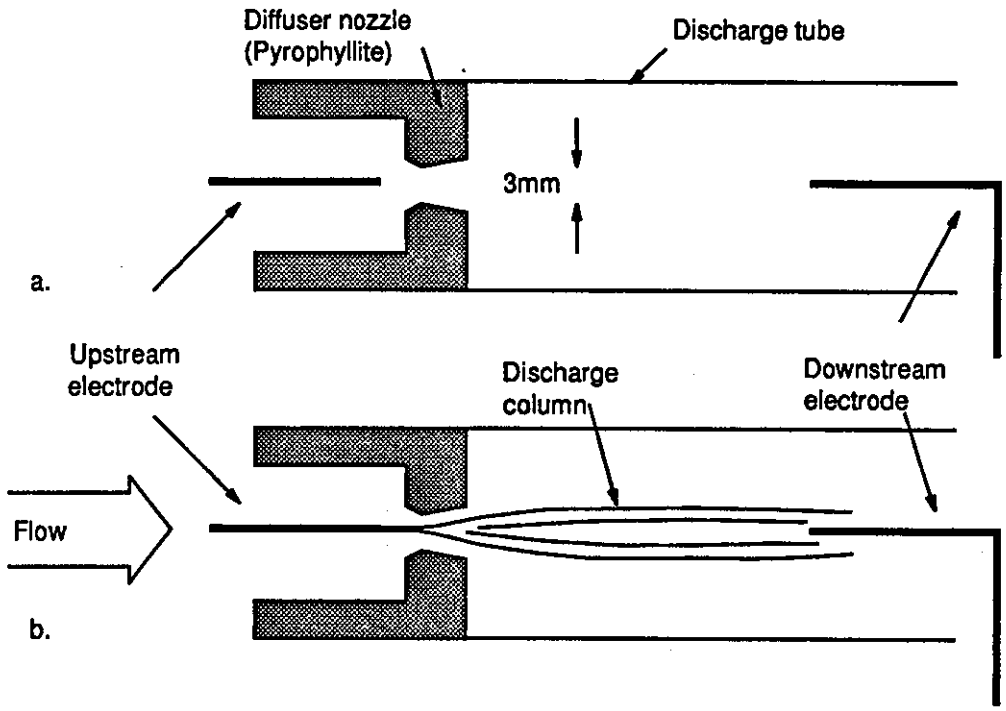

Fig. 6.18 Fast flow axial discharge using diffuser injection nozzle at atmospheric pressure

The gas velocity used here which is the same velocity used in the previous tests indicates that the gas flow regime which is identical in all the cases is not responsible for the diffusion but it is the flow profile.

6.11 SUMMARY OF RESULTS

(i) The configuration of the upstream electrode(s) is very critical and it/they dominate the discharge column characteristics.

(ii) Multiple electrodes upstream have greater advantages over a single electrode, minimising the discharge current per electrode and assisting in diffusing the discharge column over a larger cross sectional area of the discharge cavity.

(iii) The discharge column follows the gas flow streamlines therefore the downstream electrode(s) appear not to be critical and multiple downstream electrodes are not essential.

(iv) The polarity of the upstream electrode(s) has no effect on the behaviour of the positive column.

(v) The stagnation region around the upstream electrode(s) must be eliminated, otherwise, the flow shearing force will push the discharge column towards this region where once it is out of the gas flow stream and is not sufficiently cooled, the discharge column will be contracted and thermally ionised.

(vi) A steep profile adjacent to the upstream electrode(s) is necessary for effective convective cooling of the discharge column.

(vii) A turbulent flow is more effective than the laminar flow in diffusing the discharge column because it has a planar profile in the centre and steeper profile near the walls.

CHAPTER 7

A HIGH POWER FAST AXIAL GAS FLOW CO_2 LASER

7.1 INTRODUCTION

The behaviour of the discharge column in a fast axial gas flow and the interaction between the column and the flow were investigated in the previous chapter.

Multiple discharges have been used to obtain a large volume discharge at low pressure to excite a high power CO_2 laser using slow axial gas flow (Saleh 1981). Higher powers were obtained using multiple discharges combined with a fast axial gas flow injected at the anodes (Evans 1987).

This chapter investigates previous results on the 5 kW CO_2 laser head using a fast axial gas flow at low pressure (50 mb). Different electrodes configurations were used to examine the effect of the fast gas flow on the multiple discharge.

7.2 THE 5 kW CO_2 LASER

The 5 kW CO_2 laser was developed and built at Loughborough University using multiple discharges combined with recirculating gas injected at the anodes (Appendix 3). The discharge current is divided between four anodes upstream and six cathodes downstream and each of the four anodes and the six cathodes is separately stabilised. Fig. 7.1 shows the electrode arrangement and the circuit stabilisation. The gas injection anodes are cylindrical nozzles injecting the gas at 45° to the discharge tube. Fig. 7.2 shows the gas injection anode, anode head cross section and method of gas injection. The laser output power is limited by the formation of streamers (local constriction) within the discharge column at currents of about 1.8 A which limits the input power to the discharge to about 22 kW.

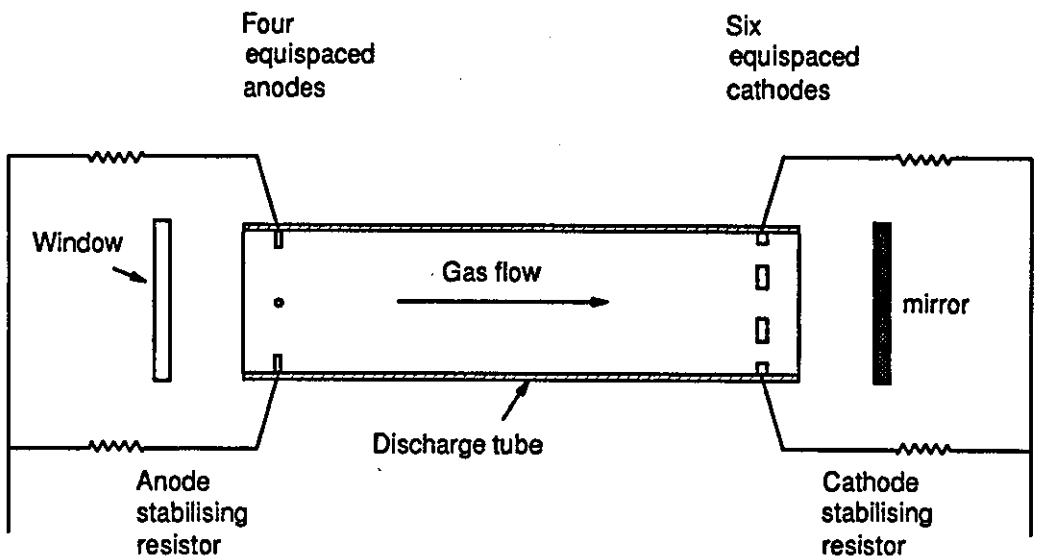

Fig. 7.1 Electrode arrangement and circuit stabilisation

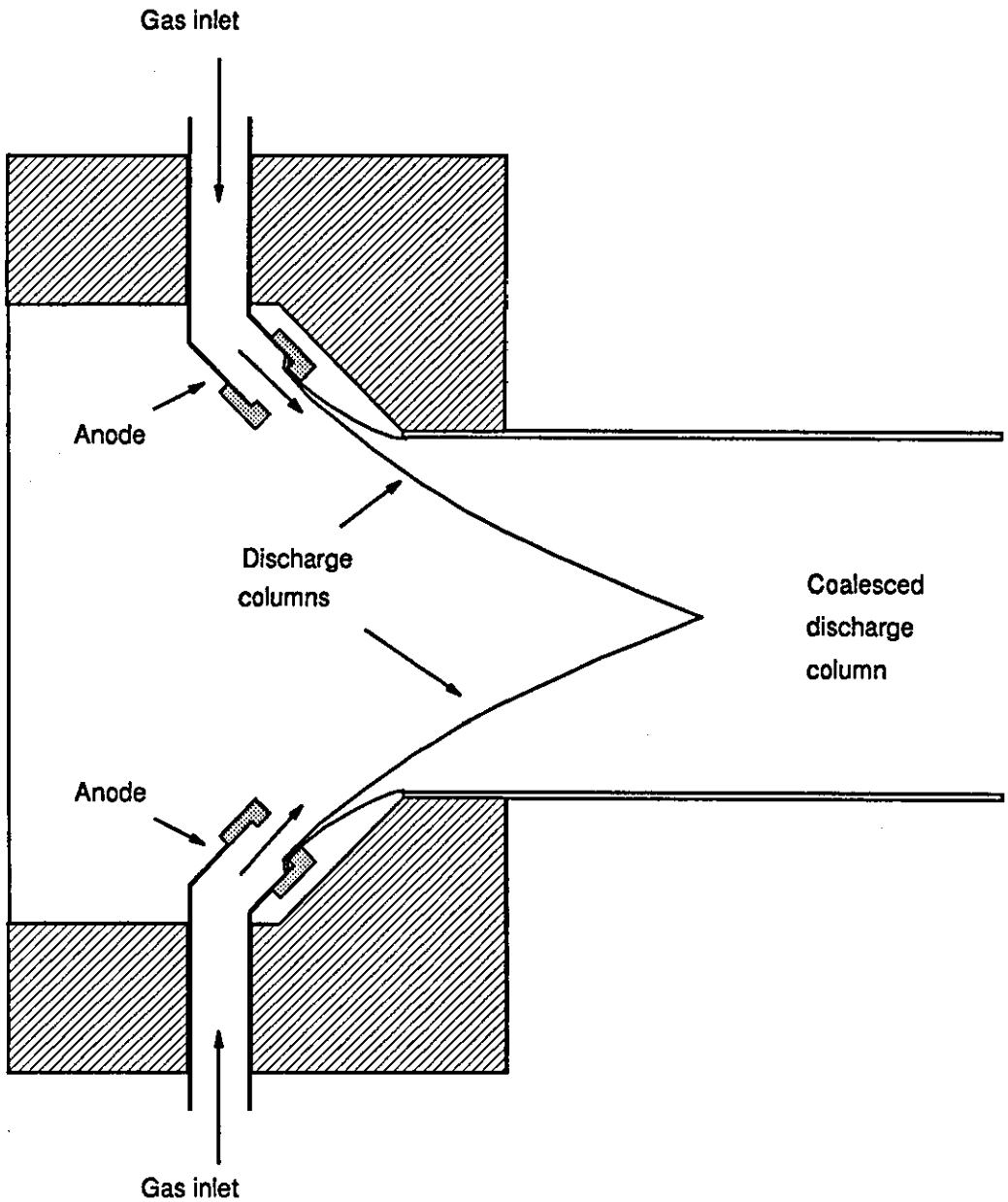

Fig. 7.2 The gas injection anode and anode head cross section and the method of gas injection.

7.3 THE GAS INJECTION ELECTRODES

It was thought that the discharge column at 50 mb in the 5 kW CO_2 laser would behave in a similar way to results obtained at atmospheric pressure by injecting the gas flow through a cylindrical nozzle (Fig. 6.9). As the gas flow was introduced through the injection anode, the anode root was driven to the stagnation region A out of the fast gas stream (Fig. 7.2), and the gas flow profile forced the low pressure discharge column to contract along side the nozzle wall similar to the behaviour at atmospheric pressure. As the gas diffused out of the nozzle into the tube, the discharge column was kept out of the fast flow region along side the tube wall at first until it was diffused by the gas injected at 45° from the opposite nozzle. As the discharge column was kept out of the fast flow region inside the nozzle and over an upstream part of the tube, the gas was not utilised efficiently in diffusing the discharge column and cooling it convectively. This results in the premature formation of streamers at an exit gas temperature of only about 105 °C although the theoretical limit on gas temperature can be increased up to about 250 °C before it quenches the selected transition.

The effect of a gas injection diffusing nozzle on the discharge was investigated at atmospheric pressure discharge in Chapter 6 which showed a considerable advantage over the cylindrical injection nozzle in using the gas for diffusing and convective cooling of the discharge column. This led to the design of a gas injection diffuser nozzle to replace the cylindrical nozzles used in the 5 kW CO_2 laser. Fig. 7.3 shows the new injection anode and anode head cross section and the behaviour of the discharge column in the gas flow. The discharge column was confined by the gas flow at the throat along the axis of the nozzle and as the gas diffused through the diffuser to the discharge tube, the discharge column followed the diverging flow streamlines as

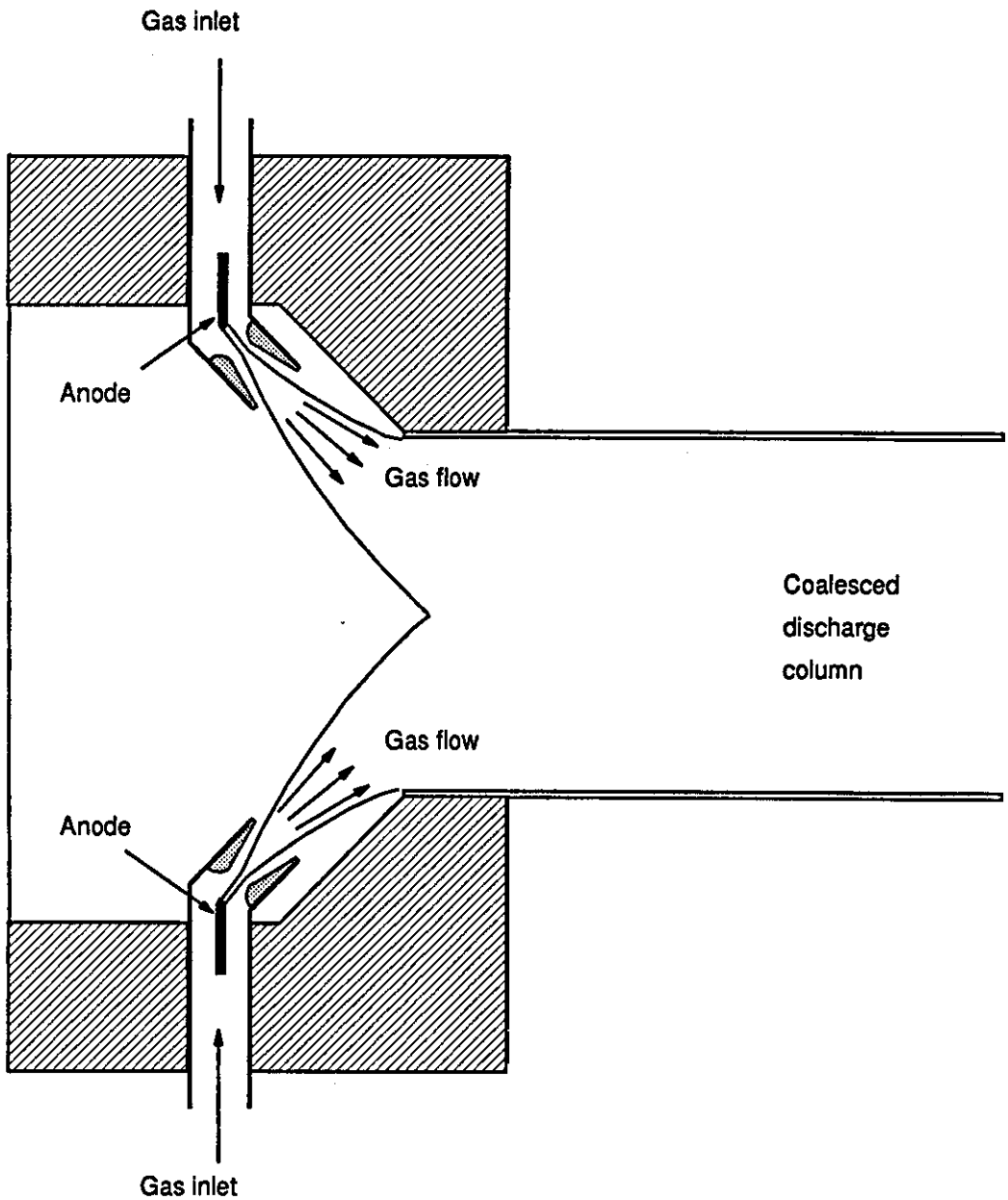

Fig. 7.3 The discharge column behaviour with the newly designed gas injection anode

discussed in Chapter 6 which resulted in a diffused discharge column starting at the nozzle, and a good utilisation of the gas to cool the column convectively.

The sum of the cross sectional area of the throats of the new injection anodes was 1134 mm^2 which is half the total cross sectional area of the original injection anodes which limited the gas mass flow rate to about 0.014 kg/s. At a pressure of 50 mb, a uniformly diffused discharge was obtained at a discharge current of up to 0.9 A at a gas mass flow rate of 0.012 kg/s before the formation of streamers occurred using the new injection anodes. This is compared with a mass flow rate of 0.023 kg/s needed with the original injection anodes to obtain a diffused discharge at the same current (0.9 A) before the streamers began to occur. The gas exit temperature at the maximum discharge current before the formation of streamers with the new injection anodes was about 150 °C compared with the 105 °C obtained with the original anodes which showed that the gas was being used more efficiently in diffusing the discharge column.

7.4 THE CONSTRICTION OF THE DISCHARGE COLUMN

A series of tests were carried out on the 5 kW CO_2 laser system to study the characteristics of the fast flow discharge at low pressure (50 mb), and to obtain reference characteristics curves for the multiple discharge so they could be compared with other characteristics for different electrode configurations.

The voltage-current characteristics of the fast axial gas flow electric discharge at 50 mb and a mass flow rate of 0.0142, 0.02 and 0.027 kg/s are shown in Figs. 7.4, 7.5 and 7.6. When the gas passed through the anodes, it passed through the discharge column, cooled it convectively and diffused it in a similar way to the test carried out at atmospheric pressure (Chapter 6). The gas

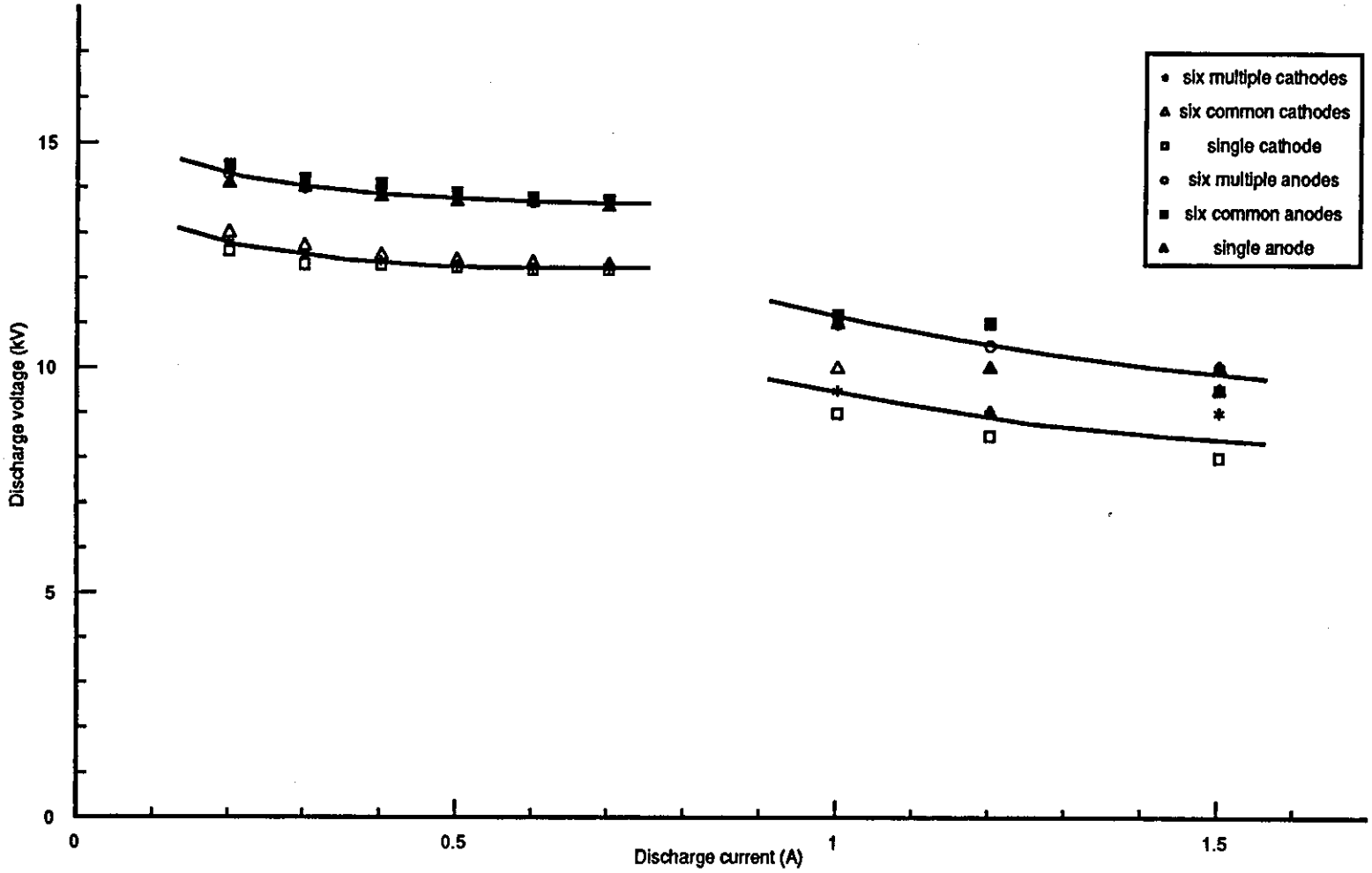

Fig. 7.4 The voltage-current characteristics at mass flow rate of 0.0142kg/s

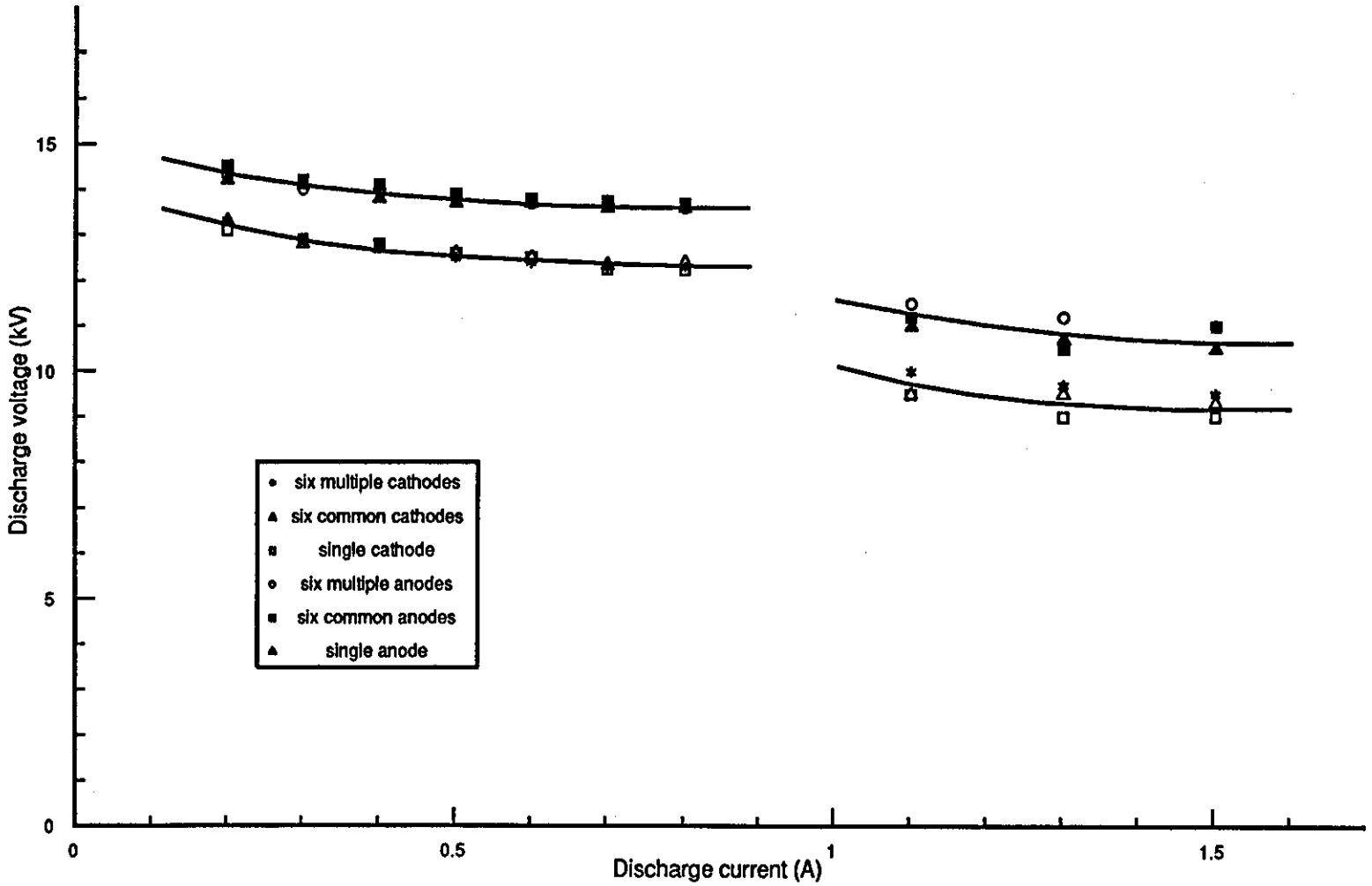

Fig. 7.5 The voltage-current characteristics at mass flow rate of 0.02kg/s

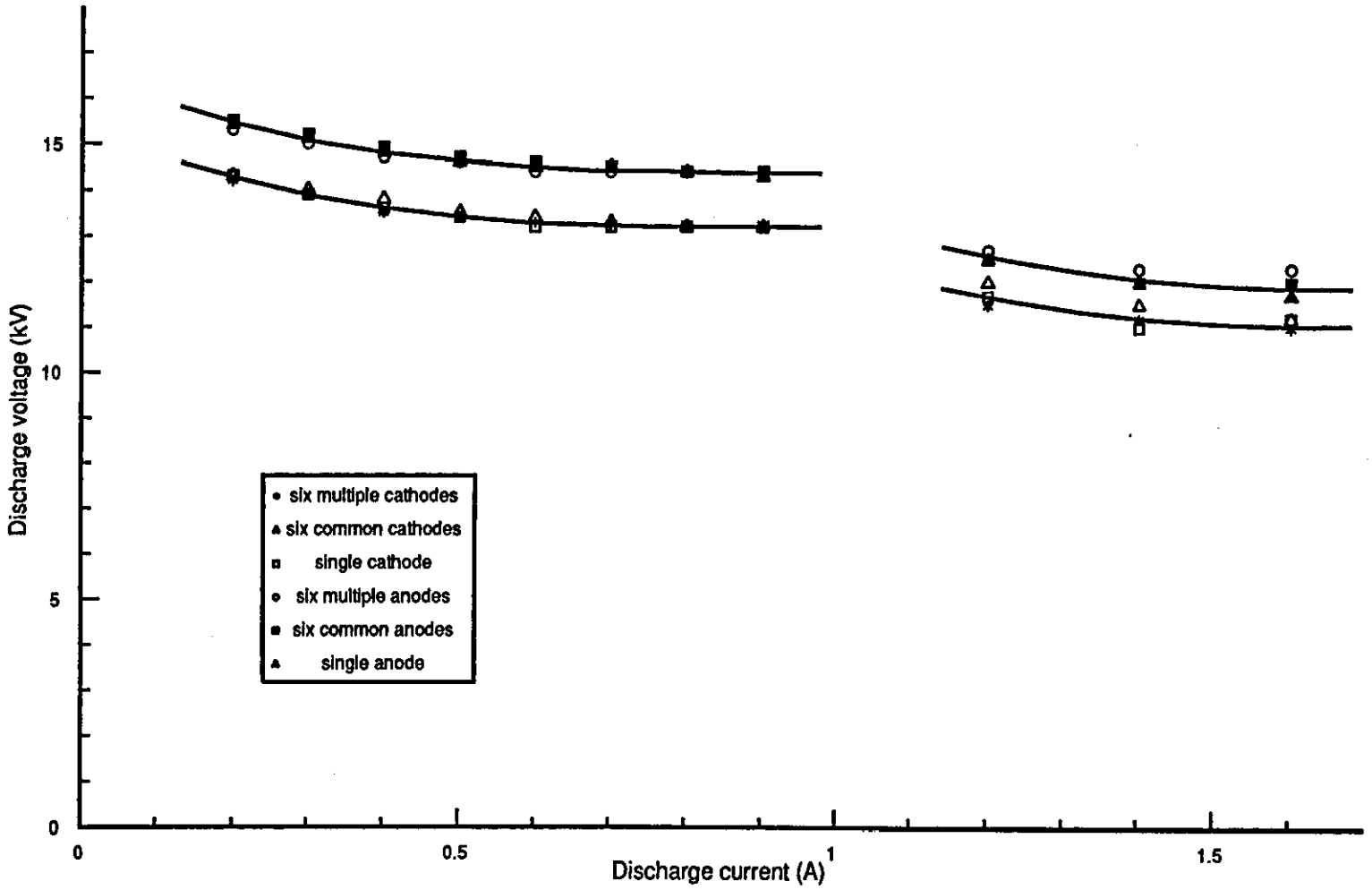

Fig. 7.6 The voltage-current characteristics at mass flow rate of 0.027kg/s

diffused out of the anodes into the Pyrex tube and the discharge column was confined along the flow streamlines emanating from the nozzles forming a homogeneous diffused discharge column (Fig. 7.7). As the current was increased, the discharge column current density increased and the discharge voltage decreased. When the discharge current was increased up to 0.7 A, 0.85 A and 0.9 A at the gas mass flow rates 0.0142, 0.02 and 0.027 kg/s respectively, random local constrictions (streamers) began to appear downstream (Fig. 7.8), without any apparent sudden change in the discharge voltage. The streamers are thought to be due to the gas becoming hot downstream as it travels along the discharge, any thermal non-homogeneity causes more current to flow through the hot region and a streamer forms. As the current increased further, the discharge column suddenly constricted between the upstream anodes and the downstream cathodes (Fig. 7.9). The sudden constriction was associated with an abrupt reduction in the discharge voltage which is shown in Figs. 7.4, 7.5 and 7.6 at total currents of 1.0 A, 1.1 A and 1.2 A respectively.

It is important to distinguish between this sudden transition in the discharge voltage which is due to the constriction of the column and the glow to arc transition which happens in the static gas flow at the cathode fall region (Chapter 4). Although the characteristics of the fast gas flow electric discharge are different from the discharge characteristics in static flow where there is a voltage-current characteristics curve for each value of gas flow rate, the fast gas flow discharge is equivalent to the subnormal glow in static gas flow in terms of the ionisation process taking place in the discharge column. Therefore, the discharge column constriction in the fast flow discharge is equivalent to a transition from point a to point b on the voltage-current characteristic curve of the positive column in the static flow (Fig. 7.10). This transition happens gradually in the discharge in a static gas flow due to the gradual domination of the

Fig. 7.7 Uniform diffused discharge column (direction of the flow is from left to right). (Vertical striations are due to reflections).

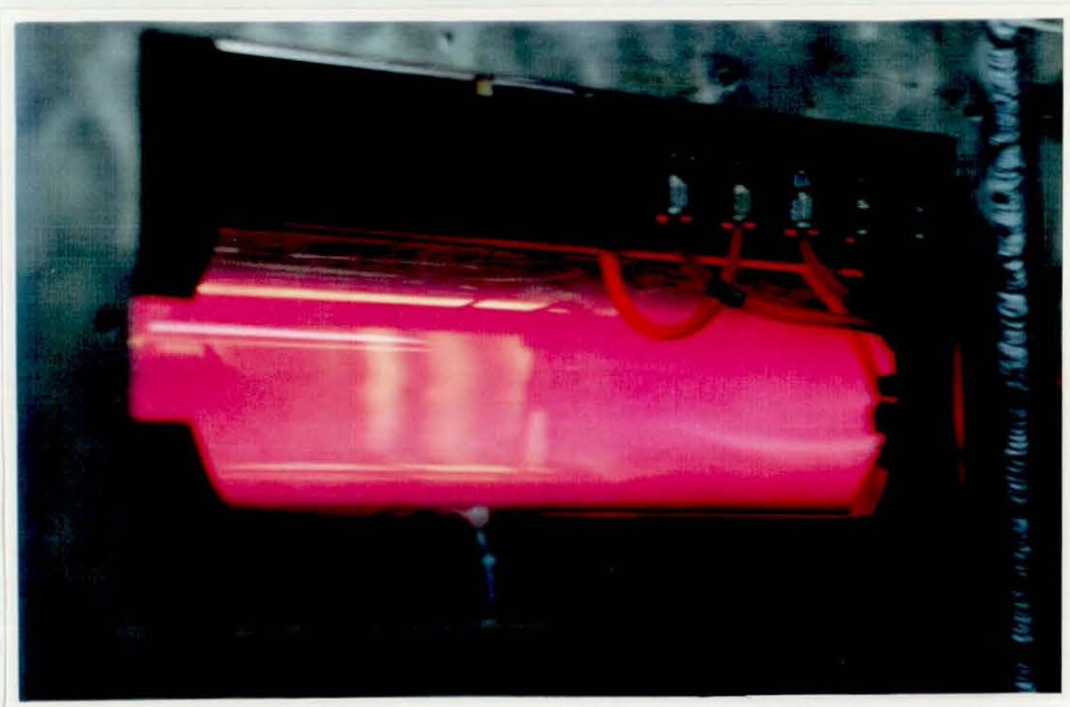

Flg. 7.8 Local constriction downstream (direction of the flow is from left to right). (Vertical striations are due to reflections).

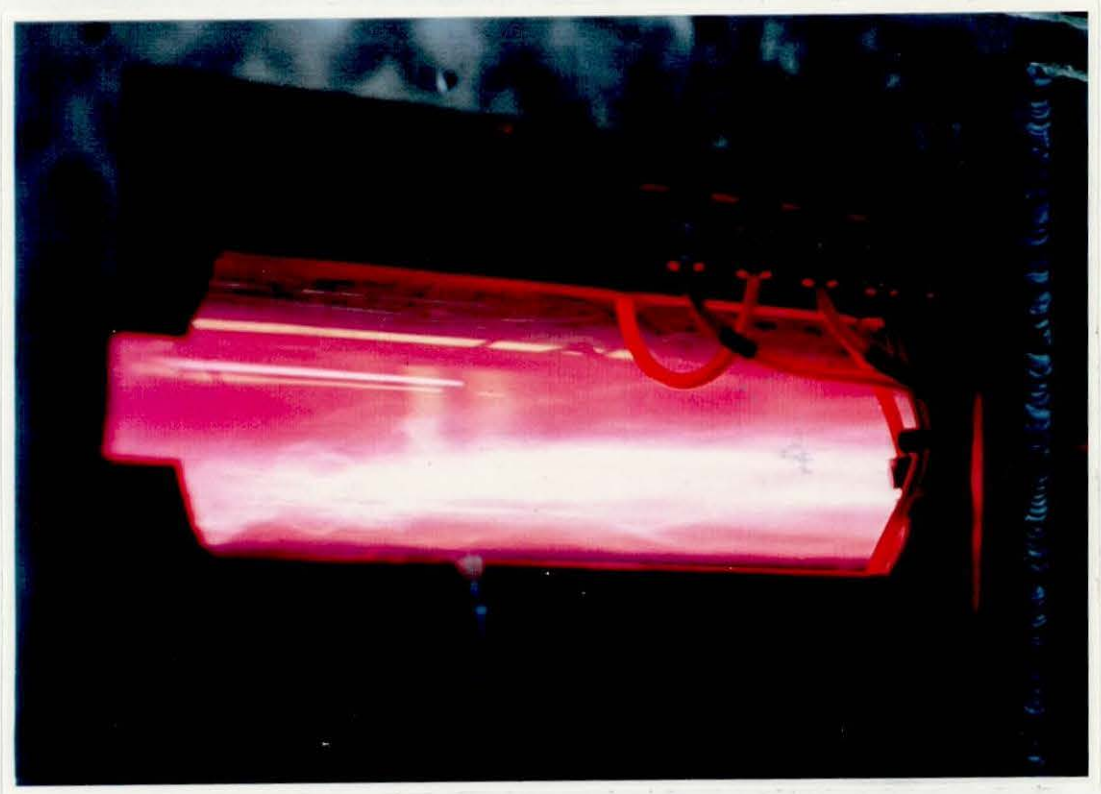

Fig. 7.9 Constriction of the column along the discharge (direction of the flow is from left to right). (Vertical striations are due to reflections).

thermal ionisation process over the field ionisation process as the discharge current is increased, while it happens suddenly in fast gas flow convectively cooled discharge due to the effect of local thermal instability.

7.5 THE DOMINATION OF THE FAST GAS FLOW ON THE DISCHARGE CHARACTERISTICS

It was concluded in Chapter 6 that once the discharge has been diffused upstream by the fast axial gas flow, it is confined by the flow streamlines and stays diffused along the discharge column, therefore, the downstream electrode configuration has no effect on the discharge column characteristic. The six downstream cathodes were connected in common to test this conclusion and to show the domination of the fast gas flow over the multiple discharge. The voltage-current characteristics of the discharge with six common cathodes at the same mass flow rates used in the test on separately stabilised cathodes were measured and are also shown in Figs. 7.4, 7.5 and 7.6. The characteristics showed no difference and the transition in the discharge voltage associated with the column constriction appeared to happen at the same values of discharge current.

To show how far the gas flow is dominating the discharge characteristic, a single cathode instead of six was used downstream. The discharge column which might be expected to constrict to one side of the tube or to show streamers at low currents as the cathode fall region was forced to a small unevenly distributed region on the surface of the cathode, Figs 7.4, 7.5 and 7.6 show again no difference in the voltage-current characteristic and the discharge current at which the transition in the discharge voltage associated with the column constriction occurs.

It was concluded in Chapter 6 that the polarity of the electrodes has no effect on the atmospheric pressure fast gas flow discharge column characteristic. To show this at low pressure, the polarity of the electrodes was reversed so that the four electrodes upstream became cathodes and the six electrodes downstream became anodes. The voltage-current characteristics of the discharge was measured with both commonly and separately stabilised anodes in addition to a single anode downstream which showed no difference in the discharge current at which the constrictions happened but showed about 10% increase in the discharge voltage than with the opposite polarity (Figs. 7.4, 7.5 and 7.6).

It was observed that as the gas flow was forcing the cathode root to a narrow region at the far end of the cathode (Fig. 7.11), the cathode fall appeared to be in the arc regime but this did not affect the constriction current which indicates that the discharge column regime can be controlled by the gas flow independently of the conditions at the fall regions at the electrodes

7.6 MEASUREMENT OF THE LASER HEAD PARAMETERS AT THE ONSET OF THE CONSTRICTION OF THE COLUMN

As the gas flow diffuses the discharge column upstream by being injected through the electrodes, the discharge column characteristic appears to be mainly dominated by the gas flow. The laser head parameters therefore were measured at different values of gas mass flow rate using different electrode configurations, six separately stabilised cathodes, six common cathodes and single cathode downstream as well as opposite polarity for the same arrangements.

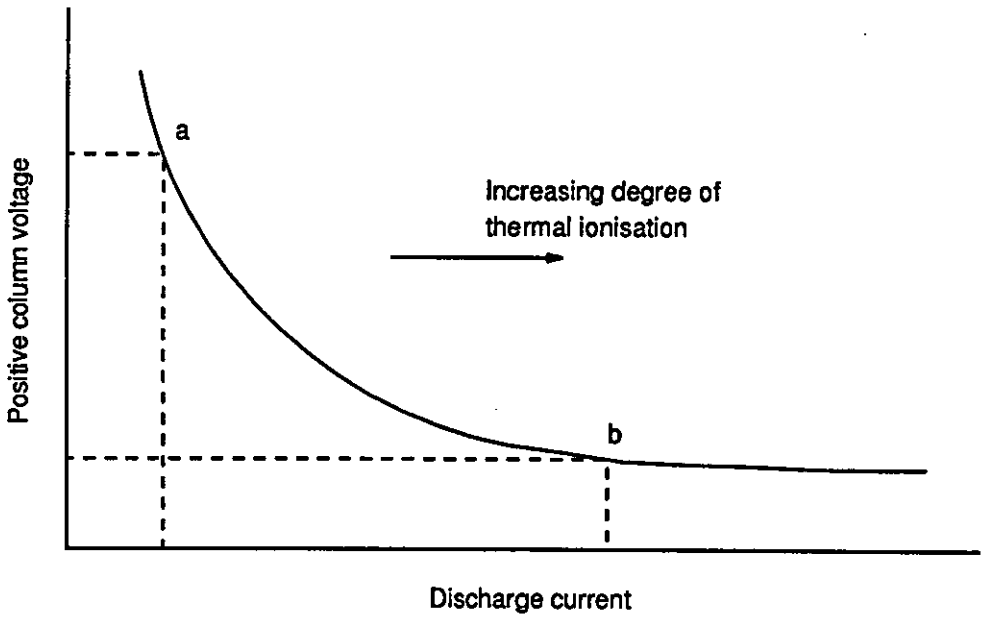

Fig. 7.10 The V-I characteristic of the positive column in a static gas flow

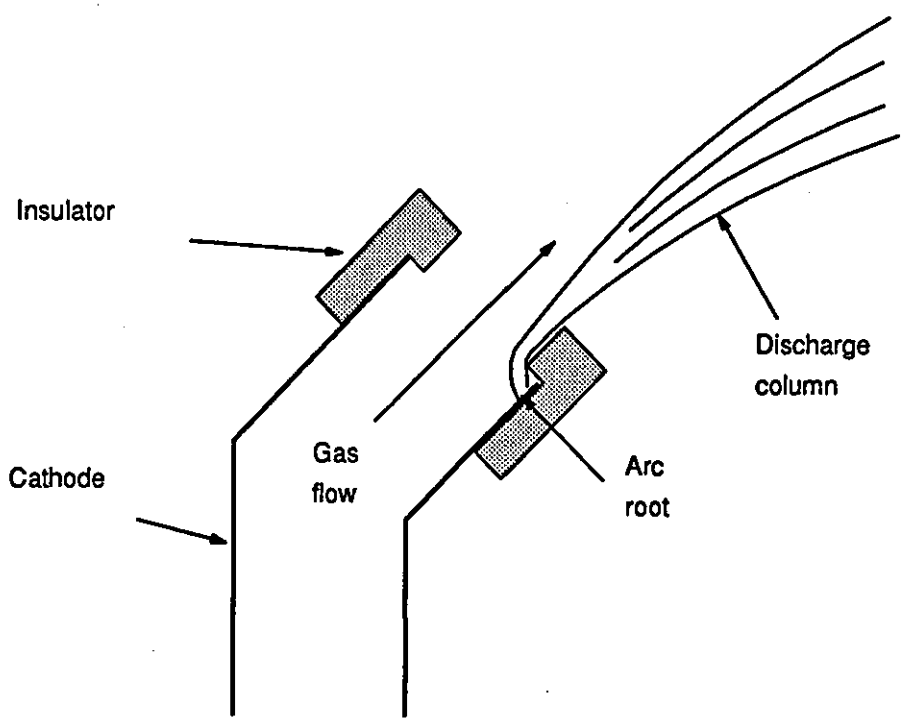

Fig. 7.11 The gas injection cathode

7.6.1 The Discharge Column Constriction Current

The relation between the mass flow rate and the discharge current at which the constriction of the column begins to appear downstream for the different electrode configurations is shown in Fig. 7.12. The relation appears to be linear implying that the maximum input power to the discharge is directly proportional to the mass flow rate. This relation appears to be irrelevant of the downstream electrode configurations or the electrode polarity which indicates that the column constrictions (streamers) are mainly due to the thermal non-homogeneity which is increased by increasing the current and decreased by increasing the gas mass flow rate.

The linear relation between the maximum input power to the discharge and the gas flow rate is only obtained for conditions where the column is immersed within the gas flow. If a stagnation region exists upstream and the discharge column passes out of the gas flow, the mass flow rate has a small effect on the input discharge power.

7.6.2 The Gas Output Temperature

The relation between the gas mass flow rate and the gas output temperature at the onset of the random local constriction within the column for the different electrodes configurations is shown in Fig. 7.13. The gas output temperature, which might be expected to remain constant, appears to increase linearly with the mass flow rate which indicates that the additional input power which results from the increase in current at which the constriction starts to appear is not totally removed by the additional gas mass flow, but still the gas flow rate is adequate to keep the discharge column homogeneously diffused. This demonstrates the domination of the gas

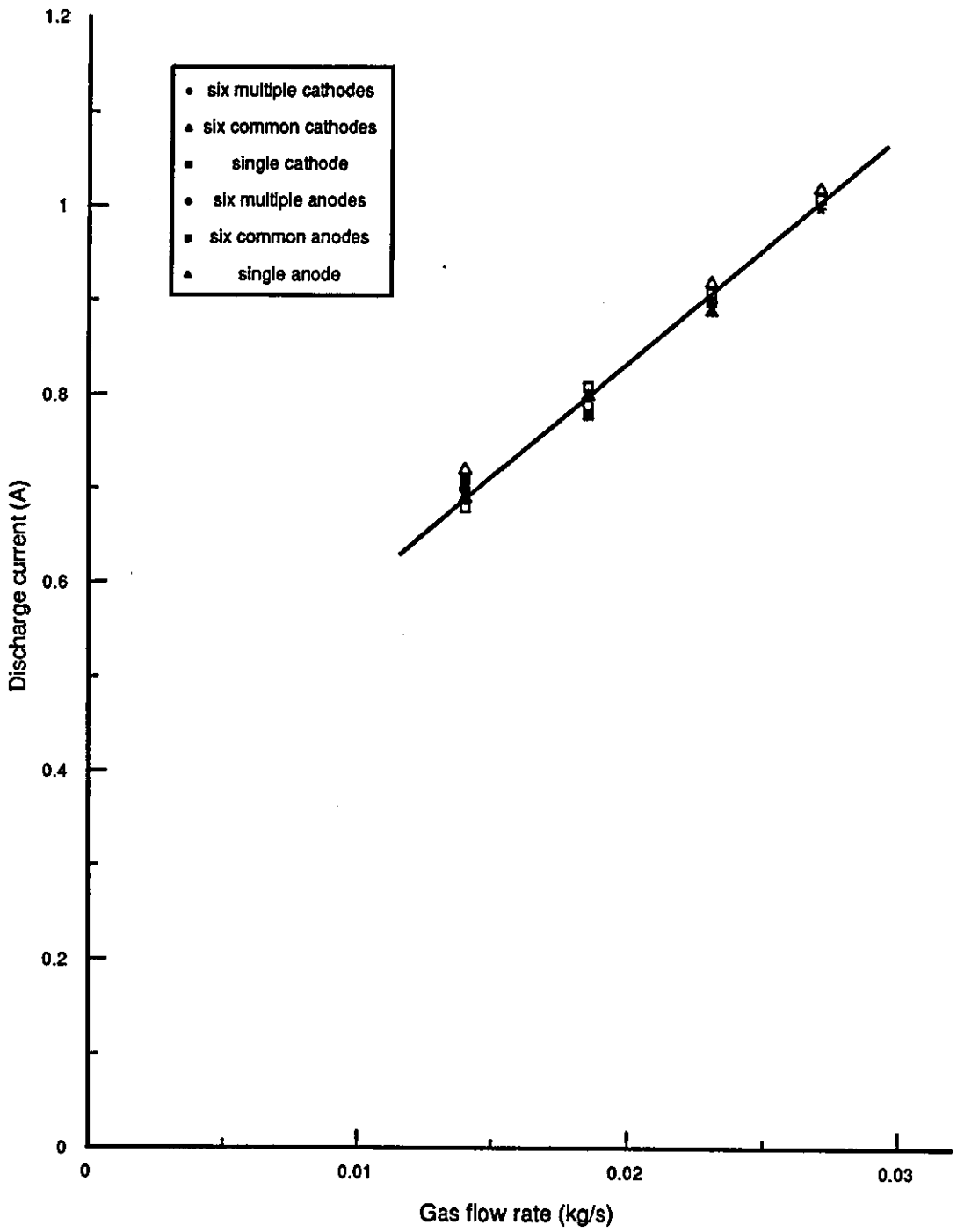

Fig. 7.12 Variation of the column constriction current with gas mass flow rate

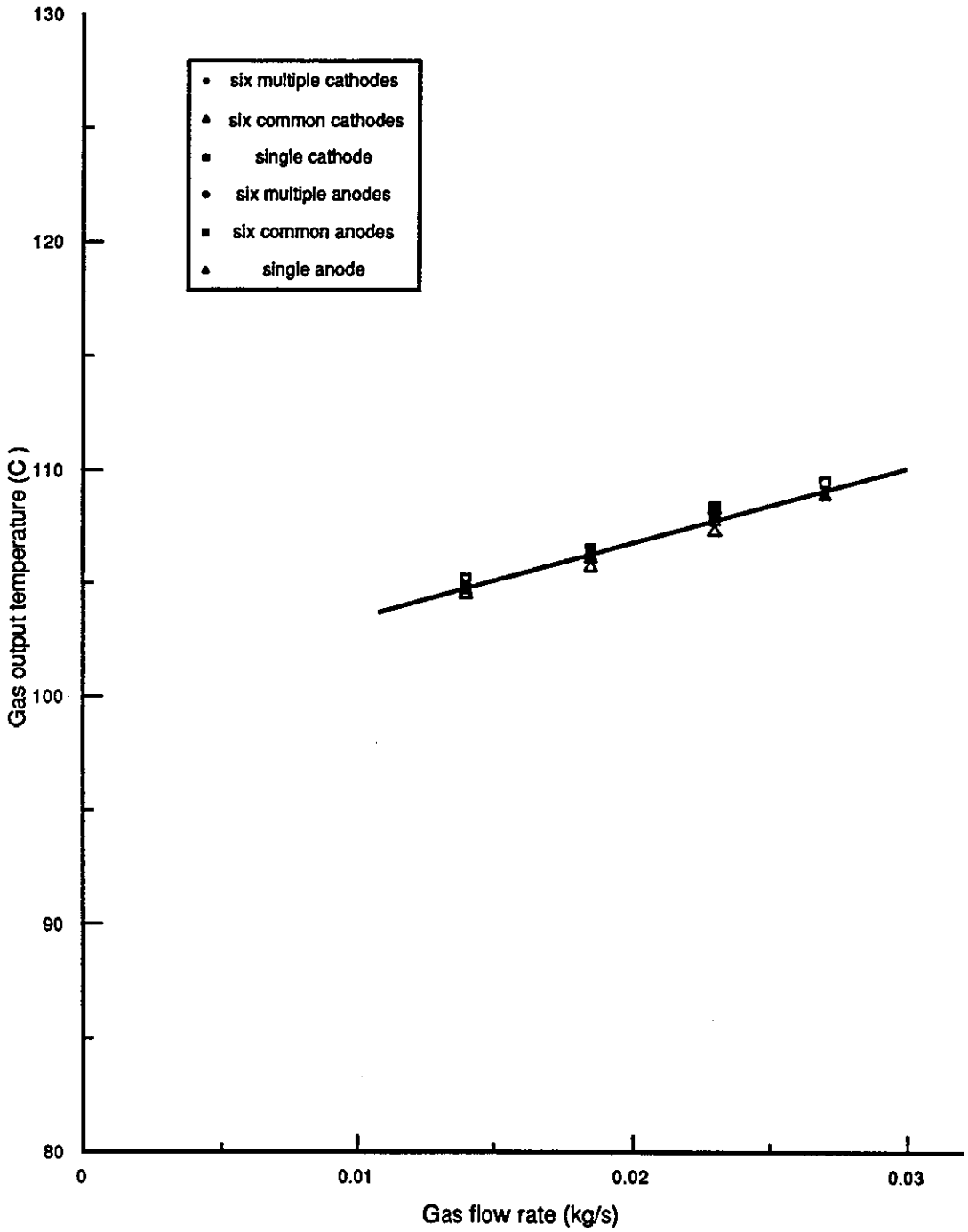

Fig. 7.13 Variation of gas output temperature with the gas mass flow rate

mass flow rate on the discharge column characteristics. The relation also appears to be unaffected by the downstream electrode configurations or their polarity

7.6.3 The Laser Output Power

The laser output power was measured for the different electrode arrangements to show if the separately stabilized downstream electrodes or their polarities have any effect on the laser output power. The relation between the gas mass flow rate and the laser output power at the discharge current at which the column constriction was just about to appear is shown in Fig. 7.14. The laser output power appears to be linearly proportional to the mass flow rate and is unaffected by the different electrode configurations used except that opposite polarity with cathode upstream and anodes downstream showed an increase of 10% laser output power. This increase in the laser output power is thought to be due to the higher discharge voltage mentioned before for this polarity arrangement which increases the E/p (or E/N) value (0.38 V/mm.mb) by 10%. Using this polarity arrangement (cathode upstream and anode downstream) is useful since the laser output power is increased without increasing the discharge current which is limited by the column constriction.

The tests have shown that multiple discharge or separately stabilised downstream electrodes are unnecessary where the fast gas flow dominates the discharge column characteristic, unlike the upstream electrodes where separately stabilised electrodes are essential for the diffusion of the discharge column upstream similarly to what was concluded from results at atmospheric pressure (Chapter 6). This conclusion is useful for a simpler design of the downstream electrode head assembly and the stabilisation circuit in terms of structure and electrical insulation.

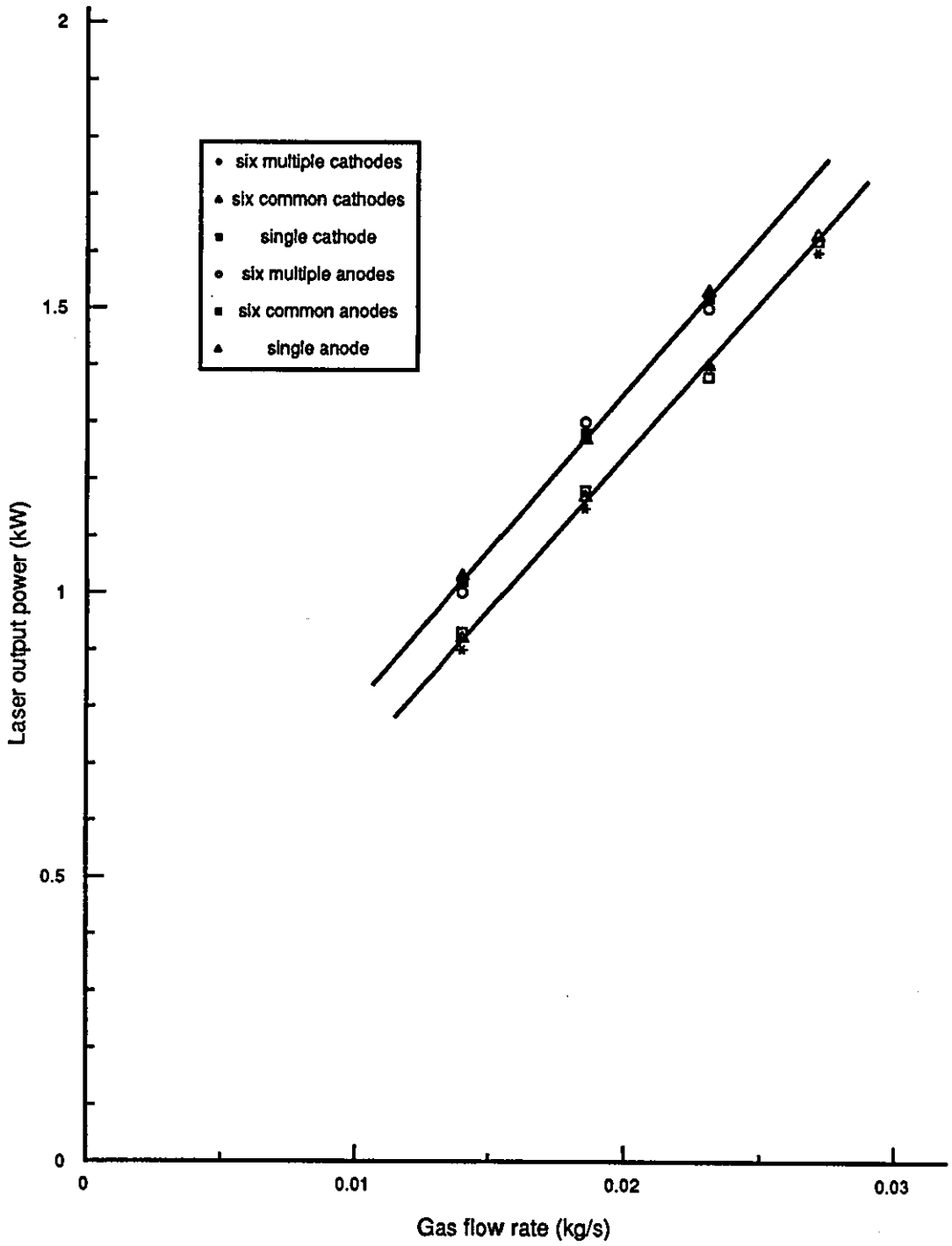

Fig. 7.14 Variation of the laser output power with the gas mass flow rate

7.7 THE E/N AND E/p RATIOS

For efficient vibrational excitation of the molecular gas mixture, the known excitation cross sections require an average electron energy determined by the E/N ratio (Nighan 1970) which could predicate operation of the discharge in diffused or constricted column mode. Experimental techniques such as using electrostatic probes or microwave radiometric techniques could be used to measure the electron energy distribution in electric discharges but they are difficult to employ and subject to varying interpretation (Papoular 1965). Nevertheless experimental results can be compared with calculated values provided E/N is known (Nighan 1970).

The E/N ratio (or E/p) is used as a measure of the average energy an electron acquires along a mean free path λ_e in the field direction where $E/P \propto E.\lambda_e$ (von Engel 1965), and the neutral particle density N is related to the pressure p by,

$$N = \frac{N_A \times p}{R \times T} \qquad 8.1$$

where N_A is Avogadro's number, R is the gas constant and T is the gas temperature.

It was shown in Chapter 4 that the voltage-current characteristic curve of the static gas flow discharge column determines the ionisation process in the column. As the column voltage gradient changes with current along the voltage-current characteristic curve due to the change from domination by either field or thermal ionisation processes, the value of E/p changes accordingly. In this case E/p could be used as a measure of the average electron energy in the column.

In the fast axial gas flow discharge, the discharge column voltage gradient E could be increased for two opposite reasons;
(i) diffusion of the discharge column by the gas flow and therefore convective cooling, or,
(ii) contraction of the discharge column by the flow accompanied by thermal ionisation.

It is well established that CO_2 lasers operated best with a ratio of electric field to pressure (E/p) of 0.76-3.8 V/mm.mb (Demaria 1973). It is believed that this wide range of E/p is due to the different discharge column regimes in the fast gas flow discharge. The E/p value for the existing 5 kW laser at its optimum operation and maximum output power of 5 kW is only 0.365 V/mm.mb (equivalent to $E/N=2.62 \times 10^{-16}$), (Evans 1987), but the electrical to optical efficiency is 23.6%.

The E/p value at 50 mb pressure, 0.027 kg/s gas flow rate and an output power of 1.6 kW is 0.38 V/mm.mb, but it is insignificantly lower (0.32 V/mm.mb) for the constricted column as the current was increased although a large reduction in the laser output power occurred (0.3 kW) which shows that the E/p (or E/N) is an ambiguous measure for assessing the suitability of the fast gas flow discharge for laser excitation.

7.8 SUMMARY OF RESULTS

(i) A gas injection diffuser nozzle was used to replace the original injection nozzle in the 5 kW CO_2 laser which allowed a 50% reduction in the gas mass flow rate due to the better utilisation of the gas flow in diffusing the discharge column. A power output of up to 7.5 kW should be possible if the full mass flow rate available is employed.

(ii) When the discharge column is diffused upstream using separately stabilised multiple electrodes combined with gas injection at the electrodes the column appears to be confined in the flow streamlines and remains diffused along the discharge cavity irrespective of the downstream electrode configurations or polarity.

(iii) Thermal instability and sudden constriction occur in the discharge column at a discharge current irrespective of the downstream electrode configurations or polarity.

(iv) Once the discharge column is diffused and immersed within the gas flow, the maximum discharge input power related to the maximum laser output power is directly proportional to the gas flow rate irrespective of the electrode fall region regime or the downstream electrode configurations or polarity.

(v) The discharge voltage was increased by 10% using the cathodes upstream and the anodes downstream and this increased the laser output power by 10%.

(vi) Separately stabilised downstream electrodes are not necessary for fast axial gas flow lasers as the separately stabilised electrodes downstream is not critical.

(vii) The E/N (or E/p) ratio is not the right measure for assessing the fast gas flow electric discharge for laser excitation.

CHAPTER 8

CONCLUSIONS AND RECOMMENDATIONS FOR FURTHER WORK

8.1 CONCLUSIONS

The characteristics of the electric discharge in a still gas have been investigated in air, He, Ar and CO_2 laser gas mixture. Glow discharges have been obtained at currents of up to 1.2 A over a wide range of pressure (50 mb up to 1 b). The characteristics and the emission spectra of the positive column have shown that the positive column is not affected by the glow to arc transition which is solely a cathode fall region phenomenon, however, the emission spectra have shown a considerable change as the discharge current is increased and the voltage gradient of the discharge column decreased, which is consistent with the change from the predominantly field ionisation to the thermal ionisation. It has been shown that the glow to arc transition oscillates between a glow and arc discharges neither of which is stable with time at the transition current.

As the pressure and/or the current is increased, the positive column contracts. It has been shown that the rate of contraction of the positive column accompanied by the reduction of its voltage gradient is higher in a gas of low thermal conductivity. It has been concluded that as the temperature of the gas in the column increases, the thermal ionisation through the molecule-molecule collision process dominates over the field ionisation process (the electron-molecule collision process). The high temperature in the column increases the degree of ionisation in the column and causes the contraction and the reduction of the voltage gradient of the column. It has been shown that enhancing the field ionisation process within the positive column leads to a higher electron energy which is possible by cooling the discharge column homogeneously.

The Steenbeck's minimum principle has been illustrated experimentally by the increase in the voltage gradient in the discharge column when the column was

contracted by an external electromagnetic field. It has been also shown that the column voltage gradient can be increased with the contraction of the column by the gas flow as well as with the diffusion which is consistent with the minimum principle. The E/N ratio of the positive column therefore is not necessarily a useful measure of the electron energy within the positive column in the fast gas flow.

The parallel multiple discharge was investigated and analysed. It has been shown that the multiple discharge coalesces so as to operate at the minimum voltage, and a simple mathematical model for the coalesced double discharge was established based on Steenbeck's minimum principle. The coalesced column of a multiple discharge has the same characteristics as a single discharge column carrying the same current, however the advantage of the multiple discharge is the distribution of the discharge current between more than one electrode. The anti-parallel multiple discharge was investigated and it was shown that it is not possible to obtain a coalesced anti-parallel discharge column, therefore the anti-parallel columns are always non coalesced and they operate between the shortest electrode separations so as to operate at the minimum voltage which is also consistent with Steenbeck's minimum principle.

Fast gas flow can be used to cool the discharge column and enhance the field ionisation process within the column. It was shown that it is preferable to use multiple electrodes upstream to spread the discharge column over a larger cross section area which stays diffused along the gas flow as it is confined by the flow streamlines. As the discharge column stays diffused and confined by the flow streamlines, the downstream electrode configuration has been shown to have a minor effect on the discharge column characteristics.

The interaction of the gas flow with the discharge column has been investigated and the contraction force applied by the shear stress force, due to the gas flow profile, on the discharge column was established mathematically. A rectangular injection nozzle has been designed to illustrate the role of the shear stress force due the flow profile across the length and the height of the nozzle in the contraction of the discharge column. An injection nozzle designed so as to diffuse the discharge column and to minimise the stagnation region in front of the upstream electrode has been proposed as an optimum design.

A gas injection diffusing nozzle was used to replace the original cylindrical injection nozzle in a 5 kW CO_2 laser which resulted in a 50% reduction in the gas mass flow rate due to better utilisation of the gas flow in diffusing the discharge column and more effective cooling. Once the discharge column is diffused and immersed within the gas flow, the maximum discharge input power determined by the laser output is directly proportional to the gas flow rate irrespective of the electrode fall region regime or the downstream electrode configuration or polarity.

This study has indicated that the discharge current and the gas pressure can be increased, so that the power density is increased, by using gas injection which minimises the stagnation region in front of the upstream electrode and along the discharge tube. It was also concluded that to maximise the convective cooling of the discharge, a transverse-flow and discharge configuration is preferable with multiple electrodes upstream and common electrode downstream. The results are applicable to both CO and CO_2 lasers where higher power and power density, and more compact lasers should be possible. The results have also indicated that CW excimer lasers are possible by combining the gas flow with the atmospheric pressure discharge using gas injection to diffuse and cool the discharge column homogeneously.

8.2 RECOMMENDATIONS FOR FURTHER WORK

(1) Investigation of various gas injection techniques to explore the optimum interaction of the gas flow with the discharge column over a wide range of pressure. This could lead to increasing the pressure and the convective cooling of the discharge with the optimum electron energy for selected transition, and to obtaining a higher density discharge and more compact gas lasers such as CO and CO_2 lasers.

(2) Studying different gas injection techniques for a fast flow electric discharge at gas pressure of up to 1 b to explore the possibility of the excitation of CW excimer laser.

(3) Investigation of the fast gas flow electric discharge for chemical synthesis by optimising the pressure and the electron energy necessary for a specific the chemical reaction.

(4) Development of the 5 kW CO_2 laser by increasing the gas mass flow rate with the new injection nozzle to enable the laser output power to be increased.

REFERENCES

Beaulieu, A. J.,"High peak power gas lasers," Proc. IEEE, vol. 59, (4), pp. 667-674, April, 1971.

Boenig, H. V.,"Fundamentals of plasma chemistry and technology," Technomat, 1988.

Brau, C. A.,"In excimer lasers," ed. by C. K. Rhodes, Topics Appl. Phys. 30 (Springer, Berlin, Heidelberg, New York), 1979.

Brown, S. C.,"Introduction to electrical discharges in gases," John Wiley, New York, 1966.

Carbone, R. J.,"Long-term operation of a sealed CO_2 laser," IEEE J. Quantum Electron., vol. QE-3, pp. 373-375, Sept. 1967.

Chebotaev, V. P.,"Uncontracted type of longitudinal d.c. glow discharge at atmospheric pressure," Soviet Physics-Doklady, vol. 17, (9), pp. 923-924, March, 1973.

Cheo, P. K.,"Effect of gas flow on gain of 10.6 micron CO_2 laser amplifier," IEEE J. Quantum Electron., vol. QE-3, pp. 683-689, Dec., 1967.

Clark, P. O. and Wada, J. Y.,"The influence of xenon on sealed-off CO_2 lasers," IEEE J. Quantum Electron., vol. QE-4, pp. 263-266, May, 1968.

Cobine, J. D.,"Gaseous conductors," McGraw-Hill, New York, 2nd ed., 1958.

Cool, T. A. and Shirley, J. A.,"Gain measurements in a fluid mixing CO_2 laser system," Appl. Phys. Lett., vol. 14, (2), pp. 70-72, Jan., 1969.

Demaria, A. J.,"Review of CW high-power CO_2 lasers," Proc. IEEE., vol. 61, (6), pp. 731-748, 1973.

Deutsch, T. F., Horrigan, F. A., and Rudko, R. J.,"CW operation of high-pressure flow CO_2 lasers," Appl. Phys. Lett. vol. 15, pp. 88-97, Aug. 1969.

Douglas, J. F., Gasiorek, J. M., and Swaffield, J. A.,"Fluid mechanics," Pitman, 2nd ed., 1985.

Eckbreth, A. C. and Davies, J. W.,"The cross-beam electric discharge convection laser," IEEE J. Quantum Electron., vol. QE-8, (2), pp. 139-144, 1972.

Eckbreth, A. C. and Owen, F. S.,"Flow conditioning in electric discharge convection lasers," Rev. Sci. Instrum., vol. 43, (7), pp. 995-998, July, 1972.

Eppers, W. C., Osgood, R. M., and Greason, P. R.,"75 -watt CW carbone monoxide laser," IEEE J. of Quantum Electron., vol. QE-6, p. 4, 1970.

Evans, D. R.,"Multiple glow discharges for the excitation of a high power CO_2 laser," Ph.D. thesis, University of Technology, Loughborough, UK, 1987.

Fan, H. Y.,"The transition from glow discharge to arc," Phys. Rev., vol. 55, pp. 769-775, April, 1939.

Gambling, W. A. and Edels, H.,"The high-pressure glow discharge in air," Brit. J. Appl. Phys., vol. 5, pp. 36-39, Jan., 1954.

Greene, A. E. and Brau, C. A.,"Theoretical studies of UV-preionised transverse discharge KrF and ArF lasers," IEEE J. Quantum Electron., vol. QE-14, (12), pp. 951-957, Dec., 1978.

Hancox, R.,"Importance of insulating inclusions in arc initiation," Brit. J. Appl. Phys., vol. 11, pp. 468-471, 1960.

Harry, J. E.,"Industrial lasers and their applications," MaGraw-Hill, London, 1974.

Harry, J. E. and Evans, D. R.,"Multikilowatt compact axial flow CO_2 laser," Appl. Phys. Lett., vol. 50, (6), pp. 313-315, Feb., 1987.

Harry, J. E. and Evans, D. R.,"A large bore fast axial flow CO_2 laser," IEEE J. Quantum Electron., vol. QE-24, (3), pp. 503-506, March, 1988.

Harry, J. E. and Knight, R.,"Simultaneous operation of electric arcs from a common power supply," IEEE Trans., Plasma Sci., vol. PS 9, (4), pp. 248-254, 1981.

Harry, J. E. and Knight, R.,"Multiple arc discharges for metallurgical reduction or metal melting," Plasma Processing and Synthesis of Materials, Materials Research Society Symposium, Boston, 1983.

Harry, J. E. and Knight, R.,"Multiple electric discharges," IEE Proc., vol. 133, Pt. A, pp. 50-57, Jan., 1986.

Harry, J. E. and Saleh, S. N.,"Multiple electrode system for high power CO_2 laser excitation," Appl. Phys. Lett., vol. 40, (5), pp. 359-361, 1982.

Hill, A. E.,"Multijoule pulses from CO_2 lasers," Appl. Phys. Lett., vol. 12, pp. 324-327, 1968.

Hill, A. E.,"Role of thermal effects and fast flow power scaling techniques in CO_2-He-N_2 lasers," Appl. Phys. Lett., vol. 16, pp. 423-426, June, 1970.

Hill, A. E.,"Uniform electrical excitation of large-volume high-pressure near-sonic CO_2-N_2-He flowstream," Appl. Phys. Lett., vol. 18, (5), pp. 194-197, March, 1971.

Hogan, D. C., Bruzzese, R., Kearsley, A. J., and Webb, C. E.,"Long pulse operation of discharge-excited XeCl lasers," J. Phys. D: Appl. Phys., vol. 14, pp. L157-161, 1981.

Hogan, D. C., Kearsley, A. J., and Webb, C. E.,"Resistive stabilisation of a discharge-excited XeCl laser," J. Phys. D: Appl. Phys., vol. 13, pp. L225-228, 1980.

Hoyaux, M. F.,"Arc physics," Springer-Verlag, Berlin, Heidelberg, New York, 1968.

Hutchinson, M. H. R.,"Excimers and excimer lasers," Appl. Phys., vol. 21, pp. 95-114, 1980.

Javan, A., Bennett JR., W. R., and Herriott, D. R.,"Population inversion and continuous optical maser oscillation in a gas discharge containing a He-Ne mixture," Phys. Rev. Lett., vol. 6, (3), pp. 106-110, Feb., 1961.

Kasamatsu, M. and Shiratori, S.,"New bar cathode sustem for CW CO_2 transversely excited laser," Appl. Phys. Lett., vol. 48, pp. 505-507, 1986.

Kasamatsu, M., Shiratori, S., and Sato, T.,"Characteristics of two cathode systems for CW transversely excited CO_2 lasers," IEEE J. Quantum Electron., vol. QE-22, (10), pp. 2026-2031, Oct., 1986.

Kasamatsu, M., Tsukamoto, K., Shiratori, S., Obara, A., and Uchiyama, F.,"High-power TE CO_2 laser with graphite electrodes," IEEE J. Quantum Electron., vol. QE-18, pp. 173-175, 1982.

Kaufmann, W.,"Elektrodynamische eigentumlichkeiten leitender gase," Ann. Phys, vol. 2, (4), p. 158, 1900.

Knight, R.,"Multiple electric arc discharge," Ph.D. thesis, University of Technology, Loughborough, UK, 1984.

Laflamme, A. K.,"Double discharge excitation for atmospheric pressure CO_2 lasers," Rev. Sci. Inst., vol. 41(11), pp. 1578-1581, 1970.

Lancashire, R. B., Alger, D. L., Manista, E. J., Slaby, J. G., Dunning, J. W., and Stubbs, R. M.,"The NASA high-power carbone dioxide laser , a versatile tool for laser applications," Optical Eng., vol. 16(5), pp. 505-512, 1977.

Legay, R. and Legay-Sommaire, N.,"The possibility of obtaining an optical maser using vibrational energy of gases excited by active nitrogen," Academiedes sciences (Paris) Comples Reders, vol. 259, pp. 99-102, July 6, 1964.

Lutz, M. A.,"The glow to arc transition - a critical review," IEEE Trans. Plasma Sci. (USA), vol. PS 2, (1), pp. 1-10, Dec., 1974.

Machetti, R., Penco, E., Armandillo, E., and Salvetti, G.,"Ultraviolet preionised CO_2 TEA laser with high output power density utilising non conventional electrode profile," IEEE J. Quantum Electron., vol. QE-18, (2), pp. 170-173, 1982.

MaCleary, R. and Gibbs, W. E. K.,"CW CO_2 laser at atmospheric pressure," IEEE J. Quantum Electron., vol. QE-9, (8), pp. 828-833, Aug., 1973.

Maiman, T. H.,"Optical and microwave-optical experiments in Ruby," Phys. Rev. Lett., vol. 4, (11), pp. 564-466, June, 1960.

Mann, M. M.,"CO electric discharge lasers," AIAA Journal, vol. 14, pp. 549-567, May, 1976.

Maskery, J. T., Dugdale, R. A.,"The role of inclusions and surface contaminations in arc initiation at low pressures," Brit. J. Appl. Phys., vol. 17, pp. 1025-1034, 1966.

Measures, R. M.,"Laser remote sensing; fundamentals and applications," John-Wiley, New York, 1984.

Meek, J. M. and Craggs, J. D.,"Electrical breakdown of gases," Clarendon Press, Oxford, 1953.

Moeller, G. and Rigden, J. D.,"High-power laser action in CO_2-He mixture," Appl. Phys. Lett., vol. 7, pp. 274-279, Nov., 1965

Nighan, W. L.,"Effect of molecular dissociation and vibrational excitation on electron energy transfer in CO_2 laser plasmas," Appl. Phys. Lett., vol. 15, (11), pp. 355-357, 1969.

Nighan, W. L.,"Electron energy distributions and collision rates in electrically excited N_2, CO, and CO_2," Phys. Rev. A, vol. 2, (5), pp. 1989-2000, Nov., 1970.

Nighan, W. L. and Bennet, J. H.,"Electron energy distribution functions and vibrational excitation rates in CO_2 laser mixtures," Appl. Phys. Lett., vol. 14, (8), pp. 240-243, 1969.

Nighan, W. L. and Wiegand, W. J.,"Causes of arcing in CW CO_2 convection laser discharges," Appl. Phys. Lett., vol. 25, (11), pp. 633-636, Dec., 1974.

Osborn, M. R., Coutts, J., Hutchinson, M. H. R., and Webb, C. E.,"Output pulse termination of a self-sustained excimer laser," Appl. Phys. Lett., vol. 49, (1), pp. 7-9, July, 1986.

Osgood, R. M., and Eppers, W. C.,"High power CO-N_2-He laser," Appl. Phys. Lett., vol. 13, pp. 409-411, Dec., 1968.

Osgood, R. M., Eppers, W. C., and Nichols, E. R.,"An investigation on the high-power CO laser," IEEE J. of Quantum Electron., vol. QE-6, p. 173, March, 1970.

Papoular, R.,"Electrical phenomena in gases," Iliffe, London, 1965.

Patel, C. K. N.,"Continuous-wave laser action in vibrational-rotational transition of CO_2," Phys. Rev. Lett., vol. 336A, pp. 1187-1193, Nov. 30, 1964a.

Patel, C. K. N.,"Interpretation of CO_2 optical maser experiments," Phys. Rev. Lett., vol. 12, pp. 588-590, May 25, 1964,b.

Patel, C. K. N.,"Selective excitation through vibrational energy transfer and optical maser action in N_2-CO_2," Phys. Rev. Lett., vol. 13, pp. 617-619, Nov. 23, 1964c.

Patel, C. K. N.,"CW laser on vibrational-rotational transitions of CO," Appl. Phys. Lett., vol. 7, pp. 246-247, Nov., 1965

Patel, C. K. N.,"Vibrational-rotational laser action in carbone monoxide," Phys. Rev., vol. 141, pp. 71-83, Jan. 1966.

Patel, C. K. N. and Kerl, R. J.,"Laser oscillation on $X^1\Sigma^+$ vibrational-rotational transitions of CO," Appl. Phy. Lett., vol. 5, (4), pp. 81-83, Aug., 1964.

Patel, C. K. N., Tien, P. K. and McFee, J. H.,"CW high-power CO_2-N_2-He laser," Appl. Phys. Lett., vol. 7, pp. 290-292, Dec. 1965.

Roberts, T. G., Hutchinson, G. J., Ehrlich, J. J., Hales, W. L., and Barr, T. A., Jr.,"High power N_2-CO_2-He laser development," IEEE J. Quantum Electron., vol. QE-3, (11), pp. 605-612, 1967.

Saito, H., Kanasawa, H., Watanabe, K., Taira, T., Sato, S., and Fujioka, T.,"Scaling up of a closed-cycle self-sustained discharge-excited CO laser," Rev. Sci. Instrum, vol. 58, (8), pp. 1417-1421, Aug., 1987.

Saleh, S. N.,"Multiple discharge system for the excitation of a high power CO_2 laser," Ph.D. thesis, University of Technology, Loughborough, UK, 1981.

Sato, S., Iyoda, M., and Fujioka, T.,"Gas flow and chemical lasers," Plenum, New York, 1982.

Sato, S., Kiyota, M., Fujioka, T., and Saito, H.,"Improved performance of a closed-cycle self-sustained discharge-excited CW CO laser," J. Appl. Phys., vol. 58, (11), pp. 3991-3995, Dec., 1985.

Shirahata, H. and Fujisawa, A.,"Aerodynamically mixed electric discharge CO_2 laser," Appl. Phys. Lett., vol. 23, (2), pp. 80-81, July, 1973.

Smith, A. L. S.,"The effect of gas flow on the composition and power output of a CO_2:He:N_2 laser," Phys. Lett., vol. 27A, (7), pp. 432-433, 1968.

Suhr, H.,"Anwendurg von plasmaprozessen in der chemmie," Chemie, Chemie Labor Betreib 29, pp. 132-136, 1973.

Svelto, O.,"Principles of lasers," Plenum Press, London, 1982.

Targ, R. and Tiffany, W. B.,"Gain and saturation in transverse flow CO_2-N_2-He mixtures," Appl. Phys. Lett., vol. 15, pp. 302-304, Nov., 1969.

Taylor, R. s. and Leopold, K. E.,"Microsecond duration optical pulses from a UV-preionised XeCl laser," Appl. Phys. Lett., vol. 47, (2), pp. 81-83, July, 1985.

Tiffany, W. B., Targ. R., and Foster, J. D.,"Kilowatt CO_2 gas transport laser," Appl. Phys. Lett., vol. 15, pp. 91-93, Aug., 1969.

Touloukian, Y. S., Liley, P. E., and Saxena, S. C.,"Thermal conductivity; nonmetallic liguids and gases," IFI/Plenum, New York-Washington, 1970.

Traus, I., Suhr, H., Harry, J. E., and Evans, D. R.,"High temperature barrier discharges and high power discharges for the dissociation of hydrogen sulphide," 2nd Symp. on High Pressure Low Temperature Plasma Chemistry, Kazimierz, Poland, September, 1989.

Tunnen, P. D., Bletzinger, P., and Garscadden, A.,"Species composition in the CO_2 discharge laser," IEEE J. Quantum Electron., vol. QE-10, (1), pp. 6-11, 1974.

Tyte, D. C.,"A compact 20 W CW CO_2 laser," J. Phys. E: Sci Instrum., vol. 3, pp. 734-735, 1970.

Van Dyke, M.,"An album of fluid motion," Parabolic Press, Stanford, California, 1982.

Von Engel, A.,"Ionised gases," Clarendon Press, Oxford, 2nd ed., 1965.

Von Engel, A.,"Electric plasmas; their nature and uses," Taylor & Francis, London, 1983.

Wang, C. P.,"Performance of XeF/KrF lasers pumped by fast discharges," Appl. Phys. Lett., vol. 29, (2), pp. 103-105, July, 1976.

Wasserstrom, E., Crispin, Y., Rom, J., and Shwartz, J.,"The interaction between electrical discharges and gas flow," J. Appl. Phys. vol. 49, (1), pp. 81-86, Jan., 1978.

Westberg, R. G.,"Nature and role of ionising potential space waves in glow to arc transitions," Phys. Rev., vol. 114, (1), pp. 1-17, 1959.

Wiegand, W. J. and Nighan, W. L.,"Influence of fluid-dynamic phenomena on the occurrence of constriction in CW convection laser discharges," Appl. Phys. Lett., vol. 26, (10), pp. 554-557, May, 1975.

Witteman, W. J.,"High-output and long lifetime of sealed-off CO_2 lasers," Appl. Phys. Lett., vol. 11, pp. 337-338, Dec., 1967.

APPENDICES

APPENDIX 1

Specifications of the Scanning Monochromator Used to Investigate the Spectrum Emission of the Positive Column.

Basic Monochromator

Rofin (6000)

Diffraction grating	1200 lines/mm blazed at 300 nm
Optical configuration	side by side Ebert
Slit height	5 mm
Slit bandwibth	2, 5, 10 or 20 nm bandpass
Maximum optical bandwibth error with slits fixed to monochromator	-0.5 nm +3.5 nm (all slits)
Useable wavelength range of monochromator and detector	300 nm - 1100 nm (with wavelength marker unit (6001))
Wavelength measurement accuracy	±0.5 nm (with wavelength marker unit (6001)) ±0.8 nm in range 400 nm - 700 nm (using oscilloscope scale)
Input/output beam angle	f/6 nominally. Optical axes of input and output beams inclined at 6° to the slit plate normal.
Spectral scan repetition period	94 ms - 95 ms nominally.

Detector

Rofin (6030) photomultiplier

Useful wavelength range	200 nm- 930 nm
Sensitivity	2.5 nm/high

Electrical

Built in transimpedance amplifier	Virtual earth, inverting operational amplifier Gain x Bandwidth typically 20 MHz Input current 250 pA MAX Standard amplifier - high gain/medium speed. V_{out}/V_{in}= 10^8 ± 5%
Oscilloscope for display	Dual trace, external negative edge triggering. 8 divition graticule. Bandwidth 20 MHz Normal x shift and calibrated time-base 0.5 ms/div and 1 ms/div

Accessories used

(i) Wavelength marker unit	
(6001) Calibrated scale	1 -10 nm indicator pulses moveable cursor pulse
Cursor control	4 digit thumbwheel
Wave accuracy	±0.5 nm (using calibration charts)
Scan rate control	Adjustable 10 Hz- 16 Hz (INT/AC/EXT).
(ii) Sample and hold unit	
(0003) display	
External output	0 - 10 (for driving chart recorder).
Gain	Switch and variable x 0.5, x 100.

APPENDIX 2

Steenbeck's Minimum Principle

The early publications on Steenbeck's minimum principle (Steenbeck 1932, 1940) were in German. A clear statement of Steenbeck's minimum principle has been given by Hoyaux (1968, 1970), in English. The following is a paraphrase of this.

"Steenbeck's minimum principle was proposed in relation to high-pressure arc physics, and its theoretical background is still far from being understood. In its generalised form, it may be tentatively expressed as:"Each time an electric discharge phenomenon seems to have a choice between more than one configuration, it tends always to achieve that implying the minimum voltage drop." This formulation contains voluntarily "unscientific" terms. A physical phenomenon has never a "choice." It is always entirely determined (at the classical level of approximation) by the laws of nature."

"The initial formulation of a minimum energy or minimum voltage drop or minimum electric field principle seems to have been nothing more than a means to solve a difficulty born with the "channel-model" in the high-pressure arc cylindrical positive column. If the ionised channel is too narrow, there is not enough room to accommodate the arc current, whereas if the channel radius approaches the tube radius, the cooling effect of the wall becomes too great, and the degree of ionisation in the channel becomes insufficient to permit the passage of the current. The radius of the "core" may be determined by the condition that the axial electric field is a minimum at equal current, external radius, gas pressure and initial gas composition. The minimum principle seems to have a direct relationship with the Second Law of Thermodynamics."

"The thermodynamics of irreversible processes predicts a tendency to a minimum generation of entropy per unit time, and this coincides, in our case, with the condition of minimum axial electric field."

"Although the minimum principle was intended to explain the conditions in the discharge column, von Engel and Steenbeck implicitly used the same principle in an entirely different field: the theory of the voltage drop at the cathode in glow discharges. Since then, Steenbeck's minimum principle has been invoked by many authors, and in relevance to many different problems (anodic spots, division of the cathodic spot, etc.)."

As the paradox surrounding the minimum principle continues, the minimum principle provides, in general, a satisfactory results in agreement with those given by an accurate models. An example of the use of the minimum principle in an entirely different field is the treatment of the skin effect by minimising the impedance with respect to the skin depth. The same expression has been obtained for the skin depth as by the conventional analysis (Sensiper 1983).

References

Hoyaux, M. F.,"Arc physics," Springer-Verlag. Berlin. Heidelberg. New York., 1968.

Hoyaux, M. F.,"The physics of the electric discharge," High Temperature - High Pressures, (Pion, Great Britain), vol. 2, pp. 17-30, 1970.

Sensiper, D.,"The skin effect as impedance minimisation," IEEE Transactions on Education, vol. E-26, (3), pp. 118-119, Aug., 1983.

Steenbeck, M.,"Energetik der gasentladungen," Z. Phys., vol. 7, pp. 809-815, 1932.

Steenbeck, M,"Eine Prufung des Minimumprinzips fur thermische Bogensaulen an Hand neuer MeBergebnisse," Wiss. Veroff. a.d. Siemens-Konzern, vol. 19, pp 59-67, 1940.

APPENDIX 3

The 5 kW CO_2 Laser

Discharge current (A)	1.5
Discharge voltage (kV)	14.1
Laser output power (kW)	5
Electrical to optical efficiency (%)	23.6
Gas pressure downstream (mb)	60
Gas flow rate (kg/s)	0.031
Electrical power loading (kW/kg/s)	682
Laser power loading (kW/kg/s)	161
Gas mixture ($He:N_2:CO_2$ by vol.)	36:7:1
Gas exit temperature (°C)	255
E/N ($V.cm^2$)	1.36×10^{-16}
E/p (V/cm.torr)	4.8

Table A3.1 Summary of the operational characteristics of the laser at maximum power output (Evans 1987).

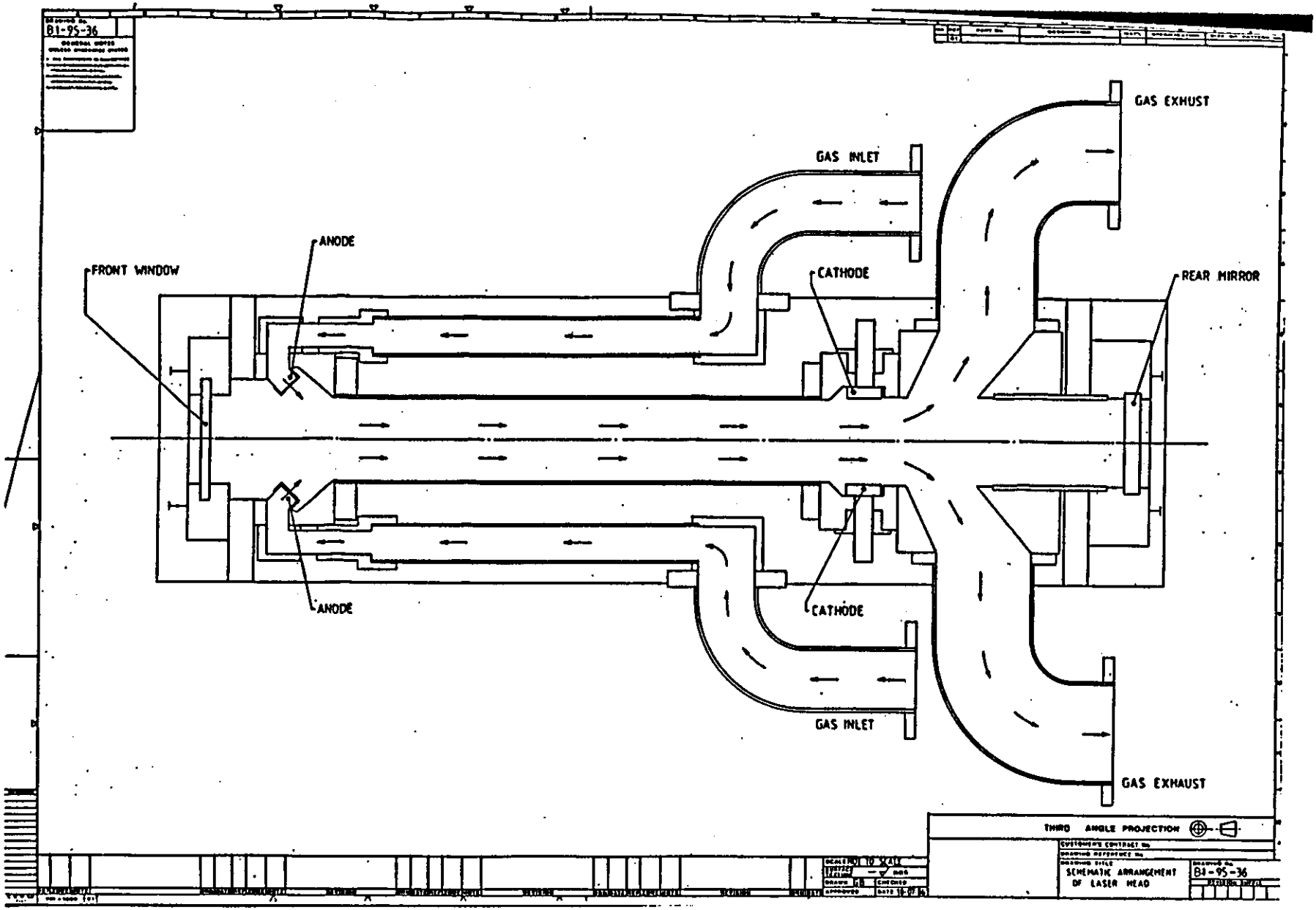

Fig. A3.1 Schematic diagram of the gas injection flow paths (Evans 1987).

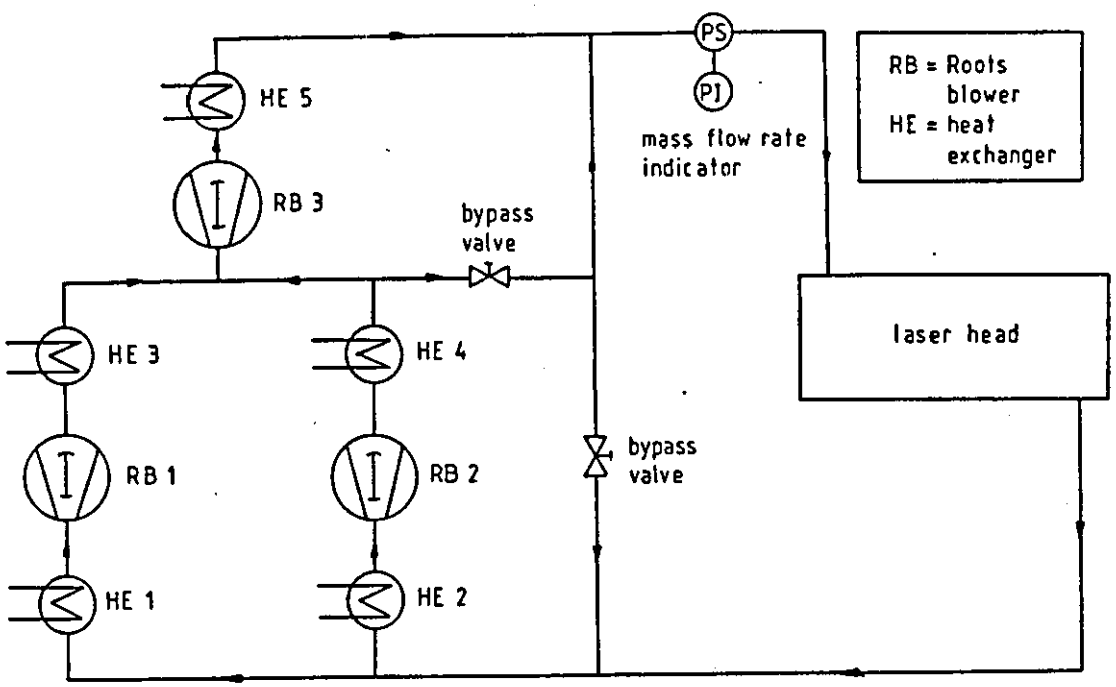

Fig. A3.2 Schematic diagram of the gas recirculating system (Evans 1987).

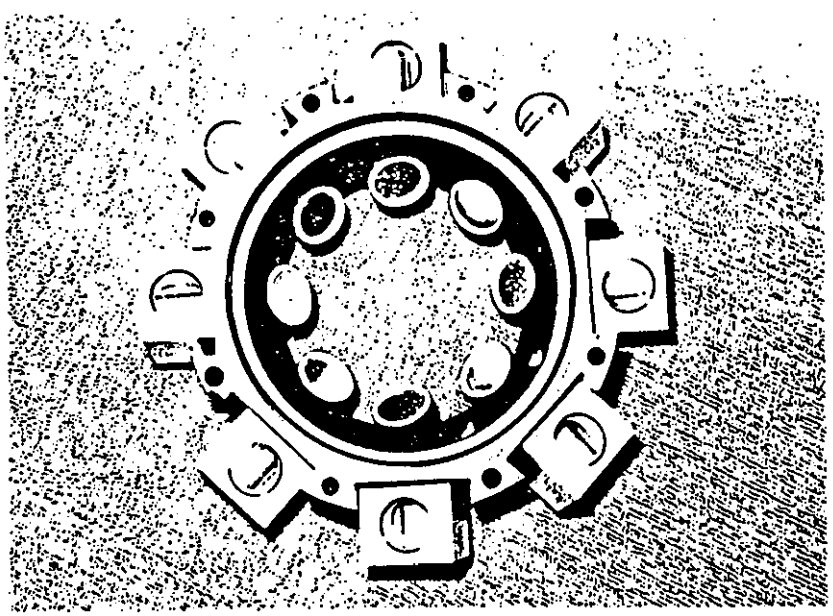

Fig. A3.3 Multiple gas injection anode head assembly (Evans 1987).